Nanoscale Energy Transport

Emerging phenomena, methods and applications

Online at: https://doi.org/10.1088/978-0-7503-1738-2

Nanoscale Energy Transport

Emerging phenomena, methods and applications

Edited by
Bolin Liao
Department of Mechanical Engineering, University of California, Santa Barbara, USA

IOP Publishing, Bristol, UK

ISBN 978-0-7503-1738-2 (ebook)
ISBN 978-0-7503-1736-8 (print)
ISBN 978-0-7503-1767-2 (myPrint)
ISBN 978-0-7503-1737-5 (mobi)

DOI 10.1088/978-0-7503-1738-2

Version: 20200301

IOP ebooks

British Library Cataloguing-in-Publication Data: A catalogue record for this book is available from the British Library.

Published by IOP Publishing, wholly owned by The Institute of Physics, London

IOP Publishing, Temple Circus, Temple Way, Bristol, BS1 6HG, UK

US Office: IOP Publishing, Inc., 190 North Independence Mall West, Suite 601, Philadelphia, PA 19106, USA

Contents

Part II Measurements and applications

Preface

Nanoscale energy transport is a fast-developing research field that studies the transport processes of fundamental energy carriers, including electrons, phonons, photons, magnons, etc, in devices and material structures with characteristic sizes in the nanometer range. Fundamentally, new physical phenomena emerge at the nanoscale due to the classical and quantum confinement effects of the energy carriers, leading to the breakdown of macroscopic constitutive laws, such as Fourier's law of heat conduction and Planck's law of blackbody radiation. Practically, as the advancement of nanotechnology has enabled routine fabrication of devices and materials at the nanoscale, a fundamental understanding of energy transport in these systems is crucial for achieving better efficiency and performance. Indeed, the improved understanding of nanoscale energy transport in the past two decades has led to better thermal management for microelectronic devices, more efficient thermoelectric modules and new strategies to efficiently harvest the full spectrum of solar power, to name a few examples. Therefore, nanoscale energy transport is a field of both fundamental interest and practical relevance. In this light, this multi-contributor volume aims to cover new developments in both the scientific basis and the practical relevance of nanoscale energy transport, with a particular emphasis on the emerging effects at the nanoscale that qualitatively differ from those at the macroscopic scale.

Excellent texts and monographs on nanoscale energy transport are available, for example by Chen [1], Zhang [2], Fisher [3], Volz [4] and others, where the fundamentals and the research developments at the time of publication are clearly elaborated. However, as this is an active field of research, new effects, experimental and computational methods, and applications are emerging at a fast pace. Complementary to these existing books, the goal of this volume is to cover recent developments in the theory, methods and applications of nanoscale energy transport from the past few years, and help researchers in this field obtain an overview of the current frontiers. To this end, I have invited active researchers in nanoscale energy transport to contribute chapters on their specialty topics and offer their expert perspectives on the important advancements in the past decade as well as future directions. In the end, 17 chapters were selected for this multi-contributor volume that cover a broad range of topics. In terms of microscopic energy carriers, the transport of phonons, electrons, photons and magnons in the nanoscale are discussed in various chapters. In terms of methods, state-of-the-art computational and experimental approaches are reviewed, including a chapter on the emerging material informatics method (chapter 5). In terms of material systems, a broad range from interfaces and molecular junctions to nanostructured bulk materials is included. While I believe this volume is a comprehensive survey of the state of the art of nanoscale energy transport, by no means does this book cover all significant new developments in the field. Notable omissions include spin caloritronics, where the coupling effects of phonons and magnons are investigated, and the energy

transport in two-dimensional materials. For these topics, the interested reader is referred to excellent recent review articles such as [5] and [6].

The chapters are organized into two parts. Part I focuses on emerging theory and computational methods. Chapter 1 by Sangyeop Lee's group at the University of Pittsburgh discusses hydrodynamic phonon transport, particularly in two-dimensional materials, where normal phonon–phonon scatterings dominate Umklapp scatterings and the phonon thermal transport mimics fluid flow. Chapter 2, by Tianli Feng from Oak Ridge National Laboratory and Xiulin Ruan from Purdue University, reviews the recent development of calculating higher order phonon scattering rates, e.g. four-phonon processes, and its relevance to thermal transport in technologically important materials. Chapter 3, by Tengfei Luo's group at the University of Notre Dame, provides a detailed account of how bulk phonon scattering events affect interfacial thermal transport from first-principles and molecular dynamics simulations. Chapter 4, by Zhiting Tian's group at Cornell University, gives an introduction to the state-of-the-art atomistic Green's function (AGF) method for calculating interfacial phonon transport properties and interfacial thermal resistance. Chapter 5, by Junichiro Shiomi's group at the University of Tokyo, elaborates on using material informatics methods, in particular Bayesian optimization, for nanoscale thermal transport problems. This is an emerging front in computational materials science that has attracted intense interest recently due to the fast advancement of data science and machine learning methods. Chapter 6, by Chengyun Hua at Oak Ridge National Laboratory, reviews the current status of resolving the phonon mean free path distribution in real materials from both the computational and experimental perspectives, which is essential for engineering materials at the nanoscale to achieve desirable thermal transport properties. Chapter 7, by Keivan Esfarjani's group at the University of Virginia, provides a historic view of incorporating the lattice anharmonicity into first-principles phonon calculations at finite temperature, which is necessary to correctly describe phonon softening and phase transitions.

Part II focuses on the developments of experimental techniques and practical applications enabled by fundamental advancements. Chapter 8, by Professors Edgar Meyhofer and Pramod Reddy's group at the University of Michigan, details state-of-the-art measurement techniques to resolve thermal and thermoelectric transport across atomic and molecular junctions with extreme sensitivity. Chapter 9, by Xiaojia Wang's group at the University of Minnesota, reviews the recent applications of emerging time-resolved magneto-optical Kerr effect (TR-MOKE) spectroscopy to characterize both phonon and magnetization dynamics. Chapter 10, by Keshav Dani's group at Okinawa Institute of Science and Technology in Japan, introduces a class of powerful tools—ultrafast electron microscopy, in particular time-resolved photoemission electron microscopy (TR-PEEM)—and their applications in nanoscale energy transport. Chapter 11, by Chen Li's group at the University of California, Riverside summarizes recent results utilizing the inelastic neutron scattering (INS) technique to understand phonons and magnons in energy materials. Chapter 12, by Renkun Chen's group at the University of California, San Diego, reviews the historic development and recent applications of suspended

micro-devices to characterize the thermal transport properties of nanomaterials. Chapters 13 and 15, by Nenad Miljkovic's group at the University of Illinois, Urbana–Champaign, discuss how micro- and nanostructured surfaces can significantly enhance condensation heat transfer and help combat frosting and icing in practical energy systems. Chapter 14, by Mona Zebarjadi's group at the University of Virginia, introduces the mechanisms and current frontiers of using thermionic emission to convert thermal energy into electricity as an alternative to thermoelectric conversion. Chapter 16, by Zhifeng Ren's group at the University of Houston, addresses a critical problem at the current development stage of thermoelectric materials—how to reliably measure the thermoelectric transport properties and energy conversion efficiency of thermoelectric materials. Chapter 17, by Andrej Lenert's group at the University of Michigan, reviews the recent development of thermophotovoltaic energy conversion, including both the material and the device aspects, and particularly the opportunities offered by the recent advancement of nanophotonics.

I wish to acknowledge all the authors for their valuable input and hard work, which have made this volume possible. I also want to thank the Institute of Physics Publishing for providing me the opportunity to work on this project, in particular Michael Slaughter and John Navas who initiated this project, and Caroline Mitchell, Daniel Heatley and Robert Trevelyan for their generous help (and patience) during the editing and production process. Last, but not least, I want to thank the support for research provided by the US Department of Energy, National Science Foundation and US Army Research Office.

Bolin Liao
University of California, Santa Barbara
November 2019

References

[1] Chen G 2005 *Nanoscale Energy Transport and Conversion: A Parallel Treatment of Electrons, Molecules, Phonons, and Photons* 1st edn (Oxford: Oxford University Press)
[2] Zhang Z 2007 *Nano/Microscale Heat Transfer* (New York: McGraw-Hill)
[3] Fisher T S 2013 *Thermal Energy At The Nanoscale* (Hackensack, NJ: WSPC)
[4] Volz S (ed) 2007 *Microscale and Nanoscale Heat Transfer* (Berlin: Springer)
[5] Boona S R, Myers R C and Heremans J P 2014 Spin caloritronics *Energy Environ. Sci.* **7** 885–910
[6] Gu X, Wei Y, Yin X, Li B and Yang R 2018 Colloquium: phononic thermal properties of two-dimensional materials *Rev. Mod. Phys.* **90** 041002

Editor biography

Bolin Liao

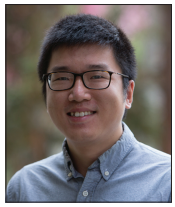

Bolin Liao is currently an assistant professor in the Department of Mechanical Engineering at the University of California, Santa Barbara. His main research interest is in nanoscale energy transport and its application to sustainable energy technologies. Specifically, his research aims to understand the transport and interaction processes of fundamental energy carriers, such as electrons, phonons, photons and magnons, at the smallest length and time scales, and then use this knowledge to develop more efficient clean energy devices, e.g. thermoelectric modules and photovoltaic cells. Current projects include first-principles and multiscale simulation of energy carrier transport, visualization of photophysics in space and time with scanning ultrafast electron microscopy, ultrafast optical techniques for thermal and thermoelectric characterization, and applied clean energy devices and systems.

Bolin obtained his PhD in mechanical engineering from MIT in March 2016, advised by Gang Chen. He was a Kavli Postdoctoral Fellow at the California Institute of Technology from May 2016 to June 2017, hosted by the late Ahmed Zewail, where he worked on scanning ultrafast electron microscopy.

Contributors

Xun Li

Xun Li received his BS degree in energy engineering from Zhejiang University, the People's Republic of China, in 2015. He is currently a PhD candidate in the Department of Mechanical Engineering and Materials Science at the University of Pittsburgh, PA. His research focuses on the computational study of first-principles based phonon transport in graphitic materials and interfacial phonon transport in semiconductors.

Sangyeop Lee

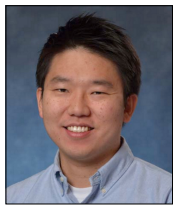

Sangyeop Lee is an Assistant Professor in the Department of Mechanical Engineering and Materials Science at the University of Pittsburgh, PA. He received his PhD from the Department of Mechanical Engineering at Massachusetts Institute of Technology in 2015. His current research interests are first-principles based simulation of hydrodynamic phonon transport and thermal transport in partially/fully disordered phases.

Tianli Feng

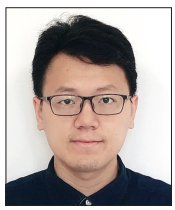

Tianli Feng is a postdoctoral fellow at Oak Ridge National Laboratory, TN. He received his BS in physics from the University of Science and Technology of China in 2011. He received his MS and PhD in mechanical engineering from Purdue University, IN in 2013 and 2017, respectively. His research interests include developing new atomistic-scale predictive simulation methods for thermal energy transport, and using these methods to guide the development of high-performance materials.

Xiulin Ruan

Xiulin Ruan is a Professor in the School of Mechanical Engineering and the Birck Nanotechnology Center at Purdue University, IN. He received his BS and MS in engineering thermophysics from Tsinghua University in 2000 and 2002, respectively. He received an MS in electrical engineering and a PhD in mechanical engineering from the University of Michigan at Ann Arbor in 2006 and 2007, respectively. His research interests include multiscale multiphysics simulations and experiments of phonon, electron, and photon transport and interactions, for various emerging applications. Ruan has been recognized with

many awards, including the NSF CAREER Award (2012), the ASME Heat Transfer Division Best Paper Award (2015) and the Air Force Summer Faculty Fellowship (2010, 2011 and 2013). He currently serves as an associate editor for the ASME *Journal of Heat Transfer*.

Tengfei Luo

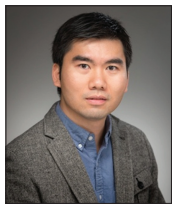

Tengfei Luo is the Dorini Family Collegiate Chair and Associate Professor in the Department of Aerospace and Mechanical Engineering (AME) at the University of Notre Dame (UND), IN. Before joining UND, he was a postdoctoral associate at Massachusetts Institute of Technology from 2009 to 2011, after obtaining his PhD from Michigan State University in 2009. At UND, Luo leads an interdisciplinary group focusing on nanoscale thermal transport, electronics thermal management, novel material design and manufacturing, and water treatment.

Eungkyu Lee

Eungkyu Lee is the Research Assistant Professor in the Department of Aerospace and Mechanical Engineering (AME) at the University of Notre Dame (UND), IN. He was a postdoctoral associate at the Department of AME at UND. He obtained his PhD from Seoul National University in 2015. At UND, Lee studies light–matter interaction involving nanophotonics and multiphase thermofluids and interfacial thermal transport.

Ruiyang Li

Ruiyang Li is currently pursuing a PhD degree at the University of Notre Dame, IN under the supervision of Tengfei Luo. He received his BS degree in energy and power engineering from Huazhong University of Science and Technology in 2018. His research interests include nanoscale thermal transport at semiconductor material interfaces, and the prediction of thermal properties using machine learning based techniques.

Zhiting Tian

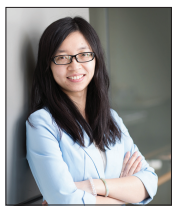

Zhiting Tian is an Assistant Professor and a Eugene A Leinroth Sesquicentennial Faculty Fellow in the Sibley School of Mechanical and Aerospace Engineering at Cornell University, NY. Between 2014 and 2018 she was an Assistant Professor of Mechanical Engineering at Virginia Tech. Zhiting obtained her PhD in mechanical engineering from MIT in 2014. Zhiting's research focuses on the fundamental understanding of nanoscale thermal

transport and energy conversion using experimental and computational tools. Zhiting's recent awards include the Office of Naval Research (ONR) Young Investigator Award, NSF CAREER Award, ACS Petroleum Research Fund Doctoral New Investigator Award and 3M Non-Tenured Faculty Award.

Jinghang Dai

Jinghang Dai is a PhD student in the Sibley School of Mechanical and Aerospace Engineering at Cornell University, NY. His research interests focus on the modeling of transport processes at interfaces and thermoelectric materials and experimental characterization of thermal transport properties.

Renjiu Hu

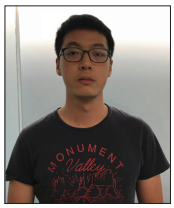

Renjiu Hu is a PhD student in the Sibley School of Mechanical and Aerospace Engineering at Cornell University, NY. His research focuses on interfacial thermal transport and Anderson localization.

Jiang Guo

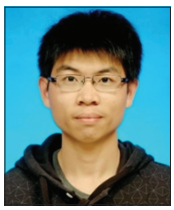

Jiang Guo is currently a PhD student in the Department of Mechanical Engineering at the University of Tokyo, working on tailoring thermal radiative properties for energy applications via optimizing metamaterials using machine learning methods.

Shenghong Ju

Shenghong Ju received his PhD in 2014 from Tsinghua University, PRC. He is now an associated professor at the China–UK Low Carbon College, Shanghai Jiao Tong University, and a visiting scholar at the University of Tokyo. He is working on developing new energy materials, fundamental nanoscale heat transfer studies and materials informatics.

Junichiro Shiomi

Junichiro Shiomi received his PhD in 2004 from the Royal Institute of Technology (KTH), Sweden. He is currently a Professor in the Department of Mechanical Engineering, The University of Tokyo. His research interests include heat conduction of nanomaterials, polymer composites, thermoelectrics, phase change and fluidics in the nanoscale, interfacial thermofluid dynamics, thermal convections and materials informatics.

Chengyun Hua

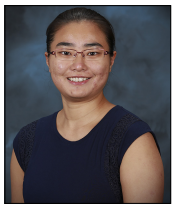

Chengyun Hua received her BS in engineering physics from the University of Michigan in 2011, and her PhD in mechanical engineering from the California Institute of Technology in 2016. She joined the Oak Ridge National Laboratory, TN, in 2016 as a Liane B Russell Fellow and is currently working as an R&D associate. Her research focuses on gaining a comprehensive picture of how heat is transported in a solid at the scales of heat carriers, i.e. electrons and phonons (quantized vibrations in the lattice). Using both computation and experiments, she is currently working on using structures at the nanoscale as a tunable physical parameter to control and manipulate heat.

Keivan Esfarjani

Keivan Esfarjani obtained his general-engineering degree at the Ecole Centrale de Paris in France. He then pursued his studies in theoretical solid-state physics with a Master's (DEA) from the University of Paris followed by a PhD at the University of Delaware and a postdoc at Washington University in Saint Louis, MO. During his career, Esfarjani has held various positions at the Institute for Materials Research of Tohoku University, Sharif University of Technology, University of California Santa Cruz, MIT and Rutgers University. Currently he is an Associate Professor at the Departments of Mechanical Engineering, Materials Science and Physics at the University of Virginia. His research interests include the electronic structure calculation of materials from first-principles, lattice dynamics and phase change, electrical and thermal transport, and finally the storage and conversion of energy and information.

Yuan Liang

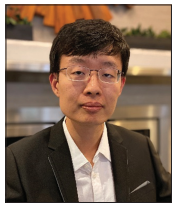

Yuan Liang received his BSc in applied physics from the University of Science and Technology of China, in Hefei, Anhui, in 2015. He was a member of the YAN Ji-Ci Elite Program in Physics, School of Gifted Young, working on the super-hydrophobicity of nano-membranes. He is currently working on his PhD in physics at the University of Virginia, Charlottesville. His current research interests include free energy computation and phase transition studies based on self-consistent phonon theory, computational schemes to extract anharmonic force constants in finite temperature—specifically stochastically designing a sampling method of lattice snapshots— and material properties analysis by applications of deep learning neural network packages.

Pramod Reddy

Pramod Reddy received a BTech and MTech in mechanical engineering from IIT-Bombay in 2002, and a PhD in applied science and technology from the University of California, Berkeley in 2007. He is currently a Professor in the Departments of Mechanical Engineering and Materials Science and Engineering at the University of Michigan, Ann Arbor.

Edgar Meyhofer

Edgar Meyhofer received a BS in biology from the University of Hannover in Germany, and an MS from Northeastern University in Boston, MA. In 1991 he earned a PhD from the University of Washington, Seattle. Since 2001 he has been a Professor of Mechanical Engineering and Biomedical Engineering at the University of Michigan in Ann Arbor. His current interests include nanoscale radiative heat transfer, energy transport in molecular junctions and nanoscale energy conversion.

Longji Cui

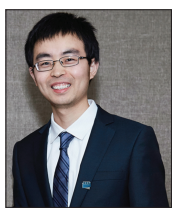

Longji Cui joined the faculty of the Mechanical Engineering and Materials Science and Engineering program of CU Boulder, CO, as an Assistant Professor in January 2020. Cui received his PhD in mechanical engineering in 2018 from the University of Michigan, Ann Arbor, under the supervision of Pramod Reddy and Edgar Meyhofer. From August 2018, he served as a Visiting Assistant Professor in the Mechanical Engineering department of CU and has been the J Evans Attwell-Welch Fellow of Rice University, and performed postdoctoral research in the Smalley-Curl Institute and Department of Physics and Astronomy (Natelson Research Group) at Rice University. Cui is a recipient of the

Robert M Caddell Memorial Award, the Richard and Eleanor Towner Prize for Outstanding PhD Research at U-M, the Chinese Government Award for Outstanding Student Abroad and the Material Research Society (MRS) Graduate Student Gold Medal.

Dustin Lattery

Dustin Lattery is currently a PhD student in mechanical engineering at the University of Minnesota, Twin Cities. He received his Bachelor's and Master's degrees in mechanical engineering from the University of Minnesota, Twin Cities in 2014 and 2017, respectively. His research focuses on magnetization dynamics in thin films. During his research, Lattery has optimized the signal from time-resolved magneto-optical Kerr effect measurements of perpendicular magnetic thin films, successfully combining both experimental and numerical methods. He has applied this method to a range of technologically important magnetic materials, for extracting information about their magnetic anisotropy and Gilbert damping.

Jie Zhu

Jie Zhu is currently an Associate Professor in the School of Energy and Power Engineering at Dalian University of Technology in China. He was previously a research associate in the Department of Mechanical Engineering at the University of Minnesota, Twin Cities. He received his BS in thermal science and energy engineering in 2004 from the University of Science and Technology of China, and a PhD from the Institute of Engineering Thermophysics, Chinese Academy of Sciences in 2011. Zhu's research interests include ultrafast non-equilibrium heat transfer, thermal transport across interfaces, the thermophysical properties of novel materials and the development of related experimental methods.

Dingbin Huang

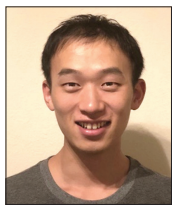

Dingbin Huang is currently a PhD student in mechanical engineering at the University of Minnesota, Twin Cities. Mr Huang received his Master's degree in mechanical engineering from Shanghai Jiao Tong University in 2018, and a Bachelor's degree from Xi'an Jiaotong University in 2015. Mr Huang's research interests are the time-resolved study of magnetization dynamics and spin-heat coupling of novel materials for spintronic and data storage applications.

Xiaojia Wang

Professor Xiaojia Wang is an assistant professor in the Department of Mechanical Engineering at the University of Minnesota, Twin Cities. Prior to this, she was a postdoctoral research associate in the Department of Materials Science and Engineering at the University of Illinois at Urbana–Champaign. She received her PhD in mechanical engineering from the Georgia Institute of Technology in 2011. She received her MS in 2007 and BS in 2004 from Xi'an Jiaotong University, China, studying mechanical engineering. Her current research explores thermal and magnetic transport in functional materials and across material interfaces, using ultrafast optical techniques. These investigative efforts have a wide range of applications, including solid-state energy conversion and harvesting, data storage and spintronic devices.

Rebecca Wong

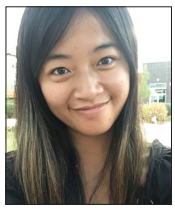

Rebecca Wong obtained her Bachelor's degree in physics and environmental science from Grinnell College. She has worked on various energy-related research projects at universities and national laboratories in the United States and abroad, and has experience in optics research at Osaka University and more recently the Okinawa Institute of Science and Technology Graduate University. Her research interests include novel semiconductor materials and devices, in particular for solar and renewable energy.

Michael Man

Michael Man received his Masters and PhD from Hong Kong University of Science and Technology. He moved to Okinawa and joined the Okinawa Institute of Science and Technology (OIST) as a postdoctoral researcher in 2012. Currently, he is a staff scientist in the Femtosecond Spectroscopy Unit at OIST. His research focuses on the development of ultrafast techniques in photoemission electron microscopy and in the study of electron dynamics and ultrafast phenomena in two-dimensional materials. He also has expertise in the field of surface science, covering phase transition, growth and magnetism in ultrathin films and two-dimensional materials.

Keshav Dani

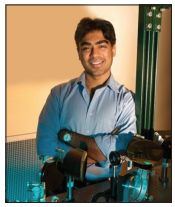

Keshav Dani is currently an Associate Professor at the Okinawa Institute of Science and Technology (OIST), Graduate University in Okinawa, Japan. He joined OIST in November 2011 as a tenure-track Assistant Professor after completing a Director's Postdoctoral Fellowship at the Center for Integrated Nanotechnologies at Los Alamos National Laboratory, NM. Keshav graduated from UC Berkeley in 2006 with a PhD in physics, where he explored the nonlinear optical response of the quantum Hall system under the supervision of Daniel Chemla at LBNL. Prior to his PhD, he obtained a BS from Caltech in mathematics with a senior thesis in quantum information theory under John Preskill and Hideo Mabuchi. His current research interests lie in the use of ultrafast techniques to study the electron dynamics of two-dimensional materials and energy materials, develop optoelectronic applications in the terahertz regimes, and pursue interdisciplinary projects with OIST colleagues in neuroscience and art conservation.

Chen Li

Chen Li joined the Department of Mechanical Engineering and Materials Science and Engineering Program at the University of California, Riverside as an assistant professor in July 2016. Prior to joining UCR, Li worked as a research scientist for EFree (Energy Frontier Research in Extreme Environment Center), a DOE Energy Frontier Research Center (EFRC) centered at the Geophysical Laboratory of the Carnegie Institute of Washington and a joint faculty at Spallation Neutron Source (SNS) at Oak Ridge National Laboratory, TN.

Li obtained a BSc in physics from the Department of Physics, Peking University, and a PhD in materials science from the Department of Applied Physics and Materials Science, California Institute of Technology. After graduation, he worked as a postdoc for the Scattering and Thermophysics Group, Materials Science and Technology Division, at Oak Ridge National Laboratory.

Qiyang Sun

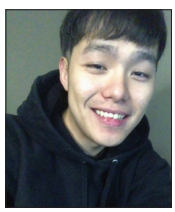

Qiyang Sun is a PhD student in the Mechanical Engineering Department, University of California, Riverside. Before joining UCR, Qiyang Sun obtained his BSc in engineering from the Energy and Power Engineering department, Huazhong University of Science and Technology, PRC.

Sunmi Shin

Sunmi Shin joined the Department of Mechanical Engineering at the National University of Singapore as a Research Assistant Professor in August 2019 and will be an Assistant Professor from July 2020. She received her PhD degree in materials science and engineering from the University of California, San Diego in 2019. She specializes in the experimental and theoretical investigation of fundamental nanoscale heat transport for thermal management and the development of personalized thermoregulators and energy harvesting devices using thermoelectric energy conversion. Her research interests include multidisciplinary approaches for efficient and active thermal energy technologies.

Renkun Chen

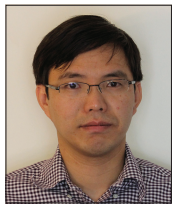

Renkun Chen is an Associate Professor in the Department of Mechanical and Aerospace Engineering at the University of California, San Diego (UCSD). He received his BS in thermophysics from Tsinghua University, Beijing in 2004, and his PhD in mechanical engineering from the University of California, Berkeley in 2008. He was a postdoctoral researcher at Berkeley prior to joining UCSD in 2009. His research group at UCSD is interested in the fundamentals and applications of thermal energy transport and conversion, including nanoscale energy transport phenomena, thermoelectric and solar–thermal energy conversion, phase-change heat transfer and thermal insulation technologies.

Hyeongyun Cha

Hyeongyun Cha received BS and MS degrees in mechanical engineering from the University of Illinois at Urbana–Champaign in 2014 and 2016, respectively, where he is currently pursuing a PhD degree in mechanical engineering. His current research focuses on the study of functional coating degradation using scanning probe microscopy techniques.

Soumyadip Sett

Soumyadip Sett received his BE degree in power engineering from Jadavpur University, India in 2011, and a PhD degree in mechanical engineering from the University of Illinois at Chicago (UIC) in 2016. He is currently a postdoctoral researcher with the University of Illinois at Urbana–Champaign (UIUC). His research interests intersect the multidisciplinary fields of thermofluid science, interfacial phenomena and renewable energy. His current work focuses on the phase-change heat transfer performance of

micro/nanostructured surfaces, in particular involving low surface tension fluids and refrigerants. He was the recipient of the Deans Graduate Fellowship from UIC in 2015 for outstanding graduate research during his PhD, and in 2014 received the Chicago Consular Corps award for academic achievements as an international student.

Patrick Birbarah

Patrick Birbarah received his BE degree (with a high distinction) in mechanical engineering from the American University of Beirut, Lebanon in 2014. He received a PhD degree in mechanical science and engineering from the University of Illinois at Urbana–Champaign in 2019, where his work focused on phase-change heat transfer enhancement. He is currently working at Trane as a thermal systems engineer.

Tarek Gebrael

Tarek Gebrael received a BE degree (with a high distinction) in mechanical engineering with a minor in applied mathematics from the American University of Beirut, Lebanon in 2017. He is currently pursuing a PhD degree in mechanical engineering at the University of Illinois at Urbana–Champaign. His current research interests include electric field actuated droplet jumping during condensation and advanced phase-change thermal management techniques for next-generation high power density electronics.

Junho Oh

Junho Oh received BS and MS degrees in mechanical engineering from Sungkyunkwan University, Seoul, South Korea in 2013 and 2015, respectively, and a PhD degree in mechanical engineering from the University of Illinois at Urbana–Champaign. He is currently a Research Fellow at University College London, UK. His current research interests include nanoengineering, fluid mechanics and interfacial sciences for enhancing phase-change heat transfer and biomedical applications.

Nenad Miljkovic

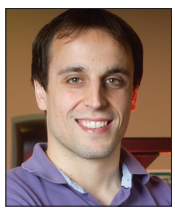

Nenad Miljkovic received a BASc degree in mechanical engineering from the University of Waterloo, ON, Canada, in 2009, and MS and PhD degrees in mechanical engineering from the Massachusetts Institute of Technology in 2011 and 2013, respectively. He is currently an Associate Professor of mechanical science and engineering with the University of Illinois at Urbana–Champaign

(UIUC) where he leads the Energy Transport Research Laboratory. He has courtesy appointments in Electrical and Computer Engineering and the Materials Research Laboratory. His group's research intersects the multidisciplinary fields of thermo-fluid science, interfacial phenomena and renewable energy. Miljkovic was a recipient of the National Science Foundation CAREER Award, the American Chemical Society Petroleum Research Fund Doctoral New Investigator Award, the Office of Naval Research Young Investigator Award, a Distinguished Visiting Fellowship from the United Kingdom Royal Academy of Engineering, a US National Academy of Sciences Arab American Frontiers Fellowship, the ASME ICNMM Young Faculty Award, the ASME Pi Tau Sigma Gold Medal, the CERL Research and Development Technical Achievement Award, and the UIUC Dean's Award for Excellence in Research. He is the associate director of the Air Conditioning and Refrigeration Center, which is an NSF-founded I/UCRC at UIUC supported by 30 industrial partners.

Mona Zebarjadi

Mona Zebarjadi is a Joint Professor of the Electrical and Computer Engineering and Materials Science and Engineering Departments at the University of Virginia, Charlottesville, where she is leading the Energy Science and Nanotechnology Laboratory (ESNL). Prior to her current appointment she was a Professor at the Mechanical Engineering Department at Rutgers University. She received her Bachelor's and Master's degree in physics from Sharif University and her PhD in electrical engineering from University of California, Santa Cruz in 2009, after which she spent three years at MIT as a postdoctoral fellow working jointly with the Electrical and Mechanical Engineering Departments. Her current research interests include electron and phonon transport in thermoelectric, thermionic and thermomagnetic materials, and devices with a focus on two-dimensional structures.

Golam Rosul

Md Golam Rosul obtained his Bachelor of Science degree in electrical and electronic engineering from the Bangladesh University of Engineering and Technology (BUET) in 2015. He joined the PhD program in electrical engineering at the University of Virginia in the fall of 2017. His current research interest is thermionic transport in two-dimensional materials.

Sabbir Akhanda

Md Sabbir Akhanda obtained BS and MS degrees in applied physics, electronics and communication engineering and in electrical and electronic engineering, respectively, from the University of Dhaka, Bangladesh, in 2013 and 2015, respectively. He is currently a PhD student with the University of Virginia, Charlottesville. His current research interest is focused on thermoelectric and thermomagnetic materials.

Shreyas Chavan

Shreyas Chavan received his Bachelor of Technology degree in mechanical engineering from the Indian Institute of Technology Bombay in 2014, and MS and PhD degrees from the University of Illinois at Urbana–Champaign in 2016 and 2019, respectively. During his PhD he worked with Nenad Miljkovic in the Energy Transport Research Laboratory. His primary research involved understanding the underlying fundamental physics of phase-change processes on structured superhydrophobic surfaces. He focused on the investigation of frosting and defrosting on superhydrophobic and biphilic surfaces.

Kalyan Boyina

Kalyan Boyina received a BS degree (Hons) in mechanical engineering from Oklahoma State University in 2014, and an MS degree from the University of Illinois, Urbana–Champaign in 2016. He is currently a doctoral student at the University of Illinois, Urbana–Champaign, where he works with Nenad Miljkovic in the Energy Transport Research Laboratory. His primary research interests include the large scale fabrication and performance characterization of anti-frosting superhydrophobic heat exchangers under a wide range of ambient conditions, optimization of superhydrophobic coating technologies, advanced defrosting techniques and brazed joint strength enhancement through surface modification.

Longnan Li

Longnan Li received a PhD degree in mechanical engineering from Sogang University, Seoul, South Korea in 2017. He was an engineer in the Haier group and Midea group before pursuing his PhD degree from 2007 to 2011. He is currently a Postdoctoral Research Associate in the Department of Mechanical Science and Engineering, University of Illinois Urbana–Champaign. His current research interests include developing durable and scalable coatings for high efficiency phase-change applications, micro/nanoscale fluid mechanics, electronics cooling and energy harvesting devices.

Qing Zhu

Qing Zhu is currently a PhD candidate in materials science and engineering at the University of Houston, TX. He received his Bachelor's degree in materials science and engineering from Northwestern Polytechnical University in China. His current research is focused on the measurement of conversion efficiency in thermoelectric materials.

Zhifeng Ren

Zhifeng Ren is the M D Anderson Chair Professor of Physics at the University of Houston, TX, and the director of the Texas Center for Superconductivity at the University of Houston (TcSUH). He received his BS degree from Xihua University in 1984, his MS degree from Huazhong University of Science and Technology in 1987, and his PhD degree from the Institute of Physics, Chinese Academy of Sciences, in 1990. He has published 510 peer-reviewed journal papers and has been awarded 55 patents. His research interests include high-performance thermoelectrics, ultrahigh thermal conductivity, amphiphilic Janus nanosheets for enhanced oil recovery, efficient catalysts for water splitting, including seawater, aligned carbon nanotubes, superconductivity, transparent flexible electrodes, etc.

Tobias Burger

Tobias Burger is a PhD candidate in chemical engineering at the University of Michigan. He received his MSE in chemical engineering from the University of Michigan and his BS in chemical engineering from the New Mexico Institute of Mining and Technology. He is working to develop thin-film PV devices for more affordable, high-performance thermophotovoltaic generators.

Caroline Sempere

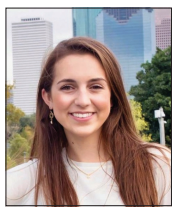

Caroline Sempere is pursuing a BSE in chemical engineering at the University of Michigan. Her research experience includes the modeling of novel self-doped semiconductors and spectral control methods for thermophotovoltaic systems.

Andrej Lenert

Andrej Lenert is an Assistant Professor in the Department of Chemical Engineering at the University of Michigan. He completed his PhD at MIT in 2014, under the supervision of Evelyn Wang. He was a postdoctoral fellow at the University of Michigan, working with the Nanoscale Transport Laboratory and the Center for Photonic and Multiscale Nanomaterials. In 2016, he was named on the Forbes 30 under 30 list in Science for his contributions to the field of thermophotovoltaic energy conversion.

Part I

Theory and Computation

IOP Publishing

Nanoscale Energy Transport
Emerging phenomena, methods and applications
Bolin Liao

Chapter 1

Hydrodynamic phonon transport: past, present and prospects

Sangyeop Lee and Xun Li

Hydrodynamic phonon transport began to be studied several decades ago to verify the quantum theory of lattice thermal transport. The recent prediction of significant hydrodynamic phonon transport in graphitic materials shows its practical importance for high thermal conductivity materials and has brought this field renewed attention. As the study of this topic had been inactive to some extent for several decades, we aim to provide a brief overview of earlier studies as well as very recent studies. The topics we discuss in this chapter include the collective motion of phonons, several approaches to solving the Peierls–Boltzmann transport equation for hydrodynamic phonon transport, the role of normal scattering for thermal resistance and the propagation of second sound. Then, we close this chapter with our perspectives for future studies and the practical implications of hydrodynamic phonon transport.

1.1 Introduction

The transport of phonons, a major heat carrier in non-metallic solids, has usually been described using the diffusive limit, since Fourier's law was suggested 200 years ago. Fourier's law has a simple form that correlates thermodynamic driving force (i.e. temperature gradient, $-\nabla T$) and the resulting heat flux (q''):

$$\frac{1}{\kappa}q'' = -\nabla T. \tag{1.1}$$

This empirical law shows that there is always a damping coefficient, $1/\kappa$, involved in transport phenomena. $1/\kappa$ is the thermal resistance which determines the extent of damping in heat flow and the resulting heat flux at a given temperature gradient. However, such a damping effect is not observed in fluid flow, although both phonons and molecules are described well by the same Boltzmann transport theory.

doi:10.1088/978-0-7503-1738-2ch1

Also, they have similar thermodynamic driving forces—molecules are driven by pressure gradient-like phonons that are driven by a temperature gradient. Assuming an infinitely large domain to exclude any effect from the boundary, the molecular flow at the macroscale can be described by Euler's equation,

$$\frac{\mathrm{D}(\rho \mathbf{u})}{\mathrm{D}t} = -\nabla p, \tag{1.2}$$

where ρ and $\mathbf{u}$ are the density and velocity of the fluid element, respectively. With the Lagrangian coordinate, equation (1.2) shows the acceleration of molecules under the pressure gradient ($-\nabla p$) without any damping effect. This is the thermodynamic limit where the entropy generation is zero.

Now, one might ask a question—why does phonon flow as described by Fourier's law exhibit a damping effect while molecular flow does not? Interestingly, Nernst speculated a century ago that heat in high thermal conductivity materials may have inertia like a fluid [1]. The different behaviors of damping in molecular and phonon flows can be associated with the difference in the scattering processes of those two particles in terms of momentum conservation. For molecular flow, the total momentum of the molecules is always conserved upon molecule–molecule scattering. Therefore, inter-molecular scattering itself cannot cease the given molecular flow. For phonon flow, however, the total momentum of phonons is not always conserved upon phonon–phonon scattering. There are two different scattering mechanisms regarding the momentum conservation: normal and Umklapp scattering (hereafter N-scattering and U-scattering, respectively), suggested by Peierls [2]. As shown in figure 1.1(a), N-scattering involves phonon states with small wavevectors and the total momentum of phonon particles is conserved ($\mathbf{q}_1 + \mathbf{q}_2 = \mathbf{q}_3$), as in the inter-molecular scattering case. However, for U-scattering, the total momentum of phonon particles is not conserved. As a result, the phonon propagation direction is reversed upon U-scattering, thus directly causing thermal resistance. Phonon scattering by impurities, as shown in figure 1.1(c), also directly causes thermal resistance as it does not conserve total momentum. Hereafter, R-scattering refers to combined U- and impurity-scattering. In most materials at room temperature, N-scattering is weak compared to R-scattering, leading to the large damping effect of heat flow in solid materials.

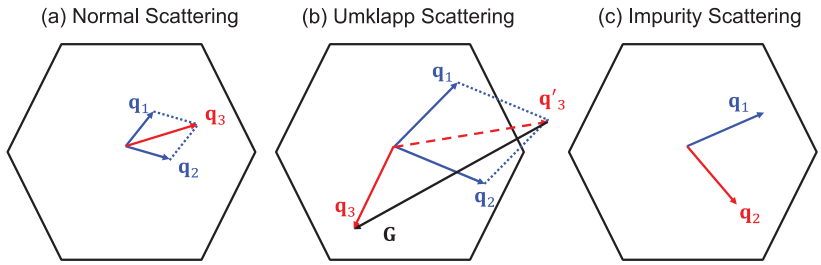

Figure 1.1. (a) Schematic of N-scattering, (b) U-scattering and (c) impurity scattering in the reciprocal space. The hexagon represents the first Brillouin zone.

We have assumed an infinitely large domain to compare the intrinsic damping of phonon flow and molecular flow. However, all solid materials have finite size, introducing phonon–boundary scattering. In most cases, the phonon–boundary scattering is diffuse boundary scattering rather than specular boundary scattering. The three types of phonon scattering (i.e. diffuse boundary scattering, N-scattering and R-scattering) influence phonon transport in different ways and thus there exist three regimes of phonon transport—the ballistic, hydrodynamic and diffusive regimes schematically shown in figure 1.2—depending on the dominant type of scattering mechanism. These three regimes occur in different ranges of temperature. The ballistic regime occurs at a low temperature where internal phonon scattering is much weaker than phonon–boundary scattering. Therefore, the phonon transport is limited by the diffuse boundary scattering and the thermal resistance is determined by the size and shape of the samples. As temperature increases, the internal phonon scattering starts to play a role in the transport process. At sufficiently low temperature, the majority of internal phonon scattering is N-scattering as phonon states with large wavevectors cannot be occupied. Because of the momentum conserving nature of N-scattering, the resulting phonon transport is similar to fluid flow and thus is called hydrodynamic phonon transport. Figure 1.2(b) shows the schematic of the heat flux profile, similar to the molecular Poiseuille flow. When temperature increases further, U-scattering becomes significant and the thermal resistance is due to the direct momentum destruction by U-scattering. As U-scattering occurs in any location, the heat flux has a spatially uniform profile as shown in figure 1.2(c).

The N- and U-scattering for phonons, since suggested by Peierls around a century ago [2], have been a foundation for the quantum theory of thermal transport in solids. Although the concept of N- and U-scattering was well accepted, the direct confirmation of N-scattering was still lacking. This led to the theoretical [4–10] and experimental efforts [11–15] for the prediction and observation of hydrodynamic phonon transport, namely, phonon Poiseuille flow and second sound, which will be discussed in more detail below. The phonon Poiseuille flow was first measured in solid He in the temperature range of 0.6–1.0 K [11]. Second sound was measured in solid ^{3}He at 0.5 K [12], in NaF at around 15 K [13, 14] and in Bi at 2 K [15]. Those experimental observations combined with the theoretical studies directly confirm the N-scattering for phonons and show remarkably different effects of N- and U-scattering on thermal transport. This was regarded as ‘one of the great triumphs of the theory of lattice vibrations’ [16].

Figure 1.2. Schematic of phonon flux profile: (a) ballistic, (b) hydrodynamic and (c) diffusive. Reproduced with permission from [3]. Copyright 2015 Macmillan Publishers Ltd.

Despite the confirmation of hydrodynamic phonon transport, the study of this topic was inactive for several decades. As can be seen from the previous measurements, hydrodynamic phonon transport was observed in very low and narrow temperature ranges and thus was considered not relevant to practical applications. The conditions for hydrodynamic phonon transport are stringent because it is rare to satisfy the conditions of weak U-scattering and strong N-scattering at the same time. The U-scattering can easily be suppressed if the temperature is much lower than the Debye temperature so as to limit the phonon population to small wavevector states. However, if the temperature is lowered, there are not enough N-scattering events and the transport easily becomes ballistic. Thus, for hydrodynamic phonon transport to be significant, a material should exhibit a high Debye temperature and large anharmonicity at the same time. This is not common; a material with a high Debye temperature such as diamond usually exhibits small anharmonicity. The quality of the sample is another issue as impurity scattering is momentum destroying scattering and weakens the hydrodynamic features. It is interesting to note that NaF was chosen for the second sound experiments [13, 14, 17] because Na and F are naturally monoisotopic elements and thus at least isotope impurities do not exist.

Hydrodynamic phonon transport has recently received renewed attention after first-principles based studies predicted significant hydrodynamic phonon transport in graphitic materials including single-wall carbon nanotubes (SWCNTs) [18], graphene [3, 19] and graphite [20]. Interestingly, those graphitic materials exhibit a high Debye temperature and large anharmonicity at the same time, leading to strong N-scattering, shown in figure 1.3, and significant hydrodynamic phonon transport [3]. The light atomic mass of carbon and strong sp^2 bonding result in the high Debye temperature and weak U-scattering. Also, the flexural phonon modes from its layered atomistic structure are largely anharmonic for small wavevector states [21], leading to strong N-scattering.

The primary objective of this chapter is to provide a brief overview of basic concepts and recent studies of hydrodynamic phonon transport for those who have previously worked on ballistic and diffusive phonon transport. Other comprehensive

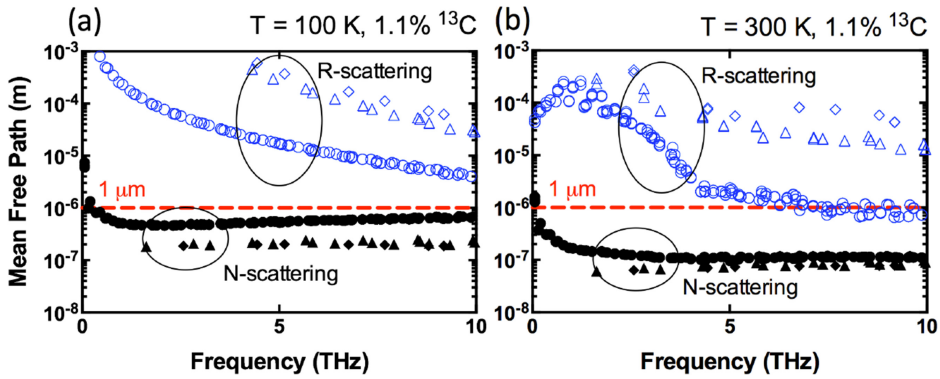

Figure 1.3. The mean free paths of N- and R-scattering in suspended graphene at 100 and 300 K from first-principles calculation.

review articles are available for advanced theoretical aspects [22, 23] and the macroscopic governing equations of the heatwave which is related to second sound [24]. This chapter is organized as follows. Section 1.2 discusses the displaced Bose–Einstein distribution as an equilibrium distribution under N-scattering and collective hydrodynamic phonon flow. Section 1.3 summarizes the methods to solve the Peierls–Boltzmann transport equation for hydrodynamic and quasi-hydrodynamic phonon transport. Section 1.4 provides our current understanding of the role of N-scattering for thermal resistance for various cases. Section 1.5 will review the theoretical and experimental studies of second sound. We then briefly discuss the future perspectives of phonon hydrodynamics in section 1.6.

We would also like to mention that the term 'hydrodynamic phonon transport' has been used in a different context in recent publications [25–31]. Those studies used phonon hydrodynamic equations that were derived assuming strong N-scattering compared to U-scattering and thus have a term similar to the viscous term of the Navier–Stokes equation [7, 8, 32]. However, to avoid any confusion, the phenomena studied in those studies are quasi-ballistic phonon transport and do not require strong N-scattering—the hydrodynamic equations were used to phenomenologically describe the quasi-ballistic transport. In this chapter, we focus on the hydrodynamic phenomena of phonon transport due to strong N-scattering and do not discuss the phenomenological hydrodynamic description of quasi-ballistic phonon transport. For the reader who is interested in the latter topic, a recent review article can provide a comprehensive summary [33].

1.2 Collective phonon flow

One unique feature of hydrodynamic transport that can be distinguished from the ballistic and diffusive regimes is the collective motion of particles. The term 'collective' is often used to describe different phenomena in solid-state physics. Here, we call the transport of particles collective when the flux of particles can be represented by a single value of velocity regardless of their quantum states. As an example, let us assume that we are able to track the movements of all molecules in a small fluid element. Assuming strong molecule–molecule scattering and small pressure gradient for the well-defined local equilibrium condition, the molecules then follow the displaced Boltzmann distribution:

$$f_{\mathrm{B}}^{\mathrm{disp}} = \left(\frac{m}{2\pi k_{\mathrm{B}} T}\right)^{3/2} \exp\left(-\frac{m\,|\mathbf{v}-\mathbf{u}|^2}{2k_{\mathrm{B}}T}\right), \tag{1.3}$$

where m, k_{B} and T represent the mass of a molecule, the Boltzmann constant and the temperature, respectively, $\mathbf{v}$ is the actual velocity of a molecule and $\mathbf{u}$ is the drift velocity. Note that the drift velocity is the same for all molecules regardless of their quantum states. Usually, the actual velocity is much larger than the drift velocity, making the movement of each molecule look random. However, the small drift velocity causes a net flow of molecules. As a result, the fluid element containing many molecules that seemingly move along random directions can move with the drift velocity as a whole. Thus, we call the molecular transport collective in this case.

Likewise, phonon particles show collective motion when the transport is hydrodynamic. The equilibrium distribution of phonons with N-scattering is the displaced Bose–Einstein distribution:

$$f^{\text{disp}} = \left[\exp\left(\frac{\hbar(\omega - \mathbf{q}\cdot\mathbf{u})}{k_{\text{B}}T}\right) - 1\right]^{-1}, \tag{1.4}$$

where $\mathbf{q}$ and $\mathbf{u}$ are the phonon wavevector and drift velocity (or displacement), respectively. In most cases where the transport is non-hydrodynamic, $\mathbf{u}$ differs for each phonon mode. However, in the hydrodynamic regime, $\mathbf{u}$ is a constant for all phonon modes. The displaced distribution function can be linearized assuming a small displacement, i.e. $\mathbf{q}\cdot\mathbf{u} \ll \omega$,

$$f^{\text{disp}} \approx f^0 + \frac{\hbar}{k_{\text{B}}T} f^0(f^0 + 1)\mathbf{q}\cdot\mathbf{u}. \tag{1.5}$$

The fact that the displaced Bose–Einstein distribution function is the equilibrium distribution upon N-scattering can be shown with Boltzmann's H-theorem [34]. For example, the rate of entropy generation upon coalescence three-phonon scattering is

$$\dot{S}_{\text{scatt}} \sim \sum_{ijk} (\phi_i + \phi_j - \phi_k)^2 P_{i,j}^k, \tag{1.6}$$

where $P_{i,j}^k$ is the equilibrium transition rate of the coalescence process where the phonon particles at states i and j are merged to state k. A similar expression can be written for the decay process. ϕ_i represents the deviation of the distribution function from the stationary Bose–Einstein distribution f_i^0 (i.e. displaced Bose–Einstein distribution with zero displacement) and is defined as $\phi_i = (f_i - f_i^0)/(f_i^0(f_i^0 + 1))$. If the three phonon states exhibit the displaced Bose–Einstein distribution,

$$\phi_i + \phi_j - \phi_k = (\mathbf{q}_i + \mathbf{q}_j - \mathbf{q}_k)\cdot\mathbf{u}. \tag{1.7}$$

Considering the momentum conservation of N-scattering, $\mathbf{q}_i + \mathbf{q}_j = \mathbf{q}_k$, the entropy generation in this case is zero, verifying that the displaced Bose–Einstein distribution is an equilibrium distribution under N-scattering. From equation (1.7), even U-scattering ($\mathbf{q}_i + \mathbf{q}_j = \mathbf{q}_k \pm \mathbf{G}_m$) does not generate any entropy if the reciprocal lattice vector $\mathbf{G}_m$ is orthogonal to $\mathbf{u}$. This was also shown through the simulation of second sound in a recent study [35].

Whether a certain scattering process is N- or U-scattering depends on the choice of the Brillouin zone, which may lead to confusion or misunderstanding about the role of N- and U-scattering on phonon transport. We would like to emphasize that the concept of momentum conservation for understanding the phonon transport is valid only when the crystal momentum is defined with the first Brillouin zone, which is the Wigner–Seitz unit cell in reciprocal space. Otherwise, the displaced distribution function in equation (1.4) is incorrect and distinguishing N- and U-scattering based on the non-Wigner–Seitz unit cell is not meaningful.

With the linearized form of the displaced distribution function in equation (1.5), it is straightforward to show that the phonon particle flux n_x'' can be described by the single value of $\mathbf{u}$:

$$n_x'' = \frac{1}{NV}\sum_i v_x f^{\text{disp}} = \left(\frac{1}{NV}\sum_i v_x \frac{\hbar}{k_B T} f^0 (f^0 + 1)\mathbf{q}\right) \cdot \mathbf{u}, \tag{1.8}$$

where N and V are the number of atoms and the volume of the unit cell, respectively. Similarly, heat flux q_x'' is

$$q_x'' = \frac{1}{NV}\sum_i \hbar\omega v_x f^{\text{disp}} = \left(\frac{1}{NV}\sum_i \hbar\omega v_x \frac{\hbar}{k_B T} f^0 (f^0 + 1)\mathbf{q}\right) \cdot \mathbf{u}. \tag{1.9}$$

It is worth noting that both particle flux and heat flux are linearly proportional to the local drift velocity $\mathbf{u}$, representing the collective motion of phonon particles. The coefficients in the parentheses are constants determined by phonon dispersion and temperature. The fact that single value $\mathbf{u}$ can describe the transport of all phonon particles is the basis for the macroscopic transport equation about $\mathbf{u}$ which will be discussed in section 1.3.

As U-scattering cannot be completely avoided, the actual phonon distribution deviates from the displaced Bose–Einstein distribution to some extent:

$$f_i \approx f_i^0 + \frac{\hbar}{k_B T} f_i^0 \left(f_i^0 + 1\right)(\mathbf{q}_i \cdot \mathbf{u} + \delta_i), \tag{1.10}$$

where δ represents the deviation from the displaced Bose–Einstein distribution. It would be interesting to see how close the actual phonon distribution is to the displaced Bose–Einstein distribution in real materials in which hydrodynamic phonon transport is expected to be significant. In figure 1.4, we show the distribution function of phonon particles along the armchair direction in graphene at 100 K from the Peierls–Boltzmann transport equation (PBE) in an infinitely large sample case, which will be discussed in section 1.3. In most cases where the transport is not hydrodynamic, δ_i in equation (1.10) is larger compared to the collective part $\mathbf{q}_i \cdot \mathbf{u}$ and thus $(f_i - f_i^0)/(f_i^0(f_i^0 + 1))$ is not linear to $q_{i,x}$. However, in graphene, $(f_i - f_i^0)/(f_i^0(f_i^0 + 1))$ is nearly linear to $q_{i,x}$ with a constant slope, representing the collective motion of phonon particles with the same displacement regardless of the phonon mode. Figure 1.5 shows the contribution of the collective motion of phonon particles to total heat flux in (20,20) SWCNTs. At low temperature below 100 K, most of the heat is carried by the collective motion of phonon particles and the contribution of collective motion gradually decreases with temperature due to U-scattering.

1.3 Peierls–Boltzmann transport equation

The phonon distribution is described by the PBE:

$$\frac{\partial f_i(t, \mathbf{x})}{\partial t} + \mathbf{v}_i \cdot \nabla f_i(t, \mathbf{x}) = \sum_j G_{ij} f_j^{\text{d}}, \tag{1.11}$$

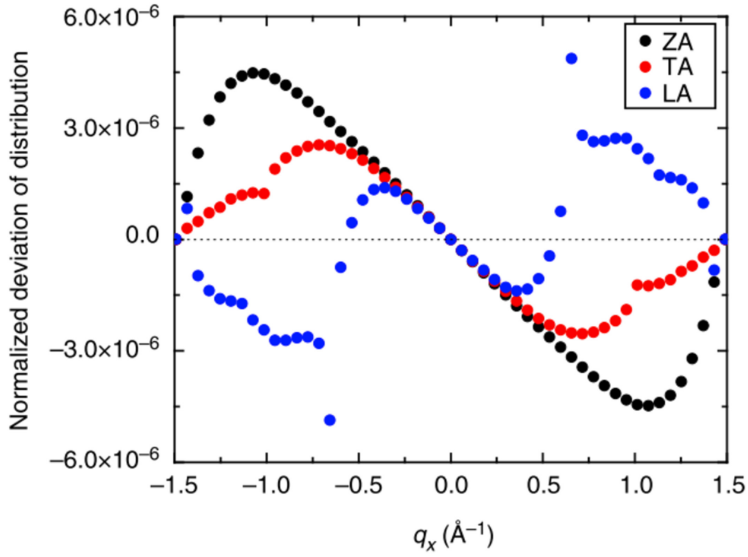

Figure 1.4. Normalized deviational distribution, $(f_i - f_i^0)/(f_i^0(f_i^0 + 1))$, in an infinitely large graphene at 100 K. Reproduced with permission from [3]. Copyright 2015 Macmillan Publishers Ltd.

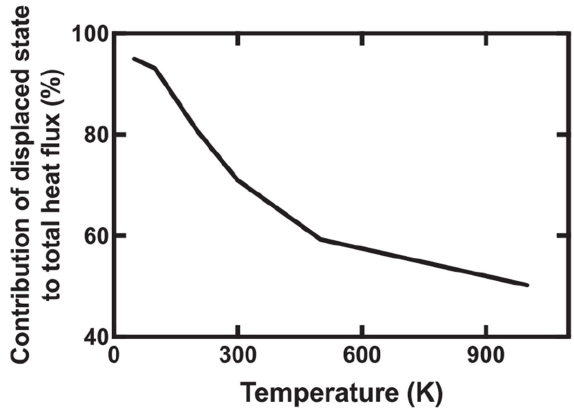

Figure 1.5. Contribution of collective motion of phonon particles to total heat flux in (20,20) SWCNT with naturally occurring ^{13}C isotope content (1.1%). Reproduced with permission from [18]. Copyright 2017 the American Physical Society.

where f_j^{d} is the deviational distribution function defined as $f_j - f_j^0$ and $\mathbf{G}$ is the scattering matrix. The original form of the PBE is known to be difficult to solve. The advection and scattering terms are in differential and integral forms and the unknown, $f_i(t, \mathbf{x})$, is a function in many dimensions including time, real space and reciprocal space domains. The equation has been often simplified assuming a steady state, a constant temperature gradient in an infinitely large sample, and very small deviation from the equilibrium distribution:

$$\mathbf{v}_i \cdot \nabla T \frac{\mathrm{d}f_i^0}{\mathrm{d}T} = \sum_j G_{ij} f_f^{\mathrm{d}}. \tag{1.12}$$

The differential advection term in equation (1.11) was replaced with the spatially homogeneous term, $\mathbf{v}_i \cdot \nabla T(\mathrm{d}f_i^0/\mathrm{d}T)$, by assuming the constant temperature gradient in an infinitely large sample. With these assumptions, the phonon distribution function is spatially homogeneous except for the change due to the temperature gradient. Then, the PBE could be simplified from the integro-differential equation to the homogeneous integral equation which is relatively easier to solve. The recently developed *ab initio* framework of lattice dynamics made it possible to calculate the scattering matrix, **G**, from first-principles [36, 37]. Also, several numerical techniques such as the full iterative method [38, 39] and the variational method [40] were developed to solve equation (1.12). Solving equation (1.12) with *ab initio* phonon dispersion and scattering matrix showed an excellent predictive power for the thermal conductivity of bulk samples [41].

For the hydrodynamic regime, however, the assumption of a spatially homogeneous distribution function is not valid. As schematically shown in figure 1.2(b), the heat flux and phonon distribution largely depend on the location in real space, and the advection term, $\mathbf{v}_i \cdot \nabla f_i$, in equation (1.11) cannot be homogeneous. Also, second sound is the temporal and spatial fluctuation of the temperature field which requires a description under an unsteady condition. Therefore, we would need to solve the PBE as an original form containing both differential and integral terms. We briefly review the past approaches used several decades ago to solve the PBE with several assumptions and also introduce recent approaches with minimal assumptions from first-principles.

One of the most challenging parts of solving the PBE is how to handle the integral scattering term. In the PBE, all phonon states are coupled to each other through the integral scattering term. Callaway suggested a simple form of scattering model from the fact that N-scattering and U-scattering tend to relax a phonon system to displaced and stationary Bose–Einstein distributions, respectively [42]. Although Callaway's scattering model was from intuition without rigorous theoretical considerations, it was later shown that the model can be formally derived by ignoring the off-diagonal terms of the N- and U-scattering matrices [43].

Early theoretical studies of phonon hydrodynamics derived macroscopic transport equations, such as the Navier–Stokes equation of fluid flow [4, 5, 7, 8, 32]. The work by Sussmann and Thellung [4] solved the PBE to the first order assuming no U-scattering and constructed momentum and energy balance equations. Some of Krumhansl group's work extended the transport equations to the case where U-scattering exists [5, 6]. The notable work by Guyer and Krumhansl [7, 8] solved the PBE in the eigenstate space of scattering operator which led to the concept of relaxon that will be discussed later. The derivation of these early studies was carefully examined and compared later by Hardy [32]. Although the details of derivation in the early studies are slightly different, they share the same basic idea. The idea is similar to how the Navier–Stokes equation is derived from the

Boltzmann transport equation with the BGK scattering model, which is analogous to the N-scattering term of Callaway's scattering model. We briefly discuss Sussmann and Thellung's derivation here.

The momentum and energy balance equations can be simply derived from the PBE by taking momentum ($\hbar\mathbf{q}$) and energy ($\hbar\boldsymbol{\omega}$) as a moment of the PBE:

$$\frac{\partial E}{\partial t} + \nabla_\alpha Q_\alpha = 0 \tag{1.13}$$

$$\frac{\partial P_\alpha}{\partial t} + \nabla_\beta p_{\alpha\beta} = 0, \tag{1.14}$$

where

$$E = \frac{1}{NV}\sum_i \hbar\omega_i f_i \tag{1.15}$$

$$Q_\alpha = \frac{1}{NV}\sum_i \hbar\omega_i v_{\alpha,i} f_i \tag{1.16}$$

$$P_\alpha = \frac{1}{NV}\sum_i \hbar q_{\alpha,i} f_i \tag{1.17}$$

$$p_{\alpha\beta} = \frac{1}{NV}\sum_i \hbar q_{\alpha,i} v_{\beta,i} f_i\,. \tag{1.18}$$

E and Q_α are the energy density and heat flux along the α-direction. P_α and $p_{\alpha\beta}$ are the α-direction momentum density and the momentum flux along the β-direction. Note that the right-hand sides of equations (1.13) and (1.14) are zero because total momentum and energy are conserved upon N-scattering. If U-scattering is considered, the momentum destroying term by U-scattering would appear in the momentum balance equation. In order to complete those momentum and energy balance equations, the phonon distribution function is required. The phonon distribution can be found by solving the PBE with the N-scattering term of Callaway's scattering model:

$$\frac{\partial f}{\partial t} + \mathbf{v}\cdot\nabla f = -\frac{f - f^{\text{disp}}}{\tau_{\text{N}}}. \tag{1.19}$$

Equation (1.19) can be further simplified if we assume $\dot{f} \approx \dot{f}^{\text{disp}}$ and $\nabla f \approx \nabla f^{\text{disp}}$. This assumption is analogous to the Chapman–Enskog expansion to the first order and is valid when N-scattering is strong [44]. To be more specific, N-scattering is considered strong when the relaxation time and mean free path of N-scattering are much smaller than the characteristic time and size of the system (e.g. the time period of temperature fluctuation for second sound and the sample size for steady-state heat flow). With such assumptions, it is straightforward to solve equation (1.19). Based

on the phonon distribution function from equation (1.19) being plugged into equations (1.13) and (1.14), the following macroscopic governing equations can be derived:

$$\dot{T}' - \frac{1}{3}v_g^2\nabla^2 T' + \frac{1}{3}\nabla\cdot\mathbf{u} = 0 \tag{1.20}$$

$$\dot{u}_\alpha + v_g^2\nabla_\alpha T' - v_g^2\tau_N\left(\frac{2}{5}\nabla_\alpha\nabla\cdot\mathbf{u} + \frac{1}{5}\nabla^2 u_\alpha\right) = 0, \tag{1.21}$$

where v_g is the group velocity. T' is the dimensionless deviational temperature defined as $(T - T_0)/T_0$, where T_0 is an equilibrium temperature.

Although early theoretical studies [4, 5, 7, 8, 32] are slightly different from the details of derivation, they are based on the same assumptions: (i) N-scattering being much stronger than U-scattering such that f is closer to f^{disp} than f^0 and (ii) N-scattering being strong enough that $\dot{f} \approx \dot{f}^{\text{disp}}$ and $\nabla f \approx \nabla f^{\text{disp}}$. Because of these assumptions, the hydrodynamic equations derived in the early studies have several limitations. The macroscopic hydrodynamic equations may not accurately describe the following cases: (i) the characteristic size of a system being comparable to the mean free path of N-scattering, namely, phonon transport somewhere between the ballistic and hydrodynamic limits, and (ii) N-scattering being not much stronger than U-scattering, namely, phonon transport somewhere between the diffusive and hydrodynamic limits. In addition, the validity of Callaway's scattering model is questionable for quantitative purposes [45, 46].

As the full scattering matrix can now be calculated from first-principles and the hydrodynamic phonon transport has gained renewed attention, there are two recently developed methods to solve the PBE with the full scattering matrix in both real and reciprocal spaces without the assumption of strong N-scattering. Both approaches provide a solution of the PBE without any significant assumptions and thus can be useful to study complex transport phenomena where features of all three regimes exist to some extent [47].

The first approach is based on the eigenstates of the scattering matrix. The scattering matrix can be symmetrized by multiplying a factor, $2\sinh(X_i/2)$, where $X_i = \hbar\omega_i/k_B T$, to equation (1.11) such that the scattering matrix has an orthogonal set of eigenstates [43]:

$$\left(2\sinh\frac{1}{2}X_i\right)\mathbf{v}_i\cdot\nabla f_i = \sum_j G_{ij}^* f_j^{d^*}, \tag{1.22}$$

where $f_j^{d^*}$ is $(2\sinh\frac{1}{2}X_j)f_j^d$ and the scattering matrix, $\mathbf{G}^*$, is

$$G_{ij}^* = \left(\frac{2\sinh\frac{1}{2}X_i}{2\sinh\frac{1}{2}X_j}\right)G_{ij}. \tag{1.23}$$

The orthogonal eigenstates of $\mathbf{G}^*$ were later called relaxons [48]. The solution of the PBE, $f^{\mathrm{d}*}$, can then be expressed as a linear combination of relaxons and the equation for the coefficient (population) of each relaxon state can be derived from the PBE [48]. An advantage of the relaxon framework is that the relaxon has now a well-defined relaxation length and thus the thermal transport can be described with a simple kinetic description of relaxon particles. Phonons, if they experience strong N-scattering, do not have a well-defined relaxation length due to the complex interplay between N- and U-scattering processes and also its collective nature of motions.

The second approach employs the Monte Carlo (MC) method to solve the PBE with the full scattering matrix [49, 50]. The MC method was previously developed to solve the PBE with the single-mode relaxation time approximation (SMRT) for studying quasi-ballistic phonon transport [51–53]. The MC method with the SMRT stochastically determines the occurrence of scattering based on the probability of scattering. With the full scattering matrix, the MC method stochastically determines whether a certain scattering process occurs or not and the final state of phonon particles if the scattering is determined to occur. The energy-based PBE is chosen over the regular PBE due to its advantage of strict energy conservation:

$$\mathbf{v}_i \cdot \nabla(\omega_i f)_i = \sum_j B_{ij}\left(\omega_i f_j^{\mathrm{d}}\right), \tag{1.24}$$

where B_{ij} is the scattering matrix of the energy-based PBE, defined as $(\omega_i/\omega_j)G_{ij}$. The energy exchange upon scattering is described as

$$\omega_i f_i^{\mathrm{d}}(t + \Delta t) = \sum_j Z_{ij}(\Delta t)\omega_j f_j^{\mathrm{d}}(t), \tag{1.25}$$

where the energy propagator matrix $\mathbf{Z}$ can be found as

$$\mathbf{Z}(\Delta t) = \mathrm{e}^{\mathbf{B}\Delta t}. \tag{1.26}$$

If the off-diagonal terms of matrix $\mathbf{B}$ are ignored and only diagonal terms are considered, equation (1.25) is recovered to the exponential decay of energy which is equivalent to the SMRT:

$$\omega_i f_i^{\mathrm{d}}(t + \Delta t) = \exp(B_{ii}\Delta t)\omega_i f_i^{\mathrm{d}}(t). \tag{1.27}$$

Note B_{ii} is the same as $-\tau_i^{-1}$ from equation (1.24). The scattering in equation (1.25) describes the transfer of energy from phonon state j to i. In an MC simulation, the destination state i can be stochastically determined and its detailed MC algorithm can be found in the literature [49, 50].

1.4 Steady-state phonon hydrodynamics

The N-scattering itself does not directly cause thermal resistance because of its momentum conserving nature. However, the N-scattering can affect thermal resistance when combined with momentum destroying scattering (R-scattering or diffuse boundary scattering) or thermal reservoirs that emit phonons for which the

distribution deviates from the displaced Bose–Einstein distribution. These situations are common in practical systems. We discuss the role of N-scattering for thermal resistance in three different cases: (i) an infinitely large sample, (ii) a sample with an infinite length but a finite width where diffuse boundary scattering destroys the phonon momentum along the flow direction and (iii) a sample with an infinite width but a finite length contacting hot and cold reservoirs that emit phonons with the stationary Bose–Einstein distribution.

1.4.1 Infinitely large sample

It is well known that the thermal conductivity is infinitely large when the N-scattering is the only scattering mechanism and the sample is infinitely large. Assuming that a local temperature gradient is applied and phonon flow is initiated, the phonons subsequently establish the displaced Bose–Einstein distribution through many N-scattering events. Then, the N-scattering does not further alter the displaced Bose–Einstein distribution and the phonons can continue to flow even without any temperature gradient, resulting in the infinite thermal conductivity. This leads to the simple statement that N-scattering itself does not cause thermal resistance. This simple statement, however, is true only when the distribution function is homogeneous in space as in the infinitely large sample. If there is a significant spatial variation of the distribution function, the N-scattering can cause thermal resistance. This will be discussed in section 1.4.3.

Even when the distribution function is homogeneous in space, N-scattering contributes to thermal resistance if U-scattering also exists. In general, phonon states with a small wavevector have very weak U-scattering. However, the small wavevector phonons can be scattered into larger wavevector states through N-scattering and then can be seen by U-scattering. A recent study on the thermal transport in SWCNTs [54] quantitatively shows the effect of N-scattering on thermal conductivity. The thermal conductivity of (10,10) SWCNT is 10 000 W m^{-1} K^{-1} when only U-scattering is considered, but it is significantly reduced to 2000 W m^{-1} K^{-1} when both N- and U-scattering processes are included.

1.4.2 Sample with an infinite length and a finite width

We consider a sample with an infinite length and a finite width to discuss the thermal resistance when N-scattering is combined with diffuse boundary scattering. As shown in figure 1.6, we consider a constant temperature gradient along the length direction, which drives the phonon flow.

The major mechanisms of thermal resistance in the diffusive and ballistic regimes are U-scattering and diffuse boundary scattering, respectively. In the hydrodynamic regime, we have a different mechanism for thermal resistance—the viscous damping effect which is a result of combined N- and diffuse boundary scattering. The drift velocity near boundaries is smaller than that in the middle of a sample due to diffuse boundary scattering. Thus, the drift velocity exhibits a gradient along the transverse direction (the y-direction in figure 1.6). Due to the drift velocity gradient, phonon momentum is transferred from the middle of the sample to the boundaries through

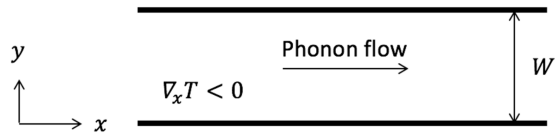

Figure 1.6. Schematic of phonon flow in an infinitely long sample with a finite width.

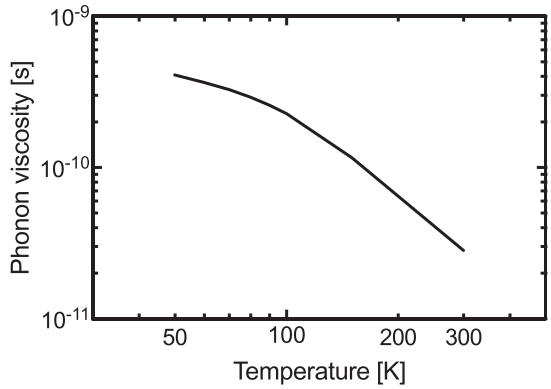

Figure 1.7. Temperature dependence of the phonon hydrodynamic viscosity of suspended graphene calculated with phonon dispersion and scattering rates from first-principles calculation. Reproduced with permission from [50]. Copyright 2018 the American Physical Society.

N-scattering processes and then finally is destroyed by the diffuse boundary scattering. The viscous damping term can be seen in the second-order derivative term in equation (1.21).

Based on the momentum balance equation from the PBE with its first-order solution discussed in section 1.3, an expression for the phonon hydrodynamic viscosity (μ_{ph}) can be derived [50]:

$$\mu_{\mathrm{ph}} = \frac{\sum_i q_x^2 v_{y,i}^2 f_i^0 \left(f_i^0 + 1\right) \tau_{\mathrm{N},i}}{\sum_i q_x v_{x,i} f_i^0 \left(f_i^0 + 1\right) \omega_i}. \tag{1.28}$$

A notable difference between the ballistic and hydrodynamic regimes is that the momentum transfer to the boundary in the hydrodynamic regime is impeded by N-scattering. As the N-scattering rate is increased, the rate of momentum transfer to the boundary, which determines the extent of viscous damping, is decreased. This can be seen in the phonon hydrodynamic viscosity as a function of temperature in figure 1.7. As temperature increases, the N-scattering rate is increased, resulting in the lower hydrodynamic phonon viscosity. The extent of viscous damping also depends on the width of the sample as indicated in the second-order derivative term in equation (1.21). The rate of momentum transfer in the hydrodynamic regime is proportional to $1/W^2$, where W is the width of a sample, while the rate in the ballistic regime is proportional to $1/W$.

The viscous damping effect of the hydrodynamic regime causes peculiar dependences of thermal conductivity on temperature and sample width, which are distinguished from the ballistic and diffusive cases. In the ballistic regime, the thermal conductivity is linearly proportional to the sample width. The thermal conductivity of the diffusive regime is constant regardless of sample width. However, the thermal conductivity of the hydrodynamic regime superlinearly increases with the sample width due to the viscous damping that decreases as W^2. In addition, the thermal conductivity of the hydrodynamic regime increases with temperature much faster than that of the ballistic regime as the viscous damping is weakened as temperature increases. The peculiar dependence of thermal conductivity on temperature was observed in solid He at a low temperature, verifying the existence of phonon Poiseuille flow [11]. Recently, these dependences have been predicted at a much higher temperature in graphene [3, 50, 55] and graphite [20], and experimentally observed in $SrTiO_3$ [56].

The peculiar dependences of thermal conductivity on temperature and sample width can be observed only when the actual transport phenomena are close to those in the ideal hydrodynamic regime without U-scattering. The thermal transport in graphitic materials at an intermediate temperature of above 100 K can exhibit all three different mechanisms of thermal resistance: U-scattering, direct diffuse boundary scattering, combined diffuse boundary and N-scattering. The significance of each mechanism can be evaluated using the momentum balance. The temperature gradient in figure 1.6 drives phonon flow and generates excess phonon momentum ($\Phi_{\nabla T}$). This momentum is balanced by momentum destructions by three different mechanisms: diffuse boundary scattering without internal phonon scattering (i.e. ballistic effect, Φ_B), diffuse boundary scattering combined with N-scattering (i.e. viscous damping or hydrodynamic effect, Φ_H) and direct momentum destruction by U-scattering (i.e. diffusive effect, Φ_D). The momentum balance can be expressed as

$$\Phi_{\nabla T} = \Phi_B + \Phi_H + \Phi_D. \tag{1.29}$$

Figure 1.8(a) shows that the thermal conductivity of an infinitely long graphene has a temperature dependence of $T^{2.03}$ when the temperature is below 90 K, much larger than that of the ballistic case $T^{1.68}$. This temperature range agrees with the momentum balance analysis of the same sample, as shown in figure 1.8(b). It is clear that below 90 K, Φ_H is the major mechanism of the momentum destruction, indicating that viscous damping is significant at this condition [47].

1.4.3 Sample with an infinite width and a finite length contacting hot and cold reservoirs

When an infinitely wide sample contacts hot and cold reservoirs, as in figure 1.9, the phonons emitted from the reservoirs do not follow the displaced Bose–Einstein distribution. They follow a Bose–Einstein distribution distorted by a spectral transmission function at the interface between the sample and the reservoir. The N-scattering processes change this non-displaced Bose–Einstein distribution (i.e. non-collective) to the displaced Bose–Einstein distribution (i.e. collective).

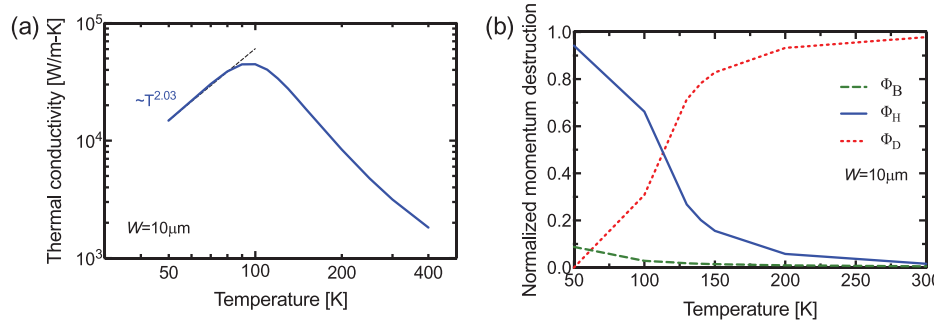

Figure 1.8. Temperature dependence of (a) thermal conductivity and (b) the momentum balance in an infinitely long graphene sample with the width of 10 μm from the MC solution of the PBE with the *ab initio* full three-phonon scattering matrix.

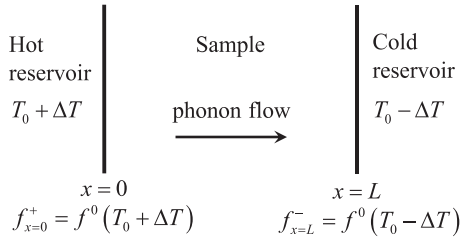

Figure 1.9. Schematic of sample geometry contacting hot and cold reservoirs.

As entropy is always generated when the distribution function is changed by scattering processes, as shown in equation (1.6), N-scattering causes thermal resistance near the interface between the sample and the reservoir where the emitted phonon flow becomes collective. The region where the thermal resistance occurs is within the order of the mean free path of N-scattering from the boundary. Figure 1.10 shows the formation of collective phonon flow at the cost of a temperature drop near the boundaries, resulting in the thermal resistance by N-scattering. Assuming N-scattering is the only scattering mechanism, the N-scattering far from the boundaries does not cause any temperature drop as the distribution function is already the displaced Bose–Einstein distribution.

The thermal resistance due to the transition between non-collective and collective phonon flows depends on materials. Figure 1.11 compares three-dimensional Debye phonon dispersion and graphite in terms of the reduction of phonon heat flux by N-scattering from the purely ballistic case. For the 3D Debye case, the reduction of heat flux is relatively small; the heat flux reduction by N-scattering is only around 5% for all three temperatures, 100, 200 and 300 K. However, for graphite, the reduction of heat flux is substantial; the heat flux is reduced by 20%, 30% and 40% at 100, 200 and 300 K, respectively. Other graphitic materials such as SWCNTs and graphene show a similar reduction of heat flux.

The large thermal resistance by N-scattering for graphitic materials can be explained with their nonlinear phonon dispersion with many phonon branches.

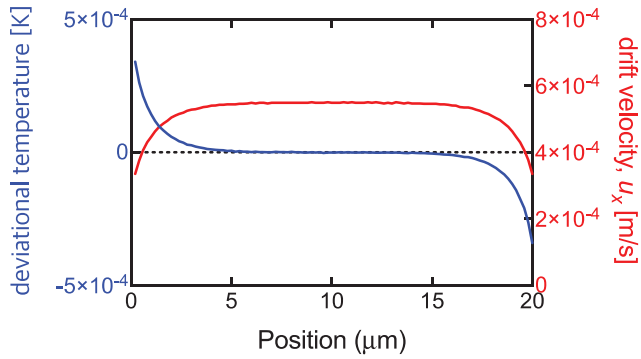

Figure 1.10. The profile of deviational temperature, defined as the difference between local temperature and global equilibrium temperature, and the drift velocity. The sample is (20,20) SWCNT contacting hot and cold reservoirs that have the deviational temperature of 0.001 and −0.001 K, respectively. The profile is calculated by the MC method of the PBE assuming Callaway's scattering model. The rate of N-scattering is assumed to be 10^{10} s^{-1} and U-scattering is ignored. Reprinted with permission from [57]. Copyright 2019 Taylor and Francis.

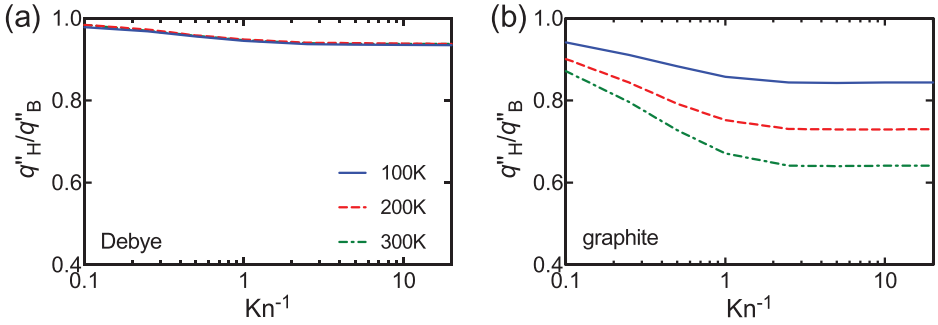

Figure 1.11. The ratio between heat flux with N-scattering (q''_H) and without any internal scattering (q''_B) as a function of inverse Knudsen number in (a) three-dimensional Debye model and (b) graphite. The heat flux is calculated with the MC solution of the PBE with Callaway's scattering model. The rate of N-scattering is assumed to be 10^{10} s^{-1} and U-scattering is ignored. Reproduced with permission from [57]. Copyright 2019 Taylor and Francis.

The rate of entropy generation due to scattering, equation (1.6), can be written as follows, assuming Callaway's scattering model and the stationary Bose–Einstein distribution for phonons emitted from the reservoirs:

$$\dot{S}_{\text{scatt}} = \left(\frac{\Delta T}{T}\right)^2 \frac{\hbar^2}{\tau_N k_B T^2 N V} \sum_i f_i^0 \left(f_i^0 + 1\right) \omega_i |q_{x,i}| \left(v_{x,i}^* - u_x'\right), \tag{1.30}$$

where $v_{x,i}^*$ is $\omega_i/|q_{x,i}|$ and u_x' is the drift velocity per temperature difference and can be found from the momentum conservation:

$$u_x' = \frac{\sum_i |q_{x,i}| \omega_i f_i^0 \left(f_i^0 + 1\right)}{\sum_i q_{x,i}^2 f_i^0 \left(f_i^0 + 1\right)}. \tag{1.31}$$

Equation (1.30) shows that the temperature difference of two reservoirs drives the phonon flow with the displacement of $v_{x,i}^*$ which may vary depending on phonon modes while the drift velocity u_x' is the same for all phonon modes. If $v_{x,i}^*$ is a constant for all phonon modes (e.g. one-dimensional Debye phonon dispersion), $v_{x,i}^*$ is the same as u_x' by equation (1.31) and the entropy generation would be zero. However, if $v_{x,i}^*$ significantly varies with phonon states, the entropy generation is expected to be large. For the three-dimensional Debye model, $v_{x,i}^*$ varies with the direction of phonon wavevector and thus causes small thermal resistance, as can be seen in figure 1.11(a). The ratio $q_{\mathrm{H}}''/q_{\mathrm{B}}''$ in this case does not change with temperature as the variance of $v_{x,i}^*$ is associated with the direction of phonon wavevector only. For graphitic materials, however, the variance of $v_{x,i}^*$ is significant compared to the Debye model as a result of non-linear dispersion with many branches, resulting in the large thermal resistance that depends on temperature in figure 1.11(b). This indicates that the resistance due to the transition between non-collective and collective phonon flows is determined by the shape of phonon dispersion.

1.5 Unsteady phonon hydrodynamics (second sound)

The fundamental difference between N- and U-scattering in terms of momentum conservation leads to a different response upon temporal perturbation to a phonon system. One simple form of the perturbation is a heat pulse being applied to one end of a sample, as shown in figure 1.12. The heat pulse causes the increased local phonon density and the response of the phonon system is largely different depending on the transport regime. For the diffusive regime, the energy balance equation with Fourier's law indicates that the peak position of the heat pulse cannot move forward and remains at its original location. Then, the thermal energy of the heat pulse diffuses into the sample and finally the sample reaches an equilibrium with a slightly elevated temperature for the entire region. For the ballistic regime, the heat pulse can propagate through the sample as there is no phonon scattering. However, the shape of the heat pulse can spread out in space unless all phonon modes have the same group velocity along the heat-pulse propagation direction. This is expected to be particularly significant in graphitic materials where flexural phonon modes with a quadratic dispersion are important for thermal energy transport. For the hydrodynamic regime, the heat pulse leads to the local fluctuation of the temperature field which can propagate as a wave through the sample. An analogous

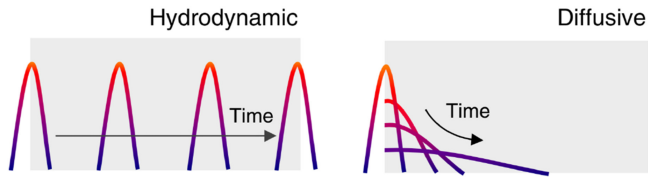

Figure 1.12. Propagation of a heat pulse in the diffusive and hydrodynamic regimes. Reproduced with permission from [3]. Copyright 2015 Macmillan Publishers Ltd.

phenomenon in the fluid system is the propagation of a pressure pulse in space, which is an acoustic sound. From the similarity of the two phenomena, the temperature pulse propagation in the form of a wave in the hydrodynamic regime is called second sound.

The second sound was first studied with superfluid He II in which the phonon is an elemental excitation of the system. The speed of second sound in liquid He was predicted by Landau using the two-fluid theory of rotons and phonons [58] and later confirmed by an experiment [59]. The predicted temperature wave was named second sound by Landau in order to distinguish it from the first sound, which is ordinary acoustic sound (i.e. pressure wave propagation). Later, it was shown that the same speed of second sound can be directly derived by using the phonon gas model without rotons [60, 61], which motivated the study of second sound in crystalline solids.

The second sound in solids can be observed with two different methods: a heat-pulse experiment [12–15, 62] and a light scattering method [10, 63–68]. In the heat pulse experiment, a heat pulse was applied to one end of a few millimeter long samples and the temperature to the opposite end was recorded as a function of time. At sufficiently low temperature such that internal phonon–phonon scattering is negligibly weak, two peaks of temperature pulse were observed, each of which represents the ballistic transport of transverse and longitudinal phonons. No significant dispersion of the temperature peak was observed because three-dimensional bulk materials where long wavelength phonons have a linear dispersion relation were used. With slightly increased temperature (around 15 K for NaF [14]), another peak in addition to those two peaks was observed. The delay time of the new peak agrees well with the predicted speed of second sound and the third peak was considered second sound. As temperature is further increased, the third peak disappears, indicating that U-scattering becomes significant. The light scattering method measures the inelastic light scattering by a local change of dielectric constants due to the second sound wave. A challenge lies in very weak coupling between light and thermal fluctuation at low temperatures. To solve this problem, a relatively strong thermal fluctuation field was induced by an optical grating method and the second sound in NaF was successfully measured [66]. The measured speed of second sound agrees well with that from the previous heat pulse experiments. Later, the light scattering measurements were carried out without inducing a thermal fluctuation field for $SrTiO_3$. $SrTiO_3$ has soft transverse optical phonons with small wavevector that are strongly anharmonic and thus cause strong N-scattering [67, 68]. The measured spectrum at around 30 K exhibits a doublet with a frequency shift (~20 GHz) that is comparable to the expected frequency of second sound in this temperature range.

As the conditions for the clear observation of second sound are narrow in the variable space, second sound measurements critically require *a priori* knowledge of the wavelength and frequency of the second sound as well as the speed of the second sound. The wavelength and frequency of second sound are determined by the mean free path and scattering rate of N- and U-scattering processes. If the pulse duration is much longer than the rate of U-scattering, the pulse can be destroyed by the

U-scattering and thus cannot propagate as a second sound. If the pulse duration is much shorter than the rate of N-scattering, phonons will travel with their own group velocity and do not have a chance to establish collective motion because of the lack of N-scattering. In this case, the pulse also cannot maintain its original shape and the thermal energy smears out.

The speed, frequency and wavelength of second sound were theoretically studied by calculating the dispersion relation of second sound. The speed of second sound was derived for the simplest case where Debye phonon dispersion is assumed and there is no U-scattering, giving the well-known relation for the speed of second sound, $v_{II} = v_g/\sqrt{3}$, where v_{II} is the speed of second sound [60, 61]. The speed of second sound was also derived for more realistic phonon dispersion consisting of one longitudinal and two degenerate transverse acoustic branches, all having Debye-type dispersion [4]. Later, theoretical studies considered the possible mechanisms for the attenuation of second sound and predicted the possible second sound frequency ranges [5–7]. In the literature, two different types of second sound called drifting and driftless second sounds were discussed [22, 69]. The driftless second sound differs from the second sound we discuss and does not require strong N-scattering; it occurs when all eigenstates of scattering operator have a similar relaxation time such that collective-looking thermal transport can occur. To our best knowledge, there was no experimental observation of the driftless second sound.

The dispersion relation of second sound can be derived from the momentum and energy balance equations in equations (1.13) and (1.14). If U-scattering is considered, the momentum destruction by U-scattering needs to be added to the right-hand side of equation (1.14). An example dispersion relation of second sound in (20,20) SWCNT is shown in figure 1.13(a). The real and imaginary frequencies represent the propagation and attenuation of a pulse, respectively. The imaginary frequency in the limit of a small wavevector (i.e. long wavelength) is mostly determined by the rate of U-scattering. As the wavevector is increased (i.e. wavelength becomes shorter), the viscous damping effect by N-scattering becomes strong, causing the significant attenuation of second sound. Figure 1.13(b) shows the required length of a sample.

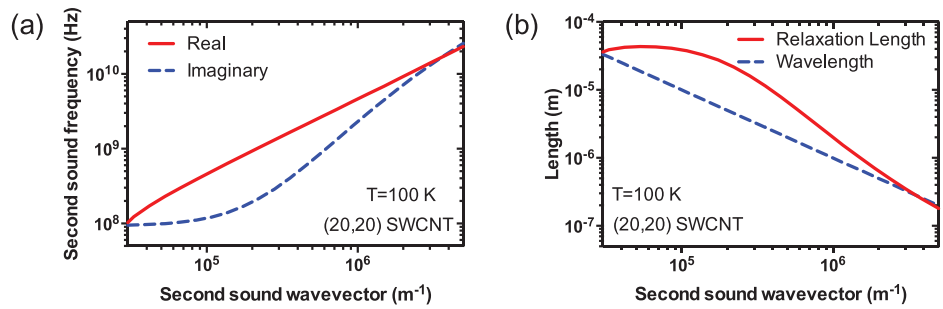

Figure 1.13. The propagation and attenuation of second sound in (20,20) SWCNT. (a) The dispersion relation of second sound showing propagation (real) and attenuation (imaginary) of second sound. (b) The comparison between relaxation length and wavelength of second sound. Reproduced with permission from [18]. Copyright 2017 the American Physical Society.

For the second sound to propagate, the sample length should be larger than the wavelength of the second sound but smaller than its relaxation length defined as $v_{II}\mathrm{Im}(\Omega)$, where v_{II} and $\mathrm{Im}(\Omega)$ are the speed of the second sound and the imaginary part of the second sound frequency, respectively.

1.6 Summary and future perspectives

In this chapter, we briefly reviewed past and recent studies on hydrodynamic phonon transport. We first discussed the displaced Bose–Einstein distribution representing the collective motion of phonon particles as an equilibrium state under N-scattering. Then, we introduced several approaches to solve the Peierls–Boltzmann transport equation for the case where N-scattering is significant. Based on the solution of the Peierls–Boltzmann transport equation, we then showed how N-scattering affects thermal phonon transport in both the steady-state and transient cases. For the steady-state cases, we discuss three scenarios: when N-scattering is combined with (i) U-scattering, (ii) diffuse boundary scattering and (iii) thermal reservoirs that emit phonons following non-displaced Bose–Einstein distribution functions. In all cases, N-scattering affects thermal transport indirectly. For the first case where N-scattering is combined with U-scattering, it transfers energy from small wavevector states where U-scattering is relatively weak to large wavevector states where U-scattering is strong, thereby contributing to thermal resistance. For the second case, the N-scattering impedes the momentum transfer to the boundaries which act as a momentum sink by diffuse boundary scattering. We discussed that stronger N-scattering leads to a lesser viscous damping effect and larger thermal conductivity. For the last case, the N-scattering itself causes thermal resistance when the distribution function is not homogeneous in space due to thermal reservoirs emitting phonons with a non-displaced distribution. The thermal resistance occurs while those non-collective phonon flows become collective through N-scattering processes. The thermal resistance by the transition between collective and non-collective phonon flows depends on the shape of phonon dispersion; while the thermal resistance due to this effect is small for Debye phonon dispersion, it can be significant in graphitic materials because of their highly nonlinear phonon dispersion with many branches. The second sound was discussed as a representative phenomenon of phonon hydrodynamics in the transient case. The N-scattering causes the damping of second sound even without U-scattering. If the fluctuation of the temperature field is fast in the time and space domains, for example, the frequency and wavelength of second sound are shorter than the rate and mean free path of N-scattering, respectively, the fluctuation can be largely damped. Thus, the N-scattering imposes the limit of frequency and wavelength of second sound for its propagation.

Although the recently developed *ab initio* framework for phonon transport has been proved for its high accuracy and predictive power [41], the significant hydrodynamic phonon transport in graphitic materials needs to be experimentally confirmed. The significant contributions from the flexural phonon modes to thermal transport were experimentally shown in [70], but its strong N-scattering due to

extremely large anharmonicity for small wavevector states has not been verified. The explicit observation of hydrodynamic phonon transport has several challenges. First, the measurements need to be done in a much smaller length and time scale compared to the previous studies performed several decades ago. The characteristic length and time scale of hydrodynamic phonon transport scales with the mean free paths and rate of internal phonon scattering. As those previous studies measured the hydrodynamic phonon transport at extremely low temperatures below 15 K, the internal phonon scattering was weak; therefore, the Poiseuille flow was measured with a several millimeter sized sample [11] and the second sound propagation was measured with a time scale of microseconds [14]. However, as the hydrodynamic phonon transport in graphitic materials is expected to occur at a much higher temperature, the internal phonon scattering is accordingly strong. Thus, the experiments need to be performed with sub-millimeter sized samples and nanosecond temporal resolution. Recent advancements on the microscale platform for the measurement of thermal conductivity [71, 72] as well as the ultrafast spectroscopy technique [73–75] are perhaps well suited for the measurement of hydrodynamic phonon transport in graphitic materials. Second, we would need a large sample with minimal defects. The *ab initio* simulation shows that the sample size should be at least 10 μm for measuring phonon Poiseuille flow and second sound at 100 K [50], but typical graphitic material samples with this sample size contain many defects. Interestingly, the observation of second sound was reported very recently using a highly oriented pyrolytic graphite (HOPG) sample [76]. This study used the transient grating method to generate the standing wave of second sound and could measure the fluctuation of temperature which is associated with the second sound. As the second sound is in standing-wave form in this study, it does not need to propagate throughout the entire sample and could be measured with less significant damping. The observation of phonon Poiseuille flow is expected to be more challenging compared to the second sound case. The theoretical prediction of phonon Poiseuille flow assumed infinitely long samples for the condition of fully developed phonon flow [50]. If a sample has a finite length, there would be the so-called entrance effect which is due to the transition from spatially uniform phonon flow to parabolic phonon flow near the entrance. This would require a sample with the length being much larger than the width. In the previous study, the phonon Poiseuille flow was predicted with the width of 10 μm, thus the length should be much longer than this value.

The recent prediction of significant hydrodynamic phonon transport indicates that the hydrodynamic regime is practically important for high thermal conductivity materials where N-scattering is often strong and cannot be ignored. Although the clear observation of hydrodynamic phonon transport is expected at sub-room temperatures, the hydrodynamic phonon transport is still important for understanding the thermal transport. As shown in figure 1.3, the mean free path of N-scattering and U-scattering has a large gap in the length ranges from sub-micrometer to micrometer for 300 K. If the sample size lies in this gap which is common in the practical applications of high thermal conductivity materials for thermal management, the diffusive–ballistic phonon transport may not correctly

describe the thermal transport phenomena; it ignores the thermal resistance due to the momentum transfer and the formation of collective phonon flow by N-scattering. Therefore, the hydrodynamic regime needs to be considered another limit of thermal transport in addition to the ballistic and diffusive limits which were extensively studied in the past [77, 78]. The detailed mechanisms of how N-scattering contributes to thermal resistance when combined with other scattering processes has not been rigorously discussed in the past. We think this is partly because of the lack of available numerical tools; it has been very challenging to solve the Peierls–Boltzmann transport equation in both real and reciprocal spaces with minimal assumptions. With the recently developed *ab initio* frameworks for solving the Peierls–Boltzmann transport equation in both real and reciprocal spaces [48, 50], it is now possible to quantitatively study the influence of N-scattering on the overall thermal transport process when it is combined with other scattering processes. This would complete the understanding of phonon transport in high thermal conductivity materials and lead to the better design of thermal devices using those high thermal conductivity materials.

Acknowledgments

We acknowledge support from the National Science Foundation (Award Nos 1705756 and 1709307).

References

[1] Nernst W 1917 *Die Theoretischen Grundlagen des Neuen Wärmesatzes* (Halle: Knapp)
[2] Peierls R 1929 Zur kinetischen Theorie der Wärmeleitung in Kristallen *Ann. Phys.* **395** 1055–101
[3] Lee S, Broido D, Esfarjani K and Chen G 2015 Hydrodynamic phonon transport in suspended graphene *Nat. Commun.* **6** 6290
[4] Sussmann J A and Thellung A 1963 Thermal conductivity of perfect dielectric crystals in the absence of Umklapp processes *Proc. Phys. Soc.* **81** 1122
[5] Prohofsky E W and Krumhansl J A 1964 Second-sound propagation in dielectric solids *Phys. Rev.* **133** A1403–10
[6] Guyer R A and Krumhansl J A 1964 Dispersion relation for second sound in solids *Phys. Rev.* **133** A1411–7
[7] Guyer R A and Krumhansl J A 1966 Thermal conductivity, second sound, and phonon hydrodynamic phenomena in nonmetallic crystals *Phys. Rev.* **148** 778–88
[8] Guyer R A and Krumhansl J A 1966 Solution of the linearized phonon Boltzmann equation *Phys. Rev.* **148** 766–78
[9] Gurzhi R 1964 Thermal conductivity of dielectrics and ferrodielectrics at low temperatures *J. Exp. Theor. Phys.* **46** 719–24
[10] Griffin A 1965 On the detection of second sound in crystals by light scattering *Phys. Lett.* **17** 208–10
[11] Mezhov-Deglin L 1965 Measurement of the thermal conductivity of crystalline He^4 *J. Exp. Theor. Phys.* **49** 66–79
[12] Ackerman C C and Overton W C 1969 Second sound in solid helium-3 *Phys. Rev. Lett.* **22** 764–6
[13] McNelly T F *et al* 1970 Heat pulses in NaF: onset of second sound *Phys. Rev. Lett.* **24** 100–2

[14] Jackson H E, Walker C T and McNelly T F 1970 Second sound in NaF *Phys. Rev. Lett.* **25** 26–8
[15] Narayanamurti V and Dynes R C 1972 Observation of second sound in bismuth *Phys. Rev. Lett.* **28** 1461–65
[16] Ashcroft N and Mermin N 1976 *Solid State Physics* (Philadelphia, PA: Saunders)
[17] Jackson H E and Walker C T 1971 Thermal conductivity, second sound, and phonon–phonon interactions in NaF *Phys. Rev.* B **3** 1428–39
[18] Lee S and Lindsay L 2017 Hydrodynamic phonon drift and second sound in a (20,20) single-wall carbon nanotube *Phys. Rev.* B **95** 184304
[19] Cepellotti A, Fugallo G, Paulatto L, Lazzeri M, Mauri F and Marzari N 2015 Phonon hydrodynamics in two-dimensional materials *Nat. Commun.* **6** 6400
[20] Ding Z, Zhou J, Song B, Chiloyan V, Li M, Liu T-H and Chen G 2018 Phonon hydrodynamic heat conduction and Knudsen minimum in graphite *Nano Lett.* **18** 638–49
[21] Schelling P K and Keblinski P 2003 Thermal expansion of carbon structures *Phys. Rev.* B **68** 035425
[22] Beck H, Meier P F and Thellung A 1974 Phonon hydrodynamics in solids *Phys. Status Solidi* a **24** 11–63
[23] Gurevich V L v 1986 *Transport in Phonon Systems Modern Problems in Condensed Matter Sciences* (Amsterdam: Elsevier)
[24] Joseph D D and Preziosi L 1989 Heat waves *Rev. Mod. Phys.* **61** 41–73
[25] Alvarez F X, Jou D and Sellitto A 2009 Phonon hydrodynamics and phonon–boundary scattering in nanosystems *J. Appl. Phys.* **105** 014317
[26] Ziabari A *et al* 2018 Full-field thermal imaging of quasiballistic crosstalk reduction in nanoscale devices *Nat. Commun.* **9** 255
[27] Torres P *et al* 2018 Emergence of hydrodynamic heat transport in semiconductors at the nanoscale *Phys. Rev. Mater.* **2** 076001
[28] Guo Y and Wang M 2018 Phonon hydrodynamics for nanoscale heat transport at ordinary temperatures *Phys. Rev.* B **97** 035421
[29] Dong Y, Cao B-Y and Guo Z-Y 2011 Generalized heat conduction laws based on thermomass theory and phonon hydrodynamics *J. Appl. Phys.* **110** 063504
[30] Cimmelli V A, Sellitto A and Jou D 2010 Nonlinear evolution and stability of the heat flow in nanosystems: beyond linear phonon hydrodynamics *Phys. Rev.* B **82** 184302
[31] Sellitto A, Alvarez F X and Jou D 2010 Temperature dependence of boundary conditions in phonon hydrodynamics of smooth and rough nanowires *J. Appl. Phys.* **107** 114312
[32] Hardy R J and Albers D L 1974 Hydrodynamic approximation to the phonon Boltzmann equation *Phys. Rev.* B **10** 3546–51
[33] Guo Y and Wang M 2015 Phonon hydrodynamics and its applications in nanoscale heat transport *Phys. Rep.* **595** 1–44
[34] Ziman J M 1960 *Electrons and Phonons: The Theory of Transport Phenomena in Solids* (Oxford: Oxford University Press)
[35] Ding Z, Zhou J, Song B, Li M, Liu T-H and Chen G 2018 Umklapp scattering is not necessarily resistive *Phys. Rev.* B **98** 180302
[36] Broido D A, Malorny M, Birner G, Mingo N and Stewart D A 2007 Intrinsic lattice thermal conductivity of semiconductors from first principles *Appl. Phys. Lett.* **91** 231922
[37] Esfarjani K, Chen G and Stokes H T 2011 Heat transport in silicon from first-principles calculations *Phys. Rev.* B **84** 085204

[38] Omini M and Sparavigna A 1996 Beyond the isotropic-model approximation in the theory of thermal conductivity *Phys. Rev.* B **53** 9064–73
[39] Omini M and Sparavigna A 1997 Heat transport in dielectric solids with diamond structure *Nuovo Cimento* D **19** 1537
[40] Fugallo G, Lazzeri M, Paulatto L and Mauri F 2013 *Ab initio* variational approach for evaluating lattice thermal conductivity *Phys. Rev.* B **88** 045430
[41] Lindsay L, Hua C, Ruan X L and Lee S 2018 Survey of *ab initio* phonon thermal transport *Mater. Today Phys.* **7** 106–20
[42] Callaway J 1959 Model for lattice thermal conductivity at low temperatures *Phys. Rev.* **113** 1046
[43] Krumhansl J A 1965 Thermal conductivity of insulating crystals in the presence of normal processes *Proc. Phys. Soc.* **85** 921
[44] Vincenti W G and Kruger C H 1965 *Introduction to Physical Gas Dynamics* (New York: Wiley)
[45] Allen P B 2013 Improved Callaway model for lattice thermal conductivity *Phys. Rev.* B **88** 144302
[46] Ma J, Li W and Luo X 2014 Examining the Callaway model for lattice thermal conductivity *Phys. Rev.* B **90** 035203
[47] Li X and Lee S 2019 Crossover of ballistic, hydrodynamic, and diffusive phonon transport in suspended graphene *Phys. Rev.* B **99** 085202
[48] Cepellotti A and Marzari N 2016 Thermal transport in crystals as a kinetic theory of relaxons *Phys. Rev.* **6** 041013
[49] Landon C D and Hadjiconstantinou N G 2014 Deviational simulation of phonon transport in graphene ribbons with *ab initio* scattering *J. Appl. Phys.* **116** 163502
[50] Li X and Lee S 2018 Role of hydrodynamic viscosity on phonon transport in suspended graphene *Phys. Rev.* B **97** 094309
[51] Majumdar A 1993 Microscale heat conduction in dielectric thin films *J. Heat Transfer* **115** 7–16
[52] Péraud J-P M and Hadjiconstantinou N G 2011 Efficient simulation of multidimensional phonon transport using energy-based variance-reduced Monte Carlo formulations *Phys. Rev.* B **84** 205331
[53] Hao Q, Chen G and Jeng M-S 2009 Frequency-dependent Monte Carlo simulations of phonon transport in two-dimensional porous silicon with aligned pores *J. Appl. Phys.* **106** 114321
[54] Lindsay L, Broido D and Mingo N 2009 Lattice thermal conductivity of single-walled carbon nanotubes: beyond the relaxation time approximation and phonon–phonon scattering selection rules *Phys. Rev.* B **80** 125407
[55] Guo Y and Wang M 2017 Heat transport in two-dimensional materials by directly solving the phonon Boltzmann equation under Callaway's dual relaxation model *Phys. Rev.* B **96** 134312
[56] Martelli V, Jiménez J L, Continentino M, Baggio-Saitovitch E and Behnia K 2018 Thermal transport and phonon hydrodynamics in strontium titanate *Phys. Rev. Lett.* **120** 125901
[57] Lee S, Li X and Guo R 2019 Thermal resistance by transition between collective and non-collective phonon flows in graphitic materials *Nanoscale Microscale Thermophys. Eng.* **2019** 1–12
[58] Landau L 1941 Theory of the superfluidity of helium II *Phys. Rev.* **60** 356–8

[59] Peshkov V 1946 Determination of the velocity of propagation of the second sound in helium II *J. Phys. USSR* **10** 389–96
[60] Ward J and Wilks J 1951 The velocity of second sound in liquid helium near the absolute zero *Philos. Mag.* **42** 314–6
[61] Ward J C and Wilks J III 1952 Second sound and the thermo-mechanical effect at very low temperatures *Philos. Mag.* **43** 48–50
[62] Rogers S J 1971 Transport of heat and approach to second sound in some isotopically pure alkali-halide crystals *Phys. Rev.* B **3** 1440–57
[63] Guyer R A 1965 Light scattering detection of thermal waves *Phys. Lett.* **19** 261
[64] Griffin A 1968 Brillouin light scattering from crystals in the hydrodynamic region *Rev. Mod. Phys.* **40** 167–205
[65] Wehner R K and Klein R 1972 Scattering of light by entropy fluctuations in dielectric crystals *Physica* **62** 161–97
[66] Pohl D W and Irniger V 1976 Observation of second sound in NaF by means of light scattering *Phys. Rev. Lett.* **36** 480–3
[67] Hehlen B, Pérou A-L, Courtens E and Vacher R 1995 Observation of a doublet in the quasielastic central peak of quantum-paraelectric $SrTiO_3$ *Phys. Rev. Lett.* **75** 2416–9
[68] Koreeda A, Takano R and Saikan S 2007 Second sound in $SrTiO_3$ *Phys. Rev. Lett.* **99** 265502
[69] Hardy R J 1970 Phonon Boltzmann equation and second sound in solids *Phys. Rev.* B **2** 1193–207
[70] Seol J H *et al* 2010 Two-dimensional phonon transport in supported graphene *Science* **328** 213–6
[71] Shi L *et al* 2003 Measuring thermal and thermoelectric properties of one-dimensional nanostructures using a microfabricated device *J. Heat Transfer* **125** 881–8
[72] Ou E, Li X, Lee S, Watanabe K and Taniguchi T 2019 Four-probe measurement of thermal transport in suspended few-layer graphene with polymer residue *J. Heat Transfer* **141** 061601–5
[73] Cahill D G 2004 Analysis of heat flow in layered structures for time-domain thermoreflectance *Rev. Sci. Instrum.* **75** 025901
[74] Johnson J A *et al* 2013 Direct measurement of room-temperature nondiffusive thermal transport over micron distances in a silicon membrane *Phys. Rev. Lett.* **110** 131–4
[75] Salcedo J R, Siegman A E, Dlott D D and Fayer M D 1978 Dynamics of energy transport in molecular crystals: the picosecond transient-grating method *Phys. Rev. Lett.* **41** 131–4
[76] Huberman S *et al* 2019 Observation of second sound in graphite at temperatures above 100 K *Science* **364** 375–9
[77] Cahill D G *et al* 2014 Nanoscale thermal transport. II. 2003–2012 *Appl. Phys. Rev.* **1** 011305
[78] Cahill D G *et al* 2003 Nanoscale thermal transport *J. Appl. Phys.* **93** 793–818

Full list of references

Prelims

[1] Chen G 2005 *Nanoscale Energy Transport and Conversion: A Parallel Treatment of Electrons, Molecules, Phonons, and Photons* 1st edn (Oxford: Oxford University Press)
[2] Zhang Z 2007 *Nano/Microscale Heat Transfer* (New York: McGraw-Hill)
[3] Fisher T S 2013 *Thermal Energy At The Nanoscale* (Hackensack, NJ: WSPC)
[4] Volz S (ed) 2007 *Microscale and Nanoscale Heat Transfer* (Berlin: Springer)
[5] Boona S R, Myers R C and Heremans J P 2014 Spin caloritronics *Energy Environ. Sci.* **7** 885–910
[6] Gu X, Wei Y, Yin X, Li B and Yang R 2018 Colloquium: phononic thermal properties of two-dimensional materials *Rev. Mod. Phys.* **90** 041002

Chapter 1

[1] Nernst W 1917 *Die Theoretischen Grundlagen des Neuen Wärmesatzes* (Halle: Knapp)
[2] Peierls R 1929 Zur kinetischen Theorie der Wärmeleitung in Kristallen *Ann. Phys.* **395** 1055–101
[3] Lee S, Broido D, Esfarjani K and Chen G 2015 Hydrodynamic phonon transport in suspended graphene *Nat. Commun.* **6** 6290
[4] Sussmann J A and Thellung A 1963 Thermal conductivity of perfect dielectric crystals in the absence of Umklapp processes *Proc. Phys. Soc.* **81** 1122
[5] Prohofsky E W and Krumhansl J A 1964 Second-sound propagation in dielectric solids *Phys. Rev.* **133** A1403–10
[6] Guyer R A and Krumhansl J A 1964 Dispersion relation for second sound in solids *Phys. Rev.* **133** A1411–7
[7] Guyer R A and Krumhansl J A 1966 Thermal conductivity, second sound, and phonon hydrodynamic phenomena in nonmetallic crystals *Phys. Rev.* **148** 778–88
[8] Guyer R A and Krumhansl J A 1966 Solution of the linearized phonon Boltzmann equation *Phys. Rev.* **148** 766–78
[9] Gurzhi R 1964 Thermal conductivity of dielectrics and ferrodielectrics at low temperatures *J. Exp. Theor. Phys.* **46** 719–24
[10] Griffin A 1965 On the detection of second sound in crystals by light scattering *Phys. Lett.* **17** 208–10
[11] Mezhov-Deglin L 1965 Measurement of the thermal conductivity of crystalline He^4 *J. Exp. Theor. Phys.* **49** 66–79
[12] Ackerman C C and Overton W C 1969 Second sound in solid helium-3 *Phys. Rev. Lett.* **22** 764–6
[13] McNelly T F *et al* 1970 Heat pulses in NaF: onset of second sound *Phys. Rev. Lett.* **24** 100–2
[14] Jackson H E, Walker C T and McNelly T F 1970 Second sound in NaF *Phys. Rev. Lett.* **25** 26–8
[15] Narayanamurti V and Dynes R C 1972 Observation of second sound in bismuth *Phys. Rev. Lett.* **28** 1461–65
[16] Ashcroft N and Mermin N 1976 *Solid State Physics* (Philadelphia, PA: Saunders)
[17] Jackson H E and Walker C T 1971 Thermal conductivity, second sound, and phonon–phonon interactions in NaF *Phys. Rev.* B **3** 1428–39

[18] Lee S and Lindsay L 2017 Hydrodynamic phonon drift and second sound in a (20,20) single-wall carbon nanotube *Phys. Rev.* B **95** 184304
[19] Cepellotti A, Fugallo G, Paulatto L, Lazzeri M, Mauri F and Marzari N 2015 Phonon hydrodynamics in two-dimensional materials *Nat. Commun.* **6** 6400
[20] Ding Z, Zhou J, Song B, Chiloyan V, Li M, Liu T-H and Chen G 2018 Phonon hydrodynamic heat conduction and Knudsen minimum in graphite *Nano Lett.* **18** 638–49
[21] Schelling P K and Keblinski P 2003 Thermal expansion of carbon structures *Phys. Rev.* B **68** 035425
[22] Beck H, Meier P F and Thellung A 1974 Phonon hydrodynamics in solids *Phys. Status Solidi* a **24** 11–63
[23] Gurevich V L v 1986 *Transport in Phonon SystemsModern Problems in Condensed Matter Sciences* (Amsterdam: Elsevier)
[24] Joseph D D and Preziosi L 1989 Heat waves *Rev. Mod. Phys.* **61** 41–73
[25] Alvarez F X, Jou D and Sellitto A 2009 Phonon hydrodynamics and phonon–boundary scattering in nanosystems *J. Appl. Phys.* **105** 014317
[26] Ziabari A *et al* 2018 Full-field thermal imaging of quasiballistic crosstalk reduction in nanoscale devices *Nat. Commun.* **9** 255
[27] Torres P *et al* 2018 Emergence of hydrodynamic heat transport in semiconductors at the nanoscale *Phys. Rev. Mater.* **2** 076001
[28] Guo Y and Wang M 2018 Phonon hydrodynamics for nanoscale heat transport at ordinary temperatures *Phys. Rev.* B **97** 035421
[29] Dong Y, Cao B-Y and Guo Z-Y 2011 Generalized heat conduction laws based on thermomass theory and phonon hydrodynamics *J. Appl. Phys.* **110** 063504
[30] Cimmelli V A, Sellitto A and Jou D 2010 Nonlinear evolution and stability of the heat flow in nanosystems: beyond linear phonon hydrodynamics *Phys. Rev.* B **82** 184302
[31] Sellitto A, Alvarez F X and Jou D 2010 Temperature dependence of boundary conditions in phonon hydrodynamics of smooth and rough nanowires *J. Appl. Phys.* **107** 114312
[32] Hardy R J and Albers D L 1974 Hydrodynamic approximation to the phonon Boltzmann equation *Phys. Rev.* B **10** 3546–51
[33] Guo Y and Wang M 2015 Phonon hydrodynamics and its applications in nanoscale heat transport *Phys. Rep.* **595** 1–44
[34] Ziman J M 1960 *Electrons and Phonons: The Theory of Transport Phenomena in Solids* (Oxford: Oxford University Press)
[35] Ding Z, Zhou J, Song B, Li M, Liu T-H and Chen G 2018 Umklapp scattering is not necessarily resistive *Phys. Rev.* B **98** 180302
[36] Broido D A, Malorny M, Birner G, Mingo N and Stewart D A 2007 Intrinsic lattice thermal conductivity of semiconductors from first principles *Appl. Phys. Lett.* **91** 231922
[37] Esfarjani K, Chen G and Stokes H T 2011 Heat transport in silicon from first-principles calculations *Phys. Rev.* B **84** 085204
[38] Omini M and Sparavigna A 1996 Beyond the isotropic-model approximation in the theory of thermal conductivity *Phys. Rev.* B **53** 9064–73
[39] Omini M and Sparavigna A 1997 Heat transport in dielectric solids with diamond structure *Nuovo Cimento* D **19** 1537
[40] Fugallo G, Lazzeri M, Paulatto L and Mauri F 2013 *Ab initio* variational approach for evaluating lattice thermal conductivity *Phys. Rev.* B **88** 045430

[41] Lindsay L, Hua C, Ruan X L and Lee S 2018 Survey of *ab initio* phonon thermal transport *Mater. Today Phys.* **7** 106–20
[42] Callaway J 1959 Model for lattice thermal conductivity at low temperatures *Phys. Rev.* **113** 1046
[43] Krumhansl J A 1965 Thermal conductivity of insulating crystals in the presence of normal processes *Proc. Phys. Soc.* **85** 921
[44] Vincenti W G and Kruger C H 1965 *Introduction to Physical Gas Dynamics* (New York: Wiley)
[45] Allen P B 2013 Improved Callaway model for lattice thermal conductivity *Phys. Rev.* B **88** 144302
[46] Ma J, Li W and Luo X 2014 Examining the Callaway model for lattice thermal conductivity *Phys. Rev.* B **90** 035203
[47] Li X and Lee S 2019 Crossover of ballistic, hydrodynamic, and diffusive phonon transport in suspended graphene *Phys. Rev.* B **99** 085202
[48] Cepellotti A and Marzari N 2016 Thermal transport in crystals as a kinetic theory of relaxons *Phys. Rev.* **6** 041013
[49] Landon C D and Hadjiconstantinou N G 2014 Deviational simulation of phonon transport in graphene ribbons with *ab initio* scattering *J. Appl. Phys.* **116** 163502
[50] Li X and Lee S 2018 Role of hydrodynamic viscosity on phonon transport in suspended graphene *Phys. Rev.* B **97** 094309
[51] Majumdar A 1993 Microscale heat conduction in dielectric thin films *J. Heat Transfer* **115** 7–16
[52] Péraud J-P M and Hadjiconstantinou N G 2011 Efficient simulation of multidimensional phonon transport using energy-based variance-reduced Monte Carlo formulations *Phys. Rev.* B **84** 205331
[53] Hao Q, Chen G and Jeng M-S 2009 Frequency-dependent Monte Carlo simulations of phonon transport in two-dimensional porous silicon with aligned pores *J. Appl. Phys.* **106** 114321
[54] Lindsay L, Broido D and Mingo N 2009 Lattice thermal conductivity of single-walled carbon nanotubes: beyond the relaxation time approximation and phonon–phonon scattering selection rules *Phys. Rev.* B **80** 125407
[55] Guo Y and Wang M 2017 Heat transport in two-dimensional materials by directly solving the phonon Boltzmann equation under Callaway's dual relaxation model *Phys. Rev.* B **96** 134312
[56] Martelli V, Jiménez J L, Continentino M, Baggio-Saitovitch E and Behnia K 2018 Thermal transport and phonon hydrodynamics in strontium titanate *Phys. Rev. Lett.* **120** 125901
[57] Lee S, Li X and Guo R 2019 Thermal resistance by transition between collective and non-collective phonon flows in graphitic materials *Nanoscale Microscale Thermophys. Eng.* **2019** 1–12
[58] Landau L 1941 Theory of the superfluidity of helium II *Phys. Rev.* **60** 356–8
[59] Peshkov V 1946 Determination of the velocity of propagation of the second sound in helium II *J. Phys. USSR* **10** 389–96
[60] Ward J and Wilks J 1951 The velocity of second sound in liquid helium near the absolute zero *Philos. Mag.* **42** 314–6
[61] Ward J C and Wilks J III 1952 Second sound and the thermo-mechanical effect at very low temperatures *Philos. Mag.* **43** 48–50

[62] Rogers S J 1971 Transport of heat and approach to second sound in some isotopically pure alkali-halide crystals *Phys. Rev.* B **3** 1440–57
[63] Guyer R A 1965 Light scattering detection of thermal waves *Phys. Lett.* **19** 261
[64] Griffin A 1968 Brillouin light scattering from crystals in the hydrodynamic region *Rev. Mod. Phys.* **40** 167–205
[65] Wehner R K and Klein R 1972 Scattering of light by entropy fluctuations in dielectric crystals *Physica* **62** 161–97
[66] Pohl D W and Irniger V 1976 Observation of second sound in NaF by means of light scattering *Phys. Rev. Lett.* **36** 480–3
[67] Hehlen B, Pérou A-L, Courtens E and Vacher R 1995 Observation of a doublet in the quasielastic central peak of quantum-paraelectric $SrTiO_3$ *Phys. Rev. Lett.* **75** 2416–9
[68] Koreeda A, Takano R and Saikan S 2007 Second sound in $SrTiO_3$ *Phys. Rev. Lett.* **99** 265502
[69] Hardy R J 1970 Phonon Boltzmann equation and second sound in solids *Phys. Rev.* B **2** 1193–207
[70] Seol J H *et al* 2010 Two-dimensional phonon transport in supported graphene *Science* **328** 213–6
[71] Shi L *et al* 2003 Measuring thermal and thermoelectric properties of one-dimensional nanostructures using a microfabricated device *J. Heat Transfer* **125** 881–8
[72] Ou E, Li X, Lee S, Watanabe K and Taniguchi T 2019 Four-probe measurement of thermal transport in suspended few-layer graphene with polymer residue *J. Heat Transfer* **141** 061601–5
[73] Cahill D G 2004 Analysis of heat flow in layered structures for time-domain thermoreflectance *Rev. Sci. Instrum.* **75** 025901
[74] Johnson J A *et al* 2013 Direct measurement of room-temperature nondiffusive thermal transport over micron distances in a silicon membrane *Phys. Rev. Lett.* **110** 131–4
[75] Salcedo J R, Siegman A E, Dlott D D and Fayer M D 1978 Dynamics of energy transport in molecular crystals: the picosecond transient-grating method *Phys. Rev. Lett.* **41** 131–4
[76] Huberman S *et al* 2019 Observation of second sound in graphite at temperatures above 100 K *Science* **364** 375–9
[77] Cahill D G *et al* 2014 Nanoscale thermal transport. II. 2003–2012 *Appl. Phys. Rev.* **1** 011305
[78] Cahill D G *et al* 2003 Nanoscale thermal transport *J. Appl. Phys.* **93** 793–818

Chapter 2

[1] Maradudin A A and Flinn P A 1961 Anharmonic contributions to vibrational thermodynamic properties of solids: Part I *Ann. Phys.* **15** 337–59
[2] Maradudin A A and Fein A E 1962 Scattering of neutrons by an anharmonic crystal *Phys. Rev.* **128** 2589
[3] Maradudin A A, Fein A E and Vineyard G H 1962 On the evaluation of phonon widths and shifts *Phys. Status Solidi* B **2** 1479–92
[4] Debernardi A, Baroni S and Molinari E 1995 Anharmonic phonon lifetimes in semiconductors from density-functional perturbation theory *Phys. Rev. Lett.* **75** 1819–22
[5] Bechstedt F, Käckell P, Zywietz A, Karch K, Adolph B, Tenelsen K and Furthmüller J 1997 Polytypism and properties of silicon carbide *Phys. Status Solidi* B **202** 35–62
[6] Debernardi A 1998 Phonon linewidth in III–V semiconductors from density-functional perturbation theory *Phys. Rev.* B **57** 12847–58

[7] Lang G, Karch K, Schmitt M, Pavone P, Mayer A, Wehner R and Strauch D 1999 Anharmonic line shift and linewidth of the Raman mode in covalent semiconductors *Phys. Rev.* B **59** 6182–8
[8] Tang X and Fultz B 2011 First-principles study of phonon linewidths in noble metals *Phys. Rev.* B **84** 054303
[9] Broido D A, Malorny M, Birner G, Mingo N and Stewart D A 2007 Intrinsic lattice thermal conductivity of semiconductors from first principles *Appl. Phys. Lett.* **91** 231922
[10] Esfarjani K, Chen G and Stokes H T 2011 Heat transport in silicon from first-principles calculations *Phys. Rev.* B **84** 085204
[11] Lindsay L, Broido D A and Reinecke T L 2013 First-principles determination of ultrahigh thermal conductivity of boron arsenide: a competitor for diamond? *Phys. Rev. Lett.* **111** 025901
[12] Seko A, Togo A, Hayashi H, Tsuda K, Chaput L and Tanaka I 2015 Prediction of low-thermal-conductivity compounds with first-principles anharmonic lattice-dynamics calculations and Bayesian optimization *Phys. Rev. Lett.* **115** 205901
[13] Feng T and Ruan X 2014 Prediction of spectral phonon mean free path and thermal conductivity with applications to thermoelectrics and thermal management: a review *J. Nanomater.* **2014** 206370
[14] Bao H, Chen J, Gu X and Cao B 2018 A review of simulation methods in micro/nanoscale heat conduction *ES Energy Environ.* **1** 16
[15] Lindsay L, Hua C, Ruan X and Lee S 2018 Survey of *ab initio* phonon thermal transport *Mater. Today Phys.* **7** 106–20
[16] Tong Z, Liu L, Li L and Bao H 2018 Temperature-dependent infrared optical properties of 3c-, 4h- and 6h-SiC *Physica* B **537** 194–201
[17] Joshi Y P, Tiwari M D and Verma G S 1970 Role of four-phonon processes in the lattice thermal conductivity of silicon from 300 to 1300 K *Phys. Rev.* B **1** 642–6
[18] Ecsedy D and Klemens P 1977 Thermal resistivity of dielectric crystals due to four-phonon processes and optical modes *Phys. Rev.* B **15** 5957
[19] Bao H, Qiu B, Zhang Y and Ruan X 2012 A first-principles molecular dynamics approach for predicting optical phonon lifetimes and far-infrared reflectance of polar materials *J. Quant. Spectrosc. Radiat. Transf.* **113** 1683–8
[20] Yang X, Feng T, Kang J S, Hu Y, Li J and Ruan X 2019 Role of higher-order phonon scattering in the zone-center optical phonon linewidth and the Lorenz oscillator model (arXiv 1908.05121)
[21] Novikov M, Ositinskaya T, Shulzhenko O, Podoba O, Sokolov O and Petrusha I 1983 Heat-conductivity of cubic boron–nitride single-crystals *Dopov. Akad. Nauk Ukrain. RSR Seriya* A 72–5
[22] Zhao L-D, Lo S-H, Zhang Y, Sun H, Tan G, Uher C, Wolverton C, Dravid V P and Kanatzidis M G 2014 Ultralow thermal conductivity and high thermoelectric figure of merit in SnSe crystals *Nature* **508** 373–7
[23] Guo R, Wang X, Kuang Y and Huang B 2015 First-principles study of anisotropic thermoelectric transport properties of IV–VI semiconductor compounds SNSE and SNS *Phys. Rev.* B **92** 115202
[24] Lindsay L and Broido D A 2008 Three-phonon phase space and lattice thermal conductivity in semiconductors *J. Phys. Condens. Matter* **20** 165209

[25] Turney J, Landry E, McGaughey A and Amon C 2009 Predicting phonon properties and thermal conductivity from anharmonic lattice dynamics calculations and molecular dynamics simulations *Phys. Rev.* B **79** 064301
[26] Feng T and Ruan X 2016 Quantum mechanical prediction of four-phonon scattering rates and reduced thermal conductivity of solids *Phys. Rev.* B **93** 045202
[27] Feng T, Lindsay L and Ruan X 2017 Four-phonon scattering significantly reduces intrinsic thermal conductivity of solids *Phys. Rev.* B **96** 161201
[28] Kang J S, Li M, Wu H, Nguyen H and Hu Y 2018 Experimental observation of high thermal conductivity in boron arsenide *Science* **361** 575–8
[29] Li S, Zheng Q, Lv Y, Liu X, Wang X, Huang P Y, Cahill D G and Lv B 2018 High thermal conductivity in cubic boron arsenide crystals *Science* **361** 579–81
[30] Tian F *et al* 2018 Unusual high thermal conductivity in boron arsenide bulk crystals *Science* **361** 582–5
[31] Feng T and Ruan X 2018 Four-phonon scattering reduces intrinsic thermal conductivity of graphene and the contributions from flexural phonons *Phys. Rev.* B **97** 045202
[32] Xia Y 2018 Revisiting lattice thermal transport in PBTE: the crucial role of quartic anharmonicity *Appl. Phys. Lett.* **113** 073901
[33] Ravichandran N K and Broido D 2018 Unified first-principles theory of thermal properties of insulators *Phys. Rev.* B **98** 085205
[34] Ziman J M 1960 *Electrons and Phonons* (London: Oxford University Press)
[35] Kaviany M 2008 *Heat Transfer Physics* (New York: Cambridge University Press)
[36] Klemens P 1958 *Solid State Physics* vol 7 (New York: Academic)
[37] Tamura S-I 1983 Isotope scattering of dispersive phonons in Ge *Phys. Rev.* B **27** 858
[38] Casimir H B G 1938 Note on the conduction of heat in crystals *Physica* **5** 495–500
[39] Berman R, Simon F E and Ziman J M 1953 The thermal conductivity of diamond at low temperatures *Proc. R. Soc. Lond.* A **220** 171–83
[40] Berman R, Foster E L and Ziman J M 1955 Thermal conduction in artificial sapphire crystals at low temperatures. I. Nearly perfect crystals *Proc. R. Soc. Lond.* A **231** 130–44
[41] Omini M and Sparavigna A 1995 An iterative approach to the phonon Boltzmann equation in the theory of thermal conductivity *Physica* B **212** 101–12
[42] Omini M and Sparavigna A 1997 Heat transport in dielectric solids with diamond structure *Nuovo Cimento Soc. Ital. Fis.* D **19D** 1537–63
[43] Broido D A, Ward A and Mingo N 2005 Lattice thermal conductivity of silicon from empirical interatomic potentials *Phys. Rev.* B **72** 014308
[44] Togo A and Tanaka I 2015 First principles phonon calculations in materials science *Scr. Mater.* **108** 1–5
[45] Tersoff J 1989 Modeling solid-state chemistry: interatomic potentials for multicomponent systems *Phys. Rev.* B **39** 5566–8
[46] Tersoff J 1990 Erratum: Modeling solid-state chemistry: interatomic potentials for multicomponent systems *Phys. Rev.* B **41** 3248
[47] Li W, Mingo N, Lindsay L, Broido D A, Stewart D A and Katcho N A 2012 Thermal conductivity of diamond nanowires from first principles *Phys. Rev.* B **85** 195436
[48] Li W, Lindsay L, Broido D A, Stewart D A and Mingo N 2012 Thermal conductivity of bulk and nanowire $Mg_2Si_xSn_{1-x}$ alloys from first principles *Phys. Rev.* B **86** 174307

[49] Lindsay L, Broido D and Mingo N 2009 Lattice thermal conductivity of single-walled carbon nanotubes: beyond the relaxation time approximation and phonon–phonon scattering selection rules *Phys. Rev.* B **80** 125407
[50] Lindsay L and Broido D A 2012 Theory of thermal transport in multilayer hexagonal boron nitride and nanotubes *Phys. Rev.* B **85** 035436
[51] Lindsay L, Broido D A and Reinecke T L 2012 Thermal conductivity and large isotope effect in GaN from first principles *Phys. Rev. Letters* **109** 095901
[52] Ruf T, Henn R, Asen-Palmer M, Gmelin E, Cardona M, Pohl H-J, Devyatych G and Sennikov P 2000 Thermal conductivity of isotopically enriched silicon *Solid State Commun.* **115** 243–7
[53] Abeles B, Beers D, Cody G and Dismukes J 1962 Thermal conductivity of Ge–Si alloys at high temperatures *Phys. Rev.* **125** 44
[54] Glassbrenner C J and Slack G A 1964 Thermal conductivity of silicon and germanium from 3 K to the melting point *Phys. Rev.* **134** A1058
[55] Feng T, Yang X and Ruan X 2018 Phonon anharmonic frequency shift induced by four-phonon scattering calculated from first principles *J. Appl. Phys.* **124** 145101
[56] Morelli D T, Jovovic V and Heremans J P 2008 Intrinsically minimal thermal conductivity in cubic I–V–vi_2 semiconductors *Phys. Rev. Lett.* **101** 035901
[57] El-Sharkawy A, El-Azm A A, Kenawy M, Hillal A and Abu-Basha H 1983 Thermophysical properties of polycrystalline PBS, PBSE, and PBTE in the temperature range 300–700 K *Int. J. Thermophys.* **4** 261–9
[58] Håkansson B and Andersson P 1986 Thermal conductivity and heat capacity of solid NaCl and NaI under pressure *J. Phys. Chem. Solids* **47** 355–62
[59] McCarthy K A and Ballard S S 1960 Thermal conductivity of eight halide crystals in the temperature range 220 K to 390 K *J. Appl. Phys.* **31** 1410–12
[60] Yukutake H and Shimada M 1978 Thermal conductivity of NaCl, MgO, coesite and stishovite up to 40 kbar *Phys. Earth Planet. Inter.* **17** 193–200
[61] Wei L, Kuo P K, Thomas R L, Anthony T R and Banholzer W F 1993 Thermal conductivity of isotopically modified single crystal diamond *Phys. Rev. Lett.* **70** 3764–7
[62] Onn D G, Witek A, Qiu Y Z, Anthony T R and Banholzer W F 1992 Some aspects of the thermal conductivity of isotopically enriched diamond single crystals *Phys. Rev. Lett.* **68** 2806–9
[63] Olson J R, Pohl R O, Vandersande J W, Zoltan A, Anthony T R and Banholzer W F 1993 Thermal conductivity of diamond between 170 and 1200 K and the isotope effect *Phys. Rev.* B **47** 14850–6
[64] Berman R, Hudson P R W and Martinez M 1975 Nitrogen in diamond: evidence from thermal conductivity *J. Phys. C: Solid State Phys.* **8** L430
[65] Zheng Q, Li S, Li C, Lv Y, Liu X, Huang P Y, Broido D A, Lv B and Cahill D G 2018 High thermal conductivity in isotopically enriched cubic boron phosphide *Adv. Funct. Mater.* **28** 1805116
[66] Yang X, Feng T, Li J and Ruan X 2019 Stronger role of four-phonon scattering than three-phonon scattering in thermal conductivity of III-V semiconductors at room temperature *Phys. Rev.* B **100** 245203
[67] Jeżowski A, Stachowiak P, Plackowski T, Suski T, Krukowski S, Boćkowski M, Grzegory I, Danilchenko B and Paszkiewicz T 2003 Thermal conductivity of GaN crystals grown by high pressure method *Phys. Status Solidi* B **240** 447–50

[68] Hess S, Taylor R, O'Sullivan E, Ryan J, Cain N, Roberts V and Roberts J 1999 Hot carrier relaxation by extreme electron–LO phonon scattering in GaN *Phys. Status Solidi* B **216** 51–5
[69] Gervais F and Piriou B 1975 Temperature dependence of transverse and longitudinal optic modes in the α and β phases of quartz *Phys. Rev.* B **11** 3944–50
[70] Dean K, Sherman W and Wilkinson G 1982 Temperature and pressure dependence of the Raman active modes of vibration of α-quartz *Spectrochim. Acta* A **38** 1105–8
[71] Ulrich C, Debernardi A, Anastassakis E, Syassen K and Cardona M 1999 Raman linewidths of phonons in Si, Ge, and Sic under pressure *Phys. Status Solidi* B **211** 293–300
[72] Herchen H and Cappelli M A 1993 Temperature dependence of the cubic boron nitride Raman lines *Phys. Rev.* B **47** 14193–9
[73] Hadjiev V G, Iliev M N, Lv B, Ren Z F and Chu C W 2014 Anomalous vibrational properties of cubic boron arsenide *Phys. Rev.* B **89** 024308
[74] Lockwood D, Yu G and Rowell N 2005 Optical phonon frequencies and damping in AlAs, GaP, GaAs, InP, InAs and InSb studied by oblique incidence infrared spectroscopy *Solid State Commun.* **136** 404–9
[75] Turner W J and Reese W E 1962 Infrared lattice bands in AlSb *Phys. Rev.* **127** 126–31
[76] McCluskey M D, Haller E E and Becla P 2001 Carbon acceptors and carbon–hydrogen complexes in AlSb *Phys. Rev.* B **65** 045201
[77] Cuscó R, Domènech-Amador N, Novikov S, Foxon C T and Artús L 2015 Anharmonic phonon decay in cubic GaN *Phys. Rev.* B **92** 075206
[78] Irmer G, Wenzel M and Monecke J 1996 The temperature dependence of the LO(T) and TO(T) phonons in GaAs and InP *Phys. Status Solidi* B **195** 85–95
[79] Stimets R W and Lax B 1970 Reflection studies of coupled magnetoplasma–phonon modes *Phys. Rev.* B **1** 4720–35
[80] Hass M and Henvis B 1962 Infrared lattice reflection spectra of III–V compound semiconductors *J. Phys. Chem. Solids* **23** 1099–104
[81] Lindsay L and Broido D A 2011 Enhanced thermal conductivity and isotope effect in single-layer hexagonal boron nitride *Phys. Rev.* B **84** 155421
[82] Lindsay L, Broido D A and Mingo N 2010 Flexural phonons and thermal transport in graphene *Phys. Rev.* B **82** 115427
[83] Lindsay L, Li W, Carrete J, Mingo N, Broido D A and Reinecke T L 2014 Phonon thermal transport in strained and unstrained graphene from first principles *Phys. Rev.* B **89** 155426
[84] Fugallo G, Cepellotti A, Paulatto L, Lazzeri M, Marzari N and Mauri F 2014 Thermal conductivity of graphene and graphite: collective excitations and mean free paths *Nano Lett.* **14** 6109–14
[85] Faugeras C, Faugeras B, Orlita M, Potemski M, Nair R R and Geim A K 2010 Thermal conductivity of graphene in corbino membrane geometry *ACS Nano* **4** 1889–92
[86] Chen S, Wu Q, Mishra C, Kang J, Zhang H, Cho K, Cai W, Balandin A A and Ruoff R S 2012 Thermal conductivity of isotopically modified graphene *Nature Mater.* **11** 203–7
[87] Xu X *et al* 2014 Length-dependent thermal conductivity in suspended single-layer graphene *Nat. Commun.* **5** 3689
[88] Ghosh S, Calizo I, Teweldebrhan D, Pokatilov E P, Nika D L, Balandin A A, Bao W, Miao F and Lau C N 2008 Extremely high thermal conductivity of graphene: prospects for thermal management applications in nanoelectronic circuits *Appl. Phys. Lett.* **92** 151911

[89] Ghosh S, Bao W, Nika D L, Subrina S, Pokatilov E P, Lau C N and Balandin A A 2010 Dimensional crossover of thermal transport in few-layer graphene *Nat. Mater.* **9** 555–8
[90] Vallabhaneni A K, Singh D, Bao H, Murthy J and Ruan X 2016 Reliability of Raman measurements of thermal conductivity of single-layer graphene due to selective electron–phonon coupling: a first-principles study *Phys. Rev.* B **93** 125432
[91] Gu X, Fan Z, Bao H and Zhao C Y 2019 Revisiting phonon–phonon scattering in single-layer graphene *Phys. Rev.* B **100** 064306
[92] Lindsay L and Broido D A 2010 Optimized Tersoff and Brenner empirical potential parameters for lattice dynamics and phonon thermal transport in carbon nanotubes and graphene *Phys. Rev.* B **81** 205441
[93] Xie H, Chen L, Yu W and Wang B 2013 Temperature dependent thermal conductivity of a free-standing graphene nanoribbon *Appl. Phys. Lett.* **102** 111911
[94] Li Q-Y, Takahashi K, Ago H, Zhang X, Ikuta T, Nishiyama T and Kawahara K 2015 Temperature dependent thermal conductivity of a suspended submicron graphene ribbon *J. Appl. Phys.* **117** 065102
[95] Chen S *et al* 2011 Raman measurements of thermal transport in suspended monolayer graphene of variable sizes in vacuum and gaseous environments *ACS Nano* **5** 321–8
[96] Lee J-U, Yoon D, Kim H, Lee S W and Cheong H 2011 Thermal conductivity of suspended pristine graphene measured by Raman spectroscopy *Phys. Rev.* B **83** 081419
[97] Lindsay L, Broido D A and Mingo N 2011 Flexural phonons and thermal transport in multilayer graphene and graphite *Phys. Rev.* B **83** 235428
[98] Kim S I *et al* 2015 Dense dislocation arrays embedded in grain boundaries for high-performance bulk thermoelectrics *Science* **348** 109–14
[99] Hong M, Chasapis T C, Chen Z-G, Yang L, Kanatzidis M G, Snyder G J and Zou J 2016 *n*-type $Bi_2Te_{3-x}Se_x$ nanoplates with enhanced thermoelectric efficiency driven by wide-frequency phonon scatterings and synergistic carrier scatterings *ACS Nano* **10** 4719
[100] Xu B *et al* 2017 Nanocomposites from solution-synthesized PbTe–BiSbTe nanoheterostructure with unity figure of merit at low–medium temperatures (500–600 K) *Adv. Mater.* **29** 1605140
[101] Joshi Y P, Tiwari M D and Verma G S 1969 Role of four-phonon processes in the lattice thermal conductivity of silicon from 300 to 1300 K *Phys. Rev.* B **1** 642
[102] Carruthers P 1962 Resonance in phonon–phonon scattering *Phys. Rev.* **125** 123–5
[103] Ravichandran N K and Broido D 2019 Non-monotonic pressure dependence of the thermal conductivity of boron arsenide *Nat. Commun.* **10** 827
[104] Mukhopadhyay S, Parker D S, Sales B C, Puretzky A A, McGuire M A and Lindsay L 2018 Two-channel model for ultralow thermal conductivity of crystalline Tl_3VSe_4 *Science* **360** 1455–8

Chapter 3

[1] Pop E, Sinha S and Goodson K E 2006 Heat generation and transport in nanometer-scale transistors *Proc. IEEE* **94** 1587–601
[2] Pop E 2010 Energy dissipation and transport in nanoscale devices *Nano Res.* **3** 147–69
[3] Borkar S 2001 Low power design challenges for the decade *Proc. of the ASP-DAC 2001 Asia and South Pacific Design Automation Conf. 2001 (Cat. No. 01EX455) (IEEE)* pp 293–6
[4] Mahajan R, Nair R, Wakharkar V, Swan J, Tang J and Vandentop G 2002 Emerging directions for packaging technologies *Intel Technol. J.* **6** 62

[5] Cahill D G *et al* 2014 Nanoscale thermal transport. II. 2003–2012 *Appl. Phys. Rev.* **1** 011305
[6] Swartz E T and Pohl R O 1989 Thermal boundary resistance *Rev. Mod. Phys.* **61** 605–68
[7] Swartz E T and Pohl R O 1987 Thermal resistance at interfaces *Appl. Phys. Lett.* **51** 2200–2
[8] Little W A 1959 The transport of heat between dissimilar solids at low temperatures *Can. J. Phys.* **37** 334–49
[9] Cahill D G, Ford W K, Goodson K E, Mahan G D, Majumdar A, Maris H J, Merlin R and Phillpot S R 2003 Nanoscale thermal transport *J. Appl. Phys.* **93** 793–818
[10] Majumdar A and Reddy P 2004 Role of electron–phonon coupling in thermal conductance of metal–nonmetal interfaces *Appl. Phys. Lett.* **84** 4768–70
[11] Hopkins P E and Norris P M 2007 Effects of joint vibrational states on thermal boundary conductance *Nanoscale Microscale Thermophys. Eng.* **11** 247–57
[12] Lyeo H-K and Cahill D G 2006 Thermal conductance of interfaces between highly dissimilar materials *Phys. Rev.* B **73** 144301
[13] Hua C, Chen X, Ravichandran N K and Minnich A J 2017 Experimental metrology to obtain thermal phonon transmission coefficients at solid interfaces *Phys. Rev.* B **95** 205423
[14] Gaskins J T *et al* 2018 Thermal boundary conductance across heteroepitaxial ZnO/GaN interfaces: assessment of the phonon gas model *Nano Lett.* **18** 7469–77
[15] Reddy P, Castelino K and Majumdar A 2005 Diffuse mismatch model of thermal boundary conductance using exact phonon dispersion *Appl. Phys. Lett.* **87** 211908
[16] Prasher R 2009 Acoustic mismatch model for thermal contact resistance of van der Waals contacts *Appl. Phys. Lett.* **94** 041905
[17] Shin S, Kaviany M, Desai T and Bonner R 2010 Roles of atomic restructuring in interfacial phonon transport *Phys. Rev.* B **82** 081302
[18] Hopkins P E, Duda J C and Norris P M 2011 Anharmonic phonon interactions at interfaces and contributions to thermal boundary conductance *J. Heat Trans. ASME* **133** 062401
[19] Mingo N and Yang L 2003 Phonon transport in nanowires coated with an amorphous material: an atomistic Green's function approach *Phys. Rev.* B **68** 245406
[20] Tian Z, Esfarjani K and Chen G 2012 Enhancing phonon transmission across a Si/Ge interface by atomic roughness: first-principles study with the Green's function method *Phys. Rev.* B **86** 235304
[21] Zhang W, Fisher T S and Mingo N 2006 Simulation of interfacial phonon transport in Si–Ge heterostructures using an atomistic Green's function method *J. Heat Transfer* **129** 483–91
[22] Mingo N 2006 Anharmonic phonon flow through molecular-sized junctions *Phys. Rev.* B **74** 125402
[23] Luo T and Chen G 2013 Nanoscale heat transfer—from computation to experiment *Phys. Chem. Chem. Phys.* **15** 3389–412
[24] Baker C H, Jordan D A and Norris P M 2012 Application of the wavelet transform to nanoscale thermal transport *Phys. Rev.* B **86** 104306
[25] Schelling P K, Phillpot S R and Keblinski P 2002 Phonon wave-packet dynamics at semiconductor interfaces by molecular-dynamics simulation *Appl. Phys. Lett.* **80** 2484–6
[26] Schelling P K, Phillpot S R and Keblinski P 2004 Kapitza conductance and phonon scattering at grain boundaries by simulation *J. Appl. Phys.* **95** 6082–91
[27] Luo T and Lloyd J R 2012 Enhancement of thermal energy transport across graphene/graphite and polymer interfaces: a molecular dynamics study *Adv. Funct. Mater.* **22** 2495–502

[28] Jiang T, Zhang X, Vishwanath S, Mu X, Kanzyuba V, Sokolov D A, Ptasinska S, Go D B, Xing H G and Luo T 2016 Covalent bonding modulated graphene–metal interfacial thermal transport *Nanoscale* **8** 10993–1001
[29] Lee E, Zhang T, Hu M and Luo T 2016 Thermal boundary conductance enhancement using experimentally achievable nanostructured interfaces—analytical study combined with molecular dynamics simulation *Phys. Chem. Chem. Phys.* **18** 16794–801
[30] Zhang T, Gans-Forrest A R, Lee E, Zhang X, Qu C, Pang Y, Sun F and Luo T 2016 Role of hydrogen bonds in thermal transport across hard/soft material interfaces *ACS Appl. Mater. Interfaces* **8** 33326–34
[31] Lee E, Menumerov E, Hughes R A, Neretina S and Luo T 2018 Low-cost nanostructures from nanoparticle-assisted large-scale lithography significantly enhance thermal energy transport across solid interfaces *ACS Appl. Mater. Interfaces* **10** 34690–8
[32] Giri A, Hopkins P E, Wessel J G and Duda J C 2015 Kapitza resistance and the thermal conductivity of amorphous superlattices *J. Appl. Phys.* **118** 165303
[33] Lee E and Luo T 2017 The role of optical phonons in intermediate layer-mediated thermal transport across solid interfaces *Phys. Chem. Chem. Phys.* **19** 18407–15
[34] Cahill D G 2004 Analysis of heat flow in layered structures for time-domain thermoreflectance *Rev. Sci. Instrum.* **75** 5119–22
[35] Schmidt A J, Chen X and Chen G 2008 Pulse accumulation, radial heat conduction, and anisotropic thermal conductivity in pump–probe transient thermoreflectance *Rev. Sci. Instrum.* **79** 114902
[36] Schmidt A J, Cheaito R and Chiesa M 2009 A frequency-domain thermoreflectance method for the characterization of thermal properties *Rev. Sci. Instrum.* **80** 094901
[37] Lee E, Zhang T, Yoo T, Guo Z and Luo T 2016 Nanostructures significantly enhance thermal transport across solid interfaces *ACS Appl. Mater. Interfaces* **8** 35505–12
[38] Kazan M 2009 First principles calculation of the thermal conductance of GaN/Si and GaN/SiC interfaces as functions of the interface conditions *Appl. Phys. Lett.* **95** 141904
[39] Yates L *et al* 2018 Low thermal boundary resistance interfaces for GaN-on-diamond devices *ACS Appl. Mater. Interfaces* **10** 24302–9
[40] Giri A *et al* 2018 Interfacial defect vibrations enhance thermal transport in amorphous multilayers with ultrahigh thermal boundary conductance *Adv. Mater.* **30** e1804097
[41] Chalopin Y and Volz S 2013 A microscopic formulation of the phonon transmission at the nanoscale *Appl. Phys. Lett.* **103** 051602
[42] Murakami T, Hori T, Shiga T and Shiomi J 2014 Probing and tuning inelastic phonon conductance across finite-thickness interface *Appl. Phys. Exp.* **7** 121801
[43] Sääskilahti K, Oksanen J, Tulkki J and Volz S 2014 Role of anharmonic phonon scattering in the spectrally decomposed thermal conductance at planar interfaces *Phys. Rev.* B **90** 134312
[44] Gordiz K and Henry A 2015 A formalism for calculating the modal contributions to thermal interface conductance *New J. Phys.* **17** 103002
[45] Gordiz K and Henry A 2016 Phonon transport at interfaces: determining the correct modes of vibration *J. Appl. Phys.* **119** 015101
[46] Zhou Y and Hu M 2017 Full quantification of frequency-dependent interfacial thermal conductance contributed by two- and three-phonon scattering processes from nonequilibrium molecular dynamics simulations *Phys. Rev.* B **95** 115313

[47] Wu X and Luo T 2014 The importance of anharmonicity in thermal transport across solid–solid interfaces *J. Appl. Phys.* **115** 014901
[48] Wu X and Luo T 2015 Effect of electron–phonon coupling on thermal transport across metal–nonmetal interface—a second look *EPL (Europhys. Lett.)* **110** 67004
[49] Lee E and Luo T 2018 Thermal transport across solid–solid interfaces enhanced by pre-interface isotope–phonon scattering *Appl. Phys. Lett.* **112** 011603
[50] Carlborg C F, Shiomi J and Maruyama S 2008 Thermal boundary resistance between single-walled carbon nanotubes and surrounding matrices *Phys. Rev.* B **78** 205406
[51] Shenogina N, Keblinski P and Garde S 2008 Strong frequency dependence of dynamical coupling between protein and water *J. Chem. Phys.* **129** 155105
[52] Luo T and Lloyd J R 2010 Non-equilibrium molecular dynamics study of thermal energy transport in Au–SAM–Au junctions *Int. J. Heat Mass Transfer* **53** 1–11
[53] An M, Song Q, Yu X, Meng H, Ma D, Li R, Jin Z, Huang B and Yang N 2017 Generalized two-temperature model for coupled phonons in nanosized graphene *Nano Lett.* **17** 5805–10
[54] Luo T, Garg J, Shiomi J, Esfarjani K and Chen G 2013 Gallium arsenide thermal conductivity and optical phonon relaxation times from first-principles calculations *EPL (Europhys. Lett.)* **101** 16001
[55] Yang N, Zhang G and Li B 2008 Ultralow thermal conductivity of isotope-doped silicon nanowires *Nano Lett.* **8** 276–80
[56] Chen S, Wu Q, Mishra C, Kang J, Zhang H, Cho K, Cai W, Balandin A A and Ruoff R S 2012 Thermal conductivity of isotopically modified graphene *Nat. Mater.* **11** 203–7
[57] Lindsay L, Broido D A and Reinecke T L 2012 Thermal conductivity and large isotope effect in GaN from first principles *Phys. Rev. Lett.* **109** 095901
[58] Novikov S V, Morris R D, Kent A J, Geen H L and Foxon C T 2007 MBE growth of GaN using ^{15}N isotope for nuclear magnetic resonance applications *J. Cryst. Growth* **301–302** 417–9

Chapter 4

[1] Datta S 1997 *Electronic Transport in Mesoscopic Systems* (Cambridge: Cambridge University Press)
[2] Mingo N and Yang L 2003 Phonon transport in nanowires coated with an amorphous material: an atomistic Green's function approach *Phys. Rev.* B **68** 245406
[3] Zhang W, Fisher T S and Mingo N 2007 Simulation of interfacial phonon transport in Si–Ge heterostructures using an atomistic Green's function method *J. Heat Transfer* **129** 483
[4] Zhang W, Mingo N and Fisher T S 2007 Simulation of phonon transport across a non-polar nanowire junction using an atomistic Green's function method *Phys. Rev.* B **76** 195429
[5] Tian Z, Esfarjani K and Chen G 2012 Enhancing phonon transmission across a Si/Ge interface by atomic roughness: first-principles study with the Green's function method *Phys. Rev.* B **86** 235304
[6] Mingo N, Stewart D A, Broido D A and Srivastava D 2008 Phonon transmission through defects in carbon nanotubes from first principles *Phys. Rev.* B **77** 033418
[7] Esfarjani K and Stokes H T 2008 Method to extract anharmonic force constants from first principles calculations *Phys. Rev.* B **77** 144112
[8] Ong Z-Y and Zhang G 2015 Efficient approach for modeling phonon transmission probability in nanoscale interfacial thermal transport *Phys. Rev.* B **91** 174302

[9] Sadasivam S, Waghmare U V and Fisher T S 2017 Phonon-eigenspectrum-based formulation of the atomistic Green's function method *Phys. Rev.* B **96** 174302
[10] Mingo N 2006 Anharmonic phonon flow through molecular-sized junctions *Phys. Rev.* B **74** 125402
[11] Sadasivam S, Ye N, Feser J P, Charles J, Miao K, Kubis T and Fisher T S 2017 Thermal transport across metal silicide-silicon interfaces: first-principles calculations and Green's function transport simulations *Phys. Rev.* B **95** 085310
[12] Ryndyk D 2016 *Theory of Quantum Transport at Nanoscale* (Berlin: Springer), p 184
[13] Sadasivam S *et al* 2014 The atomistic Green's function method for interfacial phonon transport *Annu. Rev. Heat Transf.* **17** 89–145
[14] Teichert F, Zienert A, Schuster J and Schreiber M 2017 Improved recursive Green's function formalism for quasi one-dimensional systems with realistic defects *J. Comput. Phys.* **334** 607–19
[15] Sancho M L, Sancho J L and Rubio J 2001 Highly convergent scheme for the calculation of bulk and surface Green functions *J. Phys.* F **15** 851
[16] Velev J and Butler W 2004 On the equivalence of different techniques for evaluating the Green function for a semi-infinite system using a localized basis *J. Phys.: Condens. Matter.* **16** R637
[17] Huang Z, Murthy J Y and Fisher T S 2011 Modeling of polarization-specific phonon transmission through interfaces *J. Heat Transfer* **133** 114502
[18] Ong Z 2018 Tutorial: concepts and numerical techniques for modeling individual phonon transmission at interfaces *J. Appl. Phys.* **124** 151101
[19] Schwinger J 1961 Brownian motion of a quantum oscillator *J. Math. Phys.* **2** 407–32
[20] Kadanoff L P, Baym G and Trimmer J D 1963 Quantum statistical mechanics *Am. J. Phys.* **31** 309
[21] Keldysh L V 1965 Diagram technique for nonequilibrium processes *Sov. Phys. JETP* **20** 1018–26
[22] Economou E N 1983 *Green's Functions in Quantum Physics* (Berlin: Springer)
[23] Lifshitz E M and Pitaevskii L P 1981 *Course of Theoretical Physics: Physical Kinetics* (Oxford: Pergamon)
[24] Dai J and Tian Z 2019 Rigorous formalism of anharmonic atomistic Green's function for three-dimensional interfaces *Phys. Rev.* B **101** 041301

Chapter 5

[1] Chu S and Majumdar A 2012 Opportunities and challenges for a sustainable energy future *Nature* **488** 294–303
[2] Goldemberg J 2007 Ethanol for a sustainable energy future *Science* **315** 808–10
[3] Chu S, Cui Y and Liu N 2017 The path towards sustainable energy *Nat. Mater.* **16** 16–22
[4] Lund H 2007 Renewable energy strategies for sustainable development *Energy* **32** 912–9
[5] Baños R, Manzano-Agugliaro F, Montoya F G, Gil C, Alcayde A and Gómez J 2011 Optimization methods applied to renewable and sustainable energy: a review *Renew. Sustain. Energy Rev.* **15** 1753–66
[6] Sarı A and Karaipekli A 2007 Thermal conductivity and latent heat thermal energy storage characteristics of paraffin/expanded graphite composite as phase change material *Appl. Therm. Eng.* **27** 1271–7

[7] Mills A, Farid M, Selman J R and Al-Hallaj S 2006 Thermal conductivity enhancement of phase change materials using a graphite matrix *Appl. Therm. Eng.* **26** 1652–61
[8] Pei Q-X, Zhang Y-W, Sha Z-D and Shenoy V B 2013 Tuning the thermal conductivity of silicene with tensile strain and isotopic doping: a molecular dynamics study *J. Appl. Phys.* **114** 033526
[9] Guo Y, Cortes C L, Molesky S and Jacob Z 2012 Broadband super-Planckian thermal emission from hyperbolic metamaterials *Appl. Phys. Lett.* **101** 131106
[10] Marquier F, Joulain K, Mulet J P, Carminati R and Greffet J J 2004 Engineering infrared emission properties of silicon in the near field and the far field *Opt. Commun.* **237** 379–88
[11] Basu S, Zhang Z M and Fu C J 2009 Review of near-field thermal radiation and its application to energy conversion *Int. J. Energy Res.* **33** 1203–32
[12] Coppens Z J and Valentine J G 2017 Spatial and temporal modulation of thermal emission *Adv. Mater.* **29** 1701275
[13] Motayed A, Davydov A V, Vaudin M D, Levin I, Melngailis J and Mohammad S N 2006 Fabrication of GaN-based nanoscale device structures utilizing focused ion beam induced Pt deposition *J. Appl. Phys.* **100** 024306
[14] Xia Y, Rogers J A, Paul K E and Whitesides G M 1999 Unconventional methods for fabricating and patterning nanostructures *Chem. Rev.* **99** 1823–48
[15] Li X, Chang W-C, Chao Y J, Wang R and Chang M 2004 Nanoscale structural and mechanical characterization of a natural nanocomposite material:â the shell of red abalone *Nano Lett.* **4** 613–7
[16] Schmitt J *et al* 1997 Metal nanoparticle/polymer superlattice films: fabrication and control of layer structure *Adv. Mater.* **9** 61–5
[17] Jordan M I and Mitchell T M 2015 Machine learning: trends, perspectives, and prospects *Science* **349** 255–60
[18] LeCun Y, Bengio Y and Hinton G 2015 Deep learning *Nature* **521** 436–44
[19] Ghahramani Z 2015 Probabilistic machine learning and artificial intelligence *Nature* **521** 452–9
[20] Mnih V *et al* 2015 Human-level control through deep reinforcement learning *Nature* **518** 529–33
[21] Lengauer T, Sander O, Sierra S, Thielen A and Kaiser R 2007 Bioinformatics prediction of HIV coreceptor usage *Nat. Biotechnol.* **25** 1407–10
[22] Schadt E E, Linderman M D, Sorenson J, Lee L and Nolan G P 2011 Cloud and heterogeneous computing solutions exist today for the emerging big data problems in biology *Nat. Rev. Genet.* **12** 224
[23] Murphy R F 2011 An active role for machine learning in drug development *Nat. Chem. Biol.* **7** 327–30
[24] Ross D T *et al* 2000 Systematic variation in gene expression patterns in human cancer cell lines *Nat. Genet.* **24** 227–35
[25] Sanchez-Lengeling B and Aspuru-Guzik A 2018 Inverse molecular design using machine learning: generative models for matter engineering *Science* **361** 360–5
[26] Chakradhar S 2017 Predictable response: finding optimal drugs and doses using artificial intelligence *Nat. Med.* **23** 1244–7
[27] Zhang L, Tan J, Han D and Zhu H 2017 From machine learning to deep learning: progress in machine intelligence for rational drug discovery *Drug Discovery Today* **22** 1680–5

[28] Raccuglia P *et al* 2016 Machine-learning-assisted materials discovery using failed experiments *Nature* **533** 73–6
[29] Ahneman D T, Estrada J G, Lin S, Dreher S D and Doyle A G 2018 Predicting reaction performance in C–N cross-coupling using machine learning *Science* **360** 186–90
[30] Langley P 1988 Machine learning as an experimental science *Mach. Learn.* **3** 5–8
[31] Berman H M *et al* 2000 The protein data bank *Nucleic Acids Res.* **28** 235–42
[32] Snoek J, Larochelle H and Adams R P 2012 Practical Bayesian optimization of machine learning algorithms *Advances in Neural Information Processing Systems* vol 25 ed F Pereira, C J C Burges, L Bottou and K Q Weinberger (New York: Curran Associates), pp 2951–9
[33] Riniker S and Landrum G A 2015 Better informed distance geometry: using what we know to improve conformation generation *J. Chem. Inf. Model.* **55** 2562–74
[34] Hernández-Lobato J M, Requeima J, Pyzer-Knapp E O and Aspuru-Guzik A 2017 Parallel and distributed Thompson sampling for large-scale accelerated exploration of chemical space *Int. Conf. on Machine Learning* pp 1470–9
[35] Srinivas N, Krause A, Kakade S and Seeger M 2010 Gaussian process optimization in the bandit setting: no regret and experimental design *Int. Conf. on Machine Learning* pp 1015–22
[36] Shahriari B, Swersky K, Wang Z, Adams R P and de Freitas N 2016 Taking the human out of the loop: a review of Bayesian optimization *Proc. IEEE* **104** 148–75
[37] Brochu E, Cora V M and de Freitas N 2010 A tutorial on Bayesian optimization of expensive cost functions, with application to active user modeling and hierarchical reinforcement learning (arXiv:1012.2599)
[38] Swersky K, Snoek J and Adams R P 2013 Multi-task Bayesian optimization *Advances in Neural Information Processing Systems* vol 26 ed C J C Burges, L Bottou, M Welling, Z Ghahramani and K Q Weinberger (New York: Curran Associates), pp 2004–12
[39] Pedregosa F *et al* 2011 Scikit-learn: machine learning in Python *J. Mach. Learn. Res.* **12** 2825–30
[40] GPy 2012 GPy: A Gaussian process framework in python http://github.com/SheffieldML/GPy
[41] Ueno T, Rhone T D, Hou Z, Mizoguchi T and Tsuda K 2016 COMBO: an efficient Bayesian optimization library for materials science *Mater. Discovery* **4** 18–21
[42] Yamashita T, Sato N, Kino H, Miyake T, Tsuda K and Oguchi T 2018 Crystal structure prediction accelerated by Bayesian optimization *Phys. Rev. Mater.* **2** 013803
[43] Ju S, Shiga T, Feng L, Hou Z, Tsuda K and Shiomi J 2017 Designing nanostructures for phonon transport via Bayesian optimization *Phys. Rev.* X **7** 021024
[44] Yamawaki M, Ohnishi M, Ju S and Shiomi J 2018 Multifunctional structural design of graphene thermoelectrics by Bayesian optimization *Sci. Adv.* **4** eaar4192
[45] Sakurai A *et al* 2019 Ultranarrow-band wavelength-selective thermal emission with aperiodic multilayered metamaterials designed by Bayesian optimization *ACS Cent. Sci.* **5** 319–26
[46] Seko A, Togo A, Hayashi H, Tsuda K, Chaput L and Tanaka I 2015 Prediction of low-thermal-conductivity compounds with first-principles anharmonic lattice-dynamics calculations and Bayesian optimization *Phys. Rev. Lett.* **115** 205901

[47] Tian Z, Esfarjani K and Chen G 2012 Enhancing phonon transmission across a Si/Ge interface by atomic roughness: first-principles study with the Green's function method *Phys. Rev.* B **86** 235304
[48] Merabia S and Termentzidis K 2014 Thermal boundary conductance across rough interfaces probed by molecular dynamics *Phys. Rev.* B **89** 054309
[49] Liu Y, Hu C, Huang J, Sumpter B G and Qiao R 2015 Tuning interfacial thermal conductance of graphene embedded in soft materials by vacancy defects *J. Chem. Phys.* **142** 244703
[50] Arora A, Hori T, Shiga T and Shiomi J 2017 Thermal rectification in restructured graphene with locally modulated temperature dependence of thermal conductivity *Phys. Rev.* B **96** 165419
[51] Sakata M, Oyake T, Maire J, Nomura M, Higurashi E and Shiomi J 2015 Thermal conductance of silicon interfaces directly bonded by room-temperature surface activation *Appl. Phys. Lett.* **106** 081603
[52] Lanzara A *et al* 2001 Evidence for ubiquitous strong electron–phonon coupling in high-temperature superconductors *Nature* **412** 510–4
[53] Yan J, Zhang Y, Kim P and Pinczuk A 2007 Electric field effect tuning of electron–phonon coupling in graphene *Phys. Rev. Lett.* **98** 166802
[54] Lin Z, Zhigilei L V and Celli V 2008 Electron–phonon coupling and electron heat capacity of metals under conditions of strong electron–phonon nonequilibrium *Phys. Rev.* B **77** 075133
[55] Brorson S D *et al* 1990 Femtosecond room-temperature measurement of the electron–phonon coupling constant γ in metallic superconductors *Phys. Rev. Lett.* **64** 2172–5
[56] Hameau S *et al* 1999 Strong electron–phonon coupling regime in quantum dots: evidence for everlasting resonant polarons *Phys. Rev. Lett.* **83** 4152–5
[57] Sood A K, Chandrabhas N, Muthu D V S and Jayaraman A 1995 Phonon interference in $BaTiO_3$: high-pressure Raman study *Phys. Rev.* B **51** 8892–6
[58] Han H, Potyomina L G, Darinskii A A, Volz S and Kosevich Y A 2014 Phonon interference and thermal conductance reduction in atomic-scale metamaterials *Phys. Rev.* B **89** 180301
[59] Feng L, Shiga T, Han H, Ju S, Kosevich Y A and Shiomi J 2017 Phonon-interference resonance effects by nanoparticles embedded in a matrix *Phys. Rev.* B **96** 220301
[60] Lim M, Lee S S and Lee B J 2015 Near-field thermal radiation between doped silicon plates at nanoscale gaps *Phys. Rev.* B **91** 195136
[61] Tang G and Wang J-S 2018 Heat transfer statistics in extreme-near-field radiation *Phys. Rev.* B **98** 125401
[62] Ilic O, Jablan M, Joannopoulos J D, Celanovic I, Buljan H and Soljačić M 2012 Near-field thermal radiation transfer controlled by plasmons in graphene *Phys. Rev.* B **85** 155422
[63] Messina R, Jin W and Rodriguez A W 2016 Strongly coupled near-field radiative and conductive heat transfer between planar bodies *Phys. Rev.* B **94** 121410
[64] Worthing P T and Barnes W L 2001 Efficient coupling of surface plasmon polaritons to radiation using a bi-grating *Appl. Phys. Lett.* **79** 3035–7
[65] Zhong R, Yu C, Hu M and Liu S 2018 Surface plasmon polaritons light radiation source with asymmetrical structure *AIP Adv.* **8** 015327

[66] Le Gall J, Olivier M and Greffet J-J 1997 Experimental and theoretical study of reflection and coherent thermal emissionby a SiC grating supporting a surface-phonon polariton *Phys. Rev.* B **55** 10105–14
[67] Lee B J and Zhang Z M 2008 Lateral shifts in near-field thermal radiation with surface phonon polaritons *Nanoscale Microscale Thermophys. Eng.* **12** 238–50
[68] Mulet J-P, Joulain K, Carminati R and Greffet J-J 2002 Enhanced radiative heat transfer at nanometric distances *Microscale Thermophys. Eng.* **6** 209–22
[69] Gramotnev D K and Bozhevolnyi S I 2014 Nanofocusing of electromagnetic radiation *Nat. Photonics* **8** 13–22
[70] Nielsen M G, Pors A, Albrektsen O and Bozhevolnyi S I 2012 Efficient absorption of visible radiation by gap plasmon resonators *Opt. Express* **20** 13311–9
[71] Ginzburg P, Arbel D and Orenstein M 2006 Gap plasmon polariton structure for very efficient microscale-to-nanoscale interfacing *Opt. Lett.* **31** 3288–90
[72] Bharadwaj P, Bouhelier A and Novotny L 2011 Electrical excitation of surface plasmons *Phys. Rev. Lett.* **106** 226802
[73] Yang Y and Wang L 2016 Spectrally enhancing near-field radiative transfer between metallic gratings by exciting magnetic polaritons in nanometric vacuum gaps *Phys. Rev. Lett.* **117** 044301
[74] Wang L P and Zhang Z M 2009 Resonance transmission or absorption in deep gratings explained by magnetic polaritons *Appl. Phys. Lett.* **95** 111904
[75] Lee B J, Wang L P and Zhang Z M 2008 Coherent thermal emission by excitation of magnetic polaritons between periodic strips and a metallic film *Opt. Express* **16** 11328–36
[76] Pendry J B, Martín-Moreno L and Garcia-Vidal F J 2004 Mimicking surface plasmons with structured surfaces *Science* **305** 847–8
[77] Zayats A V and Smolyaninov I I 2003 Near-field photonics: surface plasmon polaritons and localized surface plasmons *J. Opt. A: Pure Appl. Opt.* **5** S16–50
[78] Maier S A, Andrews S R, Martín-Moreno L and García-Vidal F J 2006 Terahertz surface plasmon–polariton propagation and focusing on periodically corrugated metal wires *Phys. Rev. Lett.* **97** 176805
[79] Caldwell J D *et al* 2015 Low-loss, infrared and terahertz nanophotonics using surface phonon polaritons *Nanophotonics* **4** 44–68
[80] Feng K *et al* 2015 Localized surface phonon polariton resonances in polar gallium nitride *Appl. Phys. Lett.* **107** 081108
[81] Huber A J, Ocelic N and Hillenbrand R 2008 Local excitation and interference of surface phonon polaritons studied by near-field infrared microscopy *J. Microsc.* **229** 389–95
[82] Hillenbrand R, Taubner T and Keilmann F 2002 Phonon-enhanced light–matter interaction at the nanometre scale *Nature* **418** 159–62
[83] Meijer G I 2010 Cooling energy-hungry data centers *Science* **328** 318–9
[84] Garner R 2018 Cutting-edge heat shield installed on NASA's Parker Solar Probe, NASA, Available from: http://nasa.gov/feature/goddard/2018/cutting-edge-heat-shield-installed-on-nasa-s-parker-solar-probe (Accessed: 28 February 2019)
[85] Zhang W, Fisher T S and Mingo N 2006 Simulation of interfacial phonon transport in Si–Ge heterostructures using an atomistic Green's function method *J. Heat Transfer* **129** 483–91
[86] Wang J-S, Wang J and Lü J T 2008 Quantum thermal transport in nanostructures *Eur. Phys. J.* B **62** 381–404

[87] Oyake T, Feng L, Shiga T, Isogawa M, Nakamura Y and Shiomi J 2018 Ultimate confinement of phonon propagation in silicon nanocrystalline structure *Phys. Rev. Lett.* **120** 045901
[88] Ju S, Shiga T, Feng L and Shiomi J 2018 Revisiting PbTe to identify how thermal conductivity is really limited *Phys. Rev.* B **97** 184305
[89] Gaskins J T *et al* 2018 Thermal boundary conductance across heteroepitaxial ZnO/GaN interfaces: assessment of the phonon gas model *Nano Lett.* **18** 7469–77
[90] Jia L, Ju S, Liang X and Zhang X 2016 Tuning phonon transmission and thermal conductance by roughness at rectangular and triangular Si/Ge interface *Mater. Res. Express* **3** 095024
[91] Hopkins P E, Norris P M, Tsegaye M S and Ghosh A W 2009 Extracting phonon thermal conductance across atomic junctions: nonequilibrium Green's function approach compared to semiclassical methods *J. Appl. Phys.* **106** 063503
[92] Hyldgaard P 2004 Resonant thermal transport in semiconductor barrier structures *Phys. Rev.* B **69** 193305
[93] Wang J, Li L and Wang J-S 2011 Tuning thermal transport in nanotubes with topological defects *Appl. Phys. Lett.* **99** 091905
[94] Wäckelgård E and Hultmark G 1998 Industrially sputtered solar absorber surface *Sol. Energy Mater. Sol. Cells* **54** 165–70
[95] Rephaeli E and Fan S 2008 Tungsten black absorber for solar light with wide angular operation range *Appl. Phys. Lett.* **92** 211107
[96] Hsu P-C *et al* 2016 Radiative human body cooling by nanoporous polyethylene textile *Science* **353** 1019–23
[97] Hsu P-C *et al* 2017 A dual-mode textile for human body radiative heating and cooling *Sci. Adv.* **3** e1700895
[98] Ilic O, Bermel P, Chen G, Joannopoulos J D, Celanovic I and Soljačić M 2016 Tailoring high-temperature radiation and the resurrection of the incandescent source *Nat. Nanotechnol.* **11** 320–4
[99] Raman A P, Anoma M A, Zhu L, Rephaeli E and Fan S 2014 Passive radiative cooling below ambient air temperature under direct sunlight *Nature* **515** 540–4
[100] Lee B J and Zhang Z M 2006 Design and fabrication of planar multilayer structures with coherent thermal emission characteristics *J. Appl. Phys.* **100** 063529
[101] Huang Z and Ruan X 2017 Nanoparticle embedded double-layer coating for daytime radiative cooling *Int. J. Heat Mass Transfer* **104** 890–96
[102] Atiganyanun S *et al* 2018 Effective radiative cooling by paint-format microsphere-based photonic random media *ACS Photonics* **5** 1181–7
[103] Basu S and Wang L 2013 Near-field radiative heat transfer between doped silicon nanowire arrays *Appl. Phys. Lett.* **102** 053101
[104] Chang J-Y, Wang H and Wang L 2017 Tungsten nanowire metamaterials as selective solar thermal absorbers by excitation of magnetic polaritons *J. Heat Transfer* **139** 052401
[105] Xia F, Wang H, Xiao D, Dubey M and Ramasubramaniam A 2014 Two-dimensional material nanophotonics *Nat. Photonics* **8** 899–907
[106] Zhao B and Zhang Z M 2015 Strong plasmonic coupling between graphene ribbon array and metal gratings *ACS Photonics* **2** 1611–8
[107] Dai S *et al* 2014 Tunable phonon polaritons in atomically thin van der Waals crystals of boron nitride *Science* **343** 1125–9

[108] Wang L P and Zhang Z M 2011 Phonon-mediated magnetic polaritons in the infrared region *Opt. Express* **19** A126–35
[109] Liu D, Tan Y, Khoram E and Yu Z 2018 Training deep neural networks for the inverse design of nanophotonic structures *ACS Photonics* **5** 1365–9
[110] Liu Z, Zhu D, Rodrigues S P, Lee K-T and Cai W 2018 Generative model for the inverse design of metasurfaces *Nano. Lett.* **18** 6570–6
[111] Ma W, Cheng F and Liu Y 2018 Deep-learning-enabled on-demand design of chiral metamaterials *ACS Nano.* **12** 6326–34
[112] Ma W, Cheng F, Xu Y, Wen Q and Liu Y 2019 Probabilistic Representation and inverse design of metamaterials based on a deep generative model with semi-supervised learning strategy *Adv. Mater.* **31** 1901111

Chapter 6

[1] Phelan D, Millican J N, Thomas E L, Leão J B, Qiu Y and Paul R 2009 Neutron scattering measurements of the phonon density of states of $FeSe_{1-x}$ superconductors *Phys. Rev.* B **79** 014519
[2] Piovano A 2015 Inelastic neutron scattering applied to materials for energy *EPJ Web Conf.* **104** 01006
[3] Mukhopadhyay S, Bansal D, Delaire O, Perrodin D, Bourret-Courchesne E, Singh D J and Lindsay L 2017 The curious case of cuprous chloride: giant thermal resistance and anharmonic quasiparticle spectra driven by dispersion nesting *Phys. Rev.* B **96** 100301
[4] Li C W *et al* 2014 Phonon self-energy and origin of anomalous neutron scattering spectra in SnTe and PbTe thermoelectrics *Phys. Rev. Lett.* **112** 175501
[5] Tian Z, Li M, Ren Z, Ma H, Alatas A, Wilson S D and Li J 2015 Inelastic x-ray scattering measurements of phonon dispersion and lifetimes in $PbTe_{1-x}$ Se_x alloys *J. Phys. Condens. Matter.* **27** 375403
[6] Ma H, Li C, Tang S, Yan J, Alatas A, Lindsay L, Sales B C and Tian Z 2016 Boron arsenide phonon dispersion from inelastic x-ray scattering: potential for ultrahigh thermal conductivity *Phys. Rev.* B **94** 220303
[7] Menendez J and Cardona M 1984 Temperature dependence of the first-order Raman scattering by phonons in Si, Ge, and α-Sn: anharmonic effects *Phys. Rev.* B **29** 2051–9
[8] Cusca R, Gil B, Cassabois G and Artus L 2016 Temperature dependence of Raman-active phonons and anharmonic interactions in layered hexagonal BN *Phys. Rev.* B **94** 155435
[9] Ponosov Y S and Streltsov S V 2017 Raman-active E_{2g} phonon in MgB_2: electron–phonon interaction and anharmonicity *Phys. Rev.* B **96** 214503
[10] Ziegler F, Gibhardt H, Leist J and Eckold G 2015 High-resolution polarised Raman scattering study on spin-phonon coupling in multiferroic $MnWO_4$ *Mater. Res. Exp.* **2** 096103
[11] Blumberg G, Klein M V, Börjesson L, Liang R and Hardy W N 1994 Investigation of the temperature dependence of electron and phonon Raman scattering in single crystal $YBa_2Cu_3O_{6.952}$ *J. Superconduct* **7** 445–8
[12] Perez-Osorio M A, Lin Q, Phillips R T, Milot R L, Herz L M, Johnston M B and Giustino F 2018 Raman spectrum of the organic–inorganic halide perovskite CH_3NH_3 PbI_3 from first principles and high-resolution low-temperature Raman measurements *J. Phys. Chem.* C **122** 21703–17

[13] Mukhopadhyay S, Parker D S, Sales B C, Puretzky A A, McGuire M A and Lindsay L 2018 Two-channel model for ultralow thermal conductivity of crystalline Tl_3VSe_4 *Science* **360** 1455–8
[14] Yan R, Simpson J R, Bertolazzi S, Brivio J, Watson M, Wu X, Kis A, Luo T, Hight Walker A R and Xing H G 2014 Thermal conductivity of monolayer molybdenum disulfide obtained from temperature-dependent Raman spectroscopy *ACS Nano* **8** 986–93
[15] Calizo I, Balandin A A, Bao W, Miao F and Lau Temperature C N 2007 Dependence of the Raman spectra of graphene and graphene multilayers *Nano Lett.* **7** 2645–9
[16] Neumann C *et al* 2015 Raman spectroscopy as probe of nanometre-scale strain variations in graphene *Nat. Commun.* **6** 8429
[17] Lee J-U, Yoon D, Kim H, Lee S W and Cheong Thermal H 2011 Conductivity of suspended pristine graphene measured by Raman spectroscopy *Phys. Rev.* B **83** 081419
[18] Chen S *et al* 2011 Raman measurements of thermal transport in suspended monolayer graphene of variable sizes in vacuum and gaseous environments *ACS Nano* **5** 321–8
[19] Minnich A J 2012 Determining phonon mean free paths from observations of quasiballistic thermal transport *Phys. Rev. Lett.* **109** 205901
[20] Cuffe J *et al* 2015 Reconstructing phonon mean-free-path contributions to thermal conductivity using nanoscale membranes *Phys. Rev.* B **91** 245423
[21] Hu Y, Zeng L, Minnich A J, Dresselhaus M S and Chen G 2015 Spectral mapping of thermal conductivity through nanoscale ballistic transport *Nat. Nanotechnol.* **10** 701–6
[22] Zeng L *et al* Measuring phonon mean free path distributions by probing quasiballistic phonon transport in grating nanostructures *Sci. Rep.* **5** 17131
[23] Hoogeboom-Pot K M *et al* A new regime of nanoscale thermal transport: collective diffusion increases dissipation efficiency**112** 4846–51
[24] Regner K, Sellan D, Su Z, Amon C, McGaughey A and Malen J 2012 Broadband phonon mean free path contributions to thermal conductivity measured using frequency-domain thermoreflectance *Nat. Commun.* **4** 1640
[25] Hua C, Chen X, Ravichandran N K and Minnich A J 2017 Experimental metrology to obtain thermal phonon transmission coefficients at solid interfaces *Phys. Rev.* B **95** 205423
[26] Ravichandran N K, Zhang H and Minnich A J 2018 Spectrally resolved specular reflections of thermal phonons from atomically rough surfaces *Phys. Rev.* X **8** 041004
[27] Forghani M and Hadjiconstantinou N G 2019 Phonon relaxation time reconstruction from transient thermal grating experiments and comparison with density functional theory predictions *Appl. Phys. Lett.* **114** 023106
[28] Casimir H B G 1938 Note on the conduction of heat in crystals *Physica* **5** 495–500
[29] Lan Y, Jerome Minnich A, Chen G and Ren Z 2010 Enhancement of thermoelectric figure-of-merit by a bulk nanostructuring approach *Adv. Funct. Mater.* **20** 357–76
[30] Biswas K, He J, Blum I V, Wu C I, Hogan T P, Seidman D N, Dravid V P and Kanatzidis M G 2012 High-performance bulk thermoelectrics with all-scale hierarchical architectures *Nature* **489** 414–8
[31] Hsiao T-K, Chang H-K, Liou S-C, Chu M-W, Lee S-C and Chang C-W 2013 Observation of room-temperature ballistic thermal conduction persisting over 8.3 μm in SiGe nanowires *Nat. Nanotechnol* **8** 534–8
[32] Li D, Wu Y, Kim P, Shi L, Yang P and Majumdar A 2003 Thermal conductivity of individual silicon nanowires *Appl. Phys. Lett.* **83** 2934–6

[33] Boukai A I, Bunimovich Y, Tahir-Kheli J, Yu J-K, Goddard W A III and Heath J R 2008 Silicon nanowires as efficient thermoelectric materials *Nature* **451** 168–71
[34] Chang C W, Okawa D, Garcia H, Majumdar A and Zettl A 2008 Breakdown of Fourier's law in nanotube thermal conductors *Phys. Rev. Lett.* **101** 075903
[35] Mei S and Knezevic I 2015 Thermal conductivity of III–V semiconductor superlattices *J. Appl. Phys.* **118** 175101
[36] Zhang H, Hua C, Ding D and Minnich A J 2015 Length dependent thermal conductivity measurements yield phonon mean free path spectra in nanostructures *Sci. Rep.* **5** 9121
[37] Sverdrup P G, Sinha S, Asheghi M, Uma S and Goodson K E 2001 Measurement of ballistic phonon conduction near hotspots in silicon *Appl. Phys. Lett.* **78** 3331–3
[38] Highland M, Gundrum B C, Koh Y K, Averback R S, Cahill D G, Elarde V C, Coleman J J, Walko D A and Landahl E C 2007 Ballistic-phonon heat conduction at the nanoscale as revealed by time-resolved x-ray diffraction and time-domain thermoreflectance *Phys. Rev.* B **76** 075337
[39] Siemens M E, Li Q, Yang R, Nelson K A, Anderson E H, Margaret M and Kapteyn H C 2010 Quasi-ballistic thermal transport from nanoscale interfaces observed using ultrafast coherent soft x-ray beams *Nat. Mater.* **9** 29–30
[40] Johnson J A, Maznev A A, Cuffe J, Eliason J K, Minnich A J, Kehoe T, Sotomayor Torres C M, Chen G and Nelson K A 2015 Direct measurement of room-temperature nondiffusive thermal transport over micron distances in a silicon membrane *Phys. Rev. Lett.* **110** 025901
[41] Robbins A B, Drakopoulos S X, Ignacio M-F, Ronca S and Minnich A J 2019 Ballistic thermal phonons traversing nanocrystalline domains in oriented polyethylene *Proc. Natl Acad. Sci.* **116** 17163–8
[42] Cahill D G *et al* 2014 Nanoscale thermal transport II: 2003–2012 *Appl. Phys. Rev.* **1** 011305
[43] Koh Y K and Cahill D G 2007 Frequency dependence of the thermal conductivity of semiconductor alloys *Phys. Rev.* B **76** 075207
[44] Minnich A J, Johnson J A, Schmidt A J, Esfarjani K, Dresselhaus M S, Nelson K A and Chen G 2015 Thermal conductivity spectroscopy technique to measure phonon mean free paths *Phys. Rev. Lett.* **107** 095901
[45] English T S, Phinney L M, Hopkins P E and Serrano J R 2013 Mean free path effects on the experimentally measured thermal conductivity of single-crystal silicon microbridges *J. Heat Transfer* **135** 091103
[46] Peierls R 1929 On the kinetic theory of thermal conduction in crystals *Ann. Phys.* **3** 1055
[47] Guyer R A and Krumhansl J A 1966 Solution of the linearized phonon Boltzmann equation *Phys. Rev.* **148** 766–78
[48] Hamilton R A H and Parrott J E 1969 Variational calculation of the thermal conductivity of germanium *Phys. Rev.* **178** 1284–92
[49] Srivastava G P 1976 Derivation and calculation of complementary variational principles for the lattice thermal conductivity *J. Phys. C: Solid State Phys.* **9** 3037
[50] Levinson I B 1980 Nonlocal phonon heat conductivity *J. Exp. Theor. Phys.* **52** 704
[51] Ward A, Broido D A, Stewart D A and Deinzer G 2009 *Ab initio* theory of the lattice thermal conductivity in diamond *Phys. Rev.* B **80** 125203
[52] Broido D A, Ward A and Mingo N 2005 Lattice thermal conductivity of silicon from empirical interatomic potentials *Phys. Rev.* B **72** 014308
[53] Li W, Carrete J, Katcho N A and Mingo N 2014 ShengBTE: a solver of the Boltzmann transport equation for phonons *Comput. Phys. Commun.* **185** 1747–58

[54] Carrete J, Vermeersch B, Katre A, van Roekeghem A, Wang T, Madsen G K H and Mingo N 2017 almaBTE: a solver of the space-time dependent Boltzmann transport equation for phonons in structured materials *Comput. Phys. Commun.* **220** 351–62
[55] Omini M and Sparavigna A 1995 An iterative approach to the phonon Boltzmann equation in the theory of thermal conductivity *Physica* B **212** 101–12
[56] Fugallo G, Lazzeri M, Paulatto L and Mauri F 2013 *Ab initio* variational approach for evaluating lattice thermal conductivity *Phys. Rev.* B **88** 045430
[57] Chaput L 2013 Direct solution to the linearized phonon Boltzmann equation *Phys. Rev. Lett.* **110** 265506
[58] Cepellotti A and Marzari N 2016 Thermal transport in crystals as a kinetic theory of relaxons *Phys. Rev.* X **6** 041013
[59] Hardy R J 1970 Phonon Boltzmann equation and second sound in solids *Phys. Rev.* B **2** 1193–207
[60] Hardy R J 1965 Lowest-order contribution to the lattice thermal conductivity *J. Math. Phys.* **6** 1749–61
[61] Cepellotti A and Marzari N 2017 Boltzmann transport in nanostructures as a friction effect *Nano Lett.* **17** 4675–82
[62] Wilson R B, Feser J P, Hohensee G T and Cahill D G 2013 Two-channel model for nonequilibrium thermal transport in pump–probe experiments *Phys. Rev.* B **88** 144305
[63] Yang F and Dames C 2015 Heating-frequency-dependent thermal conductivity: an analytical solution from diffusive to ballistic regime and its relevance to phonon scattering measurements *Phys. Rev.* B **91** 165311
[64] Torres P, Ziabari A, Torelló A, Bafaluy J, Camacho J, Cartoixà X, Shakouri A and Alvarez F X 2018 Emergence of hydrodynamic heat transport in semiconductors at the nanoscale *Phys. Rev. Mater* **2** 076001
[65] Vermeersch B, Carrete J, Mingo N and Shakouri A 2015 Superdiffusive heat conduction in semiconductor alloys. I. Theoretical foundations *Phys. Rev.* B **91** 085202
[66] Maznev A A, Johnson J A and Nelson K A 2011 Onset of nondiffusive phonon transport in transient thermal grating decay *Phys. Rev.* B **84** 195206
[67] Maassen J and Lundstrom M 2015 Steady-state heat transport: ballistic-to-diffusive with Fourier's law *J. Appl. Phys.* **117** 035104
[68] Mahan G D and Claro F 1988 Nonlocal theory of thermal conductivity *Phys. Rev.* B **38** 1963–9
[69] Hua C and Minnich A J 2014 Analytical Green's function of the multidimensional frequency-dependent phonon Boltzmann equation *Phys. Rev.* B **90** 214306
[70] Allen P B and Perebeinos V 2018 Temperature in a Peierls–Boltzmann treatment of nonlocal phonon heat transport *Phys. Rev.* B **98** 085427
[71] Collins K C, Maznev A A, Tian Z, Esfarjani K, Nelson K A and Chen G 2013 Non-diffusive relaxation of a transient thermal grating analyzed with the Boltzmann transport equation *J. Appl. Phys.* **114** 104302
[72] Hua C and Minnich A J 2015 Semi-analytical solution to the frequency-dependent Boltzmann transport equation for cross-plane heat conduction in thin films *J. Appl. Phys.* **117** 175306
[73] Kan Koh Y, Cahill D G and Sun B 2014 Nonlocal theory for heat transport at high frequencies *Phys. Rev.* B **90** 205412

[74] Ramu A T and Ma Y 2014 An enhanced Fourier law derivable from the Boltzmann transport equation and a sample application in determining the mean-free path of nondiffusive phonon modes *J. Appl. Phys.* **116** 093501
[75] Regner K T, McGaughey A J H and Malen J A 2014 Analytical interpretation of nondiffusive phonon transport in thermoreflectance thermal conductivity measurements *Phys. Rev.* B **90** 064302
[76] Zeng L and Chen G 2014 Disparate quasiballistic heat conduction regimes from periodic heat sources on a substrate *J. Appl. Phys.* **116** 064307
[77] Vermeersch B, Carrete J, Mingo N and Shakouri A 2015 Superdiffusive heat conduction in semiconductor alloys. I. Theoretical foundations *Phys. Rev.* B **91** 085202
[78] Peraud J-P M and Hadjiconstantinou N G 2011 Efficient simulation of multidimensional phonon transport using energy-based variance-reduced Monte Carlo formulations *Phys. Rev.* B **84** 205331
[79] Peraud J-P M and Hadjiconstantinou N G 2012 An alternative approach to efficient simulation of micro/nanoscale phonon transport *Appl. Phys. Lett.* **101** 15311
[80] Hua C and Minnich A J 2014 Importance of frequency-dependent grain boundary scattering in nanocrystalline silicon and silicongermanium thermoelectrics *Semicond. Sci. Technol.* **29** 124004
[81] Minnich A J, Chen G, Mansoor S and Yilbas B S 2011 Quasiballistic heat transfer studied using the frequency-dependent Boltzmann transport equation *Phys. Rev.* B **84** 235207
[82] Péraud J-P M and Hadjiconstantinou N G 2015 Adjoint-based deviational Monte Carlo methods for phonon transport calculations *Phys. Rev.* B **91** 235321
[83] Hua C, Lindsay L, Chen X and Minnich A A generalized Fourier's law for non-diffusive thermal transport: theory and experiment *Phys. Rev.* B **100** 085203
[84] Xu X *et al* 2014 Length-dependent thermal conductivity in suspended single-layer graphene *Nat. Commun.* **5** 3689
[85] Grant M and Boyd S 2014 CVX: Matlab software for disciplined convex programming, version 2.1. Available from: http://cvxr.com/cvx March 2014
[86] Grant M and Boyd S 2008 Graph implementations for nonsmooth convex programs *Recent Advances in Learning and Control, Lecture Notes* ed V Blondel, S Boyd and H Kimura (Berlin: Springer), pp 95–110 http://stanford.edu/boyd/graph_dcp.html
[87] Hastings W K 1970 Monte Carlo sampling methods using Markov chains and their applications *Biometrika* **57** 97–109
[88] Nelder J A and Mead R 1965 A simplex method for function minimization *Comput. J.* **7** 308–13
[89] Forghani M, Hadjiconstantinou N G and Péraud J-P M 2016 Reconstruction of the phonon relaxation times using solutions of the Boltzmann transport equation *Phys. Rev.* B **94** 155439
[90] Forghani M and Hadjiconstantinou N G 2018 Reconstruction of phonon relaxation times from systems featuring interfaces with unknown properties *Phys. Rev.* B **97** 195440
[91] Wei Z, Yang J, Chen W, Bi K, Li D and Chen Y 2014 Phonon mean free path of graphite along the *c*-axis *Appl. Phys. Lett.* **104** 081903
[92] Hua C and Minnich A J 2014 Transport regimes in quasiballistic heat conduction *Phys. Rev.* B **89** 094302
[93] Sondheimer E H 1952 *The Mean Free Path of Electrons in Metals* (Oxford: Taylor and Francis)

[94] Fuchs K 1938 The conductivity of thin metallic films according to the electron theory of metals *Math. Proc. Camb. Phil. Soc.* **34** 100–8
[95] Ravichandran N K and Minnich A J 2016 Role of thermalizing and nonthermalizing walls in phonon heat conduction along thin films *Phys. Rev.* B **93** 035314
[96] Koh Y K and Cahill D G 2007 Frequency dependence of the thermal conductivity of semiconductor alloys *Phys. Rev.* B **76** 075207
[97] Kang J S, Li M, Wu H, Nguyen H and Hu Y 2018 Experimental observation of high thermal conductivity in boron arsenide *Science* **361** 575–8
[98] Li S, Zheng Q, Lv Y, Liu X, Wang X, Huang P Y, Cahill D G and Lv B 2018 High thermal conductivity in cubic boron arsenide crystals *Science* **361** 579–81
[99] Capinski W S and Maris H J 1996 Improved apparatus for picosecond pump and probe optical measurements *Rev. Sci. Instrum.* **67** 2720–6
[100] Schmidt A J, Chen X and Chen G 2008 Pulse accumulation, radial heat conduction, and anisotropic thermal conductivity in pump–probe transient thermoreflectance *Rev. Sci. Instrum.* **79** 114902
[101] Ding D, Chen X and Minnich A J 2014 Radial quasiballistic transport in time-domain thermoreflectance studied using Monte Carlo simulations *Appl. Phys. Lett.* **104** 143104
[102] Tian F *et al* 2018 Unusual high thermal conductivity in boron arsenide bulk crystals *Science* **361** 582–5
[103] Lindsay L, Broido D A and Reinecke T L 2013 First-principles determination of ultrahigh thermal conductivity of boron arsenide: a competitor for diamond? *Phys. Rev. Lett.* **111** 025901
[104] Broido D A, Lindsay L and Reinecke T L 2013 *Ab initio* study of the unusual thermal transport properties of boron arsenide and related materials *Phys. Rev.* B **88** 214303
[105] Feng T, Lindsay L and Ruan X 2017 Four-phonon scattering significantly reduces intrinsic thermal conductivity of solids *Phys. Rev.* B **96** 161201
[106] Chen X, Hua C, Zhang H, Ravichandran N K and Minnich A J 2018 Quasiballistic thermal transport from nanoscale heaters and the role of the spatial frequency *Phys. Rev. Appl.* **10** 054068
[107] Hua C and Minnich A J 2018 Heat dissipation in the quasiballistic regime studied using the Boltzmann equation in the spatial frequency domain *Phys. Rev.* B **97** 014307

Chapter 7

[1] De Wette F W, Nosanow L H and Werthamer N R 1967 Calculation of phonon frequencies and thermodynamic properties of crystalline bcc helium *Phys. Rev.* **162** 824
[2] Maradudin A A and Fein A E 1962 Scattering of neutrons by an anharmonic crystal *Phys. Rev.* **128** 2589
[3] Born M and Hooton D J 1955 Statistische Dynamik mehrfach periodischer Systeme *Z. Phys.* **142** 201
[4] Hooton D 1955 LI. a new treatment of anharmonicity in lattice thermodynamics: I *Lond. Edinb. Dubl. Philos. Mag. J. Sci.* **46** 422
[5] Boccara N and Sarma G 1965 Theorie microscopique des transitions s'accompagnant d' une modification de la structure cristalline *Phys. Phys. Fiz.* **1** 219
[6] Wick G C 1950 The evaluation of the collision matrix *Phys. Rev.* **80** 268
[7] Horner H 1967 Lattice dynamics of quantum crystals *Z. Phys.* **205** 72

[8] Gillis N S, Werthamer N R and Koehler T R 1968 Properties of crystalline argon and neon in the self-consistent phonon approximation *Phys. Rev.* **165** 951
[9] Feynman R P 1972 *Statistical Mechanics, a Set of Lectures* (Reading, MA: Benjamin/Cummings)
[10] Isihara A 1968 The Gibbs–Bogoliubov inequality *J. Phys. A: Gen. Phys.* **1** 539
[11] Bauer E and Wu T Y 1956 Thermal expansion of a linear chain *Phys. Rev.* **104** 914
[12] Car R and Parrinello M 1985 Unified approach for molecular dynamics and density-functional theory *Phys. Rev. Lett.* **55** 2471
[13] Ceperley D M 1995 Path integrals in the theory of condensed helium *Rev. Mod. Phys.* **67** 279
[14] Hooton D J 1958 The use of a model in anharmonic lattice dynamics *Philos. Mag. J. Theor. Exp. Appl. Phys.* **3** 49
[15] Koehler T R 1966 Theory of the self-consistent harmonic approximation with application to solid neon *Phys. Rev. Lett.* **17** 89
[16] Bernardes N 1958 Theory of solid Ne, A, Kr, and Xe at 0 K *Phys. Rev.* **112** 1534
[17] Nosanow L H and Shaw G L 1962 Hartree calculations for the ground state of solid He and other noble gas crystals *Phys. Rev.* **128** 546
[18] Nosanow L H and Werthamer N R 1965 Calculations of sound velocities in crystalline helium at zero temperature *Phys. Rev. Lett.* **15** 618
[19] Ranninger J 1965 Lattice thermal conductivity *Phys. Rev.* **140** A2031
[20] Choquard P 1967 *The Anharmonic Crystal* (New York: W A Benjamin)
[21] Goldman V V, Horton G K and Klein M L 1968 An improved self-consistent phonon approximation *Phys. Rev. Lett.* **21** 1527
[22] Feldman J L and Horton G K 1967 Anharmonic contributions to the Helmholtz free energy of a simple crystal model: high-temperature limit and zero-point energy *Proc. Phys. Soc.* **92** 227
[23] Werthamer N R 1970 Self-consistent phonon formulation of anharmonic lattice dynamics *Phys. Rev.* B **1** 572
[24] Koehler T R 1969 Theoretical temperature-dependent phonon spectra of solid neon *Phys. Rev. Lett.* **22** 777
[25] Horton G K and Maradudin A A 1974 *Dynamical Properties of Solids* vol 1 (Amsterdam: North Holland), p 433
[26] Samathiyakanit V and Glyde H R 1973 Path integral theory of anharmonic crystals *J. Phys. C: Solid State Phys.* **6** 1180
[27] Baroni S, Giannozzi P and Testa A 1987 Green's-function approach to linear response in solids *Phys. Rev. Lett.* **58** 1861
[28] Gonze X and Vigneron J P 1989 Density-functional approach to nonlinear-response coefficients of solids *Phys. Rev.* B **39** 13120
[29] Debernardi A, Baroni S and Molinari E 1995 Anharmonic phonon lifetimes in semiconductors from density-functional perturbation theory *Phys. Rev. Lett.* **75** 1819
[30] Vanderbilt D, Louie S G and Cohen M L 1984 Calculation of phonon–phonon interactions and the absence of two-phonon bound states in diamond *Phys. Rev. Lett.* **53** 1477
[31] Narasimhan S and Vanderbilt D 1991 Anharmonic self-energies of phonons in silicon *Phys. Rev.* B **43** 4541
[32] Parlinski K, Li Z Q and Kawazoe Y 1997 First-principles determination of the soft mode in cubic (ZrO_2) *Phys. Rev. Lett.* **78** 4063

[33] Esfarjani K and Stokes H T 2008 Method to extract anharmonic force constants from first principles calculations *Phys. Rev.* B **77** 144112
[34] Li W, Carrete J, Katcho N A and Mingo N 2014 ShengBTE: a solver of the Boltzmann transport equation for phonons *Comp. Phys. Commun.* **185** 1747–58
[35] Togo A and Tanaka I 2015 First principles phonon calculations in materials science *Scr. Mater.* **108** 1
[36] Tadano T and Tsuneyuki S 2018 First-principles lattice dynamics method for strongly anharmonic crystals *J. Phys. Soc. Jpn.* **87** 041015
[37] Hellman O, Steneteg P, Abrikosov I A and Simak S I 2013 Temperature dependent effective potential method for accurate free energy calculations of solids *Phys. Rev.* B **87** 104111
[38] Giannozzi P, de Gironcoli S, Pavone P and Baroni S 1991 *Ab initio* calculation of phonon dispersions in semiconductors *Phys. Rev.* B **43** 7231
[39] Broido D A, Malorny M, Birner G, Mingo N and Stewart D A 2007 Intrinsic lattice thermal conductivity of semiconductors from first principles *Appl. Phys. Lett.* **91** 231922
[40] Deinzer G, Birner G and Strauch D 2003 *Ab initio* calculation of the linewidth of various phonon modes in germanium and silicon *Phys. Rev.* B **67** 144304
[41] Rousseau B and Bergara A 2010 Giant anharmonicity suppresses superconductivity in AlH_3 under pressure *Phys. Rev.* B **82** 104504
[42] Alfè D 2009 PHON: a program to calculate phonons using the small displacement method *Comput. Phys. Commun.* **180** 2622
[43] Li W, Mingo N, Lindsay L, Broido D A, Stewart D A and Katcho N A 2012 Thermal conductivity of diamond nanowires from first principles *Phys. Rev.* B **85** 195436
[44] Detraux F, Ghosez P H and Gonze X 1998 Long-range Coulomb interaction in ZrO_2 *Phys. Rev. Lett.* **81** 3297
[45] Parlinski K, Li Z Q and Kawazoe Y 1998 Parlinski, Li, and Kawazoe reply *Phys. Rev. Lett.* **81** 3298
[46] Wang Y, Wang J J, Wang W Y, Mei Z G, Shang S L, Chen L Q and Liu Z K 2010 A mixed-space approach to first-principles calculations of phonon frequencies for polar materials *J. Phys. Condens. Matter* **22** 202201
[47] Parlinski K 2018 *Ab initio* determination of anharmonic phonon peaks *Phys. Rev.* B **98** 054305
[48] Tadano T, Gohda Y and Tsuneyuki S 2014 Anharmonic force constants extracted from first-principles molecular dynamics: applications to heat transfer simulations *J. Phys. Condens. Matter* **26** 225402
[49] Hellman O, Abrikosov I A and Simak S I 2011 Lattice dynamics of anharmonic solids from first principles *Phys. Rev.* B **84** 180301
[50] Eriksson F, Fransson E and Erhart P 2019 The Hiphive package for the extraction of high-order force constants by machine learning *Adv. Theory Simul.* **2** 1800184
[51] Fu L, Kornbluth M, Cheng Z and Marianetti C A 2019 Group theoretical approach to computing phonons and their interactions *Phys. Rev.* B **100** 014303
[52] Shang H, Carbogno C, Rinke P and Scheffler M 2017 Lattice dynamics calculations based on density-functional perturbation theory in real space *Comput. Phys. Commun.* **215** 26
[53] Baroni S, de Gironcoli S, Dal Corso A and Giannozzi P 2001 Phonons and related crystal properties from density-functional perturbation theory *Rev. Mod. Phys.* **73** 515

[54] Souvatzis P, Eriksson O, Katsnelson M I and Rudin S P 2008 Entropy driven stabilization of energetically unstable crystal structures explained from first principles theory *Phys. Rev. Lett.* **100** 095901
[55] Souvatzis P, Eriksson O, Katsnelson M and Rudin S 2009 The self-consistent *ab initio* lattice dynamical method *Comput. Mater. Sci.* **44** 888
[56] Zhang H Y, Niu Z W, Cai L C, Chen X R and Xi F 2018 *Ab initio* dynamical stability of tungsten at high pressures and high temperatures *Comput. Mater. Sci.* **144** 32
[57] Hellman O and Abrikosov I A 2013 Temperature-dependent effective third-order interatomic force constants from first principles *Phys. Rev.* B **88** 144301
[58] West D and Estreicher S K 2006 First-principles calculations of vibrational lifetimes and decay channels: hydrogen-related modes in Si *Phys. Rev. Lett.* **96** 115504
[59] Yang F C, Hellman O, Lucas M S, Smith H L, Saunders C N, Xiao Y, Chow P and Fultz B 2018 Temperature dependence of phonons in (Pd_3Fe) through the Curie temperature *Phys. Rev.* B **98** 024301
[60] Vanderbilt D, Louie S G and Cohen M L 1986 Calculation of anharmonic phonon couplings in C, Si, and Ge *Phys. Rev.* B **33** 8740
[61] Ravichandran N K and Broido D 2018 Unified first-principles theory of thermal properties of insulators *Phys. Rev.* B **98** 085205
[62] Paulatto L, Mauri F and Lazzeri M 2013 Anharmonic properties from a generalized third-order *ab initio* approach: theory and applications to graphite and graphene *Phys. Rev.* B **87** 214303
[63] Paulatto L, Errea I, Calandra M and Mauri F 2015 First-principles calculations of phonon frequencies, lifetimes, and spectral functions from weak to strong anharmonicity: the example of palladium hydrides *Phys. Rev.* B **91** 054304
[64] Glyde H R and Goldman V V 1976 Dynamics of quantum crystals *J. Low Temp. Phys.* **25** 601
[65] Morris J R and Gooding R J 1990 Exactly solvable heterophase fluctuations at a vibrational-entropy-driven first-order phase transition *Phys. Rev. Lett.* **65** 1769
[66] Morris J R and Gooding R J 1991 Vibrational entropy effects at a diffusionless first-order solid-to-solid transition *Phys. Rev.* B **43** 6057
[67] Morris J R and Ho K M 1995 Calculating accurate free energies of solids directly from simulations *Phys. Rev. Lett.* **74** 940

Chapter 8

[1] Agrait N, Yeyati A L and van Ruitenbeek J M 2003 *Phys. Rep.* **377** 81–279
[2] Aradhya S V and Venkataraman L 2013 *Nat. Nanotechnol.* **8** 399–410
[3] Imry Y 1997 *Introduction to Mesoscopic Physics* (New York: Oxford University Press), p xiii
[4] Landauer R 1957 *IBM J. Res. Dev.* **1** 223–31
[5] Landauer R 1989 *J. Phys. Condens. Mater.* **1** 8099–110
[6] Datta S 2005 *Quantum Transport: Atom to Transistor* (Cambridge: Cambridge University Press), p xiv
[7] Cuevas J C and Scheer E 2017 *Molecular Electronics: An Introduction to Theory and Experiment* (Singapore: World Scientific), p xix
[8] Esfarjani K, Zebarjadi M and Kawazoe Y 2006 *Phys. Rev.* B **73** 085406
[9] Chiatti O, Nicholls J T, Proskuryakov Y Y, Lumpkin N, Farrer I and Ritchie D A 2006 *Phys. Rev. Lett.* **97** 056601

[10] Jezouin S, Parmentier F D, Anthore A, Gennser U, Cavanna A, Jin Y and Pierre F 2013 *Science* **342** 601–4
[11] Meschke M, Guichard W and Pekola J P 2006 *Nature* **444** 187–90
[12] Partanen M, Tan K Y, Govenius J, Lake R E, Makela M K, Tanttu T and Mottonen M 2016 *Nat. Phys.* **12** 460–4
[13] Schwab K, Henriksen E A, Worlock J M and Roukes M L 2000 *Nature* **404** 974–7
[14] Ashcroft N W and Mermin N D 1976 *Solid State Physics* (New York: Holt), p xxi
[15] Crossno J *et al* 2016 *Science* **351** 1058–61
[16] Wakeham N, Bangura A F, Xu X, Mercure J F, Greenblatt M and Hussey N E 2011 *Nat. Commun.* **2** 396
[17] Sivan U and Imry Y 1986 *Phys. Rev.* B **33** 551–8
[18] Lake R and Datta S 1992 *Phys. Rev.* B **46** 4757–63
[19] Butcher P N 1990 *J. Phys. Condens. Mat.* **2** 4869–78
[20] Paulsson M and Datta S 2003 *Phys. Rev.* B **67** 241403
[21] Cahill D G 2004 *Rev. Sci. Instrum.* **75** 5119–22
[22] Balandin A A 2011 *Nat. Mater.* **10** 569–81
[23] Majumdar A 1999 *Annu. Rev. Mater. Sci.* **29** 505–85
[24] Kim K, Jeong W H, Lee W C and Reddy P 2012 *ACS Nano* **6** 4248–57
[25] Menges F, Mensch P, Schmid H, Riel H, Stemmer A and Gotsmann B 2016 *Nat. Commun.* **7** 10874
[26] Cui L, Jeong W, Fernandez-Hurtado V, Feist J, Garcia-Vidal F J, Cuevas J C, Meyhofer E and Reddy P 2018 *Nat. Commun.* **9** 14479
[27] Jeong W, Hur S, Meyhofer E and Reddy P 2015 *Nanosc. Microsc. Therm.* **19** 279–302
[28] Cui L, Miao R, Jiang C, Meyhofer E and Reddy P 2017 *J. Chem. Phys.* **146** 092201
[29] Cui L, Jeong W, Hur S, Matt M, Klockner J C, Pauly F, Nielaba P, Cuevas J C, Meyhofer E and Reddy P 2017 *Science* **355** 1192–5
[30] Yanson A I, Bollinger G R, van den Brom H E, Agrait N and van Ruitenbeek J M 1998 *Nature* **395** 783–5
[31] Scheer E, Agrait N, Cuevas J C, Yeyati A L, Ludoph B, Martin-Rodero A, Bollinger G R, van Ruitenbeek J M and Urbina C 1998 *Nature* **394** 154–7
[32] Xu B Q and Tao N J J 2003 *Science* **301** 1221–3
[33] Olesen L, Laegsgaard E, Stensgaard I, Besenbacher F, Schiotz J, Stoltze P, Jacobsen K W and Norskov J K 1994 *Phys. Rev. Lett.* **72** 2251–4
[34] Krans J M, Muller C J, Vanderpost N, Postma F R, Sutton A P, Todorov T N and Vanruitenbeek J M 1995 *Phys. Rev. Lett.* **74** 2146
[35] Olesen L, Laegsgaard E, Stensgaard I, Besenbacher F, Schiotz J, Stoltze P, Jacobsen K W and Norskov J K 1995 *Phys. Rev. Lett.* **74** 2147
[36] Mosso N, Drechsler U, Menges F, Nirmalraj P, Karg S, Riel H and Gotsmann B 2017 *Nat. Nanotechnol.* **12** 430–3
[37] Lee W, Kim K, Jeong W, Zotti L A, Pauly F, Cuevas J C and Reddy P 2013 *Nature* **498** 209–13
[38] Cui L, Miao R, Wang K, Thompson D, Zotti L A, Cuevas J C, Meyhofer E and Reddy P 2018 *Nat. Nanotechnol.* **13** 122–7
[39] Markussen T 2013 *J. Chem. Phys.* **139** 244101
[40] Fermi E, Pasta J and Ulam S 1955 Los Alamos Report, LA-1940 978

[41] Cui L, Hur S, Akbar Z A, Klockner J C, Jeong W, Pauly F, Jang S Y, Reddy P and Meyhofer E 2019 *Nature* **572** 628–33
[42] Murphy P, Mukerjee S and Moore J 2008 *Phys. Rev.* B **78** 161406
[43] Sadeghi H, Sangtarash S and Lambert C J 2015 *Nano Lett.* **15** 7467–72
[44] Karlstrom O, Linke H, Karlstrom G and Wacker A 2011 *Phys. Rev.* B **84** 113415
[45] Bergfield J P, Solis M A and Stafford C A 2010 *ACS Nano* **4** 5314–20
[46] Finch C M, Garcia-Suarez V M and Lambert C J 2009 *Phys. Rev.* B **79** 033405
[47] Hou S J, Wu Q Q, Sadeghi H and Lambert C J 2019 *Nanoscale* **11** 3567–73
[48] Xu Y F, Wang X X, Zhou J W, Song B, Jiang Z, Lee E M Y, Huberman S, Gleason K K and Chen G 2018 *Sci. Adv.* **4** eaar3031
[49] Wang X J, Ho V, Segalman R A and Cahill D G 2013 *Macromolecules* **46** 4937–43
[50] Meier T, Menges F, Nirmalraj P, Holscher H, Riel H and Gotsmann B 2014 *Phys. Rev. Lett.* **113** 060801
[51] Shen S, Henry A, Tong J, Zheng R T and Chen G 2010 *Nat. Nanotechnol.* **5** 251–5
[52] Wang R Y, Segalman R A and Majumdar A 2006 *Appl. Phys. Lett.* **89** 173113
[53] Wang Z H, Carter J A, Lagutchev A, Koh Y K, Seong N H, Cahill D G and Dlott D D 2007 *Science* **317** 787–90
[54] Losego M D, Grady M E, Sottos N R, Cahill D G and Braun P V 2012 *Nat. Mater.* **11** 502–6
[55] Majumdar S, Sierra-Suarez J A, Schiffres S N, Ong W L, Higgs C F, McGaughey A J H and Malen J A 2015 *Nano Lett.* **15** 2985–91
[56] Ge Z B, Cahill D G and Braun P V 2006 *Phys. Rev. Lett.* **96** 186101
[57] O'Brien P J, Shenogin S, Liu J X, Chow P K, Laurencin D, Mutin P H, Yamaguchi M, Keblinski P and Ramanath G 2013 *Nat. Mater.* **12** 118–22
[58] Majumdar S, Malen J A and McGaughey A J H 2017 *Nano Lett.* **17** 220–7

Chapter 9

[1] Moore G E 2006 *IEEE Solid-State Circuits Soc. Newslett.* **11** 36–7
[2] Theis T N and Wong H P 2017 *Comput. Sci. Eng.* **19** 41–50
[3] Baibich M N, Broto J M, Fert A, Van Dau F N, Petroff F, Etienne P, Creuzet G, Friederich A and Chazelas J 1988 *Phys. Rev. Lett.* **61** 2472–5
[4] Binasch G, Grünberg P, Saurenbach F and Zinn W 1989 *Phys. Rev.* B **39** 4828–30
[5] Tehrani S, Slaughter J M, Chen E, Durlam M, Shi J and DeHerren M 1999 *IEEE Trans. Magn.* **35** 2814–9
[6] Slonczewski J C 1996 *J. Magn. Magn. Mater.* **159** L1–7
[7] Berger L 1996 *Phys. Rev.* B **54** 9353–8
[8] Liu L, Pai C-F, Li Y, Tseng H W, Ralph D C and Buhrman R A 2012 *Science* **336** 555–8
[9] Cubukcu M *et al* 2018 *IEEE Trans. Magn.* **54** 1–4
[10] Behin-Aein B, Datta D, Salahuddin S and Datta S 2010 *Nat. Nanotechnol.* **5** 266
[11] Kim J, Paul A, Crowell P A, Koester S J, Sapatnekar S S, Wang J and Kim C H 2015 *Proc. IEEE* **103** 106–30
[12] Camsari K Y, Faria R, Sutton B M and Datta S 2017 *Phys. Rev.* X **7** 031014
[13] Kiselev S I, Sankey J C, Krivorotov I N, Emley N C, Schoelkopf R J, Buhrman R A and Ralph D C 2003 *Nature* **425** 380
[14] Kaka S, Pufall M R, Rippard W H, Silva T J, Russek S E and Katine J A 2005 *Nature* **437** 389
[15] Houssameddine D *et al* 2007 *Nat. Mater.* **6** 447

[16] Mizushima K, Kudo K and Sato R 2007 *J. Magn. Magn. Mater.* **316** e960–2
[17] Kryder M H, Gage E C, McDaniel T W, Challener W A, Rottmayer R E, Ju G, Hsia Y and Erden M F 2008 *Proc. IEEE* **96** 1810–35
[18] Challener W A *et al* 2009 *Nat. Photonics* **3** 220
[19] Ju G *et al* 2015 *IEEE Trans. Magn.* **51** 1–9
[20] Kittel C 1948 *Phys. Rev.* **73** 155–61
[21] Kittel C 1947 *Phys. Rev.* **71** 270–1
[22] Rossing T D 1963 *J. Appl. Phys.* **34** 995
[23] Farle M, Silva T and Woltersdorf G 2013 *Magnetic Nanostructures: Spin Dynamics and Spin Transport* ed H Zabel and M Farle (Berlin: Springer), pp 37–83
[24] Cahill D G *et al* 2014 *Appl. Phys. Rev.* **1** 011305
[25] Nan C-W, Birringer R, Clarke D R and Gleiter H 1997 *J. Appl. Phys.* **81** 6692–9
[26] Goodson K E and Ju Y S 1999 *Annu. Rev. Mater. Sci.* **29** 261–93
[27] Cahill D G, Bullen A and Seung-Min L 2000 *High Temp. High Press.* **32** 135–42
[28] Soyez G, Eastman J A, Thompson L J, Bai G-R, Baldo P M, McCormick A W, DiMelfi R J, Elmustafa A A, Tambwe M F and Stone D S 2000 *Appl. Phys. Lett.* **77** 1155–7
[29] Hung M-T, Choi O, Ju Y S and Hahn H T 2006 *Appl. Phys. Lett.* **89** 023117
[30] Chiritescu C, Cahill D G, Nguyen N, Johnson D, Bodapati A, Keblinski P and Zschack P 2007 *Science* **315** 351–3
[31] Losego M D, Moh L, Arpin K A, Cahill D G and Braun P V 2010 *Appl. Phys. Lett.* **97** 011908
[32] Gundrum B C, Cahill D G and Averback R S 2005 *Phys. Rev.* B **72** 245426
[33] Hamad-Schifferli K, Schwartz J J, Santos A T, Zhang S and Jacobson J M 2002 *Nature* **415** 152
[34] Vallabhaneni A K, Qiu B, Hu J, Chen Y P, Roy A K and Ruan X 2013 *J. Appl. Phys.* **113** 064311
[35] Novoselov K S, Geim A K, Morozov S V, Jiang D, Katsnelson M I, Grigorieva I V, Dubonos S V and Firsov A A 2005 *Nature* **438** 197
[36] Ferrari A C and Basko D M 2013 *Nat. Nanotechnol.* **8** 235
[37] Rodin A S, Carvalho A and Castro Neto A H 2014 *Phys. Rev. Lett.* **112** 176801
[38] Cai Y, Zhang G and Zhang Y-W 2014 *JACS* **136** 6269–75
[39] Cahill D G 2004 *Rev. Sci. Instrum.* **75** 5119–22
[40] Zhu J, Wu X, Lattery D M, Zheng W and Wang X 2017 *Nanoscale Microscale Thermophys. Eng.* **21** 177–98
[41] Kang K, Koh Y K, Chiritescu C, Zheng X and Cahill D G 2008 *Rev. Sci. Instrum.* **79** 114901
[42] Persson A I, Koh Y K, Cahill D G, Samuelson L and Linke H 2009 *Nano Lett.* **9** 4484–8
[43] Koh Y K, Bae M-H, Cahill D G and Pop E 2011 *ACS Nano* **5** 269–74
[44] Monachon C and Weber L 2012 *Emerg. Mater. Res.* **1** 89–98
[45] Cheaito R, Duda J C, Beechem T E, Hattar K, Ihlefeld J F, Medlin D L, Rodriguez M A, Campion M J, Piekos E S and Hopkins P E 2012 *Phys. Rev. Lett.* **109** 195901
[46] Wang X, Liman C D, Treat N D, Chabinyc M L and Cahill D G 2013 *Phys. Rev.* B **88** 075310
[47] Zhu J, Zhu Y, Wu X, Song H, Zhang Y and Wang X 2016 *Appl. Phys. Lett.* **108** 231903
[48] Zhu J, Feng T, Mills S, Wang P, Wu X, Zhang L, Pantelides S T, Du X and Wang X 2018 *ACS Appl. Mater. Interfaces* **10** 40740–7

[49] Prakash A, Xu P, Wu X, Haugstad G, Wang X and Jalan B 2017 *J. Mater. Chem.* C **5** 5730–6
[50] Liu J, Wang X, Li D, Coates N E, Segalman R A and Cahill D G 2015 *Macromolecules* **48** 585–91
[51] Wang X, Ho V, Segalman R A and Cahill D G 2013 *Macromolecules* **46** 4937–43
[52] Mai C-K, Schlitz R A, Su G M, Spitzer D, Wang X, Fronk S L, Cahill D G, Chabinyc M L and Bazan G C 2014 *JACS* **136** 13478–81
[53] Xu D, Wang Q, Wu X, Zhu J, Zhao H, Xiao B, Wang X, Wang X and Hao Q 2018 *Front. Energy* **12** 127–36
[54] Hopkins P E, Beechem T, Duda J C, Hattar K, Ihlefeld J F, Rodriguez M A and Piekos E S 2011 *Phys. Rev.* B **84** 125408
[55] Losego M D, Grady M E, Sottos N R, Cahill D G and Braun P V 2012 *Nat. Mater.* **11** 502
[56] Hohensee G T, Wilson R B and Cahill D G 2015 *Nat. Commun.* **6** 6578
[57] Zheng K, Sun F, Zhu J, Ma Y, Li X, Tang D, Wang F and Wang X 2016 *ACS Nano* **10** 7792–8
[58] Wu X, Ni Y, Zhu J, Burrows N D, Murphy C J, Dumitrica T and Wang X 2016 *ACS Appl. Mater. Interfaces* **8** 10581–9
[59] Feser J P and Cahill D G 2012 *Rev. Sci. Instrum.* **83** 104901
[60] Feser J P, Liu J and Cahill D G 2014 *Rev. Sci. Instrum.* **85** 104903
[61] Jang H, Ryder C R, Wood J D, Hersam M C and Cahill D G 2017 *Adv. Mater.* **29** 1700650
[62] Jang H, Wood J D, Ryder C R, Hersam M C and Cahill D G 2015 *Adv. Mater.* **27** 8017–22
[63] Liu J, Choi G-M and Cahill D G 2014 *J. Appl. Phys.* **116** 233107
[64] van Kampen M, Jozsa C, Kohlhepp J T, LeClair P, Lagae L, de Jonge W J M and Koopmans B 2002 *Phys. Rev. Lett.* **88** 227201
[65] Barman A, Kimura T, Otani Y, Fukuma Y, Akahane K and Meguro S 2008 *Rev. Sci. Instrum.* **79** 123905
[66] Zhu J *et al* 2016 *Adv. Electron. Mater.* **2** 1600040
[67] Kerr J 1900 *The Effects of a Magnetic Field on Radiation* ed E P Lewis (New York: American Book), pp 27–52
[68] Pedrotti F L, Pedrotti L M and Pedrotti L S 2007 *Introduction to Optics* (London: Pearson Education), p 562
[69] Yang Z J and Scheinfein M R 1993 *J. Appl. Phys.* **74** 6810–23
[70] You C Y and Shin S C 1996 *Appl. Phys. Lett.* **69** 1315–7
[71] You C-Y and Shin S-C 1998 *J. Appl. Phys.* **84** 541–6
[72] Landau L D and Lifshitz E M 1984 *Electrodynamics of Continuous Media* ed L D Landau and E M Lifshitz (Amsterdam: Pergamon), pp 257–89
[73] Krinchik G S and Arem'ev V A 1968 *Sov. Phys. JETP* **26** 1080–5
[74] Qiu Z Q and Bader S D 2000 *Rev. Sci. Instrum.* **71** 1243–55
[75] Huang B *et al* 2017 *Nature* **546** 270
[76] Schmidt F, Rave W and Hubert A 1985 *IEEE Trans. Magn.* **21** 1596–8
[77] Rave W, Schäfer R and Hubert A 1987 *J. Magn. Magn. Mater.* **65** 7–14
[78] Agranat M B, Ashitkov S I, Granovskii A B and Rukman G I 1984 *Sov. Phys. JETP* **59** 804–6
[79] Vaterlaus A, Beutler T, Guarisco D, Lutz M and Meier F 1992 *Phys. Rev.* B **46** 5280–6
[80] Beaurepaire E, Merle J C, Daunois A and Bigot J Y 1996 *Phys. Rev. Lett.* **76** 4250–3

[81] Ju G, Nurmikko A V, Farrow R F C, Marks R F, Carey M J and Gurney B A 1999 *Phys. Rev. Lett.* **82** 3705–8
[82] Ju G, Chen L, Nurmikko A V, Farrow R F C, Marks R F, Carey M J and Gurney B A 2000 *Phys. Rev.* B **62** 1171–7
[83] Gilbert T L 2004 *IEEE Trans. Magn.* **40** 3443–9
[84] Koopmans B 2003 *Spin Dynamics in Confined Magnetic Structures II* ed B Hillebrands and K Ounadjela (Berlin: Springer), pp 253–316
[85] Chen J-Y, Zhu J, Zhang D, Lattery D M, Li M, Wang J-P and Wang X 2016 *J. Phys. Chem. Lett.* **7** 2328–32
[86] Güdde J, Conrad U, Jähnke V, Hohlfeld J and Matthias E 1999 *Phys. Rev.* B **59** R6608–11
[87] Melnikov A, Bovensiepen U, Radu I, Krupin O, Starke K, Matthias E and Wolf M 2004 *J. Magn. Magn. Mater.* **272–276** 1001–2
[88] Wietstruk M, Melnikov A, Stamm C, Kachel T, Pontius N, Sultan M, Gahl C, Weinelt M, Dürr H A and Bovensiepen U 2011 *Phys. Rev. Lett.* **106** 127401
[89] Koopmans B, Malinowski G, Dalla Longa F, Steiauf D, Fähnle M, Roth T, Cinchetti M and Aeschlimann M 2010 *Nat. Mater.* **9** 259–65
[90] Roth T, Schellekens A J, Alebrand S, Schmitt O, Steil D, Koopmans B, Cinchetti M and Aeschlimann M 2012 *Phys. Rev.* X **2** 021006
[91] Hohensee G T, Wilson R B, Feser J P and Cahill D G 2014 *Phys. Rev.* B **89** 024422
[92] Kimling J, Kimling J, Wilson R B, Hebler B, Albrecht M and Cahill D G 2014 *Phys. Rev.* B **90** 224408
[93] Kimling J, Philippi-Kobs A, Jacobsohn J, Oepen H P and Cahill D G 2017 *Phys. Rev.* B **95** 184305
[94] Wang X J, Mori T, Kuzmych-Ianchuk I, Michiue Y, Yubuta K, Shishido T, Grin Y, Okada S and Cahill D G 2014 *APL Mater.* **2** 046113
[95] Li W, Carrete J and Mingo N 2013 *Appl. Phys. Lett.* **103** 253103
[96] Gu X and Yang R 2014 *Appl. Phys. Lett.* **105** 131903
[97] Mansuripur M 1995 *The Physical Principles of Magneto-optical Recording* (Cambridge: Cambridge University Press), pp 128–79
[98] Acremann Y, Back C H, Buess M, Portmann O, Vaterlaus A, Pescia D and Melchior H 2000 *Science* **290** 492–5
[99] Iida S 1963 *J. Phys. Chem. Solids* **24** 625–30
[100] Smit J and Beljers H G 1955 *Philips Res. Rep.* **10** 113–30
[101] Suhl H 1955 *Phys. Rev.* **97** 555–7
[102] Mizukami S 2015 *J. Magn. Soc. Jpn.* **39** 1–7
[103] Mangin S, Ravelosona D, Katine J A, Carey M J, Terris B D and Fullerton E E 2006 *Nat. Mater.* **5** 210
[104] Meng H and Wang J-P 2006 *Appl. Phys. Lett.* **88** 172506
[105] Iihama S, Mizukami S, Naganuma H, Oogane M, Ando Y and Miyazaki T 2014 *Phys. Rev.* B **89** 174416
[106] Lattery D M, Zhang D, Zhu J, Hang X, Wang J-P and Wang X 2018 *Sci. Rep.* **8** 13395
[107] Zhang B *et al* 2017 *Appl. Phys. Lett.* **110** 012405
[108] Song H-S, Lee K-D, Sohn J-W, Yang S-H, Parkin S S P, You C-Y and Shin S-C 2013 *Appl. Phys. Lett.* **103** 022406
[109] Mizukami S, Watanabe D, Kubota T, Zhang X, Naganuma H, Oogane M, Ando Y and Miyazaki T 2010 *Appl. Phys. Exp.* **3** 123001

[110] Iihama S, Sakuma A, Naganuma H, Oogane M, Miyazaki T, Mizukami S and Ando Y 2014 *Appl. Phys. Lett.* **105** 142403
[111] Wu D, Li W, Tang M, Zhang Z, Lou S and Jin Q Y 2016 *J. Magn. Magn. Mater.* **409** 143–7
[112] Iihama S, Sakuma A, Naganuma H, Oogane M, Mizukami S and Ando Y 2016 *Phys. Rev.* B **94** 174425
[113] Becker J, Mosendz O, Weller D, Kirilyuk A, Maan J C, Christianen P C M, Rasing T and Kimel A 2014 *Appl. Phys. Lett.* **104** 152412
[114] Takahashi Y K *et al* 2017 *Appl. Phys. Lett.* **110** 252409
[115] Capua A, Yang S-h, Phung T and Parkin S S P 2015 *Phys. Rev.* B **92** 224402
[116] Morrish A H 1965 *The Physical Principles of Magnetism* (New York: Wiley), p 555
[117] Lattery D M, Zhu J, Zhang D, Wang J-P, Crowell P A and Wang X 2018 *Appl. Phys. Lett.* **113** 162405
[118] Qiao S, Nie S, Zhao J, Huo Y, Wu Y and Zhang X 2013 *Appl. Phys. Lett.* **103** 152402
[119] Sparks M 1964 *Ferromagnetic-Relaxation Theory* (New York: McGraw-Hill)
[120] McMichael R D and Krivosik P 2004 *IEEE Trans. Magn.* **40** 2–11
[121] Landeros P, Arias R E and Mills D L 2008 *Phys. Rev.* B **77** 214405
[122] Beaujour J M, Ravelosona D, Tudosa I, Fullerton E E and Kent A D 2009 *Phys. Rev.* B **80** 180415
[123] Tserkovnyak Y, Brataas A and Bauer G E W 2002 *Phys. Rev. Lett.* **88** 117601
[124] Ikeda S, Miura K, Yamamoto H, Mizunuma K, Gan H D, Endo M, Kanai S, Hayakawa J, Matsukura F and Ohno H 2010 *Nat. Mater.* **9** 721
[125] Kittel C 1958 *Phys. Rev.* **110** 1295–7
[126] Weber R 1968 *IEEE Trans. Magn.* **4** 28–31
[127] Kajiwara Y *et al* 2010 *Nature* **464** 262
[128] Iihama S, Sasaki Y, Sugihara A, Kamimaki A, Ando Y and Mizukami S 2016 *Phys. Rev.* B **94** 020401
[129] Yun S-J, Cho C-G and Choe S-B 2015 *Appl. Phys. Exp.* **8** 063009
[130] Wessels P, Vogel A, Tödt J-N, Wieland M, Meier G and Drescher M 2016 *Sci. Rep.* **6** 22117
[131] Qiu T Q, Juhasz T, Suarez C, Bron W E and Tien C L 1994 *Int. J. Heat Mass Transfer* **37** 2799–808
[132] Choi G-M, Min B-C, Lee K-J and Cahill D G 2014 *Nat. Commun.* **5** 4334
[133] Kimling J and Cahill D G 2017 *Phys. Rev.* B **95** 014402
[134] Kazantseva N, Nowak U, Chantrell R W, Hohlfeld J and Rebei A 2008 *Europhys. Lett.* **81** 27004
[135] Chubykalo-Fesenko O, Nowak U, Chantrell R W and Garanin D 2006 *Phys. Rev.* B **74** 094436
[136] Kazantseva N, Hinzke D, Nowak U, Chantrell R W, Atxitia U and Chubykalo-Fesenko O 2008 *Phys. Rev.* B **77** 184428
[137] Atxitia U and Chubykalo-Fesenko O 2011 *Phys. Rev.* B **84** 144414
[138] Joule J 1842 *Ann. Electr. Magn. Chem* **8** 219–24
[139] O'Hara K E, Hu X and Cahill D G 2001 *J. Appl. Phys.* **90** 4852–8
[140] Hohensee G T, Hsieh W-P, Losego M D and Cahill D G 2012 *Rev. Sci. Instrum.* **83** 114902
[141] Kim J-W, Vomir M and Bigot J-Y 2012 *Phys. Rev. Lett.* **109** 166601
[142] Jäger J V *et al* 2013 *Appl. Phys. Lett.* **103** 032409

[143] Jäger J V, Scherbakov A V, Glavin B A, Salasyuk A S, Campion R P, Rushforth A W, Yakovlev D R, Akimov A V and Bayer M 2015 *Phys. Rev.* B **92** 020404
[144] Uchida K, Takahashi S, Harii K, Ieda J, Koshibae W, Ando K, Maekawa S and Saitoh E 2008 *Nature* **455** 778
[145] Uchida K *et al* 2010 *Nat. Mater.* **9** 894
[146] Bauer G E W, Saitoh E and van Wees B J 2012 *Nat. Mater.* **11** 391
[147] Boona S R, Myers R C and Heremans J P 2014 *Energy Env. Sci.* **7** 885–910
[148] Jaworski C M, Yang J, Mack S, Awschalom D D, Heremans J P and Myers R C 2010 *Nat. Mater.* **9** 898
[149] Jaworski C M, Yang J, Mack S, Awschalom D D, Myers R C and Heremans J P 2011 *Phys. Rev. Lett.* **106** 186601
[150] Choi G-M, Moon C-H, Min B-C, Lee K-J and Cahill D G 2015 *Nat. Phys.* **11** 576

Chapter 10

[1] Axt V M and Kuhn T 2004 Femtosecond spectroscopy in semiconductors: a key to coherences, correlations and quantum kinetics *Rep. Prog. Phys.* **67** 433
[2] Kim G H, Shao L, Zhang K and Pipe K P 2013 Engineered doping of organic semiconductors for enhanced thermoelectric efficiency *Nat. Mater.* **12** 719–23
[3] López N, Reichertz L A, Yu K M, Campman K and Walukiewicz W 2011 Engineering the electronic band structure for multiband solar cells *Phys. Rev. Lett.* **106** 028701
[4] Blochwitz J *et al* 2001 Interface electronic structure of organic semiconductors with controlled doping levels *Org. Electron.* **2** 97–104
[5] Yankowitz M *et al* 2018 Dynamic band-structure tuning of graphene moiré superlattices with pressure *Nature* **557** 404–8
[6] Zheng R, Gao J, Wang J and Chen G 2011 Reversible temperature regulation of electrical and thermal conductivity using liquid–solid phase transitions *Nat. Commun.* **2** 289
[7] Largent R and Wenham S 2003 *Solar Cells Resources for the Secondary Science Teacher* (Sydney: UNSW Photovoltaics)
[8] Sze S M and Ng K K 2006 *Physics of Semiconductor Devices* 3rd edn (Hoboken, NJ: Wiley)
[9] Othonos A 1998 Probing ultrafast carrier and phonon dynamics in semiconductors *J. Appl. Phys.* **83** 1789
[10] Rossi F and Kuhn T 2002 Theory of ultrafast phenomena in photoexcited semiconductors *Rev. Mod. Phys.* **74** 895
[11] Iwai H, Kakushima K and Wong H 2006 Challenges for future semiconductor manufacturing *Int. J. High Speed Electron. Syst.* **16** 43–81
[12] Peercy P S 2000 The drive to miniaturization *Nature* **406** 1023–6
[13] Zhai X, Wu S, Shang A and Li X 2015 Limiting efficiency calculation of silicon single-nanowire solar cells with considering Auger recombination *Appl. Phys. Lett.* **106** 063904
[14] García-Santamaría F *et al* 2009 Suppressed Auger recombination in 'giant' nanocrystals boosts optical gain performance *Nano Lett.* **9** 3482–8
[15] Bulashevich K A and Karpov S Y 2008 Is Auger recombination responsible for the efficiency rollover in III-nitride light-emitting diodes? *Phys. Status Solidi* **5** 2066–9
[16] Saari J I *et al* 2013 Ultrafast electron trapping at the surface of semiconductor nanocrystals: excitonic and biexcitonic processes *J. Phys. Chem.* B **117** 4412–21

[17] Liao B and Najafi E 2017 Scanning ultrafast electron microscopy: a novel technique to probe photocarrier dynamics with high spatial and temporal resolutions *Mater. Today Phys.* **2** 46–53
[18] Jin C, Ma E Y, Karni O, Regan E C, Wang F and Heinz T F 2018 Ultrafast dynamics in van der Waals heterostructures *Nat. Nanotechnol.* **13** 994–1003
[19] Miller R J D 1995 Time scale issues for charge transfer and energy storage using semiconductor junctions *Sol. Energy Mater. Sol. Cells* **38** 331–3
[20] Vanacore G M, Fitzpatrick A W P and Zewail A H 2016 Four-dimensional electron microscopy: ultrafast imaging, diffraction and spectroscopy in materials science and biology *Nano Today* **11** 228–9
[21] Freundlich M M 1963 Origin of the electron microscope *Sci.* **142** 185–8
[22] Smith D J 2008 Development of aberration-corrected electron microscopy *Microsc. Microanal.* **14** 2–15
[23] Barwick B, Flannigan D J and Zewail A H 2009 Photon-induced near-field electron microscopy *Nature* **462** 902–6
[24] Barwick B and Zewail A H 2015 Photonics and plasmonics in 4D ultrafast electron microscopy *ACS Photonics* **2** 1391–402
[25] Kim J S *et al* 2008 Imaging of transient structures using nanosecond *in situ* TEM *Science* **321** 1472–5
[26] Zhang Q and Luo Y 2016 Probing the ultrafast dynamics in nanomaterial complex systems by femtosecond transient absorption spectroscopy *High Power Laser Sci. Eng.* **4** 1–10
[27] Krehl P and Engemann S 1995 August Toepler—the first who visualized shock waves *Shock Waves* **5** 1–18
[28] Dantus M and Gross P 1998 Ultrafast spectroscopy *Encycl. Appl. Phys.* **22** 431–56
[29] Corkum P B and Krausz F 2007 Attosecond science *Nat. Phys.* **3** 381–7
[30] Krausz F and Ivanov M 2009 Attosecond physics *Rev. Mod. Phys.* **81** 163
[31] Shah J 1999 *Ultrafast Spectroscopy of Semiconductors and Semiconductor Nanostructures* vol 115 (Berlin: Springer)
[32] Keller U 2003 Recent developments in compact ultrafast lasers *Nature* **424** 831–8
[33] Lundstrom M 2000 *Fundamentals of Carrier Transport* 2nd edn (New York: Cambridge University Press)
[34] Elsaesser T and Woerner M 1999 Femtosecond infrared spectroscopy of semiconductors and semiconductor nanostructures *Phys. Rep.* **321** 253–305
[35] Simpson M J, Doughty B, Yang B, Xiao K and Ma Y Z 2016 Separation of distinct photoexcitation species in femtosecond transient absorption microscopy *ACS Photonics* **3** 434–42
[36] Davydova D, de la Cadena A, Akimov D and Dietzek B 2016 Transient absorption microscopy: advances in chemical imaging of photoinduced dynamics *Laser Photon. Rev.* **10** 62–81
[37] Guo Z, Manser J S, Wan Y, Kamat P V and Huang L 2015 Spatial and temporal imaging of long-range charge transport in perovskite thin films by ultrafast microscopy *Nat. Commun.* **6** 7471
[38] Grancini G *et al* 2012 Dynamic microscopy study of ultrafast charge transfer in a hybrid P3HT/hyperbranched CdSe nanoparticle blend for photovoltaics *J. Phys. Chem. Lett.* **3** 517–23

[39] Huang L *et al* 2010 Ultrafast transient absorption microscopy studies of carrier dynamics in epitaxial graphene *Nano Lett.* **10** 1308–13
[40] Gao B *et al* 2011 Studies of intrinsic hot phonon dynamics in suspended graphene by transient absorption microscopy *Nano Lett.* **11** 3184–9
[41] Guo Z, Wan Y, Yang M, Snaider J, Zhu K and Huang L 2017 Long-range hot-carrier transport in hybrid perovskites visualized by ultrafast microscopy *Sci.* **356** 59–62
[42] Ruzicka B A, Wang R, Lohrman J, Ren S and Zhao H 2012 Exciton diffusion in semiconducting single-walled carbon nanotubes studied by transient absorption microscopy *Phys. Rev.* B **86** 205417
[43] Gao B, Hartland G V and Huang L 2012 Transient absorption spectroscopy and imaging of individual chirality-assigned single-walled carbon nanotubes *ACS Nano* **6** 5083–90
[44] Mehl B P, Kirschbrown J R, House R L and Papanikolas J M 2011 The end is different than the middle: spatially dependent dynamics in ZnO rods observed by femtosecond pump-probe microscopy *J. Phys. Chem. Lett.* **2** 1777–81
[45] Gabriel M M *et al* 2013 Direct imaging of free carrier and trap carrier motion in silicon nanowires by spatially-separated femtosecond pump–probe microscopy *Nano Lett.* **13** 1336–40
[46] Steeves G M, Elezzabi A Y, Freeman M R, Steeves G M, Elezzabi A Y and Freeman M R 2011 Nanometer-scale imaging with an ultrafast scanning tunneling microscope nanometer-scale imaging with an ultrafast scanning tunneling microscope**504** 1996–9
[47] Terada Y, Aoyama M and Kondo H 2007 Ultrafast photoinduced carrier dynamics in GaNAs probed using femtosecond time-resolved scanning tunnelling *Nanotechnology* **18** 04402
[48] Terada Y, Yoshida S, Takeuchi O and Shigekawa H 2010 Laser-combined scanning tunnelling microscopy for probing ultrafast transient dynamics *J. Phys. Condens. Matter* **22** 264008
[49] Cocker T L *et al* 2013 An ultrafast terahertz scanning tunnelling microscope *Nat. Photonics* **7** 620–5
[50] Shigekawa H, Takeuchi O and Aoyama M 2005 Development of femtosecond time-resolved scanning tunneling microscopy for nanoscale science and technology *Sci. Technol. Adv. Mater.* **6** 582–8
[51] Yoshida S *et al* 2014 Probing ultrafast spin dynamics with optical pump–probe scanning tunnelling microscopy *Nat. Nanotechnol.* **9** 588–93
[52] Gerstner V, Knoll A, Pfeiffer W, Thon A and Gerber G 2000 Femtosecond laser assisted scanning tunneling microscopy *J. Appl. Phys.* **88** 4851–9
[53] Loth S, Etzkorn M, Lutz C P, Eigler D M and Heinrich A J 2010 Measurement of fast electron spin relaxation times with atomic resolution *Sci.* **329** 1628–30
[54] Nechay B A, Siegner U, Morier-Genoud F, Schertel A and Keller U 1999 Femtosecond near-field optical spectroscopy of implantation patterned semiconductors *Appl. Phys. Lett.* **74** 61–3
[55] Nechay B A, Siegner U, Achermann M, Bielefeldt H and Keller U 1999 Femtosecond pump–probe near-field optical microscopy *Rev. Sci. Instrum.* **70** 2758–64
[56] Richter A *et al* 1999 Time-resolved near-field optics: exciton transport in semiconductor nanostructures *J. Microsc.* **194** 393–400

[57] Lienau C, Emiliani V, Günther T, Intonti F and Elsaesser T 1999 Picosecond and femtosecond near-field optical spectroscopy of carrier dynamics in semiconductor nanostructures *Physica* B **272** 96–100
[58] Guenther T *et al* 1999 Femtosecond near-field spectroscopy of a single GaAs quantum wire *Appl. Phys. Lett.* **75** 3500–2
[59] Huber M A *et al* 2017 Femtosecond photo-switching of interface polaritons in black phosphorus heterostructures *Nat. Nanotechnol.* **12** 207–11
[60] Schumacher Z, Spielhofer A, Miyahara Y and Grutter P 2017 The limit of time resolution in frequency modulation atomic force microscopy by a pump–probe approach *Appl. Phys. Lett.* **110** 053111
[61] Murawski J *et al* 2015 Tracking speed bumps in organic field-effect transistors via pump–probe Kelvin-probe force microscopy *J. Appl. Phys.* **118** 244502
[62] Liscio A, Palermo V and Samorì P 2010 Nanoscale quantitative measurement of the potential of charged nanostructures by electrostatic and Kelvin probe force microscopy: unraveling electronic processes in complex materials *Acc. Chem. Res.* **43** 541–50
[63] Haight R, Ross F M and Hannon J B 2011 *Handbook of Instrumentation and Techniques for Semiconductor Nanostructure Characterization* vol 1 (Singapore: World Scientific)
[64] Shorokhov D and Zewail A H 2016 Perspective: 4D ultrafast electron microscopy—evolutions and revolutions *J. Chem. Phys.* **144** 080901
[65] Zewail A H 2010 Four-dimensional electron microscopy *Sci.* **328** 187–93
[66] Zewail A H 2016 Ultrafast light and electrons: imaging the invisible *Optics in Our Time* (Berlin: Springer), pp 43–68
[67] Plemmons D A, Suri P K and Flannigan D J 2015 Probing structural and electronic dynamics with ultrafast electron microscopy *Chem. Mater.* **27** 3178–92
[68] Baskin J S and Zewail A H 2014 Seeing in 4D with electrons: development of ultrafast electron microscopy at Caltech *Compt. Rend. Phys.* **15** 176–89
[69] Seres E, Seres J and Spielmann C 2006 X-ray absorption spectroscopy in the keV range with laser generated high harmonic radiation *Appl. Phys. Lett.* **89** 1–4
[70] Adhikari A, Eliason J K, Sun J, Bose R, Flannigan D J and Mohammed O F 2017 Four-dimensional ultrafast electron microscopy: insights into an emerging technique *ACS Appl. Mater. Interfaces* **9** 3–16
[71] Park H S, Baskin J S, Kwon O H and Zewail A H 2007 Atomic-scale imaging in real and energy space developed in ultrafast electron microscopy *Nano Lett.* **7** 2545–51
[72] Bücker K *et al* 2016 Electron beam dynamics in an ultrafast transmission electron microscope with Wehnelt electrode *Ultramicroscopy* **171** 8–18
[73] Barwick B, Park H S, Kwon O-H, Baskin J S and Zewail A H 2008 4D imaging of transient structures and morphologies in ultrafast electron microscopy *Sci.* **322** 1227–31
[74] King W E *et al* 2005 Ultrafast electron microscopy in materials science, biology, and chemistry *J. Appl. Phys.* **97** 111101
[75] Yurtsever A and Zewail A H 2009 4D nanoscale diffraction observed by convergent-beam ultrafast electron microscopy *Sci.* **326** 708–12
[76] Vanacore G M, Van Der Veen R M and Zewail A H 2015 Origin of axial and radial expansions in carbon nanotubes revealed by ultrafast diffraction and spectroscopy *ACS Nano* **9** 1721–9

[77] Flannigan D J and Zewail A H 2010 Optomechanical and crystallization phenomena visualized with 4D electron microscopy: interfacial carbon nanotubes on silicon nitride *Nano Lett.* **10** 1892–9
[78] McKenna A J, Eliason J K and Flannigan D J 2016 Imaging photoinduced structural and morphological dynamics of a single MoS_2 flake with ultrafast electron microscopy *Proc. Microsc. Microanal.* **22** 1662–3
[79] Yang D-S, Mohammed O F and Zewail A H 2010 Scanning ultrafast electron microscopy *Proc. Natl Acad. Sci.* **107** 14993–8
[80] Hassan M T 2018 Attomicroscopy: from femtosecond to attosecond electron microscopy *J. Phys. B: At. Mol. Opt. Phys.* **51** 032005
[81] Mohammed O F, Yang D S, Pal S K and Zewail A H 2011 4D scanning ultrafast electron microscopy: visualization of materials surface dynamics *J. Am. Chem. Soc.* **133** 7708–11
[82] Cho J, Hwang T Y and Zewail A H 2014 Visualization of carrier dynamics in p(n)-type GaAs by scanning ultrafast electron microscopy *Proc. Natl Acad. Sci.* **111** 2094–9
[83] Liao B *et al* 2017 Spatial–temporal imaging of anisotropic photocarrier dynamics in black phosphorus *Nano Lett.* **17** 3675–80
[84] Najafi E, Scarborough T D, Tang J and Zewail A 2015 Four-dimensional imaging of carrier interface dynamics in p–n junctions *Sci.* **347** 164–7
[85] Liao B, Najafi E, Li H, Minnich A J and Zewail A H 2017 Photo-excited hot carrier dynamics in hydrogenated amorphous silicon imaged by 4D electron microscopy *Nat. Nanotechnol.* **12** 871–6
[86] Khan J I *et al* 2016 Enhanced optoelectronic performance of a passivated nanowire-based device: key information from real-space imaging using 4D electron microscopy *Small* **12** 2312
[87] Bose R *et al* 2018 Imaging localized energy states in silicon-doped InGaN nanowires using 4D electron microscopy *ACS Energy Lett.* **3** 476–81
[88] Shaheen B S, Sun J, Yang D S and Mohammed O F 2017 Spatiotemporal observation of electron-impact dynamics in photovoltaic materials using 4D electron microscopy *J. Phys. Chem. Lett.* **8** 2455–62
[89] Sun J, Melnikov V A, Khan J I and Mohammed O F 2015 Real-space imaging of carrier dynamics of materials surfaces by second-generation four-dimensional scanning ultrafast electron microscopy *J. Phys. Chem. Lett.* **6** 3884–90
[90] Meizyte G *et al* 2018 Imaging the reduction of electron trap states in shelled copper indium gallium selenide nanocrystals using ultrafast electron microscopy *J. Phys. Chem.* C **122** 15010–6
[91] Bose R *et al* 2016 Real-space mapping of surface trap states in CIGSe nanocrystals using 4D electron microscopy *Nano Lett.* **16** 4417–23
[92] Schmidt O *et al* 2002 Time-resolved two photon photoemission electron microscopy *Appl. Phys.* B **74** 223–7
[93] Kahl P *et al* 2018 Direct observation of surface plasmon polariton propagation and interference by time-resolved imaging in normal-incidence two photon photoemission microscopy *Plasmonics* **13** 239–46
[94] Mahro A K *et al* 2017 Revealing the subfemtosecond dynamics of orbital angular momentum in nanoplasmonic vortices *Sci.* **355** 1187–91

[95] Bayer D, Wiemann C, Gaier O, Bauer M and Aeschlimann M 2008 Time-resolved 2PPE and time-resolved PEEM as a probe of LSPs in silver nanoparticles *J. Nanomater.* **2008** 249514
[96] Petek H, Sametoglu V, Pontius N and Kubo A 2005 Imaging of surface plasmon dynamics in nanostructured silver films *IQEC, Int. Quantum Electronics Conf. Proc.*
[97] Mårsell E *et al* 2015 Nanoscale imaging of local few-femtosecond near-field dynamics within a single plasmonic nanoantenna *Nano Lett.* **15** 6601–8
[98] Bauer M, Wiemann C, Lange J, Bayer D, Rohmer M and Aeschlimann M 2007 Phase propagation of localized surface plasmons probed by time-resolved photoemission electron microscopy *Appl. Phys.* A **88** 473–80
[99] Fukumoto K *et al* 2014 Femtosecond time-resolved photoemission electron microscopy for spatiotemporal imaging of photogenerated carrier dynamics in semiconductors *Rev. Sci. Instrum.* **85** 083705
[100] Fukumoto K, Yamada Y, Onda K and Koshihara S Y 2014 Direct imaging of electron recombination and transport on a semiconductor surface by femtosecond time-resolved photoemission electron microscopy *Appl. Phys. Lett.* **104** 053117
[101] Fukumoto K *et al* 2014 Femtosecond time-resolved photoemission electron microscopy for spatiotemporal imaging of photogenerated carrier dynamics in semiconductors *Rev. Sci. Instrum.* **85** 083705
[102] Fukumoto K, Yamada Y, Koshihara S Y and Onda K 2015 Lifetimes of photogenerated electrons on a GaAs surface affected by nanostructural defects *Appl. Phys. Express* **8** 101201
[103] Shibuta M, Yamagiwa K, Eguchi T and Nakajima A 2016 Imaging and spectromicroscopy of photocarrier electron dynamics in C_{60} fullerene thin films *Appl. Phys. Lett.* **109** 203111
[104] Fukumoto K *et al* 2017 Ultrafast electron dynamics in twisted graphene by femtosecond photoemission electron microscopy *Carbon* **124** 49–56
[105] Man M K L *et al* 2017 Imaging the motion of electrons across semiconductor heterojunctions *Nat. Nanotechnol.* **12** 36–40
[106] Wang L, Xu C, Li M Y, Li L J and Loh Z H 2018 Unraveling spatially heterogeneous ultrafast carrier dynamics of single-layer WSe_2 by femtosecond time-resolved photoemission electron microscopy *Nano Lett.* **18** 5172–8
[107] Wong E L, Winchester A J, Pareek V, Madéo J, Man M K L and Dani K M 2018 Pulling apart photoexcited electrons by photoinducing an in-plane surface electric field *Sci. Adv.* **4** eaat9722
[108] Bauer E 2014 *Surface Microscopy with Low Energy Electrons* (New York: Springer)
[109] Man K L and Altman M S 2012 Low energy electron microscopy and photoemission electron microscopy investigation of graphene *J. Phys. Condens. Matter* **24** 314209
[110] Menteş T O, Zamborlini G, Sala A and Locatelli A 2014 Cathode lens spectromicroscopy: methodology and applications *Beilstein J. Nanotechnol.* **5** 1873–86
[111] Einstein A 1905 Über einen die Erzeugung und Verwandlung des Lichtes betreffenden heuristischen Gesichtspunkt *Ann. Phys.* **322** 132–48
[112] Mårsell E *et al* 2015 Nanoscale imaging of local few-femtosecond near-field dynamics within a single plasmonic nanoantenna *Nano Lett.* **15** 6601–8
[113] Renault O and Chabli A 2007 Energy-filtered photoelectron emission microscopy (EF-PEEM) for imaging nanoelectronic materials *AIP Conf. Proc.* **931** 502–6
[114] Hüfner S 2003 *Photoelectron Spectroscopy* vol 53 (Berlin: Springer)

[115] Suga S and Sekiyama A 2014 *Photoelectron Spectroscopy—Bulk and Surface Electronic Structures* vol 176 (Berlin: Springer)
[116] Amati M *et al* 2018 Photoelectron microscopy at Elettra: recent advances and perspectives *J. Electron Spectros. Relat. Phenomena* **224** 59–67
[117] Bostanjoglo O and Weingärtner M 1997 Pulsed photoelectron microscope for imaging laser-induced nanosecond processes *Rev. Sci. Instrum.* **68** 2456–60
[118] Schmitz C *et al* 2016 Compact extreme ultraviolet source for laboratory-based photoemission spectromicroscopy *Appl. Phys. Lett.* **108** 234101
[119] Chiang C T *et al* 2015 Boosting laboratory photoelectron spectroscopy by megahertz high-order harmonics *New J. Phys.* **17** 013035
[120] Wang H, Xu Y, Ulonska S, Robinson J S, Ranitovic P and Kaindl R A 2015 Bright high-repetition-rate source of narrowband extreme-ultraviolet harmonics beyond 22 eV *Nat. Commun.* **6** 1–7
[121] Heyl C M, Güdde J, L'Huillier A and Höfer U 2012 High-order harmonic generation with μJ laser pulses at high repetition rates *J. Phys. B: At. Mol. Opt. Phys.* **45** 074020
[122] Hellmann S *et al* 2012 Time-resolved x-ray photoelectron spectroscopy at FLASH *New J. Phys.* **14** 013062
[123] Pietzsch A *et al* 2008 Towards time resolved core level photoelectron spectroscopy with femtosecond x-ray free-electron lasers *New J. Phys.* **10** 033004
[124] Johannsen J C *et al* 2013 Direct view of hot carrier dynamics in graphene *Phys. Rev. Lett.* **111** 027403
[125] Grubišić Čabo A *et al* 2015 Observation of ultrafast free carrier dynamics in single layer MoS_2 *Nano Lett.* **15** 5883–7
[126] Wallauer R, Reimann J, Armbrust N, Güdde J and Höfer U 2016 Intervalley scattering in MoS_2 imaged by two-photon photoemission with a high-harmonic probe *Appl. Phys. Lett.* **109** 162102
[127] Ulstrup S *et al* 2017 Spin and valley control of free carriers in single-layer WS_2 *Phys. Rev.* B **95** 041405
[128] Nikogosyan D N 1991 Beta barium borate (BBO)—a review of its properties and applications *Appl. Phys.* A **52** 359–68
[129] Togashi T *et al* 2003 Generation of vacuum-ultraviolet light by an optically contacted, prism-coupled $KBe_2BO_3F_2$ crystal *Opt. Lett.* **28** 254
[130] Guo S *et al* 2016 $BaBe_2BO_3F_3$: a KBBF-type deep-ultraviolet nonlinear optical material with reinforced $[Be_2BO_3F_2]\infty$layers and short phase-matching wavelength *Chem. Mater.* **28** 8871–5
[131] Ališauskas S *et al* 2012 Bright coherent ultrahigh harmonics in the keV x-ray regime from mid-infrared femtosecond lasers *Sci.* **1287** 1287–92
[132] Pupeza I *et al* 2013 Compact high-repetition-rate source of coherent 100 eV radiation *Nat. Photonics* **7** 608–12
[133] Schmidt J *et al* 2017 Development of a 10 kHz high harmonic source up to 140 eV photon energy for ultrafast time-, angle-, and phase-resolved photoelectron emission spectroscopy on solid targets *Rev. Sci. Instrum.* **88** 083105
[134] Passlack S, Mathias S, Andreyev O, Mittnacht D, Aeschlimann M and Bauer M 2006 Space charge effects in photoemission with a low repetition, high intensity femtosecond laser source *J. Appl. Phys.* **100** 024912

[135] Buckanie N M, Göhre J, Zhou P, von der Linde D, H-von Hoegen M and Meyer Zu Heringdorf F-J 2009 Space charge effects in photoemission electron microscopy using amplified femtosecond laser pulses *J. Phys. Condens. Matter* **21** 314003
[136] Hellmann S, Rossnagel K, Marczynski-Bühlow M and Kipp L 2009 Vacuum space-charge effects in solid-state photoemission *Phys. Rev.* B **79** 1–12
[137] Schoenhense B *et al* 2018 Multidimensional photoemission spectroscopy—the space-charge limit *New J. Phys.* **20** 033004
[138] Rothhardt J *et al* 2010 High average and peak power few-cycle laser pulses delivered by fiber pumped OPCPA system *Opt. Express* **18** 12719
[139] Tavella F *et al* 2010 Fiber-amplifier pumped high average power few-cycle pulse non-collinear OPCPA *Opt. Express* **18** 4689
[140] Spiecker H *et al* 1998 Time-of-flight photoelectron emission microscopy TOF-PEEM: first results *Nucl. Instrum. Methods Phys. Res.* A **406** 499–506
[141] Oelsner A, Rohmer M, Schneider C, Bayer D, Schönhense G and Aeschlimann M 2010 Time- and energy resolved photoemission electron microscopy-imaging of photoelectron time-of-flight analysis by means of pulsed excitations *J. Electron Spectros. Relat. Phenomena* **178–179** 317–30
[142] Wolf S A *et al* 2001 Spintronics: a spin-based electronics vision for the future *Sci.* **294** 1488
[143] Hasan M Z and Kane C L 2010 Colloquium: topological insulators *Rev. Mod. Phys.* **82** 3045–67
[144] Qi X L and Zhang S C 2011 Topological insulators and superconductors *Rev. Mod. Phys.* **83** 1057
[145] Kronast F, Schlichting J, Radu F, Mishra S K, Noll T and Dürr H A 2010 Spin-resolved photoemission microscopy and magnetic imaging in applied magnetic fields *Surf. Interface Anal.* **42** 1532–6
[146] Tusche C *et al* 2011 Spin resolved photoelectron microscopy using a two-dimensional spin-polarizing electron mirror *Appl. Phys. Lett.* **99** 15–8
[147] Tusche C, Krasyuk A and Kirschner J 2015 Spin resolved bandstructure imaging with a high resolution momentum microscope *Ultramicroscopy* **159** 520–9
[148] Murphy S and Huang L 2013 Transient absorption microscopy studies of energy relaxation in graphene oxide thin film *J. Phys. Condens. Matter* **25** 144203

Chapter 11

[1] Shirane G, Shapiro S M and Tranquada J M 2002 *Neutron Scattering with a Triple-Axis Spectrometer: Basic Techniques* (Cambridge: Cambridge University Press)
[2] Squires G L 2012 *Introduction to the Theory of Thermal Neutron Scattering* (Cambridge: Cambridge University Press)
[3] Maradudin A A and Fein A E 1962 *Phys. Rev.* **128** 2589
[4] Abernathy D L, Stone M B, Loguillo M J, Lucas M S, Delaire O, Tang X, Lin J Y Y and Fultz B 2012 *Rev. Sci. Instrum.* **83** 015114
[5] Stone M B, Niedziela J L and Abernathy D L 2014 *Rev. Sci. Instrum.* **85** 045113
[6] Willendrup P, Farhi E, Knudsen E, Filges U and Lefmann K 2014 *J. Neutron Res.* **17** 35
[7] Zheludev A 2009 Reslib https://neutron.ethz.ch/research/resources/reslib.html (ResLib v3.4c)
[8] Li C W, Hong J, May A F, Bansal D, Chi S, Hong T, Ehlers G and Delaire O 2015 *Nat. Phys.* **11** 1063
[9] Cowley E R, Darby J K and Pawley G S 1969 *J. Phys. C: Solid State Phys.* **2** 1916

[10] Fultz B, Robertson J L, Stephens T A, Nagel L J and Spooner S 1998 *J. Appl. Phys.* **79** 8318
[11] Li C W, Tang X, Munoz J A, Keith J B, Tracy S J, Abernathy D L and Fultz B 2011 *Phys. Rev. Lett.* **107** 195504
[12] Kresch M, Lucas M, Delaire O, Lin J Y Y and Fultz B 2008 *Phys. Rev.* B **77** 024301
[13] May A F, Delaire O, Niedziela J L, Lara-Curzio E, Susner M A, Abernathy D L, Kirkham M and McGuire M A 2016 *Phys. Rev.* B **93** 064104
[14] Pang J W L, Buyers W J L, Chernatynskiy A, Lumsden M D, Larson B C and Phillpot S R 2013 *Phys. Rev. Lett.* **110** 157401
[15] Delaire O *et al* 2011 *Nat. Mater.* **10** 614

Chapter 12

[1] Tans S J, Verschueren A R M and Dekker C 1998 Room-temperature transistor based on a single carbon nanotube *Nature* **393** 49–52
[2] Shulaker M M, Hills G, Patil N, Wei H, Chen H Y, PhilipWong H S and Mitra S 2013 Carbon nanotube computer *Nature* **501** 526
[3] Huang Y, Duan X F, Cui Y, Lauhon L J, Kim K H and Lieber C M 2001 Logic gates and computation from assembled nanowire building blocks *Science* **294** 1313–7
[4] Tian B Z, Zheng X L, Kempa T J, Fang Y, Yu N F, Yu G H, Huang J L and Lieber C M 2007 Coaxial silicon nanowires as solar cells and nanoelectronic power sources *Nature* **449** 885
[5] Hochbaum A I, Chen R K, Delgado R D, Liang W J, Garnett E C, Najarian M, Majumdar A and Yang P D 2008 Enhanced thermoelectric performance of rough silicon nanowires *Nature* **451** 163
[6] Boukai A I, Bunimovich Y, Tahir-Kheli J, Yu J K, Goddard W A and Heath J R 2008 Silicon nanowires as efficient thermoelectric materials *Nature* **451** 168–71
[7] Wang Z L and Song J H 2006 Piezoelectric nanogenerators based on zinc oxide nanowire arrays *Science* **312** 242–6
[8] Su Y D, Liu C, Brittman S, Tang J Y, Fu A, Kornienko N, Kong Q and Yang P D 2016 Single-nanowire photoelectrochemistry *Nat. Nanotechnol.* **11** 609
[9] Chan C K, Peng H L, Liu G, McIlwrath K, Zhang X F, Huggins R A and Cui Y 2008 High-performance lithium battery anodes using silicon nanowires *Nat. Nanotechnol.* **3** 31–5
[10] Cui Y, Wei Q Q, Park H K and Lieber C M 2001 Nanowire nanosensors for highly sensitive and selective detection of biological and chemical species *Science* **293** 1289–92
[11] Cahill D G, Ford W K, Goodson K E, Mahan G D, Majumdar A, Maris H J, Merlin R and Sr P 2003 Nanoscale thermal transport *J. Appl. Phys.* **93** 793–818
[12] Cahill D G *et al* 2014 Nanoscale thermal transport. II. 2003–2012 *Appl. Phys. Rev.* **1** 011305
[13] Cahill D G, Goodson K E and Majumdar A 2002 Thermometry and thermal transport in micro/nanoscale solid-state devices and structures *J. Heat Trans.* **124** 223–41
[14] Cahill D G 2002 Erratum: "Thermal conductivity measurement from 30 to 750 K: the 3ω method" [*Rev. Sci. Instrum.* **61**, 802 (1990)] *Rev. Sci. Instrum.* **73** 3701
[15] Majumdar A 1999 Scanning thermal microscopy *Annu. Rev. Mater. Sci.* **29** 505–85
[16] Cahill D G 2004 Analysis of heat flow in layered structures for time-domain thermoreflectance *Rev. Sci. Instrum.* **75** 5119–22
[17] Schmidt A J, Cheaito R and Chiesa M 2009 A frequency-domain thermoreflectance method for the characterization of thermal properties *Rev. Sci. Instrum.* **80** 094901

[18] Shi L, Li D Y, Yu C H, Jang W Y, Kim D, Yao Z, Kim P and Majumdar A 2003 Measuring thermal and thermoelectric properties of one-dimensional nanostructures using a microfabricated device *J. Heat Trans.* **125** 881–8
[19] Kim P, Shi L, Majumdar A and McEuen P L 2001 Thermal transport measurements of individual multiwalled nanotubes *Phys. Rev. Lett.* **87** 215502
[20] Yang J K *et al* 2014 Phonon transport through point contacts between graphitic nanomaterials *Phys. Rev. Lett.* **112** 205901
[21] Yang J K, Yang Y, Waltermire S W, Gutu T, Zinn A A, Xu T T, Chen Y F and Li D Y 2011 Measurement of the intrinsic thermal conductivity of a multiwalled carbon nanotube and its contact thermal resistance with the substrate *Small* **7** 2334–40
[22] Yu C H, Shi L, Yao Z, Li D Y and Majumdar A 2005 Thermal conductance and thermopower of an individual single-wall carbon nanotube *Nano Lett.* **5** 1842–6
[23] Chang C W, Okawa D, Majumdar A and Zettl A 2006 Solid-state thermal rectifier *Science* **314** 1121–4
[24] Chen R, Hochbaum A I, Murphy P, Moore J, Yang P D and Majumdar A 2008 Thermal conductance of thin silicon nanowires *Phys. Rev. Lett.* **101** 105501
[25] Zhang Q *et al* 2018 Thermal transport in quasi-1D van der Waals crystal $Ta_2Pd_3Se_8$ nanowires: size and length dependence *ACS Nano* **12** 2634–42
[26] Shi L, Hao Q, Yu C H, Mingo N, Kong X Y and Wang Z L 2004 Thermal conductivities of individual tin dioxide nanobelts *Appl. Phys. Lett.* **84** 2638–40
[27] Roh J W, Hippalgaonkar K, Ham J H, Chen R K, Li M Z, Ercius P, Majumdar A, Kim W and Lee W 2011 Observation of anisotropy in thermal conductivity of individual single-crystalline bismuth nanowires *ACS Nano* **5** 3954–60
[28] Zhou F, Szczech J, Pettes M T, Moore A L, Jin S and Shi L 2007 Determination of transport properties in chromium disilicide nanowires via combined thermoelectric and structural characterizations *Nano Lett.* **7** 1649–54
[29] Zhou J H, Jin C G, Seol J H, Li X G and Shi L 2005 Thermoelectric properties of individual electrodeposited bismuth telluride nanowires *Appl. Phys. Lett.* **87** 133109
[30] Mavrokefalos A, Moore A L, Pettes M T, Shi L, Wang W and Li X G 2009 Thermoelectric and structural characterizations of individual electrodeposited bismuth telluride nanowires *J. Appl. Phys.* **105** 104318
[31] Wingert M C, Chen Z C Y, Dechaumphai E, Moon J, Kim J H, Xiang J and Chen R K 2011 Thermal conductivity of Ge and Ge–Si core–shell nanowires in the phonon confinement regime *Nano Lett.* **11** 5507–13
[32] Wingert M C, Kwon S, Hu M, Poulikakos D, Xiang J and Chen R K 2015 Sub-amorphous thermal conductivity in ultrathin crystalline silicon nanotubes *Nano Lett.* **15** 2605–11
[33] Yang L *et al* 2016 Thermal conductivity of individual silicon nanoribbons *Nanoscale* **8** 17895–901
[34] Li D Y, Wu Y, Fan R, Yang P D and Majumdar A 2003 Thermal conductivity of Si/SiGe superlattice nanowires *Appl. Phys. Lett.* **83** 3186–8
[35] Lee E K *et al* 2012 Large thermoelectric figure-of-merits from sige nanowires by simultaneously measuring electrical and thermal transport properties *Nano Lett.* **12** 2918–23
[36] Zhang Q *et al* 2017 Defect facilitated phonon transport through kinks in boron carbide nanowires *Nano Lett.* **17** 3550–5
[37] Li D Y, Wu Y Y, Kim P, Shi L, Yang P D and Majumdar A 2003 Thermal conductivity of individual silicon nanowires *App. Phys. Lett.* **83** 2934–6

[38] Hippalgaonkar K, Huang B L, Chen R K, Sawyer K, Ercius P and Majumdar A 2010 Fabrication of microdevices with integrated nanowires for investigating low-dimensional phonon transport *Nano Lett.* **10** 4341–8
[39] Seol J H *et al* 2010 Two-dimensional phonon transport in supported graphene *Science* **328** 213–6
[40] Shi L, Li D Y, Yu C H, Jang W Y, Kim D Y, Yao Z, Kim P and Majumdar A 2003 Erratum: "Measuring thermal and thermoelectric properties of one-dimensional nanostructures using a microfabricated device" [*Journal of Heat Transfer*, 2003, **125**(5), pp. 881–888] *J. Heat Trans.* **125** 1209
[41] Chen R 2008 Nanowires for thermal energy conversion and management *Mechanical Engineering.* (Berkeley, CA: University of California)
[42] Zheng J L, Wingert M C, Dechaumphai E and Chen R K 2013 Sub-picowatt/kelvin resistive thermometry for probing nanoscale thermal transport *Rev. Sci. Instrum.* **84** 114901
[43] Dechaumphai E and Chen R K 2014 Sub-picowatt resolution calorimetry with niobium nitride thin-film thermometer *Rev. Sci. Instrum.* **85** 094903
[44] Wingert M C, Chen Z C Y, Kwon S, Xiang J and Chen R K 2012 Ultra-sensitive thermal conductance measurement of one-dimensional nanostructures enhanced by differential bridge *Rev. Sci. Instrum.* **83** 024901
[45] Hippalgaonkar K, Seol J H, Xu D Y and Li D Y 2017 Experimental studies of thermal transport in nanostructures *Thermal Transport in Carbon-Based Nanomaterials.* ed G Zhang (Amsterdam: Elsevier), pp 319–57
[46] Yang L 2019 *Phonon Transport in Nanowires—Beyond Classical Size Effects, in Mechanical Engineering.* (Nashville, TN: Vanderbilt University)
[47] Bahadur V, Xu J, Liu Y and Fisher T S 2005 Thermal resistance of nanowire–plane interfaces *J. Heat Trans.* **127** 664–8
[48] Bahadur V, Xu J, Liu Y and Fisher T S 2006 Erratum: "Thermal resistance of nanowire-plane interfaces" [*Journal of Heat Transfer*, 2005, **127**(6), pp. 664–668] *J. Heat Trans.* **128** 858
[49] Yu C H, Saha S, Zhou J H, Shi L, Cassell A M, Cruden B A, Ngo Q and Li J 2006 Thermal contact resistance and thermal conductivity of a carbon nanofiber *J. Heat Trans.* **128** 234–9
[50] Zhong Z X, Wingert M C, Strzalka J, Wang H H, Sun T, Wang J, Chen R K and Jiang Z 2014 Structure-induced enhancement of thermal conductivities in electrospun polymer nanofibers *Nanoscale* **6** 8283–91
[51] Prasher R 2005 Predicting the thermal resistance of nanosized constrictions *Nano Lett.* **5** 2155–9
[52] Xia M G, Cheng Z F, Han J Y, Zheng M R, Sow C H, Thong J T L, Zhang S L and Li B W 2014 Gallium ion implantation greatly reduces thermal conductivity and enhances electronic one of ZnO nanowires *AIP Adv.* **4** 057128
[53] Bui C T, Xie R G, Zheng M R, Zhang Q X, Sow C H, Li B W and Thong J T L 2012 Diameter-dependent thermal transport in individual Zno nanowires and its correlation with surface coating and defects *Small* **8** 738–45
[54] Lim J W, Hippalgaonkar K, Andrews S C, Majumdar A and Yang P D 2012 Quantifying surface roughness effects on phonon transport in silicon nanowires *Nano Lett.* **12** 2475–82
[55] Shrestha R *et al* 2018 Crystalline polymer nanofibers with ultra-high strength and thermal conductivity *Nat. Commun.* **9** 1664

[56] Park Y, Lee S, Ha S S, Alunda B, Noh D Y, Lee Y J, Kim S and Seol J H 2019 Crosslinking effect on thermal conductivity of electrospun poly(acrylic acid) nanofibers *Polymers* **11** 858
[57] Park Y, You M, Shin J, Ha S, Kim D, Heo M H, Nah J, Kim Y A and Seol J H 2019 Thermal conductivity enhancement in electrospun poly(vinyl alcohol) and poly(vinyl alcohol)/cellulose nanocrystal composite nanofibers *Sci. Rep.* **9** 3026
[58] Ma J, Zhang Q, Mayo A, Ni Z H, Yi H, Chen Y F, Mu R, Bellan L M and Li D Y 2015 Thermal conductivity of electrospun polyethylene nanofibers *Nanoscale* **7** 16899–908
[59] Ma J, Zhang Q, Zhang Y, Zhou L, Yang J K and Ni Z H 2016 A rapid and simple method to draw polyethylene nanofibers with enhanced thermal conductivity *Appl. Phys. Lett.* **109** 033101
[60] Zhang Y, Zhang X, Yang L, Zhang Q, Fitzgerald M L, Ueda A, Chen Y F, Mu R, Li D Y and Bellan L M 2018 Thermal transport in electrospun vinyl polymer nanofibers: effects of molecular weight and side groups *Soft Matt.* **14** 9534–41
[61] Canetta C, Guo S and Narayanaswamy A 2014 Measuring thermal conductivity of polystyrene nanowires using the dual-cantilever technique *Rev. Sci. Instrum.* **85** 104901
[62] Zeng X L, Xiong Y C, Fu Q, Sun R, Xu J B, Xu D Y and Wong C P 2017 Structure-induced variation of thermal conductivity in epoxy resin fibers *Nanoscale* **9** 10585–9
[63] Balandin A and Wang K L 1998 Significant decrease of the lattice thermal conductivity due to phonon confinement in a free-standing semiconductor quantum well *Phys. Rev.* B **58** 1544–9
[64] Sadat S, Meyhofer E and Reddy P 2012 High resolution resistive thermometry for micro/nanoscale measurements *Rev. Sci. Instrum.* **83** 084902
[65] Zheng J L, Wingert M C, Dechaumphai E and Chen R K 2013 Sub-picowatt/kelvin resistive thermometry for probing nanoscale thermal transport *Rev. Sci. Instrum.* **84** 114901
[66] Sadat S, Meyhofer E and Reddy P 2013 Resistance thermometry-based picowatt-resolution heat-flow calorimeter *Appl. Phys. Lett.* **102** 163110
[67] Zheng J L, Wingert M C, moon J and Chen R K 2016 Simultaneous specific heat and thermal conductivity measurement of individual nanostructures *Semicond. Sci. Technol.* **31** 084005
[68] Weathers A, Bi K D, Pettes M T and Shi L 2013 Re-examination of thermal transport measurements of a low-thermal conductance nanowire with a suspended micro-device *Rev. Sci. Instrum.* **84** 084903
[69] Wang X M, Yang J K, Xiong Y C, Huang B L, Xu T T, Li D Y and Xu D Y 2018 Measuring nanowire thermal conductivity at high temperatures *Meas. Sci. Technol.* **29** 025001
[70] Fernandez-Hurtado V, Fernandez-Dominguez A I, Feist J, Garcia-Vidal F J and Cuevas J C 2018 Super-Planckian far-field radiative heat transfer *Phys. Rev.* B **97** 045408
[71] Thompson D, Zhu L X, Mittapally R, Sadat S, Xing Z, McArdle P, Qazilbash M M, Reddy P and Meyhofer E 2018 Hundred-fold enhancement in far-field radiative heat transfer over the blackbody limit *Nature* **561** 216
[72] Ravindra N M, Abedrabbo S, Chen W, Tong F M, Nanda A K and Speranza A C 1998 Temperature-dependent emissivity of silicon-related materials and structures *IEEE Trans. Semicond. Manuf.* **11** 30–9
[73] Liu D, Xie R G, Yang N, Li B W and Thong J T L 2014 Correction to Profiling nanowire thermal resistance with a spatial resolution of nanometers *Nano Lett.* **14** 4195

[74] Kim J, Ou E, Sellan D P and Shi L 2015 A four-probe thermal transport measurement method for nanostructures *Rev. Sci. Instrum.* **86** 044901
[75] Kwon S, Zheng J L, Wingert M C, Cui S and Chen R K 2017 Unusually high and anisotropic thermal conductivity in amorphous silicon nanostructures *ACS Nano* **11** 2470–6
[76] Regner K T, Sellan D P, Su Z H, Amon C H, McGaughey A J H and Malen J A 2013 Broadband phonon mean free path contributions to thermal conductivity measured using frequency domain thermoreflectance *Nat. Commun.* **4** 1640
[77] Larkin J M and McGaughey A J H 2014 Thermal conductivity accumulation in amorphous silica and amorphous silicon *Phys. Rev.* B **89** 144303
[78] DeAngelis F, Muraleedharan M G, moon J, Seyf H R, Minnich A J, McGaughey A J H and Henry A 2019 Thermal transport in disordered materials *Nanoscale Microscale Thermophys. Eng.* **23** 81–116
[79] moon J, Latour B and Minnich A J 2018 Propagating elastic vibrations dominate thermal conduction in amorphous silicon *Phys. Rev.* B **97** 024201
[80] Braun J L, Baker C H, Giri A, Elahi M, Artyushkova K, Beechem T E, Norris P M, Leseman Z C, Gaskins J T and Hopkins P E 2016 Size effects on the thermal conductivity of amorphous silicon thin films *Phys. Rev.* B **93** 140201
[81] Wingert M C, Zheng J L, Kwon S and Chen R K 2016 Thermal transport in amorphous materials: a review *Semicond. Sci. Technol.* **31** 113003
[82] Tavakoli A, Lulla K, Crozes T, Mingo N, Coilin E and Bourgeois O 2018 Heat conduction measurements in ballistic 1D phonon waveguides indicate breakdown of the thermal conductance quantization *Nat. Commun.* **9** 4287
[83] Schwab K, Henriksen E A, Worlock J M and Roukes M L 2000 Measurement of the quantum of thermal conductance *Nature* **404** 974–7
[84] Bourgeois O, Andre E, Macovei C and Chaussy J 2006 Liquid nitrogen to room-temperature thermometry using niobium nitride thin films *Rev. Sci. Instrum.* **77** 126108
[85] Nomura M, Nakagawa J, Kage Y, Maire J, Moser D and Paul O 2015 Thermal phonon transport in silicon nanowires and two-dimensional phononic crystal nanostructures *Appl. Phys. Lett.* **106** 143102
[86] Anufriev R, Ramiere A, Maire J and Nomura M 2017 Heat guiding and focusing using ballistic phonon transport in phononic nanostructures *Nat. Commun.* **8** 15505
[87] Maire J, Anufriev R and Nomura M 2017 Ballistic thermal transport in silicon nanowires *Sci. Rep.* **7** 41794
[88] Maire J, Anufriev R, Yanagisawa R, Ramiere A, Volz S and Nomura M 2017 Heat conduction tuning by wave nature of phonons *Sci. Adv.* **3** e1700027
[89] Shin S M, Elzouka M, Prasher R and Chen R K 2019 Far-field coherent thermal emission from polaritonic resonance in individual anisotropic nanoribbons *Nat. Commun.* **10** 1377
[90] Hsiao T K, Chang H K, Liou S C, Chu M W, Lee S C and Chang C W 2013 Observation of room-temperature ballistic thermal conduction persisting over 8.3 μm SiGe nanowires *Nat. Nanotechnol.* **8** 534–8
[91] Xu X F *et al* 2014 Length-dependent thermal conductivity in suspended single-layer graphene *Nat. Commun.* **5** 3689
[92] Lee V, Wu C H, Lou Z X, Lee W L and Chang C W 2017 Divergent and ultrahigh thermal conductivity in millimeter-long nanotubes *Phys. Rev. Lett.* **118** 135901

Chapter 13

[1] Beér J M 2007 High efficiency electric power generation: the environmental role *Prog. Energy Combust. Sci.* **33** 107–34

[2] Rosen M A 2001 Energy- and exergy-based comparison of coal-fired and nuclear steam power plants *Exergy Inter. J.* **1** 180–92

[3] Mazzei P, Minichiello F and Palma D 2005 HVAC dehumidification systems for thermal comfort: a critical review *Appl. Therm. Eng.* **25** 677–707

[4] Pérez-Lombard L, Ortiz J and Pout C 2008 A review on buildings energy consumption information *Energy Build.* **40** 394–8

[5] Oh J, Birbarah P, Foulkes T, Yin S L, Rentauskas M, Neely J, Pilawa-Podgurski R C N and Miljkovic N 2017 Jumping-droplet electronics hot-spot cooling *Appl. Phys. Lett.* **110** 123107

[6] Miljkovic N, Preston D J, Enright R and Wang E N 2014 Jumping-droplet electrostatic energy harvesting *Appl. Phys. Lett.* **105** 013111

[7] Humplik T, Lee J, O'hern S, Fellman B, Baig M, Hassan S, Atieh M, Rahman F, Laoui T and Karnik R 2011 Nanostructured materials for water desalination *Nanotechnology* **22** 292001

[8] Vinoth Kumar K and Kasturi Bai R 2008 Performance study on solar still with enhanced condensation *Desalination* **230** 51–61

[9] Kim H, Yang S, Rao S R, Narayanan S, Kapustin E A, Furukawa H, Umans A S, Yaghi O M and Wang E N 2017 Water harvesting from air with metal–organic frameworks powered by natural sunlight *Science* **356** 430

[10] Park K-C, Kim P, Grinthal A, He N, Fox D, Weaver J C and Aizenberg J 2016 Condensation on slippery asymmetric bumps *Nature* **531** 78

[11] Nusselt W 1916 The surface condensation of water vapor *Z. Ver. Dtsch. Ing.* **60** 541–6

[12] Rose J W 2002 Dropwise condensation theory and experiment: a review *Proc. Inst. Mech. Eng.* A **216** 115–28

[13] Boreyko J B and Chen C-H 2010 Self-propelled jumping drops on superhydrophobic surfaces *Phys. Fluids* **22** 091110

[14] Enright R, Miljkovic N, Sprittles J, Nolan K, Mitchell R and Wang E N 2014 How coalescing droplets jump *ACS Nano* **8** 10352–62

[15] Miljkovic N, Enright R, Nam Y, Lopez K, Dou N, Sack J and Wang E N 2013 Jumping-droplet-enhanced condensation on scalable superhydrophobic nanostructured surfaces *Nano Lett.* **13** 179–87

[16] Birbarah P and Miljkovic N 2017 Internal convective jumping-droplet condensation in tubes *Int. J. Heat Mass Transfer* **114** 1025–36

[17] Birbarah P and Miljkovic N 2017 External convective jumping-droplet condensation on a flat plate *Int. J. Heat Mass Transfer* **107** 74–88

[18] Kim M-K, Cha H, Birbarah P, Chavan S, Zhong C, Xu Y and Miljkovic N 2015 Enhanced jumping-droplet departure *Langmuir* **31** 13452–66

[19] Enright R, Miljkovic N, Dou N, Nam Y and Wang E N 2013 Condensation on superhydrophobic copper oxide nanostructures *J. Heat Transfer* **135** 091304–091304-12

[20] Nenad M, Daniel John P, Ryan E, Solomon A, Youngsuk N and Evelyn N W 2013 Jumping droplet dynamics on scalable nanostructured superhydrophobic surfaces *J. Heat Transfer* **135** 080907–080907-1

[21] Miljkovic N, Enright R and Wang E N 2012 Effect of droplet morphology on growth dynamics and heat transfer during condensation on superhydrophobic nanostructured surfaces *ACS Nano* **6** 1776–85
[22] Wiedenheft K F, Guo H A, Qu X, Boreyko J B, Liu F, Zhang K, Eid F, Choudhury A, Li Z and Chen C-H 2017 Hotspot cooling with jumping-drop vapor chambers *Appl. Phys. Lett.* **110** 141601
[23] Qu X, Boreyko J B, Liu F, Agapov R L, Lavrik N V, Retterer S T, Feng J J, Collier C P and Chen C-H 2015 Self-propelled sweeping removal of dropwise condensate *Appl. Phys. Lett.* **106** 221601
[24] Liu F, Ghigliotti G, Feng J J and Chen C-H 2014 Numerical simulations of self-propelled jumping upon drop coalescence on non-wetting surfaces *J. Fluid Mech.* **752** 39–65
[25] Murase T, Wang H S and Rose J W 2006 Effect of inundation for condensation of steam on smooth and enhanced condenser tubes *Int. J. Heat Mass Transfer* **49** 3180–9
[26] Belghazi M, Bontemps A and Marvillet C 2002 Condensation heat transfer on enhanced surface tubes: experimental results and predictive theory *J. Heat Transfer* **124** 754–61
[27] Guo S-P, Wu Z, Li W, Kukulka D, Sundén B, Zhou X-P, Wei J-J and Simon T 2015 Condensation and evaporation heat transfer characteristics in horizontal smooth, herring-bone and enhanced surface EHT tubes *Int. J. Heat Mass Transfer* **85** 281–91
[28] Cho H J, Preston D J, Zhu Y and Wang E N 2016 Nanoengineered materials for liquid–vapour phase-change heat transfer *Nat. Rev. Mater.* **2** 16092
[29] Shahriari A, Birbarah P, Oh J, Miljkovic N and Bahadur V 2017 Electric field-based control and enhancement of boiling and condensation *Nanoscale Microscale Thermophys. Eng.* **21** 102–21
[30] Cavallini A, Censi G, Del Col D, Doretti L, Longo G A, Rossetto L and Zilio C 2003 Condensation inside and outside smooth and enhanced tubes—a review of recent research *Int. J. Refrig.* **26** 373–92
[31] Ma X, Rose J W, Xu D, Lin J and Wang B 2000 Advances in dropwise condensation heat transfer: Chinese research *Chem. Eng. J.* **78** 87–93
[32] Tanasawa I 1991 Advances in condensation heat transfer *Advances in Heat Transfer* ed J P Hartnett, T F Irvine and Y I Cho vol 21 (Amsterdam: Elsevier), pp 55–139
[33] Attinger D, Frankiewicz C, Betz A R, Schutzius T M, Ganguly R, Das A, Kim C-J and Megaridis C M 2014 Surface engineering for phase change heat transfer: a review *MRS Energy Sustainability* **1** E4
[34] Enright R, Miljkovic N, Alvarado J L, Kim K and Rose J W 2014 Dropwise condensation on micro- and nanostructured surfaces *Nanoscale Microscale Thermophys. Eng.* **18** 223–50
[35] Dalkilic A S and Wongwises S 2009 Intensive literature review of condensation inside smooth and enhanced tubes *Int. J. Heat Mass Transfer* **52** 3409–26
[36] Zhang P and Lv F Y 2015 A review of the recent advances in superhydrophobic surfaces and the emerging energy-related applications *Energy* **82** 1068–87
[37] Miljkovic N and Wang E N 2013 Condensation heat transfer on superhydrophobic surfaces *MRS Bull.* **38** 397–406
[38] Wen R, Xu S, Ma X, Lee Y-C and Yang R 2018 Three-dimensional superhydrophobic nanowire networks for enhancing condensation heat transfer *Joule* **2** 269–79
[39] Rose J 1964 Dropwise condensation of steam on vertical planes *PhD Dissertation* University of London (Queen Mary College)

[40] Utaka Y, Saito A, Ishikawa H and Yanagida H 1986 Study on dropwise condensation curves: dropwise to filmwise transition of propylene glycol, ethylene glycol and glycerol vapors on a copper surface using a monolayer type promoter (Part 1) *Bull. JSME* **29** 4228–34

[41] Utaka Y, Saito A, Ishikawawa H and Yanagida H 1988 Study on dropwise condensation curves (dropwise to filmwise transition of propylene glycol, ethylene glycol and glycerol vapors on a copper surface using a monolayer type promoter—part 2) *JSME Inter. J.* **31** 73–80

[42] Das A K, Kilty H P, Marto P J, Andeen G B and Kumar A 1999 The use of an organic self-assembled monolayer coating to promote dropwise condensation of steam on horizontal tubes *J. Heat Transfer* **122** 278–86

[43] Vemuri S, Kim K J, Wood B D, Govindaraju S and Bell T W 2006 Long term testing for dropwise condensation using self-assembled monolayer coatings of *n*-octadecyl mercaptan *Appl. Therm. Eng.* **26** 421–9

[44] Vemuri S and Kim K J 2006 An experimental and theoretical study on the concept of dropwise condensation *Int. J. Heat Mass Transfer* **49** 649–57

[45] Pauporté T, Bataille G, Joulaud L and Vermersch F J 2010 Well-aligned ZnO nanowire arrays prepared by seed-layer-free electrodeposition and their Cassie–Wenzel transition after hydrophobization *J. Phys. Chem.* C **114** 194–202

[46] Razavi S M R *et al* 2017 Superhydrophobic surfaces made from naturally derived hydrophobic materials *ACS Sustain. Chem. Eng.* **5** 11362–70

[47] Love J C, Wolfe D B, Haasch R, Chabinyc M L, Paul K E, Whitesides G M and Nuzzo R G 2003 Formation and structure of self-assembled monolayers of alkanethiolates on palladium *JACS* **125** 2597–609

[48] Love J C, Estroff L A, Kriebel J K, Nuzzo R G and Whitesides G M 2005 Self-assembled monolayers of thiolates on metals as a form of nanotechnology *Chem. Rev.* **105** 1103–70

[49] Chen L, Liang S, Yan R, Cheng Y, Huai X and Chen S 2009 *n*-octadecanethiol self-assembled monolayer coating with microscopic roughness for dropwise condensation of steam *J. Therm. Sci.* **18** 160–5

[50] Enright R, Miljkovic N, Al-Obeidi A, Thompson C V and Wang E N 2012 Condensation on superhydrophobic surfaces: the role of local energy barriers and structure length scale *Langmuir* **28** 14424–32

[51] Boreyko J B and Chen C H 2013 Vapor chambers with jumping-drop liquid return from superhydrophobic condensers *Int. J. Heat Mass Transfer* **61** 409–18

[52] Miljkovic N, Preston D J, Enright R and Wang E N 2013 Electrostatic charging of jumping droplets *Nat. Commun.* **4** 2517

[53] Varanasi K K, Hsu M, Bhate N, Yang W S and Deng T 2009 Spatial control in the heterogeneous nucleation of water *Appl. Phys. Lett.* **95** 094101

[54] Chen X, Wu J, Ma R, Hua M, Koratkar N, Yao S and Wang Z 2011 Nanograssed micropyramidal architectures for continuous dropwise condensation *Adv. Funct. Mater.* **21** 4617–23

[55] Cha H, Chun J M, Sotelo J and Miljkovic N 2016 Focal plane shift imaging for the analysis of dynamic wetting processes *ACS Nano* **10** 8223–32

[56] Chavan S *et al* 2016 Heat transfer through a condensate droplet on hydrophobic and nanostructured superhydrophobic surfaces *Langmuir* **32** 7774–87

[57] Rykaczewski K, Scott J H J, Rajauria S, Chinn J, Chinn A M and Jones W 2011 Three dimensional aspects of droplet coalescence during dropwise condensation on superhydrophobic surfaces *Soft Matter* **7** 8749–52
[58] Paxson A T, Yagüe J L, Gleason K K and Varanasi K K 2014 Stable dropwise condensation for enhancing heat transfer via the initiated chemical vapor deposition (iCVD) of grafted polymer films *Adv. Mater.* **26** 418–23
[59] Preston D J, Mafra D L, Miljkovic N, Kong J and Wang E N 2015 Scalable graphene coatings for enhanced condensation heat transfer *Nano Lett.* **15** 2902–9
[60] Luo H, Liu T, Ma J, Wang P, Wang Y, Leprince-Wang Y and Jing G 2016 Evaporation-induced failure of hydrophobicity *Phys. Rev. Fluids* **1** 053901
[61] Crudden C M *et al* 2014 Ultra stable self-assembled monolayers of *N*-heterocyclic carbenes on gold *Nat. Chem.* **6** 409
[62] Erb R and Thelen E 1965 Promoting permanent dropwise condensation *Ind. Eng. Chem.* **57** 49–52
[63] Brown A R and Thomas M A 1966 Filmwise and dropwise condensation of steam at low pressures (International Heat Transfer Conference Digital Library) (Danbury, CT: Begell House)
[64] Ma X, Xu D and Lin J 1994 A study of dropwise condensation on the ultra-thin polymer surfaces.*International Heat Transfer Conference Digital Library* (Begell House Inc.)
[65] Oh I-K *et al* 2015 Hydrophobicity of rare earth oxides grown by atomic layer deposition *Chem. Mater.* **27** 148–56
[66] Ölçeroğlu E and McCarthy M 2016 Self-organization of microscale condensate for delayed flooding of nanostructured superhydrophobic surfaces *ACS Appl. Mater. Interfaces* **8** 5729–36
[67] Cha H, Xu C, Sotelo J, Chun J M, Yokoyama Y, Enright R and Miljkovic N 2016 Coalescence-induced nanodroplet jumping *Phys. Rev. Fluids* **1** 064102
[68] Hannemann R J and Mikic B B 1976 An experimental investigation into the effect of surface thermal conductivity on the rate of heat transfer in dropwise condensation *Int. J. Heat Mass Transfer* **19** 1309–17
[69] Rose J W 1978 The effect of surface thermal conductivity on dropwise condensation heat transfer *Int. J. Heat Mass Transfer* **21** 80–1
[70] Kuppusami S and Oskouei R H 2015 Parylene coatings in medical devices and implants: a review *Univ. J. Biomed. Eng.* **3** 9–14
[71] Chen T-N, Wuu D-S, Wu C-C, Chiang C-C, Chen Y-P and Horng R-H 2007 Improvements of permeation barrier coatings using encapsulated Parylene interlayers for flexible electronic applications *Plasma Processes Polym.* **4** 180–5
[72] Young Shik S, Keunchang C, Sun Hee L, Seok C, Sung-Jin P, Chanil C, Dong-Chul H and Jun Keun C 2003 PDMS-based micro PCR chip with Parylene coating *J. Micromech. Microeng.* **13** 768
[73] Noar J H, Wahab A, Evans R D and Wojcik A G 1999 The durability of parylene coatings on neodymium-iron-boron magnets *Eur. J. Orthod.* **21** 685–93
[74] 1965 Parylene coating promotes dropwise condensation on condenser tubes *Chem. Eng. News Archive* **43** 45
[75] Marto P J, Looney D J, Rose J W and Wanniarachchi A S 1986 Evaluation of organic coatings for the promotion of dropwise condensation of steam *Int. J. Heat Mass Transfer* **29** 1109–17

[76] Holden K M, Wanniarachchi A S, Marto P J, Boone D H and Rose J W 1987 The use of organic coatings to promote dropwise condensation of steam *J. Heat Trans.* **109** 768–74
[77] Spivack M A and Ferrante G 1969 Determination of the water vapor permeability and continuity of ultrathin Parylene membranes *J. Electrochem. Soc.* **116** 1592–4
[78] SCS Parylene Properties 2016 Specialty Coating Systems
[79] Chen C-H, Cai Q, Tsai C, Chen C-L, Xiong G, Yu Y and Ren Z 2007 Dropwise condensation on superhydrophobic surfaces with two-tier roughness *Appl. Phys. Lett.* **90** 173108
[80] Tenhaeff W E and Gleason K K 2008 Initiated and oxidative chemical vapor deposition of polymeric thin films: iCVD and oCVD *Adv. Funct. Mater.* **18** 979–92
[81] Lau K K S and Gleason K K 2006 Initiated chemical vapor deposition (iCVD) of poly (alkyl acrylates): an experimental study *Macromolecules* **39** 3688–94
[82] Chan K and Gleason K K 2005 Initiated chemical vapor deposition of linear and cross-linked poly(2-hydroxyethyl methacrylate) for use as thin-film hydrogels *Langmuir* **21** 8930–9
[83] Soto D, Ugur A, Farnham T A, Gleason K K and Varanasi K K 2018 Short-fluorinated iCVD coatings for nonwetting fabrics *Adv. Funct. Mater.* **28** 1707355
[84] Ölçeroğlu E, Hsieh C-Y, Rahman M M, Lau K K S and McCarthy M 2014 Full-field dynamic characterization of superhydrophobic condensation on biotemplated nanostructured surfaces *Langmuir* **30** 7556–66
[85] Alf M E *et al* 2010 Chemical vapor deposition of conformal, functional, and responsive polymer films *Adv. Mater.* **22** 1993–2027
[86] Yagüe J L and Gleason K K 2013 Enhanced cross-linked density by annealing on fluorinated polymers synthesized via initiated chemical vapor deposition to prevent surface reconstruction *Macromolecules* **46** 6548–54
[87] Peng C, Chen Z and Tiwari M K 2018 All-organic superhydrophobic coatings with mechanochemical robustness and liquid impalement resistance *Nat. Mater.* **17** 355–60
[88] Wang Y and Gong X 2017 Superhydrophobic coatings with periodic ring structured patterns for self-cleaning and oil–water separation *Adv. Mater.* **4** 1700190
[89] Tiwari M K, Bayer I S, Jursich G M, Schutzius T M and Megaridis C M 2010 Highly liquid-repellent, large-area, nanostructured poly(vinylidene fluoride)/poly(ethyl 2-cyanoacrylate) composite coatings: particle filler effects *ACS Appl. Mater. Interfaces* **2** 1114–9
[90] Bakir M, Henderson C N, Meyer J L, Oh J, Miljkovic N, Kumosa M, Economy J and Jasiuk I 2018 Effects of environmental aging on physical properties of aromatic thermosetting copolyester matrix neat and nanocomposite foams *Polym. Degrad. Stab.* **147** 49–56
[91] Kondrashov V and Rühe J 2014 Microcones and nanograss: toward mechanically robust superhydrophobic surfaces *Langmuir* **30** 4342–50
[92] Wu Y, Zhou S and Wu L 2016 Fabrication of robust hydrophobic and super-hydrophobic polymer films with onefold or dual inverse opal structures *Macromol. Mater. Eng.* **301** 1430–6
[93] Scarratt L R J, Hoatson B S, Wood E S, Hawkett B S and Neto C 2016 Durable superhydrophobic surfaces via spontaneous wrinkling of Teflon AF *ACS Appl. Mater. Interfaces* **8** 6743–50
[94] Hönes R, Kondrashov V, Huai H and Rühe J 2017 Wetting transitions in polymer nanograss generated by nanoimprinting *Macromol. Chem. Phys.* **218** 1700056

[95] Hönes R, Kondrashov V and Rühe J 2017 Molting materials: restoring superhydrophobicity after severe damage via snakeskin-like shedding *Langmuir* **33** 4833–9
[96] Robertson J 2002 Diamond-like amorphous carbon *Mater. Sci. Eng. Rep.* **37** 129–281
[97] Ferrari A C and Robertson J 2000 Interpretation of Raman spectra of disordered and amorphous carbon *Phys. Rev.* B **61** 14095–107
[98] Dearnaley G and Arps J H 2005 Biomedical applications of diamond-like carbon (DLC) coatings: a review *Surf. Coat. Technol.* **200** 2518–24
[99] Roy R K and Lee K-R 2007 Biomedical applications of diamond-like carbon coatings: a review *J. Biomed. Mater. Res.* B **83B** 72–84
[100] Robertson J 2008 Comparison of diamond-like carbon to diamond for applications *Phys. Status Solidi* a **205** 2233–44
[101] Treutler C P O 2005 Industrial use of plasma-deposited coatings for components of automotive fuel injection systems *Surf. Coat. Technol.* **200** 1969–75
[102] van der Kolk G J 2008 Wear resistance of amorphous DLC and metal containing DLC in industrial applications *Tribology of Diamond-Like Carbon Films: Fundamentals and Applications* ed C Donnet and A Erdemir (Boston, MA: Springer), pp 484–93
[103] Matthews A and Eskildsen S S 1994 Engineering applications for diamond-like carbon *Diamond Relat. Mater.* **3** 902–11
[104] Trojan K, Grischke M and Dimigen H 1994 Network modification of DLC coatings to adjust a defined surface energy *Phys. Status Solidi* a **145** 575–85
[105] Grischke M, Bewilogua K, Trojan K and Dimigen H 1995 Application-oriented modifications of deposition processes for diamond-like-carbon-based coatings *Surf. Coat. Technol.* **7475** 739–45
[106] Grischke M, Hieke A, Morgenweck F and Dimigen H 1998 Variation of the wettability of DLC-coatings by network modification using silicon and oxygen *Diamond Relat. Mater.* **7** 454–58
[107] Shamsa M, Liu W L, Balandin A A, Casiraghi C, Milne W I and Ferrari A C 2006 Thermal conductivity of diamond-like carbon films *Appl. Phys. Lett.* **89** 161921
[108] Koch G, Zhang D C and Leipertz A 1997 Condensation of steam on the surface of hard coated copper discs *Heat Mass Transfer* **32** 149–56
[109] Koch G, Zhang D C, Leipertz A, Grischke M, Trojan K and Dimigen H 1998 Study on plasma enhanced CVD coated material to promote dropwise condensation of steam *Int. J. Heat Mass Transfer* **41** 1899–906
[110] Azimi G, Dhiman R, Kwon H-M, Paxson A T and Varanasi K K 2013 Hydrophobicity of rare-earth oxide ceramics *Nat. Mater.* **12** 315–20
[111] Khan S, Azimi G, Yildiz B and Varanasi K K 2015 Role of surface oxygen-to-metal ratio on the wettability of rare-earth oxides *Appl. Phys. Lett.* **106** 061601
[112] Pedraza F, Mahadik S A and Bouchaud B 2015 Synthesis of ceria based superhydrophobic coating on $Ni_{20}Cr$ substrate via cathodic electrodeposition *Phys. Chem. Chem. Phys.* **17** 31750–7
[113] Carchini G, García-Melchor M, Łodziana Z and López N 2016 Understanding and tuning the intrinsic hydrophobicity of rare-earth oxides: a DFT+U study *ACS Appl. Mater. Interfaces* **8** 152–60
[114] Tam J, Palumbo G, Erb U and Azimi G 2017 Robust hydrophobic rare earth oxide composite electrodeposits *Adv. Mater. Interfaces* **4** 1700850

[115] Preston D J, Miljkovic N, Sack J, Enright R, Queeney J and Wang E N 2014 Effect of hydrocarbon adsorption on the wettability of rare earth oxide ceramics *Appl. Phys. Lett.* **105** 011601
[116] Lundy R, Byrne C, Bogan J, Nolan K, Collins M N, Dalton E and Enright R 2017 Exploring the role of adsorption and surface state on the hydrophobicity of rare earth oxides *ACS Appl. Mater. Interfaces* **9** 13751–60
[117] Külah E, Marot L, Steiner R, Romanyuk A, Jung T A, Wäckerlin A and Meyer E 2017 Surface chemistry of rare-earth oxide surfaces at ambient conditions: reactions with water and hydrocarbons *Sci. Rep.* **7** 43369
[118] Fu S-P, Rossero J, Chen C, Li D, Takoudis C G and Abiade J T 2017 On the wetting behavior of ceria thin films grown by pulsed laser deposition *Appl. Phys. Lett.* **110** 081601
[119] Shim J, Seo D, Oh S, Lee J and Nam Y 2018 Condensation heat-transfer performance of thermally stable superhydrophobic cerium-oxide surfaces *ACS Appl. Mater. Interfaces* **10** 31765–76
[120] Prakash S, Ghosh S, Patra A, Annamalai M, Motapothula M R, Sarkar S, Tan S J R, Zhunan J, Loh K P and Venkatesan T 2018 Intrinsic hydrophilic nature of epitaxial thin-film of rare-earth oxide grown by pulsed laser deposition *Nanoscale* **10** 3356–61
[121] Xu P, Coyle T W, Pershin L and Mostaghimi J 2018 Superhydrophobic ceramic coating: fabrication by solution precursor plasma spray and investigation of wetting behavior *J. Colloid Interface Sci.* **523** 35–44
[122] Mogensen M, Sammes N M and Tompsett G A 2000 Physical, chemical and electrochemical properties of pure and doped ceria *Solid State Ionics* **129** 63–94
[123] White M L 1964 The wetting of gold surfaces by water *J. Phys. Chem.* **68** 3083–85
[124] Erb R A 1965 Wettability of metals under continuous condensing conditions *J. Phys. Chem.* **69** 1306–9
[125] White M L and Drobek J 1966 The effect of residual abrasives on the wettability of polished gold surfaces *J. Phys. Chem.* **70** 3432–36
[126] Erb R A 1968 Wettability of gold *J. Phys. Chem.* **72** 2412–7
[127] Erb R A, Haigh T I and Downing T M 1970 Permanent systems for dropwise condensation for distillation plants *Symp. on Enhanced Tubes for Desalination Plants (US Dept. of Interior Washington, DC)* pp 177–201
[128] Morcos I 1971 Double layer structure and the phenomena of wetting *J. Colloid Interface Sci.* **37** 410–21
[129] Trasatti S 1971 Work function, electronegativity, and electrochemical behaviour of metals: II. Potentials of zero charge and 'electrochemical' work functions *J. Electroanal. Chem. Interfacial Electrochem.* **33** 351–78
[130] Trasatti S 1974 Operative (electrochemical) work function of gold *J. Electroanal. Chem. Interfacial Electrochem.* **54** 19–24
[131] Morcos I 1975 The electrocapillary phenomena of solid electrodes *J. Electroanal. Chem. Interfacial Electrochem.* **62** 313–40
[132] Bewig K W and Zisman W A 1965 The wetting of gold and platinum by water *J. Phys. Chem.* **69** 4238–42
[133] Bernett M K and Zisman W A 1970 Confirmation of spontaneous spreading by water on pure gold *J. Phys. Chem.* **74** 2309–12
[134] Schrader M E 1970 Ultrahigh-vacuum techniques in the measurement of contact angles II. Water on gold *J. Phys. Chem.* **74** 2313–7

[135] Wilkins D G, Bromley L A and Read S M 1973 Dropwise and filmwise condensation of water vapor on gold *AlChE J.* **19** 119–23
[136] Gardner J R and Woods R 1977 The hydrophilic nature of gold and platinum *J. Electroanal. Chem. Interfacial Electrochem.* **81** 285–90
[137] Parsegian V A, Weiss G H and Schrader M E 1977 Macroscopic continuum model of influence of hydrocarbon contaminant on forces causing wetting of gold by water *J. Colloid Interface Sci.* **61** 356–60
[138] Smith T 1980 The hydrophilic nature of a clean gold surface *J. Colloid Interface Sci.* **75** 51–5
[139] Woodruff D W and Westwater J W 1981 Steam condensation on various gold surfaces *J. Heat Transf.* **103** 685–92
[140] Westwater J W 1981 Gold surfaces for condensation heat transfer *Gold Bull.* **14** 95–101
[141] O'Neill G A and Westwater J W 1984 Dropwise condensation of steam on electroplated silver surfaces *Int. J. Heat Mass Transfer* **27** 1539–49
[142] Erb R A 1973 Dropwise condensation on gold *Gold Bull.* **6** 2–6
[143] Vorobyev A Y and Guo C 2015 Multifunctional surfaces produced by femtosecond laser pulses *J. Appl. Phys.* **117** 033103
[144] Kietzig A-M, Hatzikiriakos S G and Englezos P 2009 Patterned superhydrophobic metallic surfaces *Langmuir* **25** 4821–7
[145] Khorsand S, Raeissi K, Ashrafizadeh F and Arenas M A 2015 Super-hydrophobic nickel–cobalt alloy coating with micro-nano flower-like structure *Chem. Eng. J.* **273** 638–46
[146] Balajka J, Hines M A, DeBenedetti W J I, Komora M, Pavelec J, Schmid M and Diebold U 2018 High-affinity adsorption leads to molecularly ordered interfaces on TiO_2 in air and solution *Science* **361** 786–9
[147] Yang Z, Liu X and Tian Y 2019 Insights into the wettability transition of nanosecond laser ablated surface under ambient air exposure *J. Colloid Interface Sci.* **533** 268–77
[148] Zhang Y, Zou G, Liu L, Zhao Y, Liang Q, Wu A and Zhou Y N 2016 Time-dependent wettability of nano-patterned surfaces fabricated by femtosecond laser with high efficiency *Appl. Surf. Sci.* **389** 554–9
[149] Chang F-M, Cheng S-L, Hong S-J, Sheng Y-J and Tsao H-K 2010 Superhydrophilicity to superhydrophobicity transition of CuO nanowire films *Appl. Phys. Lett.* **96** 114101
[150] Boinovich L B, Emelyanenko A M, Pashinin A S, Lee C H, Drelich J and Yap Y K 2012 Origins of thermodynamically stable superhydrophobicity of boron nitride nanotubes coatings *Langmuir* **28** 1206–16
[151] Li L H and Chen Y 2010 Superhydrophobic properties of nonaligned boron nitride nanotube films *Langmuir* **26** 5135–40
[152] Kim G-T, Gim S-J, Cho S-M, Koratkar N and Oh I-K 2014 Wetting-transparent graphene films for hydrophobic water-harvesting surfaces *Adv. Mater.* **26** 5166–72
[153] Long J, Zhong M, Zhang H and Fan P 2015 Superhydrophilicity to superhydrophobicity transition of picosecond laser microstructured aluminum in ambient air *J. Colloid Interface Sci.* **441** 1–9
[154] Wang G and Zhang T-Y 2012 Oxygen adsorption induced superhydrophilic-to-super-hydrophobic transition on hierarchical nanostructured CuO surface *J. Colloid Interface Sci.* **377** 438–41
[155] Wang L and McCarthy T J 2016 Covalently attached liquids: instant omniphobic surfaces with unprecedented repellency *Angew. Chem. Int. Ed.* **55** 244–8

[156] Castro Y, Ferrari B, Moreno R and Durán A 2005 Corrosion behaviour of silica hybrid coatings produced from basic catalysed particulate sols by dipping and EPD *Surf. Coat. Technol.* **191** 228–35
[157] Lopez G, Biebuyck H, Frisbie C and Whitesides G 1993 Imaging of features on surfaces by condensation figures *Science* **260** 647–49
[158] Cao P, Xu K, Varghese J O and Heath J R 2011 The microscopic structure of adsorbed water on hydrophobic surfaces under ambient conditions *Nano Lett.* **11** 5581–6
[159] Cha H, Wu A, Kim M-K, Saigusa K, Liu A and Miljkovic N 2017 Nanoscale-agglomerate-mediated heterogeneous nucleation *Nano Lett.* **17** 7544–51
[160] Cognard J 1994 Blistering of glass–epoxy amine adhesive joints in water vapour at high pressure an indication of interfacial crumpling *J. Adhes.* **47** 83–93
[161] Yang X F, Vang C, Tallman D E, Bierwagen G P, Croll S G and Rohlik S 2001 Weathering degradation of a polyurethane coating *Polym. Degrad. Stab.* **74** 341–51
[162] Yang X F, Tallman D E, Bierwagen G P, Croll S G and Rohlik S 2002 Blistering and degradation of polyurethane coatings under different accelerated weathering tests *Polym. Degrad. Stab.* **77** 103–9
[163] Tucker W C and Brown R 1989 Blister formation on graphite/polymer composites galvanically coupled with steel in seawater *J. Compos. Mater.* **23** 389–95
[164] Hinkley J A 1983 A blister test for adhesion of polymer films to SiO_2 *J. Adhes.* **16** 115–25
[165] Jensen H M 1991 The blister test for interface toughness measurement *Eng. Fract. Mech.* **40** 475–86
[166] Cao Z, Wang P, Gao W, Tao L, Suk J W, Ruoff R S, Akinwande D, Huang R and Liechti K M 2014 A blister test for interfacial adhesion of large-scale transferred graphene *Carbon* **69** 390–400
[167] Perraud V *et al* 2015 The future of airborne sulfur-containing particles in the absence of fossil fuel sulfur dioxide emissions *PNAS* **112** 13514–9
[168] Aneja V P 1990 Natural sulfur emissions into the atmosphere *J. Air Waste Manage. Assoc.* **40** 469–76
[169] Bates T S, Lamb B K, Guenther A, Dignon J and Stoiber R E 1992 Sulfur emissions to the atmosphere from natural sourees *J. Atmos. Chem.* **14** 315–37
[170] Barnes I, Hjorth J and Mihalopoulos N 2006 Dimethyl sulfide and dimethyl sulfoxide and their oxidation in the atmosphere *Chem. Rev.* **106** 940–75
[171] Lana A *et al* 2011 An updated climatology of surface dimethlysulfide concentrations and emission fluxes in the global ocean *Global Biogeochem. Cycles* **25** GB1004
[172] Jardine K *et al* 2015 Dimethyl sulfide in the Amazon rain forest *Global Biogeochem. Cycles* **29** 19–32
[173] Filipy J, Rumburg B, Mount G, Westberg H and Lamb B 2006 Identification and quantification of volatile organic compounds from a dairy *Atmos. Environ.* **40** 1480–94
[174] Trabue S, Scoggin K, Mitloehner F, Li H, Burns R and Xin H 2008 Field sampling method for quantifying volatile sulfur compounds from animal feeding operations *Atmos. Environ.* **42** 3332–41
[175] Feilberg A, Liu D, Adamsen A P S, Hansen M J and Jonassen K E N 2010 Odorant emissions from intensive pig production measured by online proton-transfer-reaction mass spectrometry *Environ. Sci. Technol.* **44** 5894–900

[176] Hansen M J, Toda K, Obata T, Adamsen A P S and Feilberg A 2012 Evaluation of single column trapping/separation and chemiluminescence detection for measurement of methanethiol and dimethyl sulfide from pig production *J. Anal. Methods Chem.* **7** 489239
[177] Rumsey I C, Aneja V P and Lonneman W A 2014 Characterizing reduced sulfur compounds emissions from a swine concentrated animal feeding operation *Atmos. Environ.* **94** 458–66
[178] Gligorovski S and Abbatt J P D 2018 An indoor chemical cocktail *Science* **359** 632–3
[179] McDonald B C *et al* 2018 Volatile chemical products emerging as largest petrochemical source of urban organic emissions *Science* **359** 760–4
[180] Kürten A *et al* 2014 Neutral molecular cluster formation of sulfuric acid–dimethylamine observed in real time under atmospheric conditions *PNAS* **111** 15019–24
[181] Karl M, Gross A, Leck C and Pirjola L 2007 Intercomparison of dimethylsulfide oxidation mechanisms for the marine boundary layer: gaseous and particulate sulfur constituents *J. Geophys. Res. Atmos.* **112** D15304
[182] Dawson M L, Varner M E, Perraud V, Ezell M J, Gerber R B and Finlayson-Pitts B J 2012 Simplified mechanism for new particle formation from methanesulfonic acid, amines, and water via experiments and *ab initio* calculations *PNAS* **109** 18719–24
[183] Faghri A 1995 *Heat Pipe Science and Technology* 2nd ed (Columbia, MO: Global Digital Press)
[184] Bejan A 2002 Fundamentals of exergy analysis, entropy generation minimization, and the generation of flow architecture *Int. J. Energy Res.* **26** 0–43
[185] Landoulsi J, Genet M J, Fleith S, Touré Y, Liascukiene I, Méthivier C and Rouxhet P G 2016 Organic adlayer on inorganic materials: XPS analysis selectivity to cope with adventitious contamination *Appl. Surf. Sci.* **383** 71–83
[186] Oh J, Zhang R, Shetty P P, Krogstad J A, Braun P V and Miljkovic N 2018 Thin film condensation on nanostructured surfaces *Adv. Funct. Mater.* **28** 1707000
[187] Ölçeroğlu E, Hsieh C-Y, Lau K K S and McCarthy M 2017 Thin film condensation supported on ambiphilic microstructures *J. Heat Transfer* **139** 020910
[188] Wang R and Antao D S 2018 Capillary-enhanced filmwise condensation in porous media *Langmuir* **34** 13855–63
[189] Preston D J, Wilke K L, Lu Z, Cruz S S, Zhao Y, Becerra L L and Wang E N 2018 Gravitationally driven wicking for enhanced condensation heat transfer *Langmuir* **34** 4658–64
[190] Park K-J, Seo T and Jung D 2007 Performance of alternative refrigerants for residential air-conditioning applications *Appl. Energy* **84** 985–91
[191] Dincer I 2017 *Refrigeration Systems and Applications* (New York: Wiley)
[192] Allen D T and Shonnard D R 2001 *Green Engineering: Environmentally Conscious Design of Chemical Processes* (Upper Saddle River, NJ: Prentice Hall)
[193] Lim W, Choi K and Moon I 2013 Current status and perspectives of liquefied natural gas (LNG) plant design *Ind. Eng. Chem. Res.* **52** 3065–88
[194] Koppejan J and Van Loo S 2012 *The Handbook of Biomass Combustion and Co-firing* (London: Earthscan)
[195] Sun D-W and Zheng L 2006 Vacuum cooling technology for the agri-food industry: past, present and future *J. Food Eng.* **77** 203–14
[196] Xue Z, Cao Y, Liu N, Feng L and Jiang L 2014 Special wettable materials for oil/water separation *J. Mater. Chem.* A **2** 2445–60

[197] Gao S J, Shi Z, Zhang W B, Zhang F and Jin J 2014 Photoinduced superwetting single-walled carbon nanotube/TiO_2 ultrathin network films for ultrafast separation of oil-in-water emulsions *ACS Nano* **8** 6344–52
[198] Xue Z, Wang S, Lin L, Chen L, Liu M, Feng L and Jiang L 2011 A novel superhydrophilic and underwater superoleophobic hydrogel-coated mesh for oil/water separation *Adv. Mater.* **23** 4270–3
[199] Jin M, Wang J, Yao X, Liao M, Zhao Y and Jiang L 2011 Underwater oil capture by a three-dimensional network architectured organosilane surface *Adv. Mater.* **23** 2861–4
[200] Nishimoto S and Bhushan B 2013 Bioinspired self-cleaning surfaces with superhydrophobicity, superoleophobicity, and superhydrophilicity *RSC Adv.* **3** 671–90
[201] Wong T-S, Kang S H, Tang S K, Smythe E J, Hatton B D, Grinthal A and Aizenberg J 2011 Bioinspired self-repairing slippery surfaces with pressure-stable omniphobicity *Nature* **477** 443
[202] Pan S, Kota A K, Mabry J M and Tuteja A 2012 Superomniphobic surfaces for effective chemical shielding *JACS* **135** 578–81
[203] Kota A K, Kwon G and Tuteja A 2014 The design and applications of superomniphobic surfaces *NPG Asia Mater.* **6** e109
[204] Chen L, Liu M, Bai H, Chen P, Xia F, Han D and Jiang L 2009 Antiplatelet and thermally responsive poly (N-isopropylacrylamide) surface with nanoscale topography *JACS* **131** 10467–72
[205] Yong J, Chen F, Yang Q, Huo J and Hou X 2017 Superoleophobic surfaces *Chem. Soc. Rev.* **46** 4168–217
[206] Bellanger H, Darmanin T, Taffin de Givenchy E and Guittard F D R 2014 Chemical and physical pathways for the preparation of superoleophobic surfaces and related wetting theories *Chem. Rev.* **114** 2694–716
[207] Chu Z and Seeger S 2014 Superamphiphobic surfaces *Chem. Soc. Rev.* **43** 2784–98
[208] Tuteja A, Choi W, Ma M, Mabry J M, Mazzella S A, Rutledge G C, McKinley G H and Cohen R E 2007 Designing superoleophobic surfaces *Science* **318** 1618–22
[209] Tuteja A, Choi W, Mabry J M, McKinley G H and Cohen R E 2008 Robust omniphobic surfaces *Proc. Natl Acad. Sci.* **105** 18200–5
[210] Zhao H, Law K-Y and Sambhy V 2011 Fabrication, surface properties, and origin of superoleophobicity for a model textured surface *Langmuir* **27** 5927–35
[211] Kota A K, Li Y, Mabry J M and Tuteja A 2012 Hierarchically structured superoleophobic surfaces with ultralow contact angle hysteresis *Adv. Mater.* **24** 5838–43
[212] Ahuja A, Taylor J, Lifton V, Sidorenko A, Salamon T, Lobaton E, Kolodner P and Krupenkin T 2008 Nanonails: a simple geometrical approach to electrically tunable superlyophobic surfaces *Langmuir* **24** 9–14
[213] Liu T and Kim C-J 2014 Turning a surface superrepellent even to completely wetting liquids *Science* **346** 1096–100
[214] Wilke K L, Preston D J, Lu Z and Wang E N 2018 Towards condensation-resistant omniphobic surfaces *ACS Nano* **12** 11013–21
[215] Rykaczewski K, Paxson A T, Staymates M, Walker M L, Sun X, Anand S, Srinivasan S, McKinley G H, Chinn J and Scott J H J 2014 Dropwise condensation of low surface tension fluids on omniphobic surfaces *Sci. Rep.* **4** 4158

[216] Preston D J, Lu Z, Song Y, Zhao Y, Wilke K L, Antao D S, Louis M and Wang E N 2018 Heat transfer enhancement during water and hydrocarbon condensation on lubricant infused surfaces *Sci. Rep.* **8** 540
[217] Solomon B R, Subramanyam S B, Farnham T A, Khalil K S, Anand S and Varanasi K K 2016 Lubricant-impregnated surfaces *Non-wettable Surfaces* (Cambridge: Royal Society of Chemistry), pp 285–318
[218] Manna U and Lynn D M 2015 Fabrication of liquid-infused surfaces using reactive polymer multilayers: principles for manipulating the behaviors and mobilities of aqueous fluids on slippery liquid interfaces *Adv. Mater.* **27** 3007–12
[219] Lafuma A and Quéré D 2011 Slippery pre-suffused surfaces *Europhys Lett.* **96** 56001
[220] Smith J D, Dhiman R, Anand S, Reza-Garduno E, Cohen R E, McKinley G H and Varanasi K K 2013 Droplet mobility on lubricant-impregnated surfaces *Soft Matter* **9** 1772–80
[221] Weisensee P B, Wang Y, Hongliang Q, Schultz D, King W P and Miljkovic N 2017 Condensate droplet size distribution on lubricant-infused surfaces *Int. J. Heat Mass Transfer* **09** 187–99
[222] Vogel N, Belisle R A, Hatton B, Wong T-S and Aizenberg J 2013 Transparency and damage tolerance of patternable omniphobic lubricated surfaces based on inverse colloidal monolayers *Nat. Commun.* **4** 2176
[223] Anand S, Paxson A T, Dhiman R, Smith J D and Varanasi K K 2012 Enhanced condensation on lubricant-impregnated nanotextured surfaces *ACS Nano* **6** 10122–9
[224] Xiao R, Miljkovic N, Enright R and Wang E N 2013 Immersion condensation on oil-infused heterogeneous surfaces for enhanced heat transfer *Sci. Rep.* **3** 1988
[225] Kim S and Kim K J 2011 Dropwise condensation modeling suitable for superhydrophobic surfaces *J. Heat Transfer* **133** 081502
[226] Boreyko J B, Polizos G, Datskos P G, Sarles S A and Collier C P 2014 Air-stable droplet interface bilayers on oil-infused surfaces *Proc. Natl Acad. Sci.* 201400381
[227] Anand S, Rykaczewski K, Subramanyam S B, Beysens D and Varanasi K K 2015 How droplets nucleate and grow on liquids and liquid impregnated surfaces *Soft Matter* **11** 69–80
[228] Subramanyam S B, Rykaczewski K and Varanasi K K 2013 Ice adhesion on lubricant-impregnated textured surfaces *Langmuir* **29** 13414–8
[229] Schellenberger F, Xie J, Encinas N, Hardy A, Klapper M, Papadopoulos P, Butt H-J and Vollmer D 2015 Direct observation of drops on slippery lubricant-infused surfaces *Soft Matter* **11** 7617–26
[230] Van Oss C J, Chaudhury M K and Good R J 1988 Interfacial Lifshitz–van der Waals and polar interactions in macroscopic systems *Chem. Rev.* **88** 927–41
[231] Preston D J, Song Y, Lu Z, Antao D S and Wang E N 2017 Design of lubricant infused surfaces *ACS Appl. Mater. Interfaces* **9** 42383–92
[232] Sett S, Yan X, Barac G, Bolton L W and Miljkovic N 2017 Lubricant-infused surfaces for low-surface-tension fluids: promise versus reality *ACS Appl. Mater. Interfaces* **9** 36400–408
[233] de Gennes P-G, Brochard-Wyart F and Queré D 2013 Capillarity and wetting phenomena: drops *Bubbles, Pearls, Waves* (Berlin: Springer), pp 291
[234] Rykaczewski K, Landin T, Walker M L, Scott J H J and Varanasi K K 2012 Direct imaging of complex nano- to microscale interfaces involving solid, liquid, and gas phases *ACS Nano* **6** 9326–34

[235] Cheng Y, Suhonen H, Helfen L, Li J, Xu F, Grunze M, Levkin P A and Baumbach T 2014 Direct three-dimensional imaging of polymer–water interfaces by nanoscale hard x-ray phase tomography *Soft Matter* **10** 2982–90
[236] Wu A and Miljkovic N 2018 Droplet cloaking imaging and characterization *J. Heat Transfer* **140** 030902
[237] Etzler F M 2013 Determination of the surface free energy of solids *Rev. Adhes. Adhesiv.* **1** 3–45
[238] Donahue D J and Bartell F 1952 The boundary tension at water–organic liquid interfaces *J. Phys. Chem.* **56** 480–4
[239] Vorobev A 2014 Dissolution dynamics of miscible liquid/liquid interfaces *Curr. Opin. Colloid Interface Sci.* **19** 300–08
[240] Wexler J S, Jacobi I and Stone H A 2015 Shear-driven failure of liquid-infused surfaces *Phys. Rev. Lett.* **114** 168301
[241] Miljkovic N, Preston D J, Enright R and Wang E N 2013 Electric-field-enhanced condensation on superhydrophobic nanostructured surfaces *ACS Nano* **7** 11043–54
[242] Preston D J, Miljkovic N, Wang E N and Enright R 2014 Jumping droplet electrostatic charging and effect on vapor drag *J. Heat Transfer* **136** 080909
[243] Landau L D, Lifshitz E M and Pitaevskiĭ L P 1984 *Electrodynamics of Continuous Media* 2nd edn (Oxford: Pergamon)
[244] Velkoff H R and Miller J H 1965 Condensation of vapor on a vertical plate with a transverse electrostatic field *J. Heat Transfer* **87** 197–201
[245] Yabe A 1991 *Active Heat Transfer Enhancement by Applying Electric Fields* (New York: American Society of Mechanical Engineers)
[246] Yamashita K, Kumagai M, Sekita S, Yabe A, Taketani T and Kikuchi K 1991 *Heat Transfer Characteristics on an EHD Condenser* (New York: American Society of Mechanical Engineers)
[247] Yabe A, Taketani T, Yoshizawa Y and Sunada K 1991 *Experimental Study of EHD Pseudo-Dropwise Condensation* (New York: American Society of Mechanical Engineers)
[248] Seth A K and Lee L 1974 The effect of an electric field in the presence of noncondensable gas on film condensation heat transfer *J. Heat Transfer* **96** 257–8
[249] Bologa M K, Savin I K and Didkovsky A B 1987 Electric-field-induced enhancement of vapour condensation heat transfer in the presence of a non-condensable gas *Int. J. Heat Mass Transfer* **30** 1577–85
[250] Omidvarborna H, Mehrabani-Zeinabad A and Esfahany M N 2009 Effect of electro-hydrodynamic (EHD) on condensation of R-134a in presence of non-condensable gas *Int. Commun. Heat Mass Transfer* **36** 286–91
[251] Budov V M, Kir'yanov V A and Shemagin I A 1987 Heat transfer in the laminar-wave section of condensation of a stationary vapor *J. Eng. Phys.* **52** 647–9
[252] Butt H-J, Untch M B, Golriz A, Pihan S A and Berger R 2011 Electric-field-induced condensation: an extension of the Kelvin equation *Phys. Rev.* E **83** 061604
[253] Birbarah P, Li Z E, Pauls A and Miljkovic N 2015 A comprehensive model of electric-field-enhanced jumping-droplet condensation on superhydrophobic surfaces *Langmuir* **31** 7885–96
[254] McCarty L S and Whitesides G M 2008 Electrostatic charging due to separation of ions at interfaces: contact electrification of ionic electrets *Angew. Chem. Int. Ed.* **47** 2188–207

[255] Corson L T, Tsakonas C, Duffy B R, Mottram N J, Sage I C, Brown C V and Wilson S K 2014 Deformation of a nearly hemispherical conducting drop due to an electric field: theory and experiment *Phys. Fluids* **26** 122106
[256] Roux J M, Achard J L and Fouillet Y 2008 Forces and charges on an undeformable droplet in the dc field of a plate condenser *J. Electrostat.* **66** 283–93
[257] Glière A, Roux J-M and Achard J-L 2013 Lift-off of a conducting sessile drop in an electric field *Microfluid. Nanofluid.* **15** 207–18
[258] Lebedev N and Skalskaya I 1962 Force acting on conducting ball placed in plane capacitor field *J. Tech. Phys.* **32** 375–8
[259] Wohlhuter F K and Basaran O A 1992 Shapes and stability of pendant and sessile dielectric drops in an electric field *J. Fluid Mech.* **235** 481–510
[260] Ristenpart W D, Bird J C, Belmonte A, Dollar F and Stone H A 2009 Non-coalescence of oppositely charged drops *Nature* **461** 377
[261] Ren B and Kang Y 2018 Demulsification of oil-in-water (O/W) emulsion in bidirectional pulsed electric field *Langmuir* **34** 8923–31
[262] Aubry N, Singh P, Janjua M and Nudurupati S 2008 Micro- and nanoparticles self-assembly for virtually defect-free, adjustable monolayers *Proc. Natl Acad. Sci.* **105** 3711
[263] Pohl H A 1978 *Dielectrophoresis: The Behavior of Neutral Matter in Nonuniform Electric Fields* (Cambridge: Cambridge University Press)
[264] Aubry N and Singh P 2006 Control of electrostatic particle–particle interactions in dielectrophoresis *Europhys. Lett.* **74** 623–9

Chapter 14

[1] Kim K and Kaviany M 2016 Thermal conductivity switch: optimal semiconductor/metal melting transition *Phys. Rev.* B **94** 155203
[2] Adams M J, Verosky M, Zebarjadi M and Heremans J P 2019 High switching ratio variable-temperature solid-state thermal switch based on thermoelectric effects *Int. J. Heat Mass Transf.* **134** 114–8
[3] Zebarjadi M 2015 Electronic cooling using thermoelectric devices *Appl. Phys. Lett.* **106** 203506
[4] Schwede J W *et al* 2010 Photon-enhanced thermionic emission for solar concentrator systems *Nat. Mater.* **9** 762–7
[5] Schlichter W 1915 Die spontane Elektronenemission glühender Metalle und das glühelektrische Element *Ann. Phys.* **352** 573–640
[6] Murphy E L and Good R H 1956 Thermionic emission, field emission, and the transition region *Phys. Rev.* **102** 1464–73
[7] Hatsopoulos G N 1965 *The Thermo-Electron Engine* (Cambridge, MA: Massachusetts Institute of Technology)
[8] Ioffe A F 1957 *Semiconductor Thermoelements and Thermoelectric Cooling* (London: Infosearch Ltd)
[9] Moss H 1957 Thermionic diodes as energy converters *J. Electron. Control* **2** 305–22
[10] Hernqvist K G, Kanefsky M and Norman F H 1958 Thermionic energy converter *RCA Rev.* **19** 244–58
[11] Webster H F 1959 Calculation of the performance of a high-vacuum thermionic energy converter *J. Appl. Phys.* **30** 488–92

[12] Hatsopoulos G N and Kaye J 1958 Measured thermal efficiencies of a diode configuration of a thermo electron engine *J. Appl. Phys.* **29** 1124–5
[13] Wilson V C 1959 Conversion of heat to electricity by thermionic emission *J. Appl. Phys.* **30** 475
[14] White M C 1996 *An Overview of Thermionic Power Conversion Technology* (Gainesville, FL: University of Florida)
[15] National Research Council 2001 *Termionics Quo Vadis? An Assessment of the DTRA's Advanced Termionics Research and Development Program* (Washington DC: The National Academies Press)
[16] Usov N N P-S V M T V A 2000 Russian space nuclear power and nuclear thermal propulsion systems *Nucl. News* **43** 33–46
[17] Merrill O S 1980 The changing emphasis of the DOE thermionic program *IEEE International Conference of Plasma Science* (Piscataway, NJ: IEEE), p 14
[18] Rasor N S 1991 Thermionic energy conversion plasmas *IEEE Trans. Plasma Sci.* **19** 1191–208
[19] Shakouri A and Bowers J E 1997 Heterostructure integrated thermionic coolers *Appl. Phys. Lett.* **71** 1234–6
[20] Mahan G D, Sofo J O and Bartkowiak M 1998 Multilayer thermionic refrigerator and generator *J. Appl. Phys.* **83** 4683
[21] Mahan G D and Woods L M 1998 Multilayer thermionic refrigeration *Phys. Rev. Lett.* **80** 4016–9
[22] Saha B, Sands T D and Waghmare U V 2012 Thermoelectric properties of HfN/ScN metal/semiconductor superlattices: a first-principles study *J. Phys. Condens. Matter.* **24** 415303
[23] Saha B, Sands T D and Waghmare U V 2011 First-principles analysis of ZrN/ScN metal/semiconductor superlattices for thermoelectric energy conversion *J. Appl. Phys.* **109** 083717
[24] Sofo J O, Mahan G D and Baars J 1994 Transport coefficients and thermoelectric figure of merit of n-$Hg_{1-x}Cd_xTe$ *J. Appl. Phys.* **76** 2249–54
[25] Velicu S *et al* 2008 Thermoelectric characteristics in MBE-grown HgCdTe-based superlattices *J. Electron. Mater.* **37** 1504–8
[26] LaBounty C, Shakouri A, Abraham P and Bowers J E 2000 Monolithic integration of thin-film coolers with optoelectronic devices *Opt. Eng.* **39** 2847
[27] Shakouri A, LaBounty C, Piprek J, Abraham P and Bowers J E 1999 Thermionic emission cooling in single barrier heterostructures *Appl. Phys. Lett.* **74** 88–9
[28] Singh R *et al* 2003 Experimental characterization and modeling of InP-based microcoolers *MRS Proc.* **793** S11.4
[29] Labounty C J *et al* 2001 Experimental investigation of thin film InGaAsP coolers *Mater. Res. Soc. Symp. Proc.* **626** Z14.4.1-6
[30] Zhang J, Anderson N G and Lau K M 2003 AlGaAs superlattice microcoolers *Appl. Phys. Lett.* **83** 374–6
[31] Zhang Y *et al* 2003 Influence of doping concentration and ambient temperature on the cross-plane Seebeck coefficient of InGaAs/InAlAs superlattices *MRS Proc.* **793** S2.4
[32] LaBounty C, Almuneau G, Shakouri A and Bowers J E 2000 Sb-based III–V cooler *19th Int. Conf. on Thermoelectrics*
[33] Zeng G *et al* 1999 SiGe micro-cooler *Electron. Lett.* **35** 2146
[34] Fan X *et al* 2001 High cooling power density SiGe/Si micro-coolers *Electron. Lett.* **37** 126

[35] Fan X *et al* 2001 Integrated cooling for Si-based microelectronics *Proc. 20th Int. Conf. on Thermoelectrics* p 405–8doi: 10.1109/ICT.2001.979917
[36] Fan X *et al* 2001 SiGeC/Si superlattice microcoolers *Appl. Phys. Lett.* **78** 1580–2
[37] Chen C-C, Li Z, Shi L and Cronin S B 2015 Thermoelectric transport across graphene/hexagonal boron nitride/graphene heterostructures *Nano Res.* **8** 666–72
[38] Wang X, Zebarjadi M and Esfarjani K 2016 First principles calculations of solid-state thermionic transport in layered van der Waals heterostructures *Nanoscale* **8** 14695–704
[39] Wang X, Zebarjadi M and Esfarjani K 2018 High-performance solid-state thermionic energy conversion based on 2D van der Waals heterostructures: a first-principles study *Sci. Rep.* **8** 9303
[40] Richardson O W 1912 LI. Some applications of the electron theory of matter *Philos. Mag. J. Sci.* **23** 594–627
[41] Dushman S 1923 Electron emission from metals as a function of temperature *Phys. Rev.* **21** 623
[42] Zebarjadi M 2017 Solid-state thermionic power generators: an analytical analysis in the nonlinear regime *Phys. Rev. Appl.* **8** 014008
[43] Houston J M 1959 Theoretical efficiency of the thermionic energy converter *J. Appl. Phys.* **30** 481
[44] Mahan G D 1994 Thermionic refrigeration *J. Appl. Phys.* **76** 4362–6
[45] Dmitriev V D and Kholopo G K 1965 Radiant emissivity of tungsten in the infrared region of the spectrum *J. Appl. Spectr.* **2** 315–20
[46] Taylor J B and Langmuir I 1933 The evaporation of atoms, ions and electrons from caesium films on tungsten *Phys. Rev.* **44** 423–58
[47] Gurney R W 1935 Theory of electrical double layers in adsorbed films *Phys. Rev.* **47** 479–82
[48] Langmuir I 1932 Vapor pressures, evaporation, condensation and adsorption *J. Am. Chem. Soc.* **54** 2798–832
[49] Sinsarp A, Yamada Y, Sasaki M and Yamamoto S 2003 Microscopic study on the work function reduction induced by Cs-adsorption *Jpn J. Appl. Phys.* **42** 4882–6
[50] Desplat J-L and Papageorgopoulos C A 1980 Interaction of cesium and oxygen on W(110) *Surf. Sci.* **92** 97–118
[51] Hernqvist K G 1963 Analysis of the arc mode operation of the cesium vapor thermionic energy converter *Proc. IEEE* **51** 748–54
[52] Hishinuma Y, Geballe T H, Moyzhes B Y and Kenny T W 2001 Refrigeration by combined tunneling and thermionic emission in vacuum: use of nanometer scale design *Appl. Phys. Lett.* **78** 2572–4
[53] Morini F, Dubois E, Robillard J F, Monfray S and Skotnicki T 2014 Low work function thin film growth for high efficiency thermionic energy converter: coupled Kelvin probe and photoemission study of potassium oxide *Phys. Status Solidi.* **211** 1334–7
[54] Ortega J E, Oellig E M, Ferrón J and Miranda R 1987 Cs and O adsorption on Si(100) 2 × 1: a model system for promoted oxidation of semiconductors *Phys. Rev.* B **36** 6213–6
[55] Wu J X *et al* 1999 Photoemission study of the effect of annealing temperature on a K_2O_2/Si (100) surface *Phys. Rev.* B **60** 17102
[56] Lee J-H *et al* 2014 Microfabricated thermally isolated low work-function emitter *J. Microelectromechanical Syst.* **23** 1182–7

[57] Jin F, Liu Y and Day C M 2006 Thermionic emission from carbon nanotubes with a thin layer of low work function barium strontium oxide surface coating *Appl. Phys. Lett.* **88** 163116
[58] Fomenko V S and Samsonov G V (ed) 1966 *Handbook of Thermoionic Properties* (Boston, MA: Springer)
[59] Koeck F A M, Nemanich R J, Lazea A and Haenen K 2009 Thermionic electron emission from low work-function phosphorus doped diamond films *Diam. Relat. Mater.* **18** 789–91
[60] Koeck F A M and Nemanich R J 2006 Emission characterization from nitrogen-doped diamond with respect to energy conversion *Diam. Relat. Mater.* **217** 15
[61] Sherehiy A *et al* 2014 Thermionic emission from phosphorus (P) doped diamond nanocrystals supported by conical carbon nanotubes and ultraviolet photoelectron spectroscopy study of P-doped diamond films *Diam. Relat. Mater.* **50** 66–76
[62] Paxton W F, Wisitsoraat A, Raina S, Davidson J L and Kang W P 2010 P2.14: Characterization of the thermionic electron emission properties of nitrogen-incorporated 'ridged' nanodiamond for use in thermal energy conversion *International Vacuum Nanoelectronics Conference* pp 149–50 (Piscataway, NJ: IEEE)
[63] Nemanich R J *et al* 2010 Thermionic and field electron emission devices from diamond and carbon nanostructures *3rd International Nanoelectronics Conference (INEC)* pp 56–7 (Piscataway, NJ: IEEE)
[64] Österlund L, Chakarov D V and Kasemo B 1999 Potassium adsorption on graphite(0001) *Surf. Sci.* **420** 174–89
[65] Michel J a *et al* 2008 Synthesis and characterization of potassium metal/graphitic carbon nanofiber intercalates *J. Nanosci. Nanotechnol.* **8** 1942–50
[66] Westover T L, Franklin A D, Cola B A, Fisher T S and Reifenberger R G 2010 Photo- and thermionic emission from potassium-intercalated carbon nanotube arrays *J. Vac. Sci. Technol.* B **28** 423–34
[67] Smestad G 2004 Conversion of heat and light simultaneously using a vacuum photodiode and the thermionic and photoelectric effects *Sol. Energy Mater. Sol. Cells* **82** 227–40
[68] Belbachir R Y, An Z and Ono T 2014 Thermal investigation of a micro-gap thermionic power generator *J. Micromechanics Microengineering* **24** 085009
[69] Littau K A *et al* 2013 Microbead-separated thermionic energy converter with enhanced emission current *Phys. Chem. Chem. Phys.* **15** 14442–6
[70] Lee J-H, Bargatin I, Melosh N A and Howe R T 2012 Optimal emitter-collector gap for thermionic energy converters *Appl. Phys. Lett.* **100** 173904
[71] Meir S, Stephanos C, Geballe T H and Mannhart J 2013 Highly-efficient thermoelectronic conversion of solar energy and heat into electric power *J. Renew. Sustain. Energy* **5** 043127
[72] Wanke R *et al* 2016 Magnetic-field-free thermoelectronic power conversion based on graphene and related two-dimensional materials *J. Appl. Phys.* **119** 244507
[73] Rasor N S 1963 Emission physics of the thermionic energy converter *Proc. IEEE* **51** 733–47
[74] Ryan Smith J 2013 Increasing the efficiency of a thermionic engine using a negative electron affinity collector *J. Appl. Phys.* **114** 164514
[75] Takeuchi D *et al* 2005 Direct observation of negative electron affinity in hydrogen-terminated diamond surfaces *Appl. Phys. Lett.* **86** 152103
[76] Nemanich R J *et al* 1996 Negative electron affinity surfaces of aluminum nitride and diamond *Diam. Relat. Mater.* **5** 790–6

[77] Sugino T, Kimura C and Yamamoto T 2002 Electron field emission from boron–nitride nanofilms *Appl. Phys. Lett.* **80** 3602–4
[78] Shakouri A, LaBounty C, Abraham P, Piprek J and Bowers J E 1998 Enhanced thermionic emission cooling in high barrier superlattice heterostructures *MRS Proc.* **545** 449
[79] Vashaee D *et al* 2005 Modeling and optimization of single-element bulk SiGe thin-film coolers *Microscale Thermophys. Eng.* **9** 99–118
[80] Zebarjadi M, Shakouri A and Esfarjani K 2006 Thermoelectric transport perpendicular to thin-film heterostructures calculated using the Monte Carlo technique *Phys. Rev.* B **74** 195331
[81] Zebarjadi M, Esfarjani K and Shakouri A 2007 Nonlinear Peltier effect in semiconductors *Appl. Phys. Lett.* **91** 122104
[82] Radtke R J, Ehrenreich H and Grein C H 1999 Multilayer thermoelectric refrigeration in $Hg_{1-x}Cd_xTe$ superlattices *J. Appl. Phys.* **86** 3195–8
[83] Vining C B and Mahan G D 1999 The B factor in multilayer thermionic refrigeration *J. Appl. Phys.* **86** 6852–3
[84] Vashaee D and Shakouri A 2004 Electronic and thermoelectric transport in semiconductor and metallic superlattices *J. Appl. Phys.* **95** 1233–45
[85] Schmidt J, Ortner K, Jensen J E and Becker C R 2002 Molecular beam epitaxially grown n-type $Hg_{0.80}Cd_{0.20}Te(112)B$ using iodine *J. Appl. Phys.* **91** 451
[86] Dilhaire S *et al* 2003 Thermal and thermomechanical study of micro-refrigerators on a chip based on semiconductor heterostructures *Proceedings 22nd International Conference on Thermoelectrics (January)* pp 519–23 (Piscataway, NJ: IEEE)
[87] Zhang Y *et al* 2003 3D electrothermal simulation of heterostructure thin film micro-coolers *ASME Int. Mechanical Engineering Congress and Exposition* pp 39–48
[88] Fitting A *et al* 2001 Transient response of thin film SiGe micro coolers *Int. Mechanical Engineering Congress and Exhibition*
[89] Shakouri A and Zhang Y 2005 On-chip solid-state cooling for integrated circuits using thin-film microrefrigerators *IEEE Trans. Components Packag. Technol.* **28** 65–9
[90] Zhang Y *et al* 2003 High speed localized cooling using SiGe superlattice microrefrigerators *19th Annual IEEE Semiconductor Thermal Measurement and Management Symposium* pp 61–5 (Piscataway, NJ: IEEE)
[91] Zeng G *et al* 2003 Cooling power density of SiGe/Si superlattice micro refrigerators *MRS Proc.* **793** S2.2
[92] Rowe D M (ed) 1995 *CRC Handbook of Thermoelectrics* (Boca Raton, FL: CRC)
[93] Liu Y *et al* 2016 Van der Waals heterostructures and devices *Nat. Rev. Mater.* **1** 16042
[94] Ni Z *et al* 2012 Tunable bandgap in silicene and germanene *Nano Lett.* **12** 113–8
[95] Nayeb Sadeghi S, Zebarjadi M and Esfarjani K 2019 Non-linear enhancement of thermoelectric performance of a $TiSe_2$ monolayer due to tensile strain, from first-principles calculations *J. Mater. Chem.* C **7** 7308–17
[96] Liang S-J, Liu B, Hu W, Zhou K and Ang L K 2017 Thermionic energy conversion based on graphene van der Waals heterostructures *Sci. Rep.* **7** 46211
[97] Yuan P, Li C, Xu S, Liu J and Wang X 2017 Interfacial thermal conductance between few to tens of layered-MoS_2 and c-Si: effect of MoS_2 thickness *Acta Mater.* **122** 152–65
[98] Sadeghi H, Sangtarash S and Lambert C J 2016 Cross-plane enhanced thermoelectricity and phonon suppression in graphene/MoS_2 van der Waals heterostructures *2D Materials* **4** 015012

[99] Massicotte M *et al* 2016 Photo-thermionic effect in vertical graphene heterostructures *Nat. Commun.* **7** 12174
[100] Vogt P *et al* 2012 Silicene: compelling experimental evidence for graphenelike two-dimensional silicon *Phys. Rev. Lett.* **108** 155501
[101] Fleurence A *et al* 2012 Experimental evidence for epitaxial silicene on diboride thin films *Phys. Rev. Lett.* **108** 245501
[102] Van Hagan T H, Smith J N and Schuller M 1997 Thermionic/AMTEC cascade converter concept for high-efficiency space power *IEEE Aerosp. Electron. Syst. Mag.* **12** 10–5
[103] Begg L L *et al* 2004 Conceptual design of high power advanced low mass (HPALM) solar thermionic power system *Proc. 37th Intersoc. Energy Convers. Eng. Conf.* pp 7–11
[104] Clark P N, Desplat J L, Streckert H H, Adams S F and Smith J W 2006 Solar thermionic test in a thermal receiver *AIP Conf. Proc.* **813** 598
[105] Adams S F 2006 Solar thermionic space power technology testing: a historical perspective *AIP Conf. Proc.* **813** 590–7
[106] Fraser D A, Tanner P G and Irving A D 2005 Developments in thermionic energy converters *IEE Proc.—Sci. Meas. Technol.* **152** 1
[107] Fitzpatrick G O *et al* 1997 Updated perspective on the potential for thermionic conversion to meet 21st century energy needs *IECEC-97 Proceedings of the 32nd Intersociety Energy Conversion Engineering Conference* pp 1045–51 (Piscataway, NJ: IEEE)
[108] Page H *et al* 2001 300 K operation of a GaAs-based quantum-cascade laser at $\lambda \approx 9$ μm *Appl. Phys. Lett.* **78** 3529–31
[109] Das N K and Bertoni H L 1997 *Directions for the Next Generation of MMIC Devices and Systems* (New York: Springer)
[110] Vashaee D and Shakouri A 2006 HgCdTe superlattices for solid-state cryogenic refrigeration *Appl. Phys. Lett.* **88** 132110
[111] Adams M J, Verosky M, Zebarjadi M and Heremans J P 2019 Active Peltier coolers based on correlated and magnon-drag metals *Phys. Rev. Appl.* **11** 054008

Chapter 15

[1] Radermacher R and Kim K 1996 Domestic refrigerators: recent developments *Int. J. Refrig.* **19** 61–9
[2] U.S. Department of Energy 2011 *Buildings Energy Data Book* (Washington DC: U.S. Dept. of Energy, Office of Energy Efficiency and Renewable Energy)
[3] Huang L, Liu Z, Liu Y, Gou Y and Wang J 2009 Experimental study on frost release on fin-and-tube heat exchangers by use of a novel anti-frosting paint *Exp. Therm. Fluid. Sci.* **33** 1049–54
[4] Lv J, Song Y, Jiang L and Wang J 2014 Bio-inspired strategies for anti-icing *ACS Nano* **8** 3152–69
[5] Zhang P and Lv F Y 2015 A review of the recent advances in superhydrophobic surfaces and the emerging energy-related applications *Energy* **82** 1068–87
[6] Machielsen C H M and Kerschbaumer H G 1989 Influence of frost formation and defrosting on the performance of air coolers: standards and dimensionless coefficients for the system designer *Int. J. Refrig.* **12** 283–90
[7] Moallem E, Cremaschi L, Fisher D E and Padhmanabhan S 2012 Experimental measurements of the surface coating and water retention effects on frosting performance of microchannel heat exchangers for heat pump systems *Exp. Therm. Fluid Sci.* **39** 176–88

[8] La Due J, Muller M and Swangler M 1996 Cratering phenomena on aircraft anti-icing films *J. Aircr.* **33** 131–8
[9] Broeren A P, Lee S and Clark C 2015 Aerodynamic effects of anti-icing fluids on a thin high-performance wing section *J. Aircr.* **53** 451–62
[10] Brown J, Raghunathan S, Watterson J, Linton A and Riordon D 2002 Heat transfer correlation for anti-icing systems *J. Aircr.* **39** 65–70
[11] Harireche O, Verdin P, Thompson C P and Hammond D W 2008 Explicit finite volume modeling of aircraft anti-icing and de-icing *J. Aircr.* **45** 1924–36
[12] Özgen S, Carbonaro M and Sarma G 2002 Experimental study of wave characteristics on a thin layer of de/anti-icing fluid *Phys. Fluids* **14** 3391–402
[13] Dong W, Zhu J, Zheng M and Chen Y 2015 Thermal analysis and testing of nonrotating cone with hot-air anti-icing system *J. Propul. Power* **31** 896–903
[14] Keith T G Jr, DEWITT K J, Nathman J K, Dietrich D A and Al-Khalil K M 1990 Thermal analysis of engine inlet anti-icing systems *J. Propul. Power* **6** 628–34
[15] Zilio C and Patricelli L 2014 Aircraft anti-ice system: evaluation of system performance with a new time dependent mathematical model *Appl. Therm. Eng.* **63** 40–51
[16] Giebel G, Brownsword R, Kariniotakis G, Denhard M and Draxl C 2011 The state-of-the-art in short-term prediction of wind power: a literature overview *ANEMOS Plus*
[17] Thomas D H 2010 *Energy Efficiency through Combined Heat and Power or Cogeneration* (New York: Nova Science Publishers)
[18] Andersson A K and Chapman L 2011 The impact of climate change on winter road maintenance and traffic accidents in West Midlands, UK *Accid. Anal. Prev.* **43** 284–9
[19] Aydın D, Kizilel R, Caniaz R O and Kizilel S 2015 Gelation-stabilized functional composite-modified bitumen for anti-icing purposes *Ind. Eng. Chem. Res.* **54** 12587–96
[20] Heymsfield E, Osweiler A, Selvam P and Kuss M 2014 Developing anti-icing airfield runways using conductive concrete with renewable energy *J. Cold Reg. Eng.* **28** 04014001
[21] Klein-Paste A and Wåhlin J 2013 Wet pavement anti-icing—a physical mechanism *Cold Reg. Sci. Technol.* **96** 1–7
[22] Li B and Yao R 2009 Urbanisation and its impact on building energy consumption and efficiency in China *Ren. Ener.* **34** 1994–8
[23] Xia Y, Zhong Y, Hrnjak P and Jacobi A 2006 Frost, defrost, and refrost and its impact on the air-side thermal-hydraulic performance of louvered-fin, flat-tube heat exchangers *Int. J. Refrig.* **29** 1066–79
[24] Chang Y-S 2011 Performance analysis of frostless heat exchanger by spreading antifreeze solution on heat exchanger surface *J. Therm. Sci. Technol.* **6** 123–31
[25] Nasr M R, Fauchoux M, Besant R W and Simonson C J 2014 A review of frosting in air-to-air energy exchangers *Renew. Sustain. Energy Rev.* **30** 538–54
[26] Goetzler W, Guernsey M, Foley K, Young J and Chung G 2016 *Energy Savings Potential and RD&D Opportunities for Commercial Building Appliances (2015 Update)* (Burlington, MA: Navigant Consulting)
[27] Nath S, Ahmadi S F and Boreyko J B 2017 A review of condensation frosting *Nanosc. Microsc. Thermophys. Eng.* **21** 81–101
[28] Dooley J B 2010 *Determination and characterization of ice propagation mechanisms on surfaces undergoing dropwise condensation* (College Station, TX: Texas A&M University)
[29] Boreyko J B and Collier C P 2013 Delayed frost growth on jumping-drop superhydrophobic surfaces *ACS Nano* **7** 1618–27

[30] Boreyko J B, Hansen R R, Murphy K R, Nath S, Retterer S T and Collier C P 2016 Controlling condensation and frost growth with chemical micropatterns *Sci. Rep.* **6** 19131
[31] Guadarrama-Cetina J, Mongruel A, González-Viñas W and Beysens D 2013 Percolation-induced frost formation *Europhys. Lett.* **101** 16009
[32] Zhang Y, Klittich M R, Gao M and Dhinojwala A 2017 Delaying frost formation by controlling surface chemistry of carbon nanotube-coated steel surfaces *ACS Appl. Mater. Interf.* **9** 6512–9
[33] Kim M-H, Kim H, Lee K-S and Kim D R 2017 Frosting characteristics on hydrophobic and superhydrophobic surfaces: a review *Energy Convers. Manage.* **138** 1–11
[34] Jung S, Tiwari M K, Doan N V and Poulikakos D 2012 Mechanism of supercooled droplet freezing on surfaces *Nat. Commun.* **3** 615
[35] Kreder M J, Alvarenga J, Kim P and Aizenberg J 2016 Design of anti-icing surfaces: smooth, textured or slippery? *Nat. Rev. Mater.* **1** 15003
[36] Miljkovic N and Wang E N 2013 Condensation heat transfer on superhydrophobic surfaces *MRS Bull.* **38** 397–406
[37] Sojoudi H, Wang M, Boscher N D, McKinley G H and Gleason K K 2016 Durable and scalable icephobic surfaces: similarities and distinctions from superhydrophobic surfaces *Soft Matter* **12** 1938–63
[38] Graeber G, Dolder V, Schutzius T M and Poulikakos D 2018 Cascade freezing of supercooled water droplet collectives *ACS Nano* **12** 11274–81
[39] Schutzius T M, Jung S, Maitra T, Eberle P, Antonini C, Stamatopoulos C and Poulikakos D 2015 Physics of icing and rational design of surfaces with extraordinary icephobicity *Langmuir* **31** 4807–21
[40] Roustan J, Kienlen J, Aubas P, Aubas S and Du Cailar J 1992 Comparison of hydrophobic heat and moisture exchangers with heated humidifier during prolonged mechanical ventilation *Inten. Care Med.* **18** 97–100
[41] Restuccia G, Freni A, Russo F and Vasta S 2005 Experimental investigation of a solid adsorption chiller based on a heat exchanger coated with hydrophobic zeolite *Appl. Therm. Eng.* **25** 1419–28
[42] Sommers A D and Jacobi A M 2006 Creating micro-scale surface topology to achieve anisotropic wettability on an aluminum surface *J. Micromech. Microeng.* **16** 1571
[43] Rykaczewski K, Scott J H J, Rajauria S, Chinn J, Chinn A M and Jones W 2011 Three dimensional aspects of droplet coalescence during dropwise condensation on superhydrophobic surfaces *Soft Matter* **7** 8749–52
[44] Chen X, Wu J, Ma R, Hua M, Koratkar N, Yao S and Wang Z 2011 Nanograssed micropyramidal architectures for continuous dropwise condensation *Adv. Funct. Mater.* **21** 4617–23
[45] Enright R, Miljkovic N, Alvarado J L, Kim K and Rose J W 2014 Dropwise condensation on micro- and nanostructured surfaces *Nanoscale Microscale Thermophys. Eng.* **18** 223–50
[46] Rose J 2002 Dropwise condensation theory and experiment: a review *Proc. Inst. Mech. Eng. A* **216** 115–28
[47] Marto P, Looney D, Rose J and Wanniarachchi A 1986 Evaluation of organic coatings for the promotion of dropwise condensation of steam *Int. J. Heat Mass Transfer* **29** 1109–17
[48] Boreyko J B and Chen C-H 2009 Self-propelled dropwise condensate on superhydrophobic surfaces *Phys. Rev. Lett.* **103** 184501

[49] Chen C-H, Cai Q, Tsai C, Chen C-L, Xiong G, Yu Y and Ren Z 2007 Dropwise condensation on superhydrophobic surfaces with two-tier roughness *Appl. Phys. Lett.* **90** 173108
[50] Miljkovic N, Enright R and Wang E N 2012 Effect of droplet morphology on growth dynamics and heat transfer during condensation on superhydrophobic nanostructured surfaces *ACS Nano* **6** 1776–85
[51] Miljkovic N, Enright R, Nam Y, Lopez K, Dou N, Sack J and Wang E N 2012 Jumping-droplet-enhanced condensation on scalable superhydrophobic nanostructured surfaces *Nano Lett.* **13** 179–87
[52] Zhang Q, He M, Chen J, Wang J, Song Y and Jiang L 2013 Anti-icing surfaces based on enhanced self-propelled jumping of condensed water microdroplets *Chem. Commun.* **49** 4516–8
[53] Sun X, Damle V G, Liu S and Rykaczewski K 2015 Bioinspired stimuli-responsive and antifreeze-secreting anti-icing coatings *Adv. Mater. Interf.* **2** 1400479
[54] Zhang S, Huang J, Cheng Y, Yang H, Chen Z and Lai Y 2017 Bioinspired surfaces with superwettability for anti-icing and ice-phobic application: concept, mechanism, and design *Small* **13** 1701867
[55] Li Q and Guo Z 2018 Fundamentals of icing and common strategies for designing biomimetic anti-icing surfaces *J. Mater. Chem.* A **6** 13549–81
[56] Hoke J, Georgiadis J and Jacobi A 2004 Effect of substrate wettability on frost properties *J. Thermophys. Heat Transfer* **18** 228–35
[57] Chavan S, Carpenter J, Nallapaneni M, Chen J and Miljkovic N 2017 Bulk water freezing dynamics on superhydrophobic surfaces *Appl. Phys. Lett.* **110** 041604
[58] Lee H, Shin J, Ha S, Choi B and Lee J 2004 Frost formation on a plate with different surface hydrophilicity *Int. J. Heat Mass Transfer* **47** 4881–93
[59] Kim K and Lee K-S 2011 Frosting and defrosting characteristics of a fin according to surface contact angle *Int. J. Heat Mass Transfer* **54** 2758–64
[60] Liu K, Yao X and Jiang L 2010 Recent developments in bio-inspired special wettability *Chem. Soc. Rev.* **39** 3240–55
[61] Yao X, Song Y and Jiang L 2011 Applications of bio-inspired special wettable surfaces *Adv. Mater.* **23** 719–34
[62] Liu K and Jiang L 2011 Bio-inspired design of multiscale structures for function integration *Nano Today* **6** 155–75
[63] Nishimoto S and Bhushan B 2013 Bioinspired self-cleaning surfaces with superhydrophobicity, superoleophobicity, and superhydrophilicity *RSC Adv.* **3** 671–90
[64] Kulinich S and Farzaneh M 2009 How wetting hysteresis influences ice adhesion strength on superhydrophobic surfaces *Langmuir* **25** 8854–6
[65] Kulinich S and Farzaneh M 2009 Ice adhesion on super-hydrophobic surfaces *Appl. Surf. Sci.* **255** 8153–7
[66] Zou M, Beckford S, Wei R, Ellis C, Hatton G and Miller M 2011 Effects of surface roughness and energy on ice adhesion strength *Appl. Surf. Sci.* **257** 3786–92
[67] Bharathidasan T, Kumar S V, Bobji M, Chakradhar R and Basu B J 2014 Effect of wettability and surface roughness on ice-adhesion strength of hydrophilic, hydrophobic and superhydrophobic surfaces *Appl. Surf. Sci.* **314** 241–50

[68] Attinger D, Frankiewicz C, Betz A R, Schutzius T M, Ganguly R, Das A, Kim C-J and Megaridis C M 2014 Surface engineering for phase change heat transfer: a review *MRS Energy Sustainability* **1** E4
[69] Tian X, Shaw S, Lind K R and Cademartiri L 2016 Thermal processing of silicones for green, scalable, and healable superhydrophobic coatings *Adv. Mater.* **28** 3677–82
[70] Jhee S, Lee K-S and Kim W-S 2002 Effect of surface treatments on the frosting/defrosting behavior of a fin-tube heat exchanger *Int. J. Refrig.* **25** 1047–53
[71] Kim P, Kreder M J, Alvarenga J and Aizenberg J 2013 Hierarchical or not? Effect of the length scale and hierarchy of the surface roughness on omniphobicity of lubricant-infused substrates *Nano Lett.* **13** 1793–9
[72] Weisensee P B, Wang Y, Hongliang Q, Schultz D, King W P and Miljkovic N 2017 Condensate droplet size distribution on lubricant-infused surfaces *Int. J. Heat Mass Transfer* **109** 187–99
[73] Cao M, Guo D, Yu C, Li K, Liu M and Jiang L 2015 Water-repellent properties of superhydrophobic and lubricant-infused 'slippery' surfaces: a brief study on the functions and applications *ACS Appl. Mater. Interf.* **8** 3615–23
[74] Anand S, Paxson A T, Dhiman R, Smith J D and Varanasi K K 2012 Enhanced condensation on lubricant-impregnated nanotextured surfaces *ACS Nano* **6** 10122–9
[75] Kim P, Wong T-S, Alvarenga J, Kreder M J, Adorno-Martinez W E and Aizenberg J 2012 Liquid-infused nanostructured surfaces with extreme anti-ice and anti-frost performance *ACS Nano* **6** 6569–77
[76] Rykaczewski K, Anand S, Subramanyam S B and Varanasi K K 2013 Mechanism of frost formation on lubricant-impregnated surfaces *Langmuir* **29** 5230–8
[77] Xiao R, Miljkovic N, Enright R and Wang E N 2013 Immersion condensation on oil-infused heterogeneous surfaces for enhanced heat transfer *Sci. Rep.* **3** 1988
[78] Carey V P 2008 *Liquid-Vapor Phase-Change Phenomena* 2nd edn (Boca Raton, FL: CRC Press)
[79] Nath S and Boreyko J B 2016 On localized vapor pressure gradients governing condensation and frost phenomena *Langmuir* **32** 8350–65
[80] Parent O and Ilinca A 2011 Anti-icing and de-icing techniques for wind turbines: critical review *Cold Reg. Sci. Technol.* **65** 88–96
[81] Laforte J, Allaire M and Laflamme J 1998 State-of-the-art on power line de-icing *Atmos. Res.* **46** 143–58
[82] Schutzius T M, Jung S, Maitra T, Eberle P, Antonini C, Stamatopoulos C and Poulikakos D 2014 Physics of icing and rational design of surfaces with extraordinary icephobicity *Langmuir* **31** 4807–21
[83] Kreder M J, Alvarenga J, Kim P and Aizenberg J 2016 Design of anti-icing surfaces: smooth, textured or slippery? *Nat. Rev. Mater.* **1** 15003
[84] Jung S, Dorrestijn M, Raps D, Das A, Megaridis C M and Poulikakos D 2011 Are superhydrophobic surfaces best for icephobicity? *Langmuir* **27** 3059–66
[85] Wen M, Wang L, Zhang M, Jiang L and Zheng Y 2014 Antifogging and icing-delay properties of composite micro-and nanostructured surfaces *ACS Appl. Mater. Interfaces* **6** 3963–8
[86] Cao L, Jones A K, Sikka V K, Wu J and Gao D 2009 Anti-icing superhydrophobic coatings *Langmuir* **25** 12444–8

[87] Tourkine P, Le Merrer M and Quéré D 2009 Delayed freezing on water repellent materials *Langmuir* **25** 7214–6
[88] Alizadeh A, Yamada M, Li R, Shang W, Otta S, Zhong S, Ge L, Dhinojwala A, Conway K R and Bahadur V 2012 Dynamics of ice nucleation on water repellent surfaces *Langmuir* **28** 3180–6
[89] Boinovich L, Emelyanenko A M, Korolev V V and Pashinin A S 2014 Effect of wettability on sessile drop freezing: when superhydrophobicity stimulates an extreme freezing delay *Langmuir* **30** 1659–68
[90] Farhadi S, Farzaneh M and Kulinich S 2011 Anti-icing performance of superhydrophobic surfaces *Appl. Surf. Sci.* **257** 6264–9
[91] Guo P, Zheng Y, Wen M, Song C, Lin Y and Jiang L 2012 Icephobic/anti-icing properties of micro/nanostructured surfaces *Adv. Mater.* **24** 2642–8
[92] Boinovich L B and Emelyanenko A M 2013 Anti-icing potential of superhydrophobic coatings *Mendeleev Commun.* **1** 3–10
[93] Kulinich S, Farhadi S, Nose K and Du X 2010 Superhydrophobic surfaces: are they really ice-repellent? *Langmuir* **27** 25–9
[94] Varanasi K K, Deng T, Smith J D, Hsu M and Bhate N 2010 Frost formation and ice adhesion on superhydrophobic surfaces *Appl. Phys. Lett.* **97** 234102
[95] Meuler A J, Smith J D, Varanasi K K, Mabry J M, McKinley G H and Cohen R E 2010 Relationships between water wettability and ice adhesion *ACS Appl. Mater. Interf.* **2** 3100–10
[96] Bengaluru Subramanyam S, Kondrashov V, Rühe J r and Varanasi K K 2016 Low ice adhesion on nano-textured superhydrophobic surfaces under supersaturated conditions *ACS Appl. Mater. Interf.* **8** 12583–7
[97] Maitra T, Jung S, Giger M E, Kandrical V, Ruesch T and Poulikakos D 2015 Superhydrophobicity vs ice adhesion: the quandary of robust icephobic surface design *Adv. Mater Interfaces* **2** 1500330
[98] Tarquini S, Antonini C, Amirfazli A, Marengo M and Palacios J 2014 Investigation of ice shedding properties of superhydrophobic coatings on helicopter blades *Cold Reg. Sci. Technol.* **100** 50–8
[99] Chanda J, Ionov L, Kirillova A and Synytska A 2015 New insight into icing and de-icing properties of hydrophobic and hydrophilic structured surfaces based on core–shell particles *Soft Matter* **11** 9126–34
[100] Thomas S K, Cassoni R P and MacArthur C D 1996 Aircraft anti-icing and de-icing techniques and modeling *J. Aircr.* **33** 841–54
[101] Cancilla D A, Holtkamp A, Matassa L and Fang X 1997 Isolation and characterization of Microtox®-active components from aircraft de-icing/anti-icing fluids *Environ. Toxicol. Chem.* **16** 430–4
[102] Golovin K, Kobaku S P, Lee D H, DiLoreto E T, Mabry J M and Tuteja A 2016 Designing durable icephobic surfaces *Sci. Adv.* **2** e1501496
[103] Fletcher N 1958 Size effect in heterogeneous nucleation *J. Chem. Phys.* **29** 572–6
[104] Adamson A and Gast A 1997 *Physical Chemistry of Surfaces* 6th edn (New York: Wiley)
[105] Hoke J L, Georgiadis J G and Jacobi A M 2004 Effect of substrate wettability on frost properties *J. Thermophys. Heat Tr.* **18** 228–35
[106] Na B and Webb R L 2003 A fundamental understanding of factors affecting frost nucleation *Int. J. Heat Mass Transfer* **46** 3797–808

[107] Alizadeh A *et al* 2012 Dynamics of ice nucleation on water repellent surfaces *Langmuir* **28** 3180–6
[108] Tourkine P, Le Merrer M and Quere D 2009 Delayed freezing on water repellent materials *Langmuir* **25** 7214–6
[109] Wang H, Tang L M, Wu X M, Dai W T and Qiu Y P 2007 Fabrication and anti-frosting performance of super hydrophobic coating based on modified nano-sized calcium carbonate and ordinary polyacrylate *Appl. Surf. Sci.* **253** 8818–24
[110] Hermes C J L, Piucco R O, Barbosa J R and Melo C 2009 A study of frost growth and densification on flat surfaces *Exp. Therm. Fluid Sci.* **33** 371–9
[111] Zhang Q L, He M, Zeng X P, Li K Y, Cui D P, Chen J, Wang J J, Song Y L and Jiang L 2012 Condensation mode determines the freezing of condensed water on solid surfaces *Soft Matter* **8** 8285–8
[112] Guadarrama-Cetina J, Mongruel A, Gonzalez-Vinas W and Beysens D 2013 Percolation-induced frost formation *Europhys. Lett.* **101** 16009
[113] Meuler A J, McKinley G H and Cohen R E 2010 Exploiting topographical texture to impart icephobicity *ACS Nano* **4** 7048–52
[114] Kulinich S A and Farzaneh M 2011 On ice-releasing properties of rough hydrophobic coatings *Cold Reg. Sci. Technol.* **65** 60–4
[115] Farhadi S, Farzaneh M and Kulinich S A 2011 Anti-icing performance of superhydrophobic surfaces *Appl. Surf. Sci.* **257** 6264–9
[116] Nosonovsky M and Hejazi V 2012 Why superhydrophobic surfaces are not always icephobic *ACS Nano* **6** 8488–91
[117] Na B and Webb R L 2004 New model for frost growth rate *Int. J. Heat Mass Transfer* **47** 925–36
[118] Narhe R D, Khandkar M D, Shelke P B, Limaye A V and Beysens D A 2009 Condensation-induced jumping water drops *Phys. Rev.* E **80** 031604
[119] Kim M-K, Cha H, Birbarah P, Chavan S, Zhong C, Xu Y and Miljkovic N 2015 Enhanced jumping-droplet departure *Langmuir* **31** 13452–66
[120] Liu H, Zhang P, Liu M, Wang S and Jiang L 2013 Organogel-based thin films for self-cleaning on various surfaces *Adv. Mater.* **25** 4477–81
[121] Enright R, Miljkovic N, Al-Obeidi A, Thompson C V and Wang E N 2012 Condensation on superhydrophobic surfaces: the role of local energy barriers and structure length scale *Langmuir* **40** 14424–32
[122] Enright R, Miljkovic N, Alvarado J L, Kim K J and Rose J W 2014 Dropwise condensation on micro- and nanostructured surfaces *Nanosc. Microsc. Therm. Eng.* **18** 223–50
[123] Enright R, Miljkovic N, Dou N, Nam Y and Wang E N 2013 Condensation on superhydrophobic copper oxide nanostructures *J. Heat Transfer* **135** 091304
[124] Enright R, Miljkovic N, Sprittles J, Mitchell R, Nolan K, Thompson C V and Wang E N 2014 How coalescing droplets jump *ACS Nano* **8** 10352–62
[125] Miljkovic N, Enright R, Nam Y, Lopez K, Dou N, Sack J and Wang E N 2013 Jumping-droplet-enhanced condensation on scalable superhydrophobic nanostructured surfaces *Nano Lett.* **13** 179–87
[126] Miljkovic N, Enright R and Wang E N 2013 Modeling and optimization of superhydrophobic condensation *J. Heat Trans.* **135** 111004

[127] Miljkovic N, Preston D J, Enright R, Adera S, Nam Y and Wang E N 2013 Jumping droplet dynamics on scalable nanostructured superhydrophobic surfaces *J. Heat Transfer* **135** 080907
[128] Miljkovic N, Preston D J, Enright R and Wang E N 2013 Electric-field-enhanced condensation on superhydrophobic nanostructured surfaces *ACS Nano* **7** 11043–54
[129] Miljkovic N, Xiao R, Preston D J, Enright R, McKay I and Wang E N 2013 Condensation on hydrophilic, hydrophobic, nanostructured superhydrophobic and oil-infused surfaces *J. Heat Transfer* **135** 080906–7
[130] Miljkovic N, Preston D J, Enright R and Wang E N 2013 Electrostatic charging of jumping droplets *Nat. Commun.* **4** 2517
[131] Chavan S, Cha H, Orejon D, Nawaz K, Singla N, Yeung Y F, Park D, Kang D H, Chang Y and Takata Y 2016 Heat transfer through a condensate droplet on hydrophobic and nanostructured superhydrophobic surfaces *Langmuir* **32** 7774–87
[132] Boinovich L B and Emelyanenko A M 2013 Anti-icing potential of superhydrophobic coatings *Mendeleev Commun.* **23** 3–10
[133] Eberle P, Tiwari M K, Maitra T and Poulikakos D 2014 Rational nanostructuring of surfaces for extraordinary icephobicity *Nanoscale* **6** 4874–81
[134] Quéré D 2005 Non-sticking drops *Rep. Prog. Phys.* **68** 2495
[135] Chaudhary G and Li R 2014 Freezing of water droplets on solid surfaces: an experimental and numerical study *Exp. Therm. Fluid Sci.* **57** 86–93
[136] Aliotta F, Giaquinta P V, Ponterio R C, Prestipino S, Saija F, Salvato G and Vasi C 2014 Supercooled water escaping from metastability *Sci. Rep.* **4** 7230
[137] Feuillebois F, Lasek A, Creismeas P, Pigeonneau F and Szaniawski A 1995 Freezing of a subcooled liquid droplet *J. Colloid. Interf. Sci.* **169** 90–102
[138] Chavan S, Park D, Singla N, Sokalski P, Boyina K and Miljkovic N 2018 Effect of latent heat released by freezing droplets during frost wave propagation *Langmuir* **34** 6636–44
[139] Cheng R J 1970 Water drop freezing: ejection of microdroplets *Science* **170** 1395–6
[140] Jung S, Tiwari M K and Poulikakos D 2012 Frost halos from supercooled water droplets *Proc. Natl Acad. Sci.* **109** 16073–8
[141] Esmeryan K D, Castano C E, Mohammadi R, Lazarov Y and Radeva E I 2018 Delayed condensation and frost formation on superhydrophobic carbon soot coatings by controlling the presence of hydrophilic active sites *J. Phys. D: Appl. Phys.* **51** 055302
[142] Rose J and Glicksman L 1973 Dropwise condensation—the distribution of drop sizes *Int. J. Heat Mass Transfer* **16** 411–25
[143] Kim A, Lee C, Kim H and Kim J 2015 Simple approach to superhydrophobic nanostructured AI for practical antifrosting application based on enhanced self-propelled jumping droplets *ACS Appl. Mater. Interf.* **7** 7206–13
[144] Sanders C T 1974 The influence of frost formation and defrosting on the performance of air coolers *PhD Thesis* Technische Hogeschool, Delft
[145] Na B and Webb R L 2004 Mass transfer on and within a frost layer *Int. J. Heat Mass Transfer* **47** 899–911
[146] El Cheikh A and Jacobi A 2014 A mathematical model for frost growth and densification on flat surfaces *Int. J. Heat Mass Transfer* **77** 604–11
[147] Lee K-S, Jhee S and Yang D-K 2003 Prediction of the frost formation on a cold flat surface *Int. J. Heat Mass Transfer* **46** 3789–96

[148] Le Gall R, Grillot J and Jallut C 1997 Modelling of frost growth and densification *Int. J. Heat Mass Transfer* **40** 3177–87
[149] Brian P T, Reid R C and Shah Y T 1970 Frost deposition on cold surfaces *Industr. Eng. Chem. Fundam.* **9** 375–80
[150] Hermes C J, Loyola F R and Nascimento V S Jr 2014 A semi-empirical correlation for the frost density *Int. J. Refrig.* **46** 100–4
[151] Hermes C J 2012 An analytical solution to the problem of frost growth and densification on flat surfaces *Int. J. Heat Mass Transfer* **55** 7346–51
[152] Storey B and Jacobi A 1999 The effect of streamwise vortices on the frost growth rate in developing laminar channel flows *Int. J. Heat Mass Transfer* **42** 3787–802
[153] Schneider H 1978 Equation of the growth rate of frost forming on cooled surfaces *Int. J. Heat Mass Transfer* **21** 1019–24
[154] Lee Y and Ro S 2005 Analysis of the frost growth on a flat plate by simple models of saturation and supersaturation *Exp. Therm. Fluid Sci.* **29** 685–96
[155] Jones B and Parker J 1975 Frost formation with varying environmental parameters *J. Heat Transfer* **97** 255–9
[156] Hejazi V, Sobolev K and Nosonovsky M 2013 From superhydrophobicity to icephobicity: forces and interaction analysis *Sci. Rep.* **3** 2194
[157] Menini R and Farzaneh M 2009 Elaboration of Al_2O_3/PTFE icephobic coatings for protecting aluminum surfaces *Surf. Coat. Technol.* **203** 1941–6
[158] Alizadeh A, Bahadur V, Shang W, Zhu Y, Buckley D, Dhinojwala A and Sohal M 2013 Influence of substrate elasticity on droplet impact dynamics *Langmuir* **29** 4520–4
[159] Sokuler M, Auernhammer G K, Roth M, Liu C, Bonacurrso E and Butt H-J 2009 The softer the better: fast condensation on soft surfaces *Langmuir* **26** 1544–7
[160] Wong T-S, Kang S H, Tang S K, Smythe E J, Hatton B D, Grinthal A and Aizenberg J 2011 Bioinspired self-repairing slippery surfaces with pressure-stable omniphobicity *Nature* **477** 443
[161] Boreyko J B, Srijanto B R, Nguyen T D, Vega C, Fuentes-Cabrera M and Collier C P 2013 Dynamic defrosting on nanostructured superhydrophobic surfaces *Langmuir* **29** 9516–24
[162] Darmanin T and Guittard F 2014 Recent advances in the potential applications of bioinspired superhydrophobic materials *J. Mater. Chem.* A **2** 16319–59
[163] Li Y, Li L and Sun J 2010 Bioinspired self-healing superhydrophobic coatings *Angewandte Chemie.* **122** 6265–9
[164] Wang S and Jiang L 2007 Definition of superhydrophobic states *Adv. Mater.* **19** 3423–4
[165] Quéré D 2008 Wetting and roughness *Annu. Rev. Mater. Res.* **38** 71–99
[166] Ulman A 1996 Formation and structure of self-assembled monolayers *Chem. Rev.* **96** 1533–54
[167] Enright R, Miljkovic N, Al-Obeidi A, Thompson C V and Wang E N 2012 Condensation on superhydrophobic surfaces: the role of local energy barriers and structure length scale *Langmuir* **28** 14424–32
[168] Wier K A and McCarthy T J 2006 Condensation on ultrahydrophobic surfaces and its effect on droplet mobility: ultrahydrophobic surfaces are not always water repellant *Langmuir* **22** 2433–6
[169] Miljkovic N, Enright R and Wang E N 2013 Modeling and optimization of superhydrophobic condensation *J. Heat Transfer* **135** 111004

[170] Cho H, Kim D, Lee C and Hwang W 2013 A simple fabrication method for mechanically robust superhydrophobic surface by hierarchical aluminum hydroxide structures *Curr. Appl. Phys.* **13** 762–7
[171] Yue X, Liu W and Wang Y 2016 Effects of black silicon surface structures on wetting behaviors, single water droplet icing and frosting under natural convection conditions *Surf. Coat. Technol.* **307** 278–86
[172] Mishchenko L, Hatton B, Bahadur V, Taylor J A, Krupenkin T and Aizenberg J 2010 Design of ice-free nanostructured surfaces based on repulsion of impacting water droplets *ACS Nano* **4** 7699–707
[173] Liao R, Zuo Z, Guo C, Yuan Y and Zhuang A 2014 Fabrication of superhydrophobic surface on aluminum by continuous chemical etching and its anti-icing property *Appl. Surf. Sci.* **317** 701–9
[174] Maitra T, Tiwari M K, Antonini C, Schoch P, Jung S, Eberle P and Poulikakos D 2013 On the nanoengineering of superhydrophobic and impalement resistant surface textures below the freezing temperature *Nano Lett.* **14** 172–82
[175] Song J, Xu W and Lu Y 2012 One-step electrochemical machining of superhydrophobic surfaces on aluminum substrates *J. Mater. Sci.* **47** 162–8
[176] Miwa M, Nakajima A, Fujishima A, Hashimoto K and Watanabe T 2000 Effects of the surface roughness on sliding angles of water droplets on superhydrophobic surfaces *Langmuir* **16** 5754–60
[177] Hao Q, Pang Y, Zhao Y, Zhang J, Feng J and Yao S 2014 Mechanism of delayed frost growth on superhydrophobic surfaces with jumping condensates: more than interdrop freezing *Langmuir* **30** 15416–22
[178] Boreyko J B, Zhao Y and Chen C-H 2011 Planar jumping-drop thermal diodes *Appl. Phys. Lett.* **99** 234105
[179] Boreyko J B and Chen C-H 2013 Vapor chambers with jumping-drop liquid return from superhydrophobic condensers *Int. J. Heat Mass Transfer* **61** 409–18
[180] Zhao Y, Preston D J, Lu Z, Zhang L, Queeney J and Wang E N 2018 Effects of millimetric geometric features on dropwise condensation under different vapor conditions *Int. J. Heat Mass Transfer* **119** 931–8
[181] Ma X-H, Zhou X-D, Lan Z, Yi-Ming L and Zhang Y 2008 Condensation heat transfer enhancement in the presence of non-condensable gas using the interfacial effect of dropwise condensation *Int. J. Heat Mass Transfer* **51** 1728–37
[182] Deng X, Mammen L, Butt H-J and Vollmer D 2012 Candle soot as a template for a transparent robust superamphiphobic coating *Science* **335** 67–70
[183] Wang N, Xiong D, Deng Y, Shi Y and Wang K 2015 Mechanically robust superhydrophobic steel surface with anti-icing, UV-durability, and corrosion resistance properties *ACS Appl. Mater. Interf.* **7** 6260–72
[184] Goetz L A, Jalvo B, Rosal R and Mathew A P 2016 Superhydrophilic anti-fouling electrospun cellulose acetate membranes coated with chitin nanocrystals for water filtration *J. Membr. Sci.* **510** 238–48
[185] de Leon A C C, Pernites R B and Advincula R C 2012 Superhydrophobic colloidally textured polythiophene film as superior anticorrosion coating *Appl. Mater. Interf.* **4** 3169–76
[186] Zhang X, Wang L and Levänen E 2013 Superhydrophobic surfaces for the reduction of bacterial adhesion *RSC Adv.* **3** 12003–20

[187] Banerjee I, Pangule R C and Kane R S 2011 Antifouling coatings: recent developments in the design of surfaces that prevent fouling by proteins, bacteria, and marine organisms *Adv. Mater.* **23** 690–718
[188] Wang Y, Xue J, Wang Q, Chen Q and Ding J 2013 Verification of icephobic/anti-icing properties of a superhydrophobic surface *Appl. Mater. Interf.* **5** 3370–81
[189] Zhang Y, Ge D and Yang S 2014 Spray-coating of superhydrophobic aluminum alloys with enhanced mechanical robustness *J. Colloid. Interf. Sci.* **423** 101–7
[190] Barthwal S, Kim Y S and Lim S-H 2013 Mechanically robust superamphiphobic aluminum surface with nanopore-embedded microtexture *Langmuir* **29** 11966–74
[191] Budunoglu H, Yildirim A and Bayindir M 2012 Flexible and mechanically stable antireflective coatings from nanoporous organically modified silica colloids *J. Mater. Chem.* **22** 9671–7
[192] Chen X, Ma R, Zhou H, Zhou X, Che L, Yao S and Wang Z 2013 Activating the microscale edge effect in a hierarchical surface for frosting suppression and defrosting promotion *Sci. Rep.* **3** 2515
[193] Susoff M, Siegmann K, Pfaffenroth C and Hirayama M 2013 Evaluation of icephobic coatings—screening of different coatings and influence of roughness *Appl. Surf. Sci.* **282** 870–9
[194] Yang S, Xia Q, Zhu L, Xue J, Wang Q and Chen Q-m 2011 Research on the icephobic properties of fluoropolymer-based materials *Appl. Surf. Sci.* **257** 4956–62
[195] Zhu L, Xue J, Wang Y, Chen Q, Ding J and Wang Q 2013 Ice-phobic coatings based on silicon-oil-infused polydimethylsiloxane *Appl. Mater. Interf.* **5** 4053–62
[196] Chen J, Liu J, He M, Li K, Cui D, Zhang Q, Zeng X, Zhang Y, Wang J and Song Y 2012 Superhydrophobic surfaces cannot reduce ice adhesion *Appl. Phys. Lett.* **101** 111603
[197] Sojoudi H, McKinley G H and Gleason K K 2015 Linker-free grafting of fluorinated polymeric cross-linked network bilayers for durable reduction of ice adhesion *Mater. Horizons* **2** 91–9
[198] Chen K, Zhou S, Yang S and Wu L 2015 Fabrication of all-water-based self-repairing superhydrophobic coatings based on UV-responsive microcapsules *Adv. Funct. Mater.* **25** 1035–41
[199] Isimjan T T, Wang T and Rohani S 2012 A novel method to prepare superhydrophobic, UV resistance and anti-corrosion steel surface *Chem. Eng. J.* **210** 182–7
[200] Gao Y, Gereige I, El Labban A, Cha D, Isimjan T T and Beaujuge P M 2014 Highly transparent and UV-resistant superhydrophobic SiO_2-coated ZnO nanorod arrays *Appl. Mater. Interf.* **6** 2219–23
[201] Zhi D, Lu Y, Sathasivam S, Parkin I P and Zhang X 2017 Large-scale fabrication of translucent and repairable superhydrophobic spray coatings with remarkable mechanical, chemical durability and UV resistance *J. Mater. Chem.* A **5** 10622–31
[202] Boinovich L B, Emelyanenko A M, Ivanov V K and Pashinin A S 2013 Durable icephobic coating for stainless steel *Appl. Mater. Interf.* **5** 2549–54
[203] Lee E J, Kim J J and Cho S O 2010 Fabrication of porous hierarchical polymer/ceramic composites by electron irradiation of organic/inorganic polymers: route to a highly durable, large-area superhydrophobic coating *Langmuir* **26** 3024–30
[204] Lee S-M, Kim K-S, Pippel E, Kim S, Kim J-H and Lee H-J 2012 Facile route toward mechanically stable superhydrophobic copper using oxidation–reduction induced morphology changes *J. Phys. Chem.* C **116** 2781–90

[205] Chang Y S 2011 Performance analysis of frostless heat exchanger by spreading antifreeze solution on heat exchanger surface *J. Therm. Sci. Tech.-Jpn* **6** 123–31
[206] Stoecker W, Lux J Jr and Kooy R 1983 Energy considerations in hot-gas defrosting of industrial refrigeration coils *ASHRAE Trans.* **89** 549–73
[207] Niederer D H 1976 Frosting and defrosting effects on coil heat transfer *ASHRAE Trans.* **82** 467–73
[208] Ganesan P, Vanaki S M, Thoo K K and Chin W M 2016 Air-side heat transfer characteristics of hydrophobic and super-hydrophobic fin surfaces in heat exchangers: a review *Int. Commun. Heat Mass Transf.* **74** 27–35
[209] Nath S, Ahmadi S F and Boreyko J B 2016 A review of condensation frosting *Nanosc. Microsc. Therm. Eng.* **21** 81–101
[210] Jin M, Feng X, Xi J, Zhai J, Cho K, Feng L and Jiang L 2005 Super-hydrophobic PDMS surface with ultra-low adhesive force *Macromol. Rapid Commun.* **26** 1805–9
[211] Song X, Zhai J, Wang Y and Jiang L 2005 Fabrication of superhydrophobic surfaces by self-assembly and their water-adhesion properties *J. Phys. Chem.* B **109** 4048–52
[212] Ma M and Hill R M 2006 Superhydrophobic surfaces *Curr. Opin. Coll. Interf. Sci.* **11** 193–202
[213] Yin L, Wang Y, Ding J, Wang Q and Chen Q 2012 Water condensation on super-hydrophobic aluminum surfaces with different low-surface-energy coatings *Appl. Surf. Sci.* **258** 4063–8
[214] Xu L, Chen W, Mulchandani A and Yan Y 2005 Reversible conversion of conducting polymer films from superhydrophobic to superhydrophilic *Angew. Chem. Int. Ed.* **44** 6009–12
[215] Ma X, Ding G, Zhang Y and Wang K 2007 Airside heat transfer and friction characteristics for enhanced fin-and-tube heat exchanger with hydrophilic coating under wet conditions *Int. J. Refrig.* **30** 1153–67
[216] Motlagh N V, Birjandi F C, Sargolzaei J and Shahtahmassebi N 2013 Durable, super-hydrophobic, superoleophobic and corrosion resistant coating on the stainless steel surface using a scalable method *Appl. Surf. Sci.* **283** 636–47
[217] Rungraeng N, Cho Y-C, Yoon S H and Jun S 2012 Carbon nanotube-polytetrafluoro-ethylene nanocomposite coating for milk fouling reduction in plate heat exchanger *J. Food Eng.* **111** 218–24
[218] Zhang J, Li J and Han Y 2004 Superhydrophobic PTFE surfaces by extension *Macromol. Rapid Commun.* **25** 1105–8
[219] Wang C-C, Lee W-S, Sheu W-J and Chang Y-J 2002 A comparison of the airside performance of the fin-and-tube heat exchangers in wet conditions; with and without hydrophilic coating *Appl. Therm. Eng.* **22** 267–78
[220] Zhou Y, Yi-Zhi W, Yi-Fan Y, Mao-Gang G and Xiao-Liang X 2012 A simple way to fabricate an aluminum sheet with superhydrophobic and self-cleaning properties *Chin. Phys. Soc.* **21**
[221] Hong K and Webb R 2000 Wetting coatings for dehumidifying heat exchangers *HVAC&R Research* **6** 229–42
[222] Wang C-C and Chang C-T 1998 Heat and mass transfer for plate fin-and-tube heat exchangers, with and without hydrophilic coating *Int. J. Heat Mass Transfer* **41** 3109–20

[223] Tadanaga K, Kitamuro K, Matsuda A and Minami T 2003 Formation of superhydrophobic alumina coating films with high transparency on polymer substrates by the sol–gel method *J. Sol–Gel Sci. Technol.* **26** 705–8
[224] Thulukkanam K 2013 *Heat Exchanger Design Handbook* (Boca Raton, FL: CRC Press)
[225] Shin J, Tikhonov A V and Kim C 2003 Experimental study on frost structure on surfaces with different hydrophilicity: density and thermal conductivity *J. Heat Transfer* **125** 84–94
[226] Hosoda T 1967 Effects of frost on the heat transfer coefficient *Hitachi Hyoron* **49** 647–51
[227] Kondepudi S and O'Neal D 1989 Effect of frost growth on the performance of louvered finned tube heat exchangers *Int. J. Refrig.* **12** 151–8
[228] Song S, Bullard C and Hrnjak P 2002 Frost deposition and refrigerant distribution in microchannel heat exchangers/Discussion *ASHRAE Trans.* **108** 944
[229] Verma P, Carlson D, Wu Y, Hrnjak P and Bullard C 2002 Experimentally validated model for frosting of plain fin-round-tube heat exchangers *Proc. of IIF–IIR Commission D* p 1
[230] Moallem E, Cremaschi L and Fisher D E 2010 Experimental investigation of frost growth on microchannel heat exchangers *13th Int. Refrigeration Conf.* (*Purdue, West Lafayette, IN)* Paper 2416
[231] Xia Y, Hrnjak P S and Jacobi A M 2005 Air-side thermal-hydraulic performance of louvered-fin, flat-tube heat exchangers with sequential frost-growth cycles *ASHRAE Trans.* **111** 487–95
[232] Yonko J D 1967 An investigation of the thermal conductivity of frost while forming on a flat horizontal plate *ASHRAE Trans.* **73** 1.1–1.11
[233] Liu Y and Kulacki F 2018 An experimental study of defrost on treated surfaces: effect of frost slumping *Int. J. Heat Mass Transfer* **119** 880–90
[234] Shi Y, Tang G and Xia H 2015 Investigation of coalescence-induced droplet jumping on superhydrophobic surfaces and liquid condensate adhesion on slit and plain fins *Int. J. Heat Mass Transfer* **88** 445–55
[235] Padhmanabhan S, Fisher D, Cremaschi L and Moallem E 2011 Modeling non-uniform frost growth on a fin-and-tube heat exchanger *Int. J. Refrig.* **34** 2018–30
[236] Kondepudi S N and O'Neal D L 1993 Performance of finned-tube heat exchangers under frosting conditions: I. Simulation model *Int. J. Refrig.* **16** 175–80
[237] Kondepudi S N and O'Neal D L 1993 Performance of finned-tube heat exchangers under frosting conditions: II. Comparison of experimental data with model *Int. J. Refrig.* **16** 181–4
[238] Seker D, Karatas H and Egrican N 2004 Frost formation on fin-and-tube heat exchangers. Part I—Modeling of frost formation on fin-and-tube heat exchangers *Int. J. Refrig.* **27** 367–74
[239] Seker D, Karatas H and Egrican N 2004 Frost formation on fin-and-tube heat exchangers. Part II—Experimental investigation of frost formation on fin-and-tube heat exchangers *Int. J. Refrig.* **27** 375–7
[240] Tso C, Cheng Y and Lai A 2006 An improved model for predicting performance of finned tube heat exchanger under frosting condition, with frost thickness variation along fin *Appl. Therm. Eng.* **26** 111–20
[241] Korte C and Jacobi A 2001 Condensate retention effects on the performance of plain-fin-and-tube heat exchangers: retention data and modeling *J. Heat Transfer* **123** 926–36
[242] Wang F, Liang C, Yang M, Fan C and Zhang X 2015 Effects of surface characteristic on frosting and defrosting behaviors of fin-tube heat exchangers *Appl. Therm. Eng.* **75** 1126–32

[243] Biguria G and Wenzel L A 1970 Measurement and correlation of water frost thermal conductivity and density *Industr. Eng. Chem. Fundam.* **9** 129–38
[244] Breque F and Nemer M 2016 Frosting modeling on a cold flat plate: comparison of the different assumptions and impacts on frost growth predictions *Int. J. Refrig.* **69** 340–60
[245] Şahin A Z 2000 Effective thermal conductivity of frost during the crystal growth period *Int. J. Heat Mass Transfer* **43** 539–53
[246] Kim K and Lee K-S 2013 Frosting and defrosting characteristics of surface-treated louvered-fin heat exchangers: effects of fin pitch and experimental conditions *Int. J. Heat Mass Transfer* **60** 505–11
[247] Xia Y P, Hrnjak P S and Jacobi A M 2005 Air-side thermal-hydraulic performance of louvered-fin, flat-tube heat exchangers with sequential frost-growth cycles *ASHRAE Trans.* **111** 487–95
[248] Amer M and Wang C-C 2017 Review of defrosting methods *Renew. Sustain. Energy Rev.* **73** 53–74
[249] Ding Y, Ma G, Chai Q and Jiang Y 2004 Experiment investigation of reverse cycle defrosting methods on air source heat pump with TXV as the throttle regulator *Int. J. Refrig.* **27** 671–8
[250] Qu M, Xia L, Deng S and Jiang Y 2012 An experimental investigation on reverse-cycle defrosting performance for an air source heat pump using an electronic expansion valve *Appl. Energy* **97** 327–33
[251] Stoecker W F, Lux J J and Kooy R J 1983 Energy considerations in hot-gas defrosting of industrial refrigeration coils *ASHRAE J.* **25** 66
[252] Niederer D H 1976 Frosting and defrosting effects on coil heat transfer *ASHRAE Trans.* **82** 467–73
[253] Tso C, Wong Y, Jolly P and Ng S 2001 A comparison of hot-gas by-pass and suction modulation method for partial load control in refrigerated shipping containers *Int. J. Refrig.* **24** 544–53
[254] Reindl D, Jekel T and Elleson J 2005 *Industrial Refrigeration Energy Efficiency Guidebook* (Madison, WI: Industrial Refrigeration Consortium, The University of Wisconsin)
[255] Liu Z, Tang G and Zhao F 2003 Dynamic simulation of air-source heat pump during hot-gas defrost *Appl. Therm. Eng.* **23** 675–85
[256] Byun J-S, Lee J and Jeon C-D 2008 Frost retardation of an air-source heat pump by the hot gas bypass method *Int. J. Refrig.* **31** 328–34
[257] Dart D M 1959 Effect of fin bond on heat transfer *ASHRAE Trans.* **1** 67–71
[258] Mader G and Thybo C 2012 A new method of defrosting evaporator coils *Appl. Therm. Eng.* **39** 78–85
[259] Mei V C, Domitrovic R E, Chen F C and Kilpatrick J K 2002 A frost-less heat pump/ discussion *ASHRAE Trans.* **108** 452
[260] Kwak K and Bai C 2010 A study on the performance enhancement of heat pump using electric heater under the frosting condition: heat pump under frosting condition *Appl. Therm. Eng.* **30** 539–43
[261] Yang C, Hong S, Gao C, Zhang D and Li Y 2011 An improvement test approach of look-up table in SRAM-based FPGAs *Adv. Mater. Res.* **159** 116–23
[262] Petrenko V F, Sullivan C R, Kozlyuk V, Petrenko F V and Veerasamy V 2011 Pulse electro-thermal de-icer (PETD) *Cold Reg. Sci. Technol.* **65** 70–8

[263] Elsharkawy M, Tortorella D, Kapatral S and Megaridis C M 2016 Combating frosting with Joule-heated liquid-infused superhydrophobic coatings *Langmuir* **32** 4278–88
[264] Li D and Chen Z 2014 Experimental study on instantaneously shedding frozen water droplets from cold vertical surface by ultrasonic vibration *Exp. Therm. Fluid Sci.* **53** 17–25
[265] Schaefer V J and Langmuir I 1953 *Project cirrus Gen. Electric Res. Lab.* Final Report 52
[266] Marshall J and Gunn K 1957 A first experiment on snow crystal growth *Artificial Stimulation of Rain* (London: Pergamon), pp 340–5
[267] Ma H and Peterson G 1995 Thermodynamic analysis of the influence of electric fields on frost formation *J. Thermophys. Heat Tr.* **9** 562–4
[268] Molki M, Ohadi M and Bloshteyn M 2000 Frost reduction under intermittent electric field *National Heat Transfer Conf. (Pittsburgh, PA)*
[269] Yang S 1995 Variation of heat transfer coefficient on an oscillating circular cylinder during temperature-rising process with water vapor condensation in humid air flow *MS Thesis* (Taipei: Tatung University)
[270] Cheng C-H and Shiu C-C 2003 Oscillation effects on frost formation and liquid droplet solidification on a cold plate in atmospheric air flow *Int. J. Refrig.* **26** 69–78
[271] Wu X and Webb R L 2001 Investigation of the possibility of frost release from a cold surface *Exp. Therm. Fluid Sci.* **24** 151–6
[272] Adachi K, Saiki K and Sato H 1998 Suppression of frosting on a metal surface using ultrasonic vibrations *Ultrasonics Symposium Proceedings* (Piscataway, NJ: IEEE), pp 759–62
[273] Adachi K, Saiki K, Sato H and Ito T 2003 Ultrasonic frost suppression *Japan J. Appl. Phys.* **42** 682
[274] Ghosh A, Beaini S, Zhang B J, Ganguly R and Megaridis C M 2014 Enhancing dropwise condensation through bioinspired wettability patterning *Langmuir* **30** 13103–15
[275] Petrenko V 2009 Pulse electrothermal and heat-storage ice detachment apparatus and methods *Google patents*
[276] Petrenko V F 2010 System and method for icemaker and aircraft wing with combined electromechanical and electrothermal pulse deicing *Google patents*
[277] Petrenko V F, Higa M, Starostin M and Deresh L 2003 Pulse electrothermal de-icing *The 13th Int. Offshore and Polar Engineering Conf. (25–30 May) (Honolulu, HI)* (Int. Society of Offshore and Polar Engineers)

Chapter 16

[1] Liu W S, Hu J Z, Zhang S M, Deng M J, Han C G and Liu Y 2017 *Mater. Today Phys.* **1** 50–60
[2] Kraemer D, Sui J, McEnaney K, Zhao H, Jie Q, Ren Z F and Chen G 2015 *Energ. Environ. Sci.* **8** 1299–308
[3] Wang H, McCarty R, Salvador J R, Yamamoto A and Konig J 2014 *J. Electron. Mater.* **43** 2274–86
[4] Kim H S, Liu W S, Chen G, Chua C W and Ren Z F 2015 *P. Natl Acad. Sci. USA* **112** 8205–10
[5] Kim H S, Liu W S and Ren Z F 2017 *Energ. Environ. Sci.* **10** 69–85
[6] Rhyee J S, Lee K H, Lee S M, Cho E, Kim S I, Lee E, Kwon Y S, Shim J H and Kotliar G 2009 *Nature* **459** 965–8
[7] Toberer E S, Rauwel P, Gariel S, Tafto J and Snyder G J 2010 *J. Mater. Chem.* **20** 9877–85

[8] Saiga Y, Du B, Deng S K, Kajisa K and Takabatake T 2012 *J. Alloy Compd.* **537** 303–7
[9] Zhou M, Li J F and Kita T 2008 *J. Am. Chem. Soc.* **130** 4527–32
[10] Zhao H Z, Sui J E, Tang Z J, Lan Y C, Jie Q G, Kraemer D, McEnaney K N, Guloy A, Chen G and Ren Z F 2014 *Nano. Energy* **7** 97–103
[11] Zhang Q, Cao F, Liu W S, Lukas K, Yu B, Chen S, Opeil C, Broido D, Chen G and Ren Z F 2012 *J. Am. Chem. Soc.* **134** 10031–8
[12] Liu W S *et al* 2015 *P. Natl Acad. Sci. USA* **112** 3269–74
[13] Zhao L D, Lo S H, Zhang Y S, Sun H, Tan G J, Uher C, Wolverton C, Dravid V P and Kanatzidis M G 2014 *Nature* **508** 373
[14] Zhang Q, Chere E K, McEnaney K, Yao M L, Cao F, Ni Y Z, Chen S, Opeil C, Chen G and Ren Z F 2015 *Adv. Energy Mater.* **5** 1401977
[15] Chen X, Shi L, Zhou J S and Goodenough J B 2015 *J. Alloy Compd.* **641** 30–6
[16] Shi X, Yang J, Salvador J R, Chi M F, Cho J Y, Wang H, Bai S Q, Yang J H, Zhang W Q and Chen L D 2011 *J. Am. Chem. Soc.* **133** 7837–46
[17] Jie Q, Wang H Z, Liu W S, Wang H, Chen G and Ren Z F 2013 *Phys. Chem. Chem. Phys.* **15** 6809–16
[18] Oto Y, Iida T, Sakamoto T, Miyahara R, Natsui A, Nishio K, Kogo Y, Hirayama N and Takanashi Y 2013 *Phys. Status Solidi* C **10** 1857–61
[19] He R, Kim H S, Lan Y C, Wang D Z, Chen S and Ren Z F 2014 *RSC Adv.* **4** 64711–6
[20] Chen S, Lukas K C, Liu W S, Opeil C P, Chen G and Ren Z F 2013 *Adv. Energy Mater.* **3** 1210–4
[21] Sui J H, Li J, He J Q, Pei Y L, Berardan D, Wu H J, Dragoe N, Cai W and Zhao L D 2013 *Energ. Environ. Sci.* **6** 2916–20
[22] Jood P, Mehta R J, Zhang Y L, Peleckis G, Wang X L, Siegel R W, Borca-Tasciuc T, Dou S X and Ramanath G 2011 *Nano Lett.* **11** 4337–42
[23] Joshi G *et al* 2008 *Nano Lett.* **8** 4670–4
[24] Wang X W *et al* 2008 *Appl. Phys. Lett.* **93** 193121
[25] Liu W S, Jie Q, Kim H S and Ren Z F 2015 *Acta Mater.* **87** 357–76
[26] Muto A, Yang J, Poudel B, Ren Z F and Chen G 2013 *Adv. Energy Mater.* **3** 245–51
[27] Muto A, Kraemer D, Hao Q, Ren Z F and Chen G 2009 *Rev. Sci. Instrum.* **80** 093901
[28] Mao J *et al* 2017 *P. Natl Acad. Sci. USA* **114** 10548–53
[29] Zhang Q H, Liao J C, Tang Y S, Gu M, Ming C, Qiu P F, Bai S Q, Shi X, Uher C and Chen L D 2017 *Energ. Environ. Sci.* **10** 956–63
[30] Shi J S and Sun Y C 1997 *Rev. Sci. Instrum.* **68** 1814–7
[31] Yoshimoto S *et al* 2007 *Nano Lett.* **7** 956–9
[32] Saini S, Mele P, Miyazaki K and Tiwari A 2016 *Energ. Convers. Manag.* **114** 251–7
[33] Hu X K, Jood P, Ohta M, Kunii M, Nagase K, Nishiate H, Kanatzidis M G and Yamamoto A 2016 *Energ. Environ. Sci.* **9** 517–29
[34] Wu G X and Yu X 2014 *Energ. Convers. Manag.* **86** 99–110
[35] Skomedal G *et al* 2016 *Energ. Convers. Manag.* **110** 13–21
[36] Fabian-Mijarigos A, Min G and Alvarez-Quintana J 2017 *Energ. Convers. Manag.* **148** 1372–81
[37] Donoso-Garcia P and Henriquez-Vargas L 2015 *Energy* **93** 1189–98
[38] Rogl G and Rogl P 2017 *Mater. Today Phys.* **3** 48–69
[39] Mao J, Wu Y X, Song S W, Shuai J, Liu Z H, Pei Y Z and Ren Z F 2017 *Mater. Today Phys.* **3** 1–6

[40] He R, Zhu H T, Sun J Y, Mao J, Reith H, Chen S, Schierning G, Nielsch K and Ren Z F 2017 *Mater. Today Phys.* **1** 24–30
[41] Liu Z H *et al* 2018 *P. Natl Acad. Sci. USA* **115** 5332–7
[42] Poudel B *et al* 2008 *Science* **320** 634–8
[43] Zhu Q, Song S, Zhu H and Ren Z 2019 *J. Power Sources* **414** 393

Chapter 17

[1] Bhatt R, Kravchenko I and Gupta M 2020 High-efficiency solar thermophotovoltaic system using a nanostructure-based selective emitter *Sol. Energy* **197** 538–45
[2] Bierman D M *et al* 2016 Enhanced photovoltaic energy conversion using thermally based spectral shaping *Nat. Energy* **1** 16068
[3] Ungaro C, Gray S K and Gupta M C 2015 Solar thermophotovoltaic system using nanostructures *Opt. Express* **23** A1149–56
[4] Lenert A *et al* 2014 A nanophotonic solar thermophotovoltaic device *Nat. Nanotechnol.* **9** 126–30
[5] Rephaeli E and Fan S 2009 Absorber and emitter for solar thermo-photovoltaic systems to achieve efficiency exceeding the Shockley-Queisser limit *Opt. Express* **17** 15145–59
[6] Wang Y, Liu H and Zhu J 2019 Solar thermophotovoltaics: Progress, challenges, and opportunities *APL Mater.* **7** 080906
[7] Zhou Z, Sakr E, Sun Y and Bermel P 2016 Solar thermophotovoltaics: reshaping the solar spectrum *Nanophotonics* **5** 1–21
[8] Harder N-P and Würfel P 2003 Theoretical limits of thermophotovoltaic solar energy conversion *Semicond. Sci. Technol.* **18** S151–7
[9] Crowley C J 2005 Thermophotovoltaic converter performance for radioisotope power systems *AIP Conf. Proc.* 746 601–14
[10] Datas A and Martí A 2016 Thermophotovoltaic energy in space applications: review and future potential *Sol. Energy Mater. Sol. Cells* **161** 285–96
[11] Datas A, Ramos A, Martí A, del Cañizo C and Luque A 2016 Ultra high temperature latent heat energy storage and thermophotovoltaic energy conversion *Energy* **107** 542–9
[12] Amy C, Seyf H R, Steiner M A, Friedman D J and Henry A 2019 Thermal energy grid storage using multi-junction photovoltaics *Energy Environ. Sci.* **12** 334–43
[13] Daneshvar H, Prinja R and Kherani N P 2015 Thermophotovoltaics: fundamentals, challenges and prospects *Appl. Energy* **159** 560–75
[14] Durisch W and Bitnar B 2010 Novel thin film thermophotovoltaic system *Sol. Energy Mater. Sol. Cells* **94** 960–5
[15] Bianchi M, Ferrari C, Melino F and Peretto A 2012 Feasibility study of a thermo-photovoltaic system for CHP application in residential buildings *Appl. Energy* **97** 704–13
[16] Fraas L M, Avery J E and Huang H X 2003 Thermophotovoltaic furnace–generator for the home using low bandgap GaSb cells *Semicond. Sci. Technol.* **18** S247–53
[17] Lee K, Zimmerman J D, Xiao X, Sun and Forrest S R 2012 Reuse of GaAs substrates for epitaxial lift-off by employing protection layers *J. Appl. Phys.* **111** 033527
[18] Lee K, Zimmerman J D, Hughes T W and Forrest S R 2014 Non-destructive wafer recycling for low-cost thin-film flexible optoelectronics *Adv. Funct. Mater.* **24** 4284–91
[19] Wang C A *et al* 2004 Wafer bonding and epitaxial transfer of GaSb-based epitaxy to GaAs for monolithic interconnection of thermophotovoltaic devices *J. Electron. Mater.* **33** 213–7

[20] Omair Z *et al* 2019 Ultraefficient thermophotovoltaic power conversion by band-edge spectral filtering *Proc. Natl Acad. Sci.* **116** 15 356–61
[21] Burger T, Fan D, Lee K, Forrest S R and Lenert A 2018 Thin-film architectures with high spectral selectivity for thermophotovoltaic cells *ACS Photonics* **5** 2748–54
[22] Seyf H R and Henry A 2016 Thermophotovoltaics: a potential pathway to high efficiency concentrated solar power *Energy Environ. Sci.* **9** 2654–65
[23] Mauk M G 2006 Survey of thermophotovoltaic (TPV) devices *Mid-infrared Semiconductor Optoelectronics* vol 118 (London: Springer), pp 673–738
[24] Sakakibara R *et al* 2019 Practical emitters for thermophotovoltaics: a review *J. Photonics Energy* **9** 032713
[25] Gupta M C, Ungaro C, Foley J J and Gray S K 2017 Optical nanostructures design, fabrication, and applications for solar/thermal energy conversion *Sol. Energy* **165** 100–14
[26] Ferrari C and Melino F 2014 Overview and status of thermophotovoltaic systems *Energy Proc.* **45** 160–9
[27] Licht A, Pfiester N, DeMeo D, Chivers J and Vandervelde T E 2019 A review of advances in thermophotovoltaics for power generation and waste heat harvesting *MRS Adv.* **4** 2271–82
[28] Bauer T 2011 *Thermophotovoltaics: Basic Principles and Critical Aspects of System Design* (Berlin: Springer)
[29] Nakagawa N, Ohtsubo H, Waku Y and Yugami H 2005 Thermal emission properties of $Al_2O_3/Er_3Al_5O_{12}$ eutectic ceramics *J. Eur. Ceram. Soc.* **25** 1285–91
[30] Chirumamilla M *et al* 2019 Metamaterial emitter for thermophotovoltaics stable up to 1400 °C *Sci. Rep.* **9** 7241
[31] Kim S *et al* 2019 Optical tunneling mediated sub-skin-depth high emissivity tungsten radiators *Nano Lett.* **19** 7093
[32] Arpin K A *et al* 2013 Three-dimensional self-assembled photonic crystals with high temperature stability for thermal emission modification *Nat. Commun.* **4** 2630
[33] Wang Y *et al* 2018 Hybrid solar absorber–emitter by coherence-enhanced absorption for improved solar thermophotovoltaic conversion *Adv. Opt. Mater.* **6** 1800813
[34] Ferguson L G and Dogan F 2001 A highly efficient NiO-Doped MgO matched emitter for thermophotovoltaic energy conversion *Mater. Sci. Eng.* B **83** 35–41
[35] Rinnerbauer V, Yeng Y X, Senkevich J J, Joannopoulos J D, Soljačić M and Celanovic I 2013 Large area selective emitters/absorbers based on 2D tantalum photonic crystals for high-temperature energy applications *Proc. SPIE* **8632** 863207
[36] Rinnerbauer V *et al* 2013 High-temperature stability and selective thermal emission of polycrystalline tantalum photonic crystals *Opt. Express* **21** 11482
[37] Stelmakh V *et al* 2013 High-temperature tantalum tungsten alloy photonic crystals: stability, optical properties, and fabrication *Appl. Phys. Lett.* **103** 123903
[38] Shimizu M, Kohiyama A and Yugami H 2018 Evaluation of thermal stability in spectrally selective few-layer metallo-dielectric structures for solar thermophotovoltaics *J. Quant. Spectrosc. Radiat. Transf.* **212** 45–9
[39] Pfiester N A and Vandervelde T E 2017 Selective emitters for thermophotovoltaic applications *Phys. Status Solidi* **214** 1600410
[40] Li P *et al* 2015 Large-scale nanophotonic solar selective absorbers for high-efficiency solar thermal energy conversion *Adv. Mater.* **27** 4585–91
[41] Bitnar S *et al* 2004 Practical thermophotovoltaic generators *Semiconductors* **38** 941–5

[42] Arpin K A, Losego M D and Braun P V 2011 Electrodeposited 3D tungsten photonic crystals with enhanced thermal stability *Chem. Mater.* **23** 4783–88
[43] Kim J H, Jung S M and Shin M W 2019 Thermal degradation of refractory layered metamaterial for thermophotovoltaic emitter under high vacuum condition *Opt. Express* **27** 3039
[44] Rinnerbauer V *et al* 2012 Recent developments in high-temperature photonic crystals for energy conversion *Energy Environ. Sci.* **5** 8815–23
[45] Cui K, Lemaire P, Zhao H, Savas T, Parsons G and Hart A J 2018 Tungsten-carbon nanotube composite photonic crystals as thermally stable spectral-selective absorbers and emitters for thermophotovoltaics *Adv. Energy Mater.* **8** 1801471
[46] Chan W R, Stelmakh V, Ghebrebrhan M, Soljačić M, Joannopoulos J D and Čelanović I 2017 Enabling efficient heat-to-electricity generation at the mesoscale *Energy Environ. Sci.* **10** 1367–71
[47] Stelmakh V 2017 A practical high temperature photonic crystal for high performance thermophotovoltaics *PhD Thesis* (Massachusetts Institute of Technology)
[48] Nagpal P, Josephson D P, Denny N R, DeWilde J, Norris D J and Stein A 2011 Fabrication of carbon/refractory metal nanocomposites as thermally stable metallic photonic crystals *J. Mater. Chem.* **21** 10836
[49] Pfiester N A, Naka N and Vandervelde T E 2015 Platinum metmamaterials for thermophotovoltaic selective emitters *31st EU-PVSEC* pp 55–8
[50] Doiron C F and Naik G V 2018 Semiconductors for high selectivity thermal emitters *J. Opt.* **20** 084001
[51] Baranov D G, Xiao Y, Nechepurenko I A, Krasnok A, Alù A and Kats M A 2019 Nanophotonic engineering of far-field thermal emitters *Nat. Mater.* **18** 920–30
[52] Wernsman B *et al* 2004 Greater than 20% radiant heat conversion efficiency of a thermophotovoltaic radiator/module system using reflective spectral control *IEEE Trans. Electron Devices* **51** 512–5
[53] Fernández J, Dimroth F, Oliva E, Hermle M and Bett A W 2007 Back-surface optimization of germanium TPV cells *AIP Conf. Proc.* 890 190–97
[54] Tang L, Fraas L M, Liu Z, Zhang Y, Duan H and Xu C 2019 N-type vapor diffusion for the fabrication of GaSb thermophotovoltaic cells to increase the quantum efficiency in the long wavelength range *Sol. Energy Mater. Sol. Cells* **194** 137–41
[55] Swanson R M 1980 Recent developments in thermophotovoltaic conversion *1980 Int. Electron Devices Meeting* pp 186–9
[56] Siergiej R R *et al* 2003 20% efficient InGaAs/InPAs thermophotovoltaic cells *AIP Conf. Proc.* 653 414–23
[57] Dashiell M W *et al* 2006 Quaternary InGaAsSb thermophotovoltaic diodes *IEEE Trans. Electron Devices* **53** 2879–91
[58] Hudait M K, Brenner M and Ringel S A 2009 Metamorphic $In_{0.7}Al_{0.3}As/In_{0.69}Ga_{0.31}As$ thermophotovoltaic devices grown on graded $InAs_yP_{1-y}$ buffers by molecular beam epitaxy *Solid. State. Electron.* **53** 102–6
[59] Haase F *et al* 2018 Laser contact openings for local poly-Si-metal contacts enabling 26.1%-efficient POLO-IBC solar cells *Sol. Energy Mater. Sol. Cells* **186** 184–93
[60] Yoshikawa K *et al* 2017 Silicon heterojunction solar cell with interdigitated back contacts for a photoconversion efficiency over 26% *Nat. Energy* **2** 17032

[61] Wanlass M W 2017 Systems and methods for advanced ultra–high–performance InP solar cells *US Patent* https://patents.google.com/patent/US9590131B2/en
[62] Kayes B M *et al* 2011 27.6% conversion efficiency, a new record for single-junction solar cells under 1 Sun illumination in *2011 37th IEEE Photovoltaic Specialists Conf.* 000 004–8
[63] Green M A *et al* 2019 Solar cell efficiency tables (version 53) *Prog. Photovoltaics Res. Appl.* **27** 3–12
[64] Henry C H 1980 Limiting efficiencies of ideal single and multiple energy gap terrestrial solar cells *J. Appl. Phys.* **51** 4494–500
[65] Miller O D, Yablonovitch E and Kurtz S R 2012 Strong internal and external luminescence as solar cells approach the Shockley–Queisser limit *IEEE J. Photovoltaics* **2** 303–11
[66] Shimizu M, Kohiyama A and Yugami H 2015 High-efficiency solar-thermophotovoltaic system equipped with a monolithic planar selective absorber/emitter *J. Photonics Energy* **5** 053099
[67] Shockley W and Queisser H J 1961 Detailed balance limit of efficiency of p–n junction solar cells *J. Appl. Phys.* **32** 510–9
[68] Green M A 1982 *Solar Cells: Operating Principles, Technology, and System Applications* (Englewood Cliffs, NJ: Prentice-Hall)
[69] Woolf D N *et al* 2018 High-efficiency thermophotovoltaic energy conversion enabled by a metamaterial selective emitter *Optica* **5** 213
[70] Yeng Y X *et al* 2012 Enabling high-temperature nanophotonics for energy applications *Proc. Natl Acad. Sci.* **109** 2280–5
[71] Kim Y, Kim M-J, Kim Y, Lee H and Lee S 2019 Nanostructured radiation emitters: design rules for high-performance thermophotovoltaic systems *ACS Photonics* **6** 2260–7